The theory of electron–molecule collisions

N. F. Lane

Physics Department, Rice University, Houston, Texas 77001
and Joint Institute for Laboratory Astrophysics, National Bureau of Standards and University of Colorado, Boulder, Colorado 80309

The current state of the theory and its application to low-energy electron–molecule collisions is reviewed. The emphasis is on elastic scattering and vibrational and rotational excitation of small diatomic and polyatomic molecules. New and traditional theoretical approaches are described, and the results of calculations are compared with existing experimental measurements.

CONTENTS

I. INTRODUCTION

Electron–molecule collision processes are important in determining the energy balance and transport properties of electrons in low-temperature gases and plasmas under a wide variety of conditions. Important applications of the basic knowledge of these collision processes include MHD (magnetohydrodynamic) power generation, electron lasers such as the CO_2 laser, the upper atmospheres of the Earth and other planets, the interstellar medium of outer space, and other examples of nonequilibrium plasmas.

In the case of MHD power generation (see Spencer and Phelps, 1976) the electrical conductivity of the coal-fired plasma is limited by electron–molecule scattering, including important contributions from polar molecules such as KOH introduced into the plasma. Success in modeling such plasmas, and thereby optimizing operating conditions, will require detailed knowledge of the momentum-transfer cross sections for electron collisions with strongly polar molecules. Since direct experimental determination of such data is very difficult, theory plays a particularly important role here.

The situation is similar in applications to laser systems. For example, the CO_2 electron laser involves electron-impact excitation of vibrational and rotational states of the CO_2 molecule and other species introduced to "tune" the laser's operating characteristics (see, for example, Demaria, 1973). Knowledge of the relevant electron collision cross sections is essential to the computer modeling and optimization of this laser system. The direct experimental determination of these data, for example, by electron swarm techniques (Bulos and Phelps, 1976; Lowke, Phelps, and Irwin, 1973), is difficult, so that at present cross sections for even the most important processes are uncertain. Theory is just beginning to make real progress on this complicated problem.

In the interstellar medium, rotational excitation of molecules in electron collisions is felt to be an important mechanism for cooling the electrons and establishing the rotational-state populations and the intensities of related emission lines of the interstellar molecules (see, for example, Dalgarno and McCray, 1972; Thaddeus, 1972; and Dickinson *et al.*, 1977). Closer to home, in the upper atmospheres of the Earth and other planets, inelastic electron–molecule collision processes contribute to the slowing down of photoelectrons and other electrons produced by particle (i.e., cosmic-ray or secondary-electron) ionization of atmospheric constituents (see, for example, Dalgarno, 1968, and Takayanagi and Itikawa, 1970a). Vibrational and rotational excitation are particularly important at electron energies below electronic-excitation thresholds. Our knowledge of the relevant cross sections is still far from complete.

A. Nature of the review

This review does not deal directly with broad applications such as those described above, but rather with the underlying physical principles of the electron–molecule collision phenomena. The purpose of the review is to discuss, in some detail, recent theoretical progress in the theory of low-energy electron–molecule collisions, and to place in some perspective the large number and variety of theoretical studies that have been carried out, especially in the past ten years. In order to limit the scope of the project, emphasis has been placed on elastic scattering and rotational and vibrational excitation of simple neutral molecules (see Lane, 1979). Only a few brief comments are made on recent advances in the theory of electronic excitation. Positron scattering is not included. An entire class of interesting and important rearrangement processes, e.g., ionization, dissociation, dissociative attachment, etc., has not been included. Also missing from this review is the class of very interesting "core-excited" (or Feshbach) resonance phenomena (see reviews by Chen, 1969; Bardsley and Mandl, 1968; Taylor, 1970; Massey, 1969; and Schulz, 1973, 1976). While a considerable amount of experimental data is included for comparison, no attempt is made here to evaluate or critically analyze these data.

Relatively recent reviews of electron–molecule scattering phenomena include: "Effective Potential Approach to Electron–Molecule Scattering Theory" (Truhlar, Onda, Eades, and Dixon, 1979); "Electron Collisions with Highly Polar Molecules: Comparison of Model, Static, and Static-Exchange Calculations for Alkali-Metal Halides" (Collins and Norcross, 1978); "Resonances in Electron–Atom and Molecule Scattering" (Golden, 1978); "Electron Scattering by Polar Molecules" (Itikawa, 1978a); "Electron Scattering by Atoms and Molecules" (Burke and Williams, 1977); "Electron Scattering" (Truhlar, 1977); "Vibrational Excitation of Molecules by Electron Impact at Low Energies" (Schulz, 1976); "Low-Energy Electron Scattering from Strongly Polar Molecules" (Takayanagi, 1974); "Momentum-Transfer Cross Sections for Electron Collisions with Atoms and Molecules" (Itikawa, 1974c); "Resonances in Electron Impact on Diatomic Molecules" (Schulz, 1973); "Low-Energy Electron Scattering by Polar Molecules" (Garrett, 1972); "Low-Energy Electron-Molecule Scattering Experiments and the Theory of Rotational Excitation" (Golden, Lane, Temkin, and Gerjuoy, 1971); "Models, Interpretations and Calculations Concerning Resonant Electron Scattering Processes in Atoms and Molecules" (Taylor, 1970); "Scattering of Electrons by Diatomic Molecules" (Chandra and Joshi, 1970); "The Rotational Excitation of Molecules by Slow Electrons" (Takayanagi and Itikawa, 1970b); "Electron Impact Spectrometry" (Trajmar, Rice, and Kuppermann, 1970); "Theory of Transient Negative Ions of Simple Molecules" (Chen, 1969); "Resonant Scattering of Electrons by Molecules" (Bardsley and Mandl, 1968); and "Resonances in Electron Scattering by Atoms and Molecules" (Burke, 1968). In addition, electron–molecule scattering was the topic of the first George J. Schulz Memorial Symposium, and the proceedings are to be published (Brown, 1979). The proceedings of the 1978 Asilomar Workshop on Electron and Photon Collisions will also be published (Rescigno, McKoy, and Schneider 1979).

This review is divided into three sections: I Introduction; II Theory; and III Applications. In subsection B of the Introduction, an overview of the "nature" of the electron–molecule collision process is discussed in order to motivate some of the "physical pictures" and related approximation schemes discussed in the body of the review. In Sec. II, a brief description of the formulation of the problem is presented, and a limited selection of the more familiar approximation methods is presented. Other new techniques, such as the Glauber approximation and the $X\alpha$ multiple scattering method, are included in Sec. III along with applications to specific systems. An attempt is made throughout Sec. III to distinguish two types of theoretical investigation: (i) calculations aimed at testing a new method (e.g., "T-matrix expansion") or a new model approximation (e.g., "semiclassical exchange approximation") against accurate calculations, but at a level where only exchange effects are included and correlation effects are missing; and (ii) calculations where the goal is to apply the best available method to obtain an accurate physical result. In the first case, one compares "theory with theory," but with a well-defined purpose in mind. In the second case, one is interested in an experimental comparison. With a few exceptions, the work described was published prior to January 1979.

B. Overview of electron-molecule collisions

The scattering of electrons by molecules can provide information about the geometry and state structure of the molecular target as well as about the negative ion temporarily formed during the collision (Massey, 1969). At relatively high energies $E > 1$ keV, corresponding to de Broglie wavelengths $\lambda \lesssim 0.6\ a_0$ (0.3 Å), it is possible to probe interatomic separations and overall nuclear geometries. However, unless the molecular targets are somehow aligned, as in a crystal, on a surface, or in a strong external field, the total scattered electron angular distributions reflect statistical averages over nuclear variables including the overall orientation of the molecule. In order to recover detailed information about nuclear geometry and state structure it is necessary to separate the scattered electrons according to energy loss and to correlate a given energy loss with a particular molecular transition. Thus, electron energy-loss spectroscopy is a valuable companion to conventional spectroscopies and provides information about molecular states not readily accessible by the latter, since the electron–molecule interaction contains important contributions beyond the dipole term which dominates photon interactions. At the high electron energies relevant here, the theory is relatively straightforward since the speed of the projectile electron greatly exceeds the speeds of the nuclei and the bound electrons. Thus, an impulse approximation is appropriate, in which the internal coordinates of the target (in the present case, both bound electron and nuclear coordinates) are held constant throughout the collision. The Born approximation, valid when the scattering is weak, defines the differential scattering cross section in terms of a generalized oscillator strength. In the high-energy limit, the latter reduces to the ordinary radiative oscillator strength, for optically allowed transitions. At high energies the molecule "sees" the passing electron as a time-changing electric field.

As one lowers the electron energy, the theory becomes more complicated. The impulse approximation no longer applies to the bound electrons (although often the nuclei can still be treated in this manner). The bound electrons now must be allowed to respond to the approach of the projectile electron. This "response" is complicated and can take on different forms. At very low energies $E \lesssim 10$ eV, the bound electrons tend to relax adiabatically as the projectile approaches, thus setting up a temporary dipole moment, proportional to the dipole polarizability of the molecule and pointed in the direction of the approaching electron. This so-called "polarization interaction" strongly influences all low-energy cross sections especially small-angle scattering. The importance of polarization is particularly evident in connection with strong interference features, e.g., the Ramsauer minimum in the electron–CH_4 total cross section (Christophorou and McCorkle, 1976; Kleban and Davis, 1977; Gianturco and Thompson, 1976). The adiabatic picture breaks down when the electron is near the nuclei and at high energies in general. A striking example of this breakdown at particular energies is evident in the core-excited resonances, completely analogous to the narrow Feshbach resonances that are observed in electron–atom scattering (Burke, 1968; Bardsley and Mandl, 1968; Chen, 1969; Taylor, 1970). These arise from temporary electronic excitation of the target followed by a resonant capture of the projectile electron to form an autoionizing state of the negative ion. The capture is probable only over a narrow energy range, so the resonance can be characterized by a mean energy E_r and width Γ, the latter related to the lifetime τ of the resonance by $\tau = \hbar/\Gamma$. A second type of resonance, the "potential resonance," does not involve this strong nonadiabatic response of the target electrons, but simply arises from the temporary capture (attachment) of the projectile electron in its own centrifugal barrier, present in the effective electron–molecule interaction potential energy. Regardless of the precise capture mechanism involved, the projectile electron is strongly influenced by the target at any energy near the resonance, and weak-scattering approximations fail. If the lifetime τ of the resonance is comparable to, or exceeds, the classical period for a particular nuclear degree of freedom, it is necessary in general to properly allow for response of that nuclear variable during the collision; i.e., the impulse approximation is inappropriate for that particular nuclear variable. For most potential resonances in small molecules such as N_2, CO, and CO_2, the impulse approximation is valid for rotation of the molecule but fails for vibration (Schulz, 1973, 1976). When attachment occurs in a dissociating negative-ion state, the molecule may dissociate into fragments, stabilizing the electron attachment in the process. This "dissociative attachment" process is strongly enhanced by resonant scattering (Schulz, 1973; Bardsley and Mandl, 1968; Chen, 1969; Taylor, 1970; O'Malley, 1971; Hall, 1977). Since there is always a chance that the electron will escape (autodetach) before it is stabilized, the magnitude and variation of the lifetime of the molecule state with respect to internuclear separation are crucial in determining which process dominates. Little progress has been made in the actual calculation of dissociative-attachment cross sections; however, semiempirical studies have been successful (see, for example, Wadehra and Bardsley, 1978; Allan and Wong, 1978). The analogous process in electron collisions with molecular ions is dissociative recombination (Bardsley and Biondi, 1970; see the recent work of Dubois, Jeffries, and Dunn, 1978, and references therein).

In attempting to properly allow for electronic response of the molecule to the approaching electron, one is faced with precisely the same complicating exchange and correlation factors as encountered in the molecular structure problem. The full wave function, including spin coordinates, must be antisymmetric with respect to interchange of any two electrons. The resulting exchange integrals complicate solution of the differential or integral scattering equations just as they do in electron–atom scattering (Mott and Massey, 1965; Massey and Burhop, 1969; Burke and Williams, 1977; Bransden and McDowell, 1977, 1978). However, here the problem is much worse. The strong nonspherical character of the target molecule complicates the partial-wave analysis and thereby renders it more cumbersome than in the electron–atom case. In the more conventional theoretical treatment of low-energy electron–molecule scattering, the partial-wave expansion is still employed. However, the partial-wave angular momenta are strongly coupled to one another (Fano, 1970b), and, as a result, the numerical computations are quite involved even for relatively simple model-potential representations of the full electron–molecule interaction. New approaches, sometimes called "L^2 methods," are based on a partitioning of configuration space in such a way that the region of space near the nuclei is treated by quasimolecular-structure methods and the region away from the nuclei by more conventional means. These methods include: R-matrix, T-matrix expansion, pseudobound state, stabilization, and complex coordinate rotations. So far, no single method has distinguished itself as the "best" approach. However, the field is active and much progress has already been made.

Examining the characteristic features of a number of specific scattering processes one is led to a few relatively safe generalizations. Near threshold, the rotational excitation cross section is dominated by long-range electron–molecule interactions, in particular the dipole interaction for polar molecules, quadrupole interaction for a large class of nonpolar molecules, etc. With the exception of strongly polar molecules (dipole moment $d \gtrsim 1.0$ a.u) the scattering near threshold is weak and the Born approximation, with its accompanying selection rules, is valid, even in the limit of a "zero-energy" outgoing electron at threshold. At high energies and/or large scattering angles, other interactions, including exchange, become important and the scattering is not weak in general. Near a resonance, the rotational-excitation cross section can be large for a number of rotational transitions, i.e., rotational selection rules are less restrictive. If it were not for the existence of long-range anisotropic interactions to provide a "long lever arm" on the molecule, or resonances to capture the electron in the short-range vicinity of the nuclei for an appreciable period of time, rotational excitation cross sections would be very small. The unfavorable electron/nucleus mass ratio prevents efficient transfer of energy from scattered electron to nuclear motion. The same general argument holds for vibrational excitation. However, in this case, it is not the anisotropy of the interaction, but rather its dependence on internuclear separations, that determines the size of the cross sections. Near the vibrational threshold, the Born approximation may be useful and several such calculations have been made. However, a spectacular failure is evident in the vibrational excitation of HCl, HF, HBr, H_2O, SF_6, and a number of other molecules, where sharp resonances appear just above threshold (Linder, 1977). These resonances may be due to a virtual-state enhancement of the final-state interaction. Whatever the cause, the scattering is strong and the Born approximation fails. Broad potential resonances are evident in many molecules at somewhat higher energies (e.g., ~2 eV for N_2 and CO, and ~4 eV for CO_2). The lifetimes associated with these resonances are comparable with vibrational periods so that considerable nuclear relaxation occurs during the collision. This nuclear response gives rise to a fine structure in elastic as well as rotational- and vibrational-excitation cross sections. In all such cases, the adiabatic-nuclei approximation applied to nuclear vibration fails. Resonant scattering can induce vibrational transitions between a number of levels so that no precise selection rules apply.

In attempting to formulate a practical theory for electron–molecule collisions, one is motivated to take every advantage of reliable approximations, and occasionally a few unreliable ones. An attempt has been made in Sec. II to describe the theory in a palatable manner. In the compromise, a certain amount of rigor and completeness has been sacrificed. It is intended that this material serve as a simple introduction to the methods used in the applications of Sec. III.

II. THEORY OF ELECTRON–MOLECULE COLLISIONS

The time-independent theory of electron scattering is based on a stationary-state description of continuum states of the electron plus target system (Mott and Massey, 1965). The objective is to calculate wave functions, more precisely eigenfunctions, of the electron–molecule Hamiltonian

$$H = -\tfrac{1}{2}\nabla_{\mathbf{r}}^2 + V_{em}(\mathbf{r}, x) + H_m(x)\,, \tag{1}$$

where the three terms represent the kinetic energy of the projectile electron, the electron–molecule interaction potential energy, and the Hamiltonian of the isolated target molecule, respectively. In a space-fixed (laboratory) frame of reference, usually with the origin chosen as the center of mass of the molecule, $\mathbf{r}$ stands for the spacial coordinates of the projectile, and x, collectively, for all coordinates (electron plus nuclear) of the target molecule. (Spin coordinates will be suppressed in general expressions. Atomic units will be used throughout, where $e = \hbar = m_e = 1$, and length, mass, charge, and energy are given in units of $a_0 \cong 0.529$ Å, $m_e \cong 9.110 \times 10^{-31}$ kg, $e \cong 1.602 \times 10^{-19}$ C, and 2 Ry $\cong$ 27.2 eV, respectively.) The continuum states relevant to the scattering problem are described by wave functions $\Psi(\mathbf{r}, x)$, finite for all values of the coordinates, that satisfy the particular asymptotic boundary conditions

$$\Psi(\mathbf{r}, x) \underset{r\to\infty}{\sim} \Psi^{\mathrm{INC}}(\mathbf{r}, x) + \Psi^{\mathrm{SCATT}}(\mathbf{r}, x)\,, \tag{2}$$

where the first term represents an incident plane wave on a particular initial molecular state

$$\Psi^{\mathrm{INC}}(\mathbf{r}, x) = \exp(i\mathbf{k}_0 \cdot \mathbf{r})\psi_0(x)\,, \tag{3}$$

and the second term consists of a superposition of outgoing waves associated with all possible (i.e., energetically accessible) molecular states n

$$\Psi^{\mathrm{SCATT}}(\mathbf{r}, x) = \frac{1}{r}\sum_n \exp(ik_n r) f_{n0}(\mathbf{k}_n, \mathbf{k}_0)\psi_n(x)\,, \tag{4}$$

where $\mathbf{k}_0$ and $\mathbf{k}_n$ are initial and energetically allowed final-state momenta of the scattered electron (defined asymptotically), whose magnitudes are related by energy conservation

$$k_n^2 = k_0^2 - 2(E_n - E_0)\,, \tag{5}$$

where E_0 and E_n are initial and final energies of the molecule. The label n represents all quantum numbers necessary to specify a state of the isolated molecule. The scattering amplitude $f_{n0}(\mathbf{k}_n, \mathbf{k}_0)$ describes a quantum scattering event $0 \to n$ in which an electron incident with momentum $\mathbf{k}_0$ upon a molecule in state $\psi_0(x)$ is scattered by the molecule and leaves with momentum $\mathbf{k}_n$, the molecule being left in state $\psi_n(x)$. The differential cross section for this event is expressed in terms of the scattering amplitude by the usual expression

$$\left(\frac{d\sigma}{d\Omega}\right)_{0\to n} = \frac{k_n}{k_0}|f_{n0}(\mathbf{k}_n, \mathbf{k}_0)|^2\,. \tag{6}$$

Because of experimental difficulties in resolving small energy losses or otherwise distinguishing between final molecular states, it is often more appropriate to calculate and compare partial summations or averages over certain initial and final states of the target, e.g., the "magnetic" states m_j of a rotating molecule, or closely spaced rotational states j of large molecules. When the final direction of the scattered electron's momentum $\hat{k}_n$ is of no interest, an integral cross section

$$\sigma_{0\to n} = \frac{k_n}{k_0}\int d\hat{k}_n |f_{n0}(\mathbf{k}_n, \mathbf{k}_0)|^2 \tag{7}$$

is calculated, where the integration is over all values of the angles θ_n and ϕ_n that define $\hat{k}_n$ (of course this integration is always carried out analytically). A special class of "swarm experiments" measure transport properties such as the drift velocity of electrons in gases (Huxley and Crompton, 1962, 1974). These measurements are most conveniently interpreted in terms of momentum-transfer cross sections, which emphasize large-angle scattering as evident in the definition

$$\sigma^m_{0\to n} = \frac{k_n}{k_0}\int d\hat{k}_n (1-\cos\theta_n)|f_{n0}(\mathbf{k}_n, \mathbf{k}_0)|^2 . \tag{8}$$

The angular weighting may be understood from simple classical considerations of the momentum transferred to the molecule during a single collision.

A. Coupled-states expansion

Alternative theories of electron–molecule scattering simply reflect different approaches to solution of the Schrödinger equation

$$(H-\varepsilon)\Psi_\varepsilon(\mathbf{r}, x) = 0 \tag{9}$$

for electron–molecule system eigenfunctions $\Psi_\varepsilon(\mathbf{r}, x)$ at total energies ε of interest. The most natural approach would seem to be a "coupled-states" (often called "close-coupling" or "eigenfunction") expansion in terms of the complete set of unperturbed states of the isolated molecule, viz.

$$\Psi_\varepsilon(\mathbf{r}, x) = \mathcal{A}\sum_n F_n(\mathbf{r})\psi_n(x) , \tag{10}$$

where, assuming proper spin couplings have been carried out, $\mathcal{A}$ is the usual antisymmetrization operator. In principle, the summation in Eq. (10) includes continuum as well as bound states of the target. The one-electron "scattering functions" $F_n(\mathbf{r})$ corresponding to bound target state n play something of the role of continuum molecular orbitals, except that they depend on the initial target state specified in the boundary conditions given by Eqs. (2)–(4); these functions satisfy the set of coupled equations

$$(\nabla^2_r + k^2_n)F_n(\mathbf{r}) = 2\sum_{n'} [V_{nn'}(\mathbf{r}) + W_{nn'}(\mathbf{r})]F_{n'}(\mathbf{r}) , \tag{11}$$

where the *direct* matrix elements are defined by

$$\begin{aligned} V_{nn'}(\mathbf{r}) &= \langle n|V_{em}|n'\rangle \\ &= \int dx\, \psi_n(x)^* V_{em}(\mathbf{r}, x)\psi_{n'}(x) , \end{aligned} \tag{12}$$

and the *exchange* matrix elements $W_{nn'}(\mathbf{r})$ are operators which interchange bound orbitals in $\psi_{n'}(x)$ with "continuum orbitals" $F_{n'}(\mathbf{r})$ to the right in Eq. (11). All exchange terms decay exponentially in the asymptotic region $r\to\infty$ in the same manner as the bound orbitals. Thus, exchange effects are characterized as short range; they will have died away long before the direct matrix elements are negligible. According to Eqs. (2)–(4), the asymptotic boundary conditions on the solutions of Eq. (11) regular at the origin are

$$F_{n0}(\mathbf{r}) \underset{r\to\infty}{\sim} \exp(i\mathbf{k}_0\cdot\mathbf{r})\delta_{n0} + \frac{1}{r}\exp(ik_n r)f_{n0}(\mathbf{k}_n, \mathbf{k}_0) , \tag{13}$$

where the second subscript on F_{n0} has been appended to designate the initial target state.

The solution of Eq. (11) for electron–atom scattering is already a formidable challenge (Mott and Massey, 1965; Massey and Burhop, 1969; Bransden and McDowell, 1977, 1978; Burke, 1977). A partial-wave expansion of the functions $F_n(\mathbf{r})$ in terms of the spherical harmonics $Y_{lm}(\theta, \phi)$ reduces Eq. (11) to a set of coupled second-order differential equations which must then be truncated before numerical solution is possible. In low-energy scattering the major role of the infinity of high-lying electronic states in the expansion (10) is to participate in the electrical polarization of the atom during the collision (Castillejo *et al.*, 1960; Drachman and Temkin, 1972). One scheme for the truncation of Eqs. (10) and (11) is to replace an infinity of excited states by a few "pseudostates" carefully chosen so that the full adiabatic polarization of the atomic target is accounted for (see discussion in Bransden and McDowell, 1977). The resulting finite set of coupled equations can then be solved numerically. While this procedure is possible for electron–molecule scattering, several additional complications arise. First, the number and the nature of the target states in Eqs. (10) and (11) are very different for molecular targets. In N_2, for example, there are far more molecular states within 1 eV of the ground state than can reasonably be included in even the most ambitious coupled-state expansions. A second complicating factor in Eq. (11) is the strong nonspherical nature of the matrix elements $V_{nn'}(\mathbf{r})$ and $W_{nn'}(\mathbf{r})$. This feature causes a partial-wave expansion of the scattering function $F_n(\mathbf{r})$ to be very slowly convergent as compared to the atomic case. Finally, the molecular target may possess large permanent electric moments which result in large long-range contributions occurring in both the diagonal and off-diagonal ("coupling") matrix elements $V_{nn'}$. In such circumstances important contributions to the scattering cross sections can arise from very large electron–molecule separations. [This effect is particularly striking for polar molecules, where the rotational-excitation cross sections are strongly enhanced and tend to dominate all forward (small-angle) scattering as well as the total integral cross section at low energies. (See Sec. III.E.)]

As in other applications of theory, we seek approximations that include all important effects and permit calculations to be performed. A particularly important example is the approximation of separation of variables, here applied to electronic and nuclear coordinates. When the scattered electron is near the molecule, exchange effects are expected to be important and the electron–molecule interaction and the related matrix elements are strongly anisotropic. However, in this region of space the electron's "motion" is determined more by the instantaneous *positions* of the nuclei and the associated bound-electron charge distribution than by the *velocities* of the nuclei and the vibrational or rotational states that determine the latter. Thus, for small r the fixed-nuclei approximation is appropriate, and one need not take explicit account of the large number of rotational and vibrational states that would be required in Eqs. (10) and (11). When the electron is far from the molecule, we naturally expect its behavior to be influenced by vibration and rotation of the nuclei, but in this region of space exchange effects are negligible and the interactions are much less anisotropic than near the nuclei. So, by conceptually dividing space into two regions, we can expect a significant reduction in complexity. This is the philosophy of Chang and Fano (1972) in their exposition of the frame transformation. The power of such an approach rests on the separation of electronic and nuclear variables and the applicability of the Born–Oppenheimer (adiabatic) separation to the electron–molecule system; this is the subject of the next section.

B. Born–Oppenheimer approximation

In this and future sections it will be necessary to distinguish between electronic and nuclear coordinates within the molecule. We will continue to represent the coordinates of the scattered electron by $\mathbf{r}$, or $\mathbf{r}'$, and the electronic and nuclear coordinates of the molecule, collectively, by $\mathbf{r}_m$ and $\mathbf{R}_m$ (in the case of a diatomic molecule, $\mathbf{R}_m$ becomes the relative-position vector of the two nuclei $\mathbf{R}$). From here on, we will follow the convention that primed coordinates $\mathbf{r}'$ refer to the LAB frame and unprimed $\mathbf{r}$ to the BODY frame. Both frames are coordinate systems having a common origin at the center of mass of the system. The LAB frame has a space-fixed z axis (often chosen along the initial momentum $\mathbf{k}_0$), whereas that of the BODY frame is directed along a symmetry axis of the molecule, e.g., for a diatomic molecule, $\hat{z} = \hat{R}$. We seek wave functions $\Psi_\epsilon(\mathbf{r}', \mathbf{r}'_m, \mathbf{R}_m)$ satisfying Eq. (9) and the asymptotic conditions given in Eq. (2), where the molecular Hamiltonian in Eq. (1) can be written

$$H_m(\mathbf{r}'_m, \mathbf{R}_m) = H_m^{(e)}(\mathbf{r}'_m, \mathbf{R}_m) + H_m^{(n)}(\mathbf{R}_m), \tag{14}$$

with the electronic contribution given by

$$H_m^{(e)}(\mathbf{r}'_m, \mathbf{R}_m) = -\frac{1}{2}\sum_{j>1}^{N_e} \nabla_j^2 - \sum_{\alpha=1}^{N_n}\sum_{j=1}^{N_e} \frac{Z_\alpha}{|\mathbf{r}'_j - \mathbf{R}_\alpha|} + \sum_{i=1}^{N_e}\sum_{j>i}^{N_e} \frac{1}{|\mathbf{r}'_i - \mathbf{r}'_j|} \tag{15}$$

and the nuclear contribution by

$$H_n^{(e)}(\mathbf{R}_m) = -\frac{1}{2}\sum_{\alpha=1}^{N_n} \frac{1}{M_\alpha}\nabla_\alpha^2 + \sum_{\alpha=1}^{N_n}\sum_{\beta>\alpha}^{N_n} \frac{1}{|\mathbf{R}_\alpha - \mathbf{R}_\beta|} \tag{16}$$

for a molecule containing N_e electrons and N_n nuclei with charges and masses Z_α and M_α, respectively (see Fig. 1). The interaction potential energy is

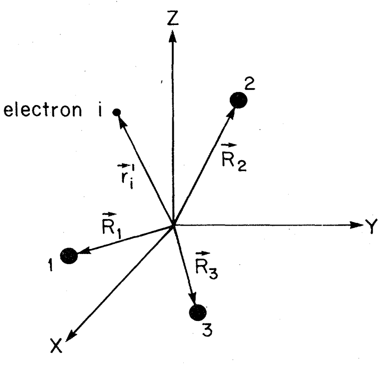

FIG. 1. Nuclear and electronic coordinates in the LAB frame.

$$V_{em}(\mathbf{r}'; \mathbf{r}'_m, \mathbf{R}_m) = -\sum_{\alpha=1}^{N_n} \frac{Z_\alpha}{|\mathbf{r}' - \mathbf{R}_\alpha|} + \sum_{j=1}^{N_e} \frac{1}{|\mathbf{r}' - \mathbf{r}'_j|}. \tag{17}$$

In the theory of molecular structure, the powerful Born–Oppenheimer approximation permits a separation of nuclear and electronic variables so that one can first solve the electronic problem with the nuclei fixed, obtaining electronic wave functions and energies that depend parametrically on the nuclear coordinates [see, for example, Flygare (1978), Chap. 6]. The nuclei are then assumed to move in response to the adiabatic potential energy corresponding to the stationary electronic state. The wave function is written as a simple product of electronic and nuclear functions. Perturbation theory may then be used to correct for the "breakdown" of the Born–Oppenheimer approximation (Herzberg, 1950; Flygare, 1978). These corrections are found to be especially important for highly excited vibrational states (large nuclear speeds), high-Rydberg electronic states (small electron speeds), or "curve crossings" where two or more electronic energy curves (or surfaces) cross or come very close to one another.

In the electron–molecule scattering problem, we are dealing with continuum (scattering) states for which the total energy is positive with respect to the ground state of the target molecule. We seek a product form for the wave function (Herzenberg and Mandl, 1962; Shugard and Hazi, 1975; Schneider, 1976)

$$\Psi_\epsilon(\mathbf{r}, \mathbf{r}_m, \mathbf{R}_m) = \Psi_\epsilon^{FN}(\mathbf{r}, \mathbf{r}_m; \mathbf{R}_m)\chi(\mathbf{R}_m), \tag{18}$$

where the fixed-nuclei (FN) electronic function $\Psi_\epsilon^{\mathrm{FN}}$ depends only parametrically on the $\mathbf{R}_m$. The most convenient electronic coordinates here are those referred to the BODY frame. The approximate form given in Eq. (18) is clearly valid in two limiting cases. When the electronic wave function $\Psi_\epsilon^{\mathrm{FN}}$ is highly localized in the vicinity of the molecule, as in the case of a narrow (long-lived) resonance, the nuclei respond adiabatically to the potential energy of the "negative-molecule-ion complex," and well-defined rotational–vibrational states, described by "resonant" wave functions χ, are established. Herzenberg and Mandl (1962) refer to this as the "compound molecule limit." At the other extreme is the "impulsive limit" appropriate for nonresonant scattering at energies sufficiently high that the velocities of the incident and outgoing electrons are considerably larger than those of the nuclei (Chang and Temkin, 1969, 1970; Hara, 1969b; Temkin and Faisal, 1971). (The impulse limit may be appropriate for nuclear rotation when it is not for vibration.) In this limiting case, the nuclear wave function χ is simply the unperturbed nuclear wave function for the molecule. When neither the adiabatic nor the impulse limits apply, it is necessary to treat the nuclei and electrons on a more equal footing. This can be accomplished by a full coupled-state (LAB-frame) approach, in which the system wave function is expanded in terms of unperturbed target wave functions as in Eq. (10), or more efficiently by some type of frame-transformation procedure wherein one takes full advantage of (Born–Oppenheimer) separation of electronic and nuclear variables when the electron is near the molecule, but relaxes this assumption at larger electron–molecule separations. When the scattering is dominated by a resonance, a "decaying electronic state" formalism is appropriate. The electronic state is represented as a bound state immersed (and decaying into) an adjacent continuum. In the Born–Oppenheimer separation of Eq. (18), $\Psi_\varepsilon^{\mathrm{FN}}$ represents the decaying (nonstationary) state, and the nuclear wave function χ is determined by a complex nuclear potential energy (Herzenberg and Mandl, 1962; see review by Bardsley and Mandl, 1968). The next section will describe the fixed-nuclei formulation of the electron–molecule scattering problem.

C. Fixed-nuclei formulation

If the nuclei are held fixed, we need only consider the electronic Hamiltonian for the electron–molecule system, viz.,

$$H^{(e)} = -\tfrac{1}{2}\nabla_{\mathbf{r}}^2 + H_m^{(e)} + V_{em}\,, \tag{19}$$

where $\nabla_{\mathbf{r}}^2$ is the Laplacian in terms of BODY-frame coordinates $\mathbf{r}$, and where the target contribution and the electron–molecule interaction potential energy are given by Eqs. (15) and (17), respectively. We will restrict the development to diatomic target molecules in order to simplify the formalism. It is convenient to refer all electronic coordinates to the BODY frame, where the polar axis is taken along the internuclear line, i.e., $\hat{z} = \hat{R}$, as shown in Fig. 2. The electronic states of the target molecule are represented by the functions $\psi_\alpha^{(e)}(\mathbf{r}_m; R)$ [we recall that $\mathbf{r}_m = (\mathbf{r}_1, \mathbf{r}_2, \ldots, \mathbf{r}_{N_e})$ represents all target-electron coordinates, collectively (spin is implicit)], where α stands for all electronic quantum numbers. These N_e-electron wave functions satisfy the target electronic Schrödinger equation

$$[H_m^{(e)} - E_\alpha^{(e)}(R)]\psi_\alpha^{(e)}(\mathbf{r}_m, R) = 0\,, \tag{20}$$

where the eigenvalues $E_\alpha^{(e)}(R)$ are the electronic "curves" for the molecular states.

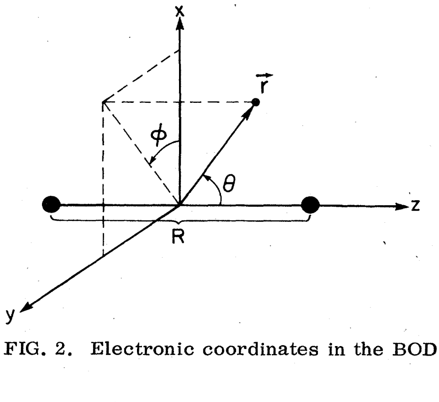

FIG. 2. Electronic coordinates in the BODY frame.

In the electron–molecule scattering problem one seeks solutions of the $N_e + 1$ electron Schrödinger equation

$$(H^{(e)} - \varepsilon)\Psi_\varepsilon^{\mathrm{FN}}(\mathbf{r}, \mathbf{r}_m; R) = 0\,, \tag{21}$$

where $(\mathbf{r}, \mathbf{r}_m) = (\mathbf{r}, \mathbf{r}_1, \ldots, \mathbf{r}_{N_e})$ denotes all $N_e + 1$ electron coordinates, collectively. In Eq. (21) the entire nuclear Hamiltonian is omitted, and this approximation eventually must be justified. For now, we will simply make the following observation. When the electrons are all close to the nuclei, their motion is dominated by the potential energy V_{em}, and any corrections arising from nuclear momentum terms are expected to be small, on classical intuitive grounds. In the asymptotic region, say as $r \to \infty$, it is much less clear how such effects can be ignored; in fact, in certain cases to be discussed, they cannot.

In the frame-transformation procedure (Fano, 1970a; Chang and Fano, 1972), one makes the fixed-nuclei approximation only in the proximity of the nuclei and performs this portion of the calculation with electronic coordinates referred to the BODY frame of the molecule. At some carefully chosen boundary, one transforms the solutions to the LAB frame, and introducing the nuclear Hamiltonian, continues solution of the resulting equations into the asymptotic region. The hope is that a transformation radius can be found such that $H^{(n)}$ can be safely ignored in the inner region and complicated exchange interactions (always short range) can be ignored in the outer region. {In general, we require that the commutator $[H^{(e)}, H^{(n)}]$, and therefore $[V_{em}, H^{(n)}]$, be small in comparison with $H^{(e)} - \varepsilon$ for all values of the coordinates (see Chang and Fano, 1972).} The details of the frame-transformation procedure will be saved for the next section, in which the LAB-frame development will be given.

There are circumstances in which the inner region can be extended to infinity, i.e., the entire problem can be solved to a very good approximation in the BODY frame, ignoring $H^{(n)}$ entirely. The frame transformation then reduces to a single step at the end of the calculation. This procedure is formally equivalent to the adiabatic approximation applied to the nuclear motion (Chang and Temkin, 1969; Hara, 1969a,b; Herzenberg and Mandl, 1962; Temkin, 1976). It is generally valid under the following circumstances: (1) the incident electron energy is well above threshold; (2) the scattering is *not* dominated by strong long-range interactions; (3) the scattering is nonresonant. These conditions are imprecise and somewhat ambiguous. The examples to be discussed later will provide some clarification. In the remainder of this section, we shall concentrate on solution of the fixed-nuclear Schrödinger Eq. (21). These solutions will be used to extract cross sections in the adiabatic nuclei approximation, and in the next section will provide the "inner solutions" for use in the more precise frame-transformation procedure.

A "close-coupling" solution of this problem involves an expansion in terms of electronic target wave functions of Eq. (20), viz.,

$$\Psi_\epsilon^{\mathrm{FN}}(\mathbf{r},\sigma,\mathbf{r}_m,\sigma_m;R)=\mathcal{A}\sum_{\alpha,m_s}C_{\alpha,m_s}F_{\alpha,m_s}(\mathbf{r};R)\times\chi_{m_s}(\sigma)\psi_\alpha^{(e)}(\mathbf{r}_m,\sigma_m;R)\,, \tag{22}$$

where the spin coordinates σ and σ_m (of the scattered and bound electrons) are shown explicitly. The coefficients C_{α,m_s} depend on the choice of spin coupling, and $\chi_{m_s}(\sigma)$ is a spin-$\frac{1}{2}$ eigenfunction. The angular dependence of F_{α,m_s} is treated by the usual partial-wave expansion

$$F_{\alpha,m_s}(\mathbf{r};R)=r^{-1}\sum_{l,m}u_{lm,m_s}(r;R)Y_{lm}(\hat{r})\,. \tag{23}$$

For problems in which the Hamiltonian does not contain magnetic (spin–spin or spin–orbit) terms it is convenient to couple the electron spins at the outset. In order to simplify notation throughout, we define a "channel index" p which labels all possible combinations of quantum numbers. Thus, the close-coupling expansion (22) becomes

$$\Psi_\epsilon^{\mathrm{FN}}(\mathbf{r},\sigma,\mathbf{r}_m,\sigma_m;R)=\mathcal{A}\sum_p r^{-1}u_p^{\mathrm{FN}}(r)\Phi_p^{\mathrm{FN}}(\hat{r},\,\sigma,\mathbf{r}_m,\sigma_m;R)\,, \tag{24}$$

where the "channel wave functions" are

$$\Phi_p^{\mathrm{FN}}(\hat{r},\sigma,\mathbf{r}_m,\sigma_m;R)=Y_{lm}(\hat{r})\sum_{m_s(M_s)_\alpha}C(\tfrac{1}{2}S_\alpha S;m_s(M_s)_\alpha)\times\chi_{m_s}(\sigma)\psi_\alpha^{(e)}(\mathbf{r}_m,\sigma_m;R)\,, \tag{25}$$

where $p=(\alpha,l,m,S,M_s)$. The radial functions $u_p(r)$ satisfy the coupled integro-differential equations

$$\left[\frac{d^2}{dr^2}+k_p^2-\frac{l(l+1)}{r^2}\right]u_p^{\mathrm{FN}}(r)=2\sum_{p'}\left[V_{pp'}^{\mathrm{FN}}(r)+W_{pp'}^{\mathrm{FN}}(r)\right]u_{p'}^{\mathrm{FN}}(r)\,, \tag{26}$$

where the total energy

$$\varepsilon=k_p^2/2+E_\alpha^{(e)}(R)=k_{p'}^2/2+E_{\alpha'}^{(e)}(R) \tag{27}$$

is given in terms of the electronic energies of the target at the fixed internuclear separation R. The "direct" matrix elements are given by

$$V_{pp'}^{\mathrm{FN}}(r)=\langle\Phi_p(\hat{r},\sigma,\mathbf{r}_m,\sigma_m;R)|V_{em}(\mathbf{r},\mathbf{r}_m;R)|\times\Phi_{p'}(\hat{r},\sigma,\mathbf{r}_m,\sigma_m;R)\rangle\,, \tag{28}$$

where integration (summation) runs over all electronic spatial (spin) coordinates except r. These matrix elements vanish unless *all* spin quantum numbers are the same in channels p and p' (i.e., no "direct" singlet-triplet coupling, etc.). The range of these matrix elements determines the way in which they influence the scattering wave function. In general, the matrix elements that are diagonal in α, i.e., $\alpha_p=\alpha_{p'}$, possess asymptotic $r^{-2},r^{-3},\ldots$ behavior, with coefficients proportional to the electric dipole, quadrupole, etc., moments for the particular electronic state involved. These long-range interactions are characteristic of electron–molecule scattering (even elastic scattering from closed-shell ground-state molecules), in contrast to the atomic case. An effective r^{-4} "induced polarization interaction" arises from virtual excitation of optically allowed electronic transitions of the molecule [i.e., from coupling in Eq. (26) with energetically inaccessible states through $V_{pp'}^{\mathrm{FN}}$] just as in electron–atom scattering (Castillejo *et al.*, 1960; Drachman and Temkin, 1972).

The "exchange" matrix element $W_{pp'}$ is an operator that interchanges coordinates of the radial part of the "scattering orbital" $u_{p'}(r)$ with those of the occupied bound orbitals; this operation may be written schematically as

$$W_{pp'}^{\mathrm{FN}}(r)\,u_{p'}(r)=\sum_\beta\left[\int_0^\infty K_{pp'\beta}(r,r')u_{p'}^{\mathrm{FN}}(r')\,dr'\right]P_\beta(r)\,, \tag{29}$$

where $P_\beta(r)$ is the radial part of a bound molecular orbital [more precisely, in the case of electron–*molecule* scattering, $P_\beta(r)$ is a single coefficient in a single-center expansion of a bound molecular orbital] and $K_{pp'\beta}(r,r')$ is an "exchange kernel." From Eq. (29) it is apparent that the exchange terms are constrained to fall off exponentially as $r\to\infty$. This is why exchange is generally regarded as a short-range effect.

The coupled equations (26) for N channels [i.e., $p=1,\ldots,N$ in Eq. (24)] possess N linearly independent regular vector solutions $u_{pp'}(r)$, where the first index labels the component of the vector and the second index labels a particular linearly independent solution. Thus, the radial solutions, i.e., radial parts of the "scattering orbitals," form a square $N\times N$ matrix $\mathbf{u}(r)$ and the coupled equations may be written simply as

$$\left[\mathbf{1}\frac{d^2}{dr^2}+\mathbf{k}^2-\frac{1}{r^2}\mathbf{L}^2\right]\mathbf{u}(r)=2[\mathbf{V}(r)+\mathbf{W}(r)]\mathbf{u}(r)\,, \tag{30}$$

where diagonal matrices $\mathbf{k}^2$ and $\mathbf{L}^2$ are defined with elements k_p^2 and $l(l+1)$, respectively.

In principle, Eqs. (30) can be solved numerically by any one of several efficient methods. In practice, accurate solution of (30) is very difficult for several reasons: (i) The expansion in Eq. (24) must be truncated at some finite number of terms and convergence with respect to the number of electronic states is often slow as in the case of electron–atom scattering; (ii) even for a finite number of electronic states, convergence in l is often slow due to the nonspherical nature of the electron–molecule interactions (Burke and Chandra, 1972; Morrison, Lane, and Collins, 1977; Morrison and Collins, 1978); (iii) the exchange terms require iteration of the solutions, or alternatively, generate many more coupled equations via a noniterative procedure (Marriott, 1958; Omidvar, 1961, 1974; see Smith, Henry, and Burke, 1966). Simply stated, the fixed-nuclei electron-scattering problem possesses all the complexity of the corresponding electron–atom problem plus the added feature that even the static field of the molecule is not spherically symmetric. Of course, when nuclear motion is properly included, additional complications arise. In the region of configuration space near the nuclei, i.e., the region where the fixed-nuclei approximation is valid, the scattering problem is most difficult. Some procedure other than solution of the coupled equations (30) is called for. Formally, the R-matrix method (see reviews by Burke and Robb, 1975; Schneider, 1977a; Fano, 1977) and related "eigenchannel" (Fano and Lee, 1973; Lee, 1974, and references therein) and "T-matrix expansion" (Rescigno, McCurdy, and McKoy, 1974a, b; 1975a) methods are designed for this task. Several applications have been successful, and the methods appear to hold promise for future studies. Applications will be discussed in Sec. III.

One approach that significantly reduces difficulties related to the multicenter character of the electron-molecule scattering problem is the "multiple-scattering method" (MSM), which is discussed in more detail in the applications in Sec. III.C.1. (See Johnson, 1973; Dill and Dehmer, 1974, 1977; Siegel and Dill, 1976; Siegel, Dill, and Dehmer, 1978. Also, see the recent article by Dehmer and Dill in Rescigno, McKoy, and Schneider, 1979.) Applications to electron–molecule scattering have been limited to fixed-nuclei calculations where the electron–molecule interaction is approximated by a local potential energy function of the "muffin-tin" form. Indeed, the convenience and efficiency of the method derives from the "muffin-tin" approximation, where a region of constant potential energy separates other regions in each of which the potential energy is spherically symmetric with respect to the respective nuclear center. The MSM is particularly useful in treating large molecules, clusters or surfaces, where there are many scattering centers.

Regardless of how the fixed-nuclei problem is solved, it is still not complete. The motion of the nuclei must be incorporated. This is properly done by means of a frame transformation from the BODY frame (with fixed nuclei) to LAB frame (with moving nuclei), to be described in Sec. II.E. However, there are many circumstances under which the adiabatic-nuclei approximation is valid, and rotational- and vibrational-excitation cross sections may be obtained directly from the fixed-nuclei scattering amplitude by simple numerical quadrature (Abram and Herzenberg, 1969; Chang and Temkin, 1969, 1970; Faisal and Temkin, 1972; Hara, 1969b; see discussions in Golden *et al.*, 1971; Takayanagi, 1973, 1975a, b; and Temkin, 1976). The general problem of an electron collision with a polyatomic molecule has been formulated by Burke, Chandra, and Gianturco (1972) and by Onda (1974).

D. Adiabatic nuclei approximation (nuclear impulse approximation)

From a classical point of view a "fast collision," in which the collision time t_c is much less than the periods for nuclear rotation, τ_R ($\gtrsim 10^{-12}$ sec), or vibration, τ_v ($\sim 10^{-14}$ sec), should be well represented by a fixed-nuclei approximation. The "fast-collision" case is alternatively described as the "impulse" and "adiabatic nuclei" limit by different authors. Indeed it is appropriate to say that the nuclei experience an *impulse* due to the collision (Herzenberg and Mandl, 1962; Bardsley and Mandl, 1968). On the other hand, the electron *adiabatically* responds to the instantaneous position of the nuclei, and therefore is *not* sensitive to the instantaneous momenta of the nuclei (Oksyuk, 1966; Chang and Temkin, 1969, 1970; Temkin, 1976). We will consider the terms "adiabatic nuclei" and "nuclear impulse" to be synonymous. The Born–Oppenheimer approximation is valid and the total (electronic and nuclear) wave function may be approximated by Eq. (18), rewritten for the diatomic case (suppressing spin coordinates) as

$$\Psi_{\epsilon\alpha_0\nu_0}(\mathbf{r}, \mathbf{r}_m, \mathrm{R}) \cong \Psi^{\mathrm{FN}}_{\epsilon\alpha_0}(\mathbf{r}, \mathbf{r}_m; \mathrm{R})\chi_{\alpha_0\nu_0}(\mathrm{R}), \tag{31}$$

where $\chi_{\alpha_0\nu_0}(\mathrm{R})$ is the *unperturbed* initial nuclear-state wave function of the target, and ν_0 represents vibrational and rotational quantum numbers for this state. Taking the overlap of the asymptotic form of Eq. (31) with an arbitrary final nuclear-state wave function $\chi_{\alpha\nu}(\mathrm{R})$, we obtain the adiabatic nuclei (AN) approximate scattering amplitude for a transition $\alpha_0\nu_0 \rightarrow \alpha\nu$

$$f^{\mathrm{AN}}_{\alpha\nu,\alpha_0\nu_0}(\mathbf{k}'_\alpha, \mathbf{k}'_0) = \langle \chi_{\alpha\nu}(\mathrm{R}) | f^{\mathrm{FN}}_{\alpha,\alpha_0}(\mathbf{k}'_\alpha, \mathbf{k}'_0; \mathrm{R}) | \chi_{\alpha_0\nu_0}(\mathrm{R})\rangle, \tag{32}$$

where $f^{\mathrm{FN}}_{\alpha,\alpha_0}$ is the fixed-nuclei (FN) scattering amplitude corresponding to an electronic transition $\alpha_0 \rightarrow \alpha$. The primes on $\mathbf{k}'_\alpha$ and $\mathbf{k}'_0$ denote LAB-frame momenta. The integration over molecular orientation $\hat{R}$ is straightforward and requires that f_{α,α_0} be calculated only once for a particular value of R, most conveniently on the BODY frame. A simple application of the rotation operator effects the transformation to the LAB frame. The integration over R requires that $f^{\mathrm{FN}}_{\alpha,\alpha_0}$ be computed for several values of R and that a numerical quadrature be performed.

At low collision energies where $t_c \cong \tau_v$ but $t_c \ll \tau_R$, the adiabatic nuclei rotation (ANR) approximation may still be valid even though vibrational motion must be treated more accurately. Instead of Eq. (32) we have for the ANR approximate scattering amplitude, the expression

$$f^{\mathrm{ANR}}_{\alpha\nu,\alpha_0\nu_0}(\mathbf{k}'_\alpha, \mathbf{k}'_0) = \langle R_{\alpha\nu}(\hat{R}) | f^{\mathrm{FNR}}_{\alpha v,\alpha_0 v_0}(\mathbf{k}'_{\alpha v}, \mathbf{k}'_{\alpha_0 v_0}; \hat{R}) | R_{\alpha_0\nu_0}(\hat{R})\rangle, \tag{33}$$

where $R_{\alpha\nu}$ is the rotational wave function corresponding to nuclear state ν, and $f^{\mathrm{FNR}}_{\alpha v,\alpha_0 v_0}$ is the fixed-nuclear rotation (FNR) scattering amplitude corresponding to an electronic-vibrational transition $\alpha_0 v_0 \rightarrow \alpha, v$, where v_0 and v are vibrational quantum numbers. The FNR amplitude in Eq. (33) can be obtained by coordinate rotation of the BODY-frame amplitude, the latter obtained by a close-coupling, R-matrix, or equivalent calculation that takes explicit account of nuclear vibration. In the remainder of this section, we will describe how the fixed-nuclei scattering amplitude $f^{\mathrm{FN}}_{\alpha,\alpha_0}$ is obtained. Formal generalization to the FNR case is direct.

The validity of the adiabatic nuclei approximation is based on the assumption that the fixed-nuclei approximation is valid even in the asymptotic region $r \rightarrow \infty$. The fixed-nuclei scattering matrices are obtained by selecting solutions of Eq. (30) that satisfy the asymptotic boundary conditions

$$\mathbf{u}(r) \underset{r\rightarrow\infty}{\simeq} \left\{ \begin{matrix} \mathbf{s}(r) + \mathbf{c}(r)(\mathbf{k}^{-1/2}\mathbf{K}\mathbf{k}^{1/2}) & \text{open channels} \\ \mathbf{b}\exp(-|\mathbf{k}|r) & \text{closed channels} \end{matrix} \right\}, \tag{34}$$

where, in terms of the Riccati Bessel and Neumann functions $\hat{j}_l(z)$ and $\hat{n}_l(z)$, respectively, we define

$$\left.\begin{aligned}[\mathbf{s}(r)]_{pp'} &= \hat{j}_l(k_p r)\delta_{pp'} \underset{r\to\infty}{\simeq} \sin(k_p r - l\pi/2)\delta_{pp'} \\ [\mathbf{c}(r)]_{pp'} &= -\hat{n}_l(k_p r)\delta_{pp'} \underset{r\to\infty}{\simeq} \cos(k_p r - l\pi/2)\delta_{pp'}\end{aligned}\right\} \tag{35}$$

and

$$(\mathbf{k}^{1/2})_{pp'} = k_p^{1/2}\delta_{pp'} . \tag{36}$$

The "standing wave" asymptotic conditions given by Eqs. (34) and (35), in terms of the reactance matrix K, are most convenient for actual computation. Alternatively, "traveling-wave" conditions in terms of the scattering matrix S may be chosen. The K, S, and T matrices are related by (Taylor, 1972; Mott and Massey, 1965)

$$\mathbf{S} = \mathbf{1} - \mathbf{T} = (1 + i\mathbf{K})(1 - i\mathbf{K})^{-1} \tag{37}$$

where S is unitary and symmetric and K is real and symmetric.

The T matrix and corresponding scattering amplitude are first determined in the BODY frame and then transformed to the LAB frame by a simple rotation of coordinates. Finally, the integrations in Eq. (32) are performed analytically over $\hat{R}$ and numerically over R. The details of this development are summarized briefly below.

Considering the asymptotic form of Eq. (24) along with the Eqs. (34)–(37), we can derive a relatively simple form for the BODY-frame (B) scattering amplitude for a transition $\alpha_0 \to \alpha$

$$f^B_{\alpha,\alpha_0}(\mathbf{k}_\alpha, \mathbf{k}_0; R) = 2\pi(k_0 k_\alpha)^{-1/2} \sum_{\substack{lm \\ l_0 m_0}} i^{l_0 - l + 1} Y^*_{l_0 m_0}(\hat{k}_0) Y_{lm}(\hat{k}_\alpha) \times T^B(\alpha l m, \alpha_0 l_0 m_0; S, R) , \tag{38}$$

where $\hat{k}_0$ and $\hat{k}_\alpha$ refer to BODY-frame coordinates and S is the total spin of the system. (The superscripts B and L will be used in this section to label BODY- and LAB-frame quantities.) A rotation of coordinates B to L is performed so as to bring $\hat{k}_0$ into coincidence with the LAB-frame z axis (see Fig. 3). The LAB-frame scattering amplitude in the fixed-nuclei approximation is

$$f^{\mathrm{FN}}_{\alpha,\alpha_0}(\mathbf{k}'_\alpha; \mathbf{R}) = (k_0 k_\alpha)^{-1/2} \sum_{l m' l_0} [\pi(2l_0 + 1)]^{1/2} i^{l_0 - l + 1} \times T^L(\alpha l m', \alpha_0 l_0 0; S, \mathbf{R}) Y_{lm'}(\hat{k}'_\alpha) , \tag{39}$$

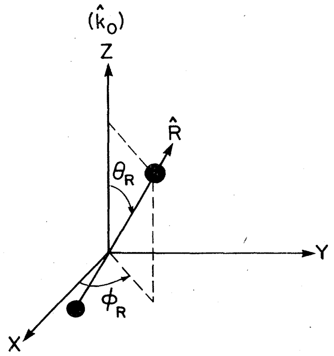

FIG. 3. Orientation of the molecule (BODY-frame) in LAB-frame coordinates.

where the LAB-frame T matrix in the fixed nuclei approximation is

$$T^L(\alpha l m', \alpha_0 l_0 0; S, \mathbf{R}) = \sum_{m, m_0} D^l_{m'm}(\hat{R}) \times T^B(\alpha l m, \alpha_0 l_0 m_0; S, R) D^{l_0}_{m_0 0}(\hat{R})^* , \tag{40}$$

and where $\mathbf{k}'_\alpha$ refers to the LAB frame, and the D-matrix elements are those of Rose (1957), in the somewhat abbreviated notation

$$D^l_{m'm}(\hat{R}) \equiv D^l_{m'm}(\phi_R, \theta_R, 0) . \tag{41}$$

[The appearance of 0 as the last index of the string $\alpha_0 l_0 0$ on T^L in Eq. (40) is a reminder that in the LAB frame we have chosen $\hat{k}_0$ as the z axis; therefore, the incident plane wave is expanded simply in terms of $Y_{l_0 0}(\hat{r}')$.] In Eq. (40), T^L now carries dependence on the orientation of the internuclear axis $\hat{R}$, arising from the rotation of coordinates BODY to LAB, as well as on the internuclear separation R, which is treated as a parameter throughout the development. The integration in Eq. (32) may now be carried out to obtain the adiabatic nuclei (AN) result for the transition $\alpha_0\nu_0 \to \alpha\nu$.

For purposes of illustration, we have chosen to represent the target diatomic molecule by a Hund's case (b) coupling scheme (Herzberg, 1950), where the nuclear wave function of the target can be written as a product

$$\chi_{\alpha\nu}(\mathbf{R}) = \phi^{(v)}_{\alpha v}(R) R_{j m_j \Lambda_\alpha}(\hat{R}) , \tag{42}$$

of the vibrational wave function $\phi^{(v)}_{\alpha v}$ and the rotational ("symmetrical top") functions

$$R_{j m_j \Lambda_\alpha}(\hat{R}) = \left(\frac{2j+1}{4\pi^2}\right)^{1/2} D^j_{m_j \Lambda_\alpha}(\hat{R})^* , \tag{43}$$

where Λ_α is the projection of electronic (target molecule) angular momentum on the internuclear axis for state α and can assume both positive and negative values. {We note here that the quantum numbers j, m_j are usually reserved for total angular momenta including spin. Here we use them to represent rotational angular momentum (usually labeled by K, M_K), and leave the molecular spin free to couple with the spin of the scattered electrons (cf. Eq. (25))}.

The adiabatic nuclei (AN) scattering amplitude for transition $\alpha_0\nu_0 \to \alpha\nu$ can now be evaluated by inserting the nuclear wave functions of Eqs. (42) and (43) into Eq. (32) and carrying out the integrations. The angular integration involves familiar properties of the D matrices (Rose, 1957). The result is

$$f^{\mathrm{AN}}_{\alpha\nu,\alpha_0\nu_0}(\mathbf{k}'_\alpha) = (k_0 k_\alpha)^{-1/2} \sum_{l l_0 m'} [\pi(2l_0 + 1)]^{1/2} i^{l_0 - l + 1} \times T^{\mathrm{AN}}(\alpha\nu l m', \alpha_0\nu_0 l_0 0; S) Y_{lm'}(\hat{k}'_\alpha) , \tag{44}$$

where the adiabatic nuclei T matrix is defined by (writing vjm_j for ν)

$$T^{\mathrm{AN}}(\alpha v j m_j l m', \alpha_0 v_0 j_0 m_{j_0} l_0 0; S) = [(2j+1)(2j_0+1)]^{1/2} \sum_J (2J+1)^{-1} \sum_{m,m_0} C(jlJ; m_j m') \times C(jlJ; \Lambda_\alpha \Lambda_{\alpha_0} - \Lambda_\alpha + m_0) C(j_0 l_0 J; m_{j_0} 0) C(j_0 l_0 J; \Lambda_{\alpha_0} m_0) \times \langle v | T^B(\alpha l m, \alpha_0 l_0 m_0; S, R) | v_0 \rangle \delta_{m+\Lambda_\alpha, m_0+\Lambda_{\alpha_0}} \delta_{m_j+m', m_{j_0}}, \tag{45}$$

and where $\mathbf{T}^B$ is the BODY-frame T matrix that results from the fixed nuclei calculation. The integration over R must be carried out numerically. Two "selection rules" arise in performing the angular integration over $\hat{R}$ leading to Eqs. (44) and (45):

$$\Lambda = m + \Lambda_\alpha = m_0 + \Lambda_{\alpha_0}, \tag{46}$$

$$M = m_j + m' = m_{j_0}. \tag{47}$$

In Eq. (46), m_0 and m are, respectively, the projections of the scattered electron's initial- and final-state orbital angular momenta on the BODY axis. Thus Eq. (46) expresses conservation of the projection of total orbital angular momentum Λ on the BODY axis. [In practice, it is convenient to alter the expansion basis of Eq. (24) slightly, defining channels with well-defined values of Λ at the outset.] In Eq. (47), m' is the projection of the scattered electron's final-state orbital angular momentum on the LAB z axis, taken here to be coincident with the incident linear momentum $\hat{k}_0$. Since the electron's initial-state angular momentum has zero projection along $\hat{k}_0$, Eq. (47) expresses conservation of the projection of total (orbital and rotational) angular momentum M on a space-fixed z axis in the LAB frame. Finally, the coupling of the rotational angular momentum j of the molecule with the orbital angular momentum $\mathbf{L}$ of the scattered electron to form a total $\mathbf{J} = \mathbf{j} + \mathbf{L}$ is evident in the Clebsch–Gordan coefficients, which vanish unless

$$|j_0 - l_0| \leq J \leq j_0 + l_0, \qquad |j - l| \leq J \leq j + l. \tag{48}$$

In a single collision event, J is conserved.

The apparent complexity of Eq. (45) arises from the presence of two unitary transformations of the T matrix. The first is a transformation from the BODY-frame basis $\langle \alpha l m R \hat{R}|$ to a coupled angular momentum representation $\langle \alpha v j l J M|$ in the LAB frame, resulting in the T matrix

$$T^{\mathrm{AN}}(\alpha v j l, \alpha_0 v_0 j_0 l_0; S, J) = \frac{[(2j+1)(2j_0+1)]^{1/2}}{2J+1} \sum_{m,m_0} C(jlJ; \Lambda_\alpha \Lambda_{\alpha_0} - \Lambda_\alpha + m_0) C(j_0 l_0 J; \Lambda_{\alpha_0} m_0) \times \langle v | T^B(\alpha l m, \alpha_0 l_0 m_0; S, R) | v_0 \rangle \delta_{m+\Lambda_\alpha, m_0+\Lambda_{\alpha_0}}. \tag{49}$$

The second transformation evident in Eq. (45) is simply an angular momentum uncoupling to the representation $\langle \alpha v j m_j l m'|$, also in the LAB frame. This transformation results in the T matrix

$$T^{\mathrm{AN}}(\alpha v j m_j l m', \alpha_0 v_0 j_0 m_{j_0} l_0 0; S) = \sum_J C(jlJ; m_j m') C(j_0 l_0 J; m_{j_0} 0) \times T^{\mathrm{AN}}(\alpha v j l, \alpha_0 v_0 j_0 l_0; S, J) \delta_{m_j+m', m_{j_0}}, \tag{50}$$

which is the same as Eq. (45).

In the general frame-transformation procedure, to be discussed in the next section, the BODY → LAB transformation is performed on the scattering wave function at some well-chosen finite value of electron–molecule separation, and the calculation is then continued outward into the asymptotic region. The adiabatic nuclei approximation is based on the assumption that this transformation can be delayed until the electron–molecule interaction has effectively vanished. The second transformation of the T matrix from the coupled to uncoupled representation is not an approximation; it is the same in an exact analysis.

Equation (44) is still not the final result since it is defined for a total spin state S, M_S of the electron–molecule system. The spin uncoupling is straightforward and takes the form

$$f^{\mathrm{AN}}_{\alpha v m_s, \alpha_0 v_0 m_{s_0}}(\mathbf{k}'_\alpha) = \sum_S C(S_\alpha \tfrac{1}{2} S; (M_{s\alpha}) m_s) C(S_{\alpha_0} \tfrac{1}{2} S; (M_s)_{\alpha_0} m_{s_0}) \times f^{\mathrm{AN}}_{\alpha v, \alpha_0 v_0, S}(\mathbf{k}'_\alpha), \tag{51}$$

where the spin label S has been made explicit for this purpose.

The differential cross section for a transition $\alpha_0 v_0 \to \alpha v$, averaged over initial and summed over final degenerate magnetic substates $m_{j_0}, (M_s)_{\alpha_0}, m_{s_0}$ and $m_j, (M_s)_\alpha, m_s$, is

$$\left(\frac{d\sigma}{d\Omega}\right)^{\mathrm{AN}}_{\alpha v j, \alpha_0 v_0 j_0} = \left(\frac{k_\alpha}{k_0}\right) \frac{1}{2(2j_0+1)(2S_{\alpha_0}+1)} \times \sum_{\substack{m_{j_0}(M_s)_{\alpha_0} m_{s_0} \\ m_j (M_s)_\alpha m_s}} |f^{\mathrm{AN}}_{\alpha v m_s, \alpha_0 v_0 m_{s_0}}(\mathbf{k}'_\alpha)|^2, \tag{52}$$

which may be expressed in terms of the corresponding T matrix elements by making use of Eqs. (44), (45), and (51). The summations in Eq. (52) permit considerable simplification of the final expressions. The integral cross section for $\alpha_0 v_0 j_0 \to \alpha v j$ corresponding to Eq. (52) becomes

$$\sigma^{\mathrm{AN}}_{\alpha v j,\alpha_0 v_0 j_0}=\frac{\pi k_0^{-2}}{2(2S_{\alpha_0}+1)(2j_0=1)}\sum_{\substack{SJ\\ ll_0}}(2S+1)(2J+1)$$

$$\times|T^{\mathrm{AN}}(\alpha vjl,\ \alpha_0 v_0 j_0 l_0;S,J)|^2 \tag{53}$$

in terms of the T matrix defined in Eq. (49).

Since the rotational energy levels of a molecule are so closely spaced, it is often impossible to resolve particular final rotational states in a scattering experiment or unimportant to do so for a particular application. It is then convenient to define a total integrated cross section, summed over all final j, viz.,

$$\sigma^{\mathrm{AN}}_{\alpha v,\alpha_0 v_0}=\sum_j \sigma^{\mathrm{AN}}_{\alpha v j,\alpha_0 v_0 j_0}, \tag{54}$$

where we have anticipated the result that in the AN (or ANR) approximation, where the rotational motion is treated adiabatically, this total cross section is independent of the initial rotational angular momentum j_0. The summation over j in Eq. (54) can be performed using Eqs. (49), (50), and (53) and the orthonormality condition on the Clebsch–Gordan coefficients. The summation over J in Eq. (53) can also be performed, resulting in

$$\sigma^{\mathrm{AN}}_{\alpha v,\alpha_0 v_0}=\frac{\pi k_0^{-2}}{2(2S_{\alpha_0}+1)}\sum_{\substack{S\\ ll_0 m_0}}(2S+1)$$

$$\times|\langle v|T^B(\alpha lm,\ \alpha_0 l_0 m_0;S,R)\,|v_0\rangle|^2, \tag{55}$$

where $m=m_0+\Lambda_{\alpha_0}-\Lambda_\alpha$. (Recall that this cross section also represents a sum over final, and average over initial spin projections.) Equation (55) can also be derived by proceeding directly from the BODY-frame scattering amplitude in Eq. (38), shown as an explicit function of molecular orientation in Eq. (39). The adiabatic nuclear vibration (ANV) approximation is made simply by forming the matrix element of the scattering amplitude in Eq. (39) $\langle v|f^L_{\alpha\alpha_0}|v_0\rangle$. However, one can bypass all the analysis associated with introducing the rotational states of the molecule. If a differential cross section is constructed directly from $\langle v|f^L_{\alpha\alpha_0}|v_0\rangle$, and is then integrated over all *molecular orientations* $\hat{R}$ as well as over final scattering momentum directions $\hat{k}$, Eq. (55) results. (Spin is handled as before.)

It may be the case that final vibrational states need not be resolved. Making use of completeness of the vibrational wave functions in Eq. (55), we can perform the v summation, obtaining

$$\sigma^{\mathrm{AN}}_{\alpha,\alpha_0 v_0}=\frac{\pi k_0^{-2}}{2(2S_{\alpha_0}+1)}\sum_{\substack{S\\ ll_0 m_0}}(2S+1)$$

$$\times|\langle v_0|T^B(\alpha lm,\ \alpha_0 l_0 m_0;SR)|v_0\rangle|^2, \tag{56}$$

where $m=m_0+\Lambda_{\alpha_0}-\Lambda_\alpha$ as before, and where now only an average of the T matrix over the initial vibrational state v_0 appears. Since the ground vibrational state wave function is localized about the equlibrium internuclear separation R_0, the approximation is often made of replacing the averaged T matrix by that evaluated at $R=R_0$. In general, the cross section defined by Eq. (56) *does* depend on initial state v_0. In contrast, the cross section defined by Eq. (54) does not depend on initial state j_0.

Under conditions where the "collision time" $t_c \ll \tau_R$ but $t_c \gtrsim \tau_v$, e.g., for energies near vibrational thresholds for states of interest, or in the vicinity of a resonance with a lifetime comparable with τ_v, the adiabatic approximation may be valid for rotation but not for vibration. In such circumstances, all the equations (45)–(55) remain valid with the replacement

$$\langle v|T^B(\alpha lm,\ \alpha_0 l_0 m_0;S,R)|v_0\rangle \rightarrow T^B(\alpha vlm,\ \alpha_0 v_0 l_0 m_0;S), \tag{57}$$

where the latter is obtained from a vibrational close-coupling treatment including vibrational as well as electronic states in the expansion of Eq. (24), or from some other method that treats molecular vibration more accurately. The calculations are necessarily more complicated.

E. General formulation

The adiabatic nuclei approximation discussed in the last section is based on a fixed-nuclear treatment throughout (i.e., at all electron–molecule separations) and must fail under certain circumstances, for example, whenever the collision time t_c is comparable to or exceeds the periods of nuclear motion τ_v and τ_R. Conditions where AN may fail include (i) energies near threshold, (ii) occurrence of resonances, and (iii) dominance of strong long-range interactions (as in scattering from polar molecules) (see Temkin, 1976).

Recently, Nesbet (1979) introduced an "energy-modified adiabatic (EMA) approximation" which formally extends the validity of the adiabatic nuclei approximation to cover all cases by including the nuclear Hamiltonian as a "parameter" in the adiabatic electronic wave function. The author shows that approximate treatments based on this theory do yield the correct results in both the resonance and impulse limits.

The general formulation of electron–molecule scattering treats the target molecule as a complicated rotating, vibrating structure capable of changes in nuclear as well as electronic states during the collision. Thus, one seeks solutions of the full electron-plus-molecule Schrödinger equation (9) subject to the asymptotic conditions of Eqs. (2)–(4). The explicit inclusion of rotational and vibrational states in a close-coupling expansion (10) introduces complications into the calculation. For relatively light molecules like N_2 and CO, the density of strongly coupled rotational states is already so high that solution of even the static-exchange problem [in which only the ground electronic state is retained in Eq. (10)] stretches the capability of the largest present-day computers. The reason for this strong rotational coupling is simply that the LAB-frame expansion (10), where the scattered electron is referred to space-fixed coordinate axes, is inappropriate at small r, where the electron is near the nuclei. To see this, let us consider a molecule like H_2 or N_2 and focus specifically on those terms in Eq. (10) that involve the ground ${}^1\Sigma_g^+$ electronic state. Such terms in the expansion may be written (ignoring spin for now)

$$\sum_{vjm_jlm'} r^{-1}u_{vjm_jlm'}(r)Y_{lm'}(\hat{r}')Y_{jm_j}(\hat{R})\chi_v(R)\psi_{\Sigma_g^+}(\mathbf{r}_m, R)\,, \tag{58}$$

where the angular coordinates $\hat{r}'$ of the scattered electron are referred to a space-fixed LAB frame, and where we have assumed that the rotational states of a diatomic molecule in a Σ electronic state may be adequately represented by spherical harmonics (rigid-rotator model). At small values of r (near the nuclei) the strong attractive interaction tends to strongly couple the angular momentum $\mathbf{L}$ of the scattered electron to the internuclear axis $\hat{R}$ (classically, $\mathbf{L}$ is caused to precess around the nuclear axis $\hat{R}$). Thus the projection $\mathbf{L}\cdot\hat{R}$ tends to be well defined near the molecule, and a representation of the scattered electron wave function in terms of eigenfunctions of $\mathbf{L}\cdot\hat{R}$, viz., $Y_{lm}(\hat{r})$, where $\hat{r}$ refers to the BODY frame, is more appropriate. In the LAB-frame treatment, the expansion (58) must somehow reflect this physical effect, and it does so by strongly coupling a large number of $lm'jm_j$ channels. Indeed, Mullaney and Truhlar (1978) have shown that in actual calculations the convergence of a rotational close-coupling calculation is much improved by employing an expansion in terms of "rotationally and orbitally adiabatic" basis functions rather than the conventional unperturbed functions.

Vibrational coupling can be understood in a very similar way. When the electron is close to the nuclei, its motion tends to respond instantaneously to any change in internuclear separation R, and therefore may be properly characterized by a Born–Oppenheimer representation in which the radial functions depend parametrically on R, viz., $\mathbf{u}(r;R)$. In Eq. (58), this kind of physical response to changes in R can be represented only by coupling of different vibrational states. It should be emphasized that most of this strong coupling of vibrational and rotational states in Eq. (58) which occurs at small r is an artifact of the type of basis functions chosen to represent the wave function, and not a true indication of the rotational and vibrational transitions that are likely to occur in a given collision.

Chang and Fano (1972) have formulated a frame-transformation (FT) procedure that takes explicit account of the physical uncoupling of the electron's angular momentum $\mathbf{L}$ from the nuclear axis as the electron moves away from the nuclei. Simply stated, the frame-transformation procedure involves a BODY-frame expansion of Ψ_ϵ when the electron is close to the molecule and a LAB-frame expansion when it is far away. The procedure also deals with the vibrational coupling problem by treating R as a parameter when the electron is near the nuclei, and introducing stationary vibrational states at larger electron–molecule separations.

Choi and Poe (1977a, b) have recently reformulated the BODY-frame treatment in a way that conveniently describes the "hybrid theory" of Chandra and Temkin (1976a) to be discussed in Sec. III.C.

1. LAB-frame formulation

In this section, we shall formulate the general LAB-frame close-coupling treatment with the understanding that this formulation, while valid for all r, will be most practical when the electron is sufficiently far from the nuclei, say $r \geq a_F$, so that its motion is not completely dominated by the electron–molecule interaction potential energy, and the rotational and vibrational portions of the Hamiltonian H are important. (It should be noted that in general, the optimum transformation radii a_R and a_v for introducing the rotational and vibrational contributions to H may be different. We won't bother with this distinction in the present discussion.)

In the complete LAB-frame formulation of the electron–molecule scattering problem, the close-coupling expansion (10) becomes, by analogy with Eq. (24),

$$\Psi_\epsilon^L(\mathbf{r}', \sigma, \mathbf{r}_m, \sigma_m, \mathbf{R}) = \mathcal{A}\sum_p r^{-1}u_p^L(r')\Phi_p^L(\hat{r}', \sigma, \mathbf{r}_m, \sigma_m, \mathbf{R})\,, \tag{59}$$

where the LAB-frame "channel wave functions" (expansion basis functions) are

$$\begin{aligned}\Phi_p^L(\hat{r}', \sigma, \mathbf{r}_m, \sigma_m, \mathbf{R}) &= \sum_{m'm_j} C(jlJ; m_jm')Y_{lm'}(\hat{r}')R_{jm_j\Lambda_\alpha}(\hat{R})\phi_{\alpha v}^{(v)}(R)\\ &\times \sum_{m_s(M_S)_\alpha} C(\tfrac{1}{2}S_\alpha S; m_s(M_S)_\alpha)\chi_{m_s}(\sigma)\psi_\alpha^{(e)}(\mathbf{r}_m, \sigma_m; R)\,.\end{aligned} \tag{60}$$

In Eq. (60) the rotational and vibrational target wave functions are those of Eqs. (42) and (43), the angular coordinates $\hat{r}'$ of the scattered electron refer to the LAB frame, and the spin coupling $\mathbf{S} = \mathbf{s} + \mathbf{S}_\alpha$ is carried out as in the fixed-nuclei treatment of Eq. (24). In this representation the orbital angular momentum of the scattered electron $\mathbf{L}$ and the rotational angular momentum of the molecule $\mathbf{j}$ are coupled, forming the total angular momentum

$$\mathbf{J} = \mathbf{j} + \mathbf{L}\,, \tag{61}$$

and the Φ_p^L are eigenfunctions of J^2 and J_z as well as S^2 and S_z, where z refers to the space-fixed LAB frame. The channel index is now $p = (\alpha, v, j, l; J, S)$. (Spatial isotropy guarantees that the radial functions and the scattering matrices are independent of M_J and M_S.) The radial functions $u_p^L(r)$ satisfy coupled integro-differential equations identical in form to (26), viz.,

$$\left[\frac{d^2}{dr^2} + k_p^2 - \frac{l(l+1)}{r^2}\right]u_p^L(r) = 2\sum_{p'}[V_{pp'}^L(r) + W_{pp'}^L(r)]u_{p'}^L(r)\,, \tag{62}$$

where the k_p^2 now include rotational and vibrational energies of the target (i.e., the matrix elements H_{VIB} and H_{ROT}, both diagonal in this representation). The direct and exchange matrix elements $V_{pp'}^L(r)$ and $W_{pp'}^L(r)$, respectively, are defined for the LAB-frame basis, Eq. (60), in complete analogy to the BODY-frame treatment leading to Eqs. (28) and (29). Although the precise forms are different, the overall structure of these matrix elements is consistent with the observations made in the last section. The coupled equations can be written in matrix form as in Eq. (30), where the radial solutions are represented by an $N \times N$ matrix $\mathbf{u}^L(r)$ with elements

$$[\mathbf{u}^L(r)]_{pq} \equiv u^L_{pq}(r)\,, \tag{63}$$

where channels are labeled by $p = 1, \dots, N$ [N = total number of channels included in the close-coupling expansion (59)], and the particular linearly independent solutions are labeled by $q = 1, \dots, q_{\max}$, where in general $q_{\max} = 2N$. If the region over which Eqs. (62) are solved includes the origin $r = 0$, then the boundary conditions requiring that $u^L_{pq}(0) = 0$ for all solutions eliminate the N irregular solutions so that $q_{\max} = N$.

If the LAB-frame treatment is being used only in an exterior region, say $r \geqslant a$, then one can still get by with only N linearly independent solutions provided sufficient information is available at the FT boundary $r = a_F$ to enable these solutions to be initialized properly and integrated into the asymptotic region. One way of incorporating this boundary information is via the R matrix (Wigner and Eisenbud, 1947; Lane and Thomas, 1958). By definition, the elements of the R matrix relate the functions and their derivatives at the FT boundary according to

$$u_{pq}(a_F) = \sum_{p'} R_{pp'} \left(\frac{du_{p'q}(r)}{dr}\right)_{r=a_F}\,. \tag{64}$$

For example, in the frame-transformation procedure the R matrix may be constructed by solving the fixed-nuclei problem in the interior region $r \leqslant a_F$, performing the frame transformation to the representation (60), and then calculating values for the radial functions and their first derivatives at the boundary $r = a_F$ from Eq. (64). Alternatively, "eigenvalue methods" have been developed which lead directly to the R matrix or its equivalent. We shall discuss some of these in the next section. It is also possible to propagate the R matrix directly into the asymptotic region, eliminating the need to obtain the radial functions themselves (Light and Walker, 1976).

2. Frame transformation

Turning now to the frame transformation itself, we have argued that in the interior region $r \leqslant a_F$ (see Fig. 4) a BODY-frame representation of the wave function is more appropriate since a strong electron–molecule interaction (rather like a strong axially symmetric electric field) is more suitably accounted for in this reference frame. A rigorous BODY-frame representation of the total wave function is given by the expansion

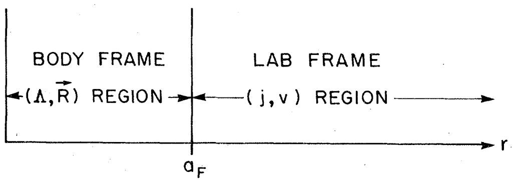

FIG. 4. Partitioning of configuration space for frame transformation.

$$\Psi^B_\epsilon(\mathbf{r}, \sigma, \mathbf{r}_m, \sigma_m, \mathbf{R}) = \mathcal{A} \sum_t r^{-1} u^B_t(r, R)\Phi^B_t(\hat{r}, \sigma, \mathbf{r}_m, \sigma_m, \mathbf{R})\,, \tag{65}$$

where the BODY-frame channel wave functions are

$$\begin{aligned}\Phi^B_t(\hat{r}, \sigma, \mathbf{r}_m, \sigma_m, \mathbf{R}) &= Y_{lm}(\hat{r})\left(\frac{2J+1}{8\pi}\right)^{1/2} D^J_{M\Lambda}(\hat{R}) \\ &\times \sum_{m_s(M_s)_\alpha} C(\tfrac{1}{2}S_\alpha S; m_s(M_s)_\alpha)\chi_{m_s}(\sigma)\psi^{(e)}_\alpha(\mathbf{r}_m, \sigma_m; R)\,,\end{aligned} \tag{66}$$

where

$$\Lambda = m + \Lambda_\alpha\,, \tag{67}$$

and where the channel index is defined as $t = (\alpha, l, m; J, S)$.

The channel functions Φ^B_t are eigenfunctions of J^2, J_z, and $\mathbf{J}\cdot\hat{R}$, with respective eigenvalues (in a.u.) $J(J+1)$, M, and Λ. The spin coupling has been carried out as before. We note that the BODY-frame channel functions Φ^B_t are *not* identical to the fixed-nuclei channel functions Φ^{FN}_p of Eq. (25) in that the $\hat{R}$-dependent factor $[(2J+1)/8\pi]^{1/2} D^J_{M\Lambda}(\hat{R})^*$ is missing from the latter. In the present section we have *not* made the fixed-nuclei approximation. The functions Φ^B_t of Eq. (66) form a complete set in the variables $\hat{R}$ as well as $\hat{r}$ and $\mathbf{r}_m$ so that the expansion (65) is exact. It differs from the LAB-frame expansion (59) largely in the choice of coordinates.

Substitution of Eq. (65) into the full Schrödinger equation yields the BODY-frame coupled radial equations

$$\left[\frac{d^2}{dr^2} + k_t^2 - \frac{l(l+1)}{r^2}\right] u^B_t(r, R) = 2\sum_{t'}[V^B_{tt'}(r, R) + W^B_{tt'}(r, R)]u^B_{t'}(r, R) + 2\sum_{t'}[\langle t|H_{\mathrm{VIB}}|t'\rangle + \langle t|H_{\mathrm{ROT}}|t'\rangle]u^B_{t'}(r, R)\,, \tag{68}$$

where in all the matrix elements, integration is performed over the nuclear variables R and $\hat{R}$ as well as $\hat{r}$, $\mathbf{r}_m$, and all spin coordinates. The direct and exchange matrix elements are given by Eqs. (28) and (29) as before. The rotational and vibrational contributions to the Hamiltonian possess eigenfunctions and eigenvalues given by

$$(H^{(\alpha)}_{\mathrm{VIB}} - E_{\alpha v})\phi^{(v)}_{\alpha v}(R) = 0\,, \tag{69}$$

where in the harmonic approximation the (discrete) eigenvalues are

$$E_{\alpha v} = \omega_\alpha(v + \tfrac{1}{2})\,, \quad v = 0, 1, 2, \dots\,,$$

and

$$(H^{(\alpha)}_{\mathrm{ROT}} - E_{\alpha j})R_{j m_j \Lambda_\alpha}(\hat{R}) = 0 , \qquad (70)$$

where, in the rigid-rotator approximation the eigenvalues are

$$E_{\alpha j} = B_\alpha j(j+1) , \quad j = 0, 1, 2, \dots ,$$

where ω_α and B_α are the vibrational and rotational constants, respectively (in a.u.). In the rigid-rotator approximation, the rotational wave function of Eq. (70) is given in Eq. (43). The channel kinetic energies k_t^2 in Eq. (68) are related by

$$\varepsilon = k_t^2/2 + E^{(e)}_\alpha(R_\alpha) = k_{t'}^2/2 + E^{(e)}_{\alpha'}(R_\alpha) , \qquad (71)$$

where R_α is the equilibrium separation for state α. The matrix elements of H_{VIB} and H_{ROT} may be calculated by transforming to the representation in which the corresponding matrices are diagonal (see Chang and Fano, 1972). The vibrational terms $\langle t|H_{\mathrm{VIB}}|t'\rangle$, though diagonal in l, m_l, and Λ, lead to an awkward continuum of coupled equations that would be very difficult to handle. The rotational terms $\langle t|H_{\mathrm{ROT}}|t'\rangle$ are less frightening; however, in general they do involve coupling in m_l and Λ. All l coupling is confined to the direct and exchange matrix elements.

Now, if we agree to work in the BODY-frame representation only in the "inner" region near the nuclei, then the direct and exchange terms in Eq. (68) are much larger than the rotational and vibrational terms, and the latter can be neglected. Chang and Fano (1972) point out that the commutators $[H_{\mathrm{ROT}}, V_{em}]$ and $[H_{\mathrm{VIB}}, V_{em}]$, although not strictly zero, nevertheless are quite small. Ignoring H_{VIB} and H_{ROT} in Eq. (68) reduces the coupled equations to those obtained in the fixed-nuclei approximation, Eqs. (26) or (30). Thus the fixed-nuclei radial solutions $u^{\mathrm{FN}}_{tq}(r,R)$ are good approximations to the electronic parts of the exact BODY-frame radial solutions $u^B_{tq}(r,R)$ for $r \le a_F$. Thus, in the sense of the Born–Oppenheimer approximation, the BODY-frame radial wave functions for $r \lesssim a_F$ may be approximated by the product form

$$u^B_{tq}(r,R) \cong u^{\mathrm{FN}}_{tq}(r,R)\chi_q(R) , \qquad (72)$$

where the fixed-nuclei functions $u^{\mathrm{FN}}_{tq}(r,R)$ are analogous to the adiabatic electronic functions in ordinary bound-state applications of the Born–Oppenheimer approximation. However, here, there exist for each channel t many acceptable linearly independent (with respect to r) functions, labeled by q. The proper choice for the corresponding "vibrational" functions $\chi_q(R)$ is somewhat ambiguous. Certainly, if the radial functions $u^{\mathrm{FN}}_{tq}(r,R)$ have been determined so as to satisfy the fixed-nuclei asymptotic boundary conditions given by Eq. (34) for each R, an appropriate choice would be

$$\chi_q(R) \equiv \phi^{(v)}_{\alpha_q v_q}(R) , \qquad (73)$$

i.e., the unperturbed target-molecule vibrational wave functions corresponding to particular initial electronic states α_q. With this choice, the adiabatic nuclei approximation [Eqs. (49)–(56)] is obtained as a limiting case, viz., when the frame-transformation radius, a_F in Fig. 4, is taken to ∞ (Henry and Chang, 1972).

The transformation at the FT boundary, $r = a_F$, is accomplished in two steps. First, the R dependence of the BODY functions $u^B_{tq}(r,R)$ is "distributed" amongst the vibrational functions by means of the expansion

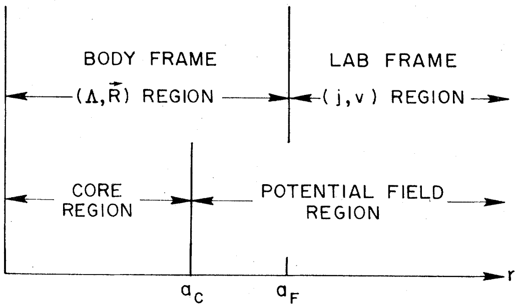

FIG. 5. Partitioning of configuration space in R-matrix method.

$$u^B_{tq}(r,R) = \sum_v u^B_{tv,q}(r)\phi^{(v)}_{\alpha v}(R) , \qquad (74)$$

where

$$u^B_{tv,q}(r) \equiv \int_0^\infty R^2 dR\, \phi^{(v)}_{\alpha v}(R) u^B_{tq}(r,R) \qquad (75)$$

$$\equiv \langle \alpha v | u^B_{tq}(r,R)\rangle_R . \qquad (76)$$

Thus from Eq. (76) we note that the BODY-frame representation of the total wave function in Eq. (65) becomes

$$\Psi^B_{\varepsilon q}(\mathbf{r}, \sigma, \mathbf{r}_m, \sigma_m, \mathbf{R}) = \mathcal{A} \sum_{tv} r^{-1} u^B_{tv,q}(r) \times \phi^{(v)}_{\alpha v}(R)\Phi^B_t(\hat{r}, \sigma, \mathbf{r}_m, \sigma_m, \mathbf{R}) , \qquad (77)$$

where the subscript q has been appended to denote a particular linearly independent solution. To compare Eq. (77) directly with the LAB-frame representation [Eq. (59)] we merely write $\phi^{(v)}_{\alpha v}\Phi^B_t$ in terms of the LAB-frame channel functions Φ^L_p defined in Eq. (60). The transformation matrix elements are defined by

$$\phi^{(v)}_{\alpha v}(R)\Phi^B_t(\hat{r}, \sigma, \mathbf{r}_m, \sigma_m, \mathbf{R}) = \sum_j A_{tp}\Phi^L_p(\hat{r}', \sigma, \mathbf{r}_m, \sigma_m, \mathbf{R}) , \qquad (78)$$

where the summation runs only over j, the rotational quantum number associated with the LAB channels $p = (\alpha, v, j, l; J, S)$. The inverse transformation involves summation only over m, associated with the BODY channels $t = (\alpha, l, m; J, S)$. The coefficients in Eq. (78) may be obtained by projecting onto particular channel functions (this involves integration over $\hat{R}$ and $\hat{r}'$). We obtain

$$A_{tp} = \left[\frac{2j+1}{2(2J+1)}\right]^{1/2} C(jlJ; \Lambda_\alpha m) = (A^{-1})_{pt} \qquad (79)$$

for the elements of the orthogonal transformation. [Note that Eq. (79) deceptively seems much simpler than the Chang and Fano (1972) result given in their Eq. (A9). The difference is that they construct channel functions Φ^B and Φ^L that are eigenfunctions of the parity operator for the electron–molecule system, thus taking advantage of this additional symmetry.] Now, Eq. (77) can be written as

$$\Psi^{B}_{\epsilon q}(\mathbf{r},\sigma,\mathbf{r}_m,\sigma_m,\mathbf{R})=\mathcal{A}\sum_{p} r^{-1}u_{pq}(r)\Phi^{L}_{p}(\hat{r}',\sigma,\mathbf{r}_m,\sigma_m,\mathbf{R}), \tag{80}$$

where

$$u_{pq}(r)=\sum_{m}\tilde{A}_{pt}u^{B}_{tv,q}(r)$$

$$=\sum_{m}\tilde{A}_{pt}\int_{0}^{\infty}R^{2}dR\,\phi^{(v)}_{\alpha v}(R)u^{B}_{tq}(r,R), \tag{81}$$

but by Eq. (59) this must agree with the LAB radial solutions $u^{L}_{pq}(r)$. Thus we have at the transformation radius $r=a_F$

$$\mathbf{u}^{L}(a_F)=\tilde{\mathbf{A}}\langle\alpha v|\mathbf{u}^{B}(a_F,R)\rangle_R, \tag{82}$$

and a similar expression for the first derivative. [In passing, we note that if the BODY-frame radial function in Eq. (76) is approximated by Eq. (72) with the choice of vibrational function (73), and the transformation is applied in the asymptotic region, i.e., $a_F\to\infty$, then with a little effort we recover Eq. (32), i.e., the adiabatic nuclei approximation.] Alternatively, the more compact R matrix can be employed. In the LAB frame, the matrix $\mathbf{R}^{L}$ is defined [cf. Eq. (64)] by

$$\mathbf{u}^{L}(a_F)=\mathbf{R}^{L}\left[\frac{d}{dr}\mathbf{u}^{L}(r)\right]_{a_F}, \tag{83}$$

and in the BODY frame the matrix $\mathbf{R}^{B}(R)$, which depends on the internuclear separation R, is defined by

$$\mathbf{u}^{B}(a_F,R)=\mathbf{R}^{B}(R)\left[\frac{d}{dr}\mathbf{u}^{B}(r,R)\right]_{a_F}. \tag{84}$$

Of course, the matrices are defined over different bases in Eqs. (83) and (84). In particular, it is important to remember that the LAB-frame channel index p includes the vibrational quantum number v. Use of Eq. (82) in Eqs. (83) and (84) leads to the R-matrix transformation

$$\mathbf{R}^{L}=\tilde{\mathbf{A}}\langle\alpha v|\mathbf{R}^{B}(R)|\alpha v'\rangle\mathbf{A}. \tag{85}$$

The procedure, then, is to develop a number of linearly independent fixed-nuclei, BODY-frame radial solutions $u^{B}_{tq}(r,R)$ at a sufficient number of internuclear separations R so that the integrals in Eq. (81) can be evaluated. At a suitable FT boundary $r=a_F$, the frame transformation (82) is applied to the functions and their first derivatives (hence, the R matrix), or the functions at two adjacent points. The LAB-frame solutions $u^{L}_{pq}(r)$ are then integrated into the asymptotic region using Eq. (62). If a_F can be chosen sufficiently large, the exchange terms $W^{L}_{pp'}$ can be set to zero.

In the asymptotic region where all electron–molecule interactions are negligible, we select LAB-frame solutions that satisfy boundary conditions identical in form to Eqs. (34)–(36) except that the LAB-frame channels are labeled by $p=(\alpha,v,j,l;J,S)$ and the channel kinetic energies k_p^2 are related by

$$\varepsilon=k_p^2/2+E_p=k_{p'}^2/2+E_{p'}, \tag{86}$$

where

$$E_p\cong E^{(e)}_{\alpha}(R_\alpha)+\omega_\alpha(v+\tfrac{1}{2})+B_\alpha j(j+1). \tag{87}$$

The LAB-frame K, S, and T matrices are related by Eq. (37). Thus the T matrix is defined with elements

$$T_{pp_0}=T(\alpha vjl,\alpha_0v_0j_0l_0;S,J). \tag{88}$$

In Eq. (49) we gave an *approximate* form (adiabatic nuclei approximation) for this quantity. In contrast, the frame-transformation procedure leading up to Eq. (88) is "exact," in the sense that in principle it can be made as accurate as desired. The angular momentum decoupling transformation is given by Eq. (50). The scattering amplitude for the transition $\alpha_0v_0\to\alpha v$ (i.e., $\alpha_0v_0j_0m_{j_0}\to\alpha vjm_j$) is given by Eq. (44) in terms of the exact T-matrix elements. Finally, Eqs. (51)–(53) for the spin-decoupled scattering amplitude, and the differential and integral cross sections hold for the exact T matrix as well, and will not be rewritten.

Weatherford and Henry (1978) discuss the frame-transformation procedure as applied to electronically elastic scattering for $^1\Sigma^+$ target molecules and in the context of the noniterative static-exchange integral equation method. They have applied the method to rotational and vibrational excitation in electron–H_2 scattering (Weatherford and Henry, 1979).

The degree of success one expects in applying the frame-transformation procedure, of course, depends on the smallness of the neglected terms. In elastic scattering and rotational excitation of polar molecules by slow electrons, the optimum choice of transformation radius a_F can be elusive (Chandra, 1977; see Sec. II.E.1.a). Lan, Dourneuf, and Schneider (1979) suggest that this special problem with polar-molecule scattering can be efficiently dealt with by including the diagonal contribution of H_{ROT} in the BODY-frame calculation.

F. R-matrix and T-matrix expansion methods

1. R-matrix method

In the previous section, the R matrix was introduced in Eqs. (64) and (83)–(85) as a convenient device for transferring information about the scattering wave function across a boundary at $r=a_F$ from an interior region of space to an exterior region. In this section, we will describe alternative methods for calculation of the R matrix that have features in common with standard bound-state methods used in molecular structure calculations (Schneider, 1975a, b and 1977a, b; Schneider and Hay, 1976; Morrison and Schneider, 1977; Burke, Mackey, and Shimamura, 1977; and Shimamura, 1977a, b). It is convenient to partition configuration space into regions as shown in Fig. 5 (Burke *et al.*, 1977). The (Λ,R) and (j,v) regions are those described earlier, in connection with the frame-transformation procedure. In the R-matrix method, a further partitioning is appropriate into a "core region," $r\leqslant a_c$, and "potential-field region," $r\geqslant a_c$. The "core region" is chosen so that all important exchange and short-range correlation effects are contained therein. Thus, the physics of the "core region" is analogous to that of a bound-state molecular structure problem.

The R matrix will be calculated in this region by employing techniques similar to those developed for structure calculations. The "potential-field" region, $r > a_c$, is sufficiently far removed from the nuclei and the regions of greatest bound-electron density (for target states of interest) that the electron–molecule interaction can be replaced by a local potential energy term in the Hamiltonian. In particular applications it may be convenient to set $a_c = a_F$, so that the frame transformation is carried out at the edge of the core region. It should be emphasized once again that the proper selection of a_F is related to the rotational and vibrational energy-level separations of the target (see Sec. II.E), and in general two different radii a_R and a_v, in place of the single a_F, might be necessary for the rotational $(\Lambda \to j)$ and vibrational $(R \to v)$ segments of the frame transformations, respectively. As described previously, under conditions such that the adiabatic nuclei approximation is valid for rotation, vibration, or both, then the relevant FT radii can be taken to be infinite (i.e., the FT reduces to a constant transformation at $r = \infty$). In contrast, the radius a_c of the core region is determined by the range of exchange interactions and complex short-range correlation effects. It is largely a "trial and error" determination (see Chandra, 1977).

The R matrix can be defined for any choice of reference frame and corresponding set of channel functions. In electron–molecule scattering, the power of the R-matrix method derives from the fact that a fixed-nuclei, BODY-frame calculation of the R matrix is sufficient in the "core region," $r \leqslant a_c$, followed by relatively straightforward integration of the scattering equations in the outer regions. Thus in terms of the fixed-nuclei radial solutions of Eq. (26), we define the BODY-frame R matrix at $r = a_c$ by

$$u_p^B(a_c) = \sum_{p'} R_{pp'}^B \left[\left(\frac{d}{dr} u_{p'}^B(r) \right)_{a_c} - \frac{b}{a_c} u_{p'}^B(a_c) \right], \tag{89}$$

for each linearly independent solution $u_{pq}^B, q = 1, \ldots, N$. The value of b is arbitrary, and is usually chosen to be zero, as in Eqs. (64), (83), and (84). In matrix form, Eq. (89) becomes

$$\mathbf{u}^B(a_c) = \mathbf{R}^B \left[\left(\frac{d}{dr} \mathbf{u}^B(r) \right)_{a_c} - \frac{b}{a_c} \mathbf{u}^B(a_c) \right], \tag{90}$$

where the second index of the radial solutions matrix labels a particular linearly independent solution. With $b = 0$, we see that the R matrix is proportional to the inverse of a generalized logarithmic derivative matrix.

The calculation of the R matrix is based on the expansion of the electron–molecule system wave function Ψ_ϵ^B in terms of a complete set of "bound-state" wave functions Ψ_k, defined for $r \leqslant a_F$ by imposing a particular type of boundary condition at a finite "core" radius a_c of Fig. 5. The "bound-state" functions can be calculated by diagonalizing the full fixed-nuclei Hamiltonian $H^{(e)}$ in a basis set in which the basis functions themselves are constrained so that their logarithmic derivatives possess particular values at the boundary $r = a_c$. Alternatively, the Bloch operator (Bloch, 1957)

$$L_b = \sum_p |\Phi_p^B\rangle \delta(r - a_c) \left[\frac{d}{dr} - \frac{b}{a_c} \right] \langle \Phi_p^B| \tag{91}$$

can be introduced, and the modified Hamiltonian $H^{(e)} + L_b$ then diagonalized in terms of an *arbitrary* basis set in which no particular constraints are placed on the basis functions. Since the Φ_p^B in Eq. (91) are the channel functions of Eq. (24), the individual terms in Eq. (91) correspond to channel projections of the Bloch operator. The use of the Bloch operator L_b has the advantages that: (i) it is much more convenient to employ arbitrary basis functions; (ii) the resulting Ψ_k and hence Ψ_ϵ^B do not possess the annoying discontinuity in their first derivatives at $r = a_c$; and (iii) the expression for the R matrix [see Eq. (99) below] is more rapidly convergent.

Thus, in terms of the Bloch operator L_b, the eigenvalue problem becomes (Burke, 1977)

$$(H^{(e)} + L_b - E_k)\Psi_k = 0\,, \quad r \lesssim a_F\,, \tag{92}$$

where the eigenfunctions are expressed (spin coordinates and parametric dependence on R suppressed) as

$$\Psi_k(\mathbf{r}, \mathbf{r}_m) = r^{-1} \mathfrak{A} \sum_{pj} a_{pjk} \Phi_p^B(\hat{r}, \mathbf{r}_m) w_j^{(0)}(r)\,, \quad r \leqslant a_F \tag{93}$$

where the $w_j^{(0)}(r)$ are arbitrary, fixed, radial functions, chosen so that the radial expanse of configuration space out to $r = a_c$ is spanned by the set of $w_j^{(0)}$. The a_{pjk} are determined as the eigenvectors corresponding to eigenvalues E_k of the linear variational problem. In actual applications, additional short-range correlation terms are usually added to Eq. (93) to provide additional variational flexibility inside the core boundary $r = a_c$ (Burke *et al.*, 1977; Schneider, 1977a, b). Now, expressing the scattering wave function in terms of the functions Ψ_k as

$$\Psi_\epsilon^B = \sum_k \Psi_k\,, \quad r \leqslant a_F\,, \tag{94}$$

we obtain the relation between the scattering radial solutions and the radial basis functions

$$u_p^B(r) = \sum_k u_{pk}^B(r) = \sum_{jk} a_{pjk} w_j^{(0)}(r)\,, \quad r \leqslant a_F\,. \tag{95}$$

The expression for the R matrix is derived by expressing the formal solution of

$$(H^{(e)} + L_b - \varepsilon)\Psi_\epsilon^B = L_b \Psi_\epsilon^B \tag{96}$$

in terms of the eigenfunctions Ψ_k (Burke *et al.*, 1977; Schneider, 1977a) as

$$\Psi_\epsilon^B = \sum_k \left[\frac{\langle \Psi_k | L_b | \Psi_\epsilon^B \rangle}{E_k - \varepsilon} \right] \Psi_k\,, \quad r \leqslant a_F\,. \tag{97}$$

Then, by projecting out particular channels, one obtains the scattering radial functions

$$u_p^B(r) = \langle \Phi_p^B | \Psi_\epsilon^B \rangle\,, \quad r \leqslant a_F\,, \tag{98}$$

where the integration (summation) includes all spatial (spin) variables except r. The Dirac delta function $\delta(r - a_c)$ in L_b selects the values of the first derivatives of the scattering radial functions at $r = a_c$. Thus, at $r = a_c$, Eq. (98) becomes Eq. (89) with the R matrix elements given by

$$R_{pp'}^B = \sum_k \frac{u_{pk}^B(a_c) u_{p'k}^B(a_c)}{E_k - \varepsilon}\,, \tag{99}$$

where the $u_{pk}^B(r)$, according to Eq. (95), are the radial functions occurring in p-channel projection of the eigenfunctions Ψ_k. It is possible to "correct" Eq. (99) by a method devised by Buttle (1967). However, provided enough terms are retained in Eq. (99) the "Buttle correction" is unnecessary [see Burke *et al.* (1977) and Schneider (1977a)]. Once the matrix $\mathbf{R}^B$ is determined, it can be used to generate radial solutions at the "core" boundary $r=a_c$ (see Fig. 5), which are then continued outward by numerically integrating the "potential-scattering" radial equations. The frame transformation, if required, can then be performed at the FT boundary $r=a_F$. Alternatively, the R matrix can itself be propagated outward to the FT boundary, transformed to the LAB frame by Eq. (88), and then propagated into the asymptotic region (Light and Walker, 1976).

The details of derivations and the description of numerical techniques are not given here. The original papers of Wigner (1964a, b), Wigner and Eisenbud (1947), and the comprehensive review of Lane and Thomas (1958) lay out the basic theory in the context of nuclear physics. Burke and Robb (1975), Burke (1977), and Robb (1977) review the application of R-matrix theory to a variety of atomic physics problems (see also Burke 1974). Shimamura (1977a, b) discusses general questions of implementation and the connections with related eigenchannel methods introduced into atomic physics by Fano and Lee (1973) and Lee (1974). (See also Fano, 1977.) Applications to elastic scattering and rotational excitation in electron–molecule collisions are described by Schneider (1975a, b) for H_2, Schneider and Hay (1976) for F_2, and Morrison and Schneider (1977) for N_2. These applications are reviewed by Schneider (1977a), and results will be discussed in the later sections on particular processes. A detailed description of an R-matrix approach to the electron–molecule scattering problem is given by Burke *et al.* (1977).

An extension of the R-matrix method to vibrational excitation and dissociative attachment is described by Schneider, Le Dourneuf, and Burke (1979), and a recent application to vibrational excitation of N_2 has been carried out by Schneider, Le Dourneuf, and Lan (1979).

2. T-matrix expansion method

An alternative new method that does not involve the explicit partitioning of configuration space into different regions is the T-matrix expansion technique of Rescigno, McCurdy, and McKoy (1974a, b). Only a very brief description will be given here. The results of calculations using this method will be described in the relevant sections on applications to specific processes. So far, applications have been restricted to elastic scattering and rotational and vibrational excitation of ground-state molecules via the adiabatic nuclei approximation. For simplicity, therefore, we shall restrict attention here to the fixed-nuclei approximation for elastic scattering in the BODY frame. Furthermore, we will assume that the electronic state of the molecule is $^1\Sigma$. The expression (38) for the BODY-frame, elastic-scattering amplitude for momentum $\mathbf{k}_0 \rightarrow \mathbf{k}$ reduces to

$$f^B(\mathbf{k},\mathbf{k}_0) = 2\pi k^{-1} \sum_{l,l_0,m_0} i^{l_0-l+1} Y^*_{l_0 m_0}(\hat{k}_0) Y_{l m_0}(\hat{k}) T^B(l m_0, l_0 m_0)\,, \tag{100}$$

where we suppress the parametric dependence on the fixed internuclear separation R. From a more formal point of view, Eq. (100) may be recognized (see Taylor, 1972) as the matrix element between "free-particle" states $\langle\mathbf{k}|$ and $\langle\mathbf{k}_0|$ of the T operator

$$f^B(\mathbf{k},\mathbf{k}_0) = -2\pi^2 \langle\mathbf{k}|T|\mathbf{k}_0\rangle\,, \tag{101}$$

where the normalization of the plane-wave states is defined by

$$\langle\mathbf{r}|\mathbf{k}\rangle = (2\pi)^{-3/2} \exp(i\mathbf{k}\cdot\mathbf{r})\,. \tag{102}$$

In Eq. (100), the plane-wave functions have been expanded in terms of spherical harmonics. The T operator satisfies the Lippmann–Schwinger equation

$$T = U + U G_0^+ T\,, \tag{103}$$

where $U=2V$, and V is an "optical potential" defined in such a way that the electron–molecule Hamiltonian may be written simply as

$$\begin{aligned} H^{(e)} &= -\tfrac{1}{2}\nabla_r^2 + V(\mathbf{r},R) \\ &\equiv H_0 + V\,. \end{aligned} \tag{104}$$

In Eq. (103), G_0^+ is the (outgoing-wave) free-particle Green function defined in terms of H_0 by

$$(E-H_0)G_0^+ = 1\,. \tag{105}$$

The T-matrix expansion method is based on the solution of an approximate (i.e., truncated) matrix representation of Eq. (103). Thus choosing a convenient *finite* basis set $\{\phi_\alpha\}$, complete over the region of space where V is important, the matrix equation corresponding to Eq. (103) can be solved for the "truncated" T matrix

$$\mathbf{T}^t = (1-\mathbf{U}^t\mathbf{G}_0^+)^{-1}\mathbf{U}^t\,, \tag{106}$$

where the matrix elements of $\mathbf{U}^t$, for example, are

$$\begin{aligned} U^t_{\alpha\beta} &= \langle\alpha|U|\beta\rangle \\ &= 2\int d\mathbf{r}\, \phi^*_\alpha(\mathbf{r}) V(\mathbf{r},R) \phi_\beta(\mathbf{r})\, dr\,. \end{aligned} \tag{107}$$

In order to calculate the scattering amplitude of Eq. (101), one need only transform the matrix elements according to

$$\langle\mathbf{k}|T^t|\mathbf{k}_0\rangle = \sum_{\alpha,\beta} \langle\mathbf{k}|\alpha\rangle\langle\alpha|T|\beta\rangle\langle\beta|\mathbf{k}_0\rangle\,. \tag{108}$$

The trick to all this lies in a careful selection of basis set $\{\phi_\alpha\}$, and a realistic choice for the "optical potential" V. A convenient choice for all the basis functions are the Cartesian Gaussian-type orbitals (GTO) centered on the nuclei and the center of mass of the molecule. This choice of basis functions permits efficient calculation of all the integrals.

Applications of the T-matrix expansion method include fixed-nuclei calculations of the total cross sections (elastic + rotational excitation) for electrons scattered by H_2 and N_2 in the static-exchange approximation, i.e., with the optical potential V replaced by the static-exchange potential (Rescigno, McCurdy, and McKoy, 1974a,b; Fliflet, Levin, Ma, and McKoy, 1978; and Fliflet and McKoy, 1978, a, b). A recent application to e–H_2 elastic and rotational excitation (Kaldor and Klonover, 1977; Klonover and Kaldor, 1978, 1979a) in the adiabatic nuclear rotation approximation includes some allowance for correlation effects (in particular, polarization) by means of a diagrammatic-perturbation-series correction to the static-exchange approximation of the optical potential. This approach has been extended to vibrational excitation (in the adiabatic nuclear vibration approximation) as well (Klonover and Kaldor, 1979b, c). Kaldor (1979a) has suggested that a full vibrational (or rotational) close-coupling calculation is feasible using the T-matrix expansion technique.

G. Static-exchange and model-potential approximations

1. STATIC EXCHANGE

In the static-exchange approximation, the theory takes into account only the static and exchange interactions of the electron with an *unperturbed* ground electronic state of the molecule. There is no allowance for polarization or other correlation effects. Electronic excitation and the (resonant) temporary electronic excitation of the molecule are not possible. Most applications have been BODY-frame calculations in the fixed-nuclei approximation. For simplicity, we will restrict attention here to that case and the example of a nonpolar closed-shell ${}^1\Sigma_g^+$ diatomic molecule. The general fixed-nuclei close-coupling expansion (22) reduces, in the static-exchange approximation, to

$$\Psi_\epsilon(\mathbf{r},\sigma,\mathbf{r}_m,\sigma_m;R)=\mathcal{A}F_{m_s}(\mathbf{r},R)\chi_{m_s}(\sigma)\psi_0^{(e)}(\mathbf{r}_m,\sigma_m;R)\,, \tag{109}$$

where $\Psi_0^{(e)}$ designates the unperturbed ground electronic state of the target. Substitution of Ψ_ϵ into the fixed-nuclei Schrödinger equation results in the partial integro-differential equation (suppressing the parameter R)

$$\begin{aligned}&[-\tfrac{1}{2}\nabla_r^2-\tfrac{1}{2}k^2+V_S(\mathbf{r})]F(\mathbf{r})\\&\quad=(h-\tfrac{1}{2}k^2)\sum_i\left[\int d\mathbf{r}'\,\phi_i(\mathbf{r}')F(\mathbf{r}')\right]\phi_i(\mathbf{r})\\&\qquad+\sum_i\left[\int d\mathbf{r}'\,\phi_i(\mathbf{r}')\frac{1}{|\mathbf{r}-\mathbf{r}'|}F(\mathbf{r}')\right]\phi_i(\mathbf{r})\,,\end{aligned} \tag{110}$$

where V_S is the static potential energy

$$\begin{aligned}V_S(\mathbf{r})&=\int d\mathbf{r}_m|\psi_0^{(e)}(\mathbf{r}_m,\sigma_m)|^2V_{em}(\mathbf{r},\mathbf{r}_m)\\&=2\sum_i\int d\mathbf{r}'|\phi_i(\mathbf{r}')|^2\frac{1}{|\mathbf{r}-\mathbf{r}'|}-\frac{Z_a}{r_a}-\frac{Z_b}{r_b}\,,\end{aligned} \tag{111}$$

where the operator h is defined by

$$h=-\frac{1}{2}\nabla_r^2-\frac{Z_a}{r_a}-\frac{Z_b}{r_b}+\sum_i\int d\mathbf{r}'|\phi_i(\mathbf{r}')|^2\frac{1}{|\mathbf{r}-\mathbf{r}'|}\,, \tag{112}$$

and where the summations over i in Eqs. (110)–(112) include all occupied spatial orbitals of the ground-state wave function (here assumed to be of single-configuration form). The subscript m_s on $F(\mathbf{r})$ has been dropped since the same equation holds for both spins. Equation (110) is simply the (continuum) Hartree–Fock equation. The exchange terms on the right-hand side of Eq. (110) may be considered corrections to the pure static potential. The Pauli exclusion principle, which states that the total wave function Ψ_ϵ of Eq. (109) must be antisymmetric with respect to the interchange of the coordinates (both spatial and spin) of any two electrons, has the effect of preventing two electrons of like spin from being found near one another. Each bound electron is surrounded by a "Fermi hole" where the repulsive Coulomb interaction between two electrons of like spin vanishes. Thus, for a closed-shell target molecule, exchange behaves as an effective short-range *attractive* interaction. Note that with the single-configuration representation of $\psi_0^{(e)}$ in Eq. (109), the total wave function Ψ_ϵ is unchanged if a multiple of any one of the occupied orbitals $\phi_i(\mathbf{r})$ is added to the "continuum orbital" $F(\mathbf{r})$; hence, $F(\mathbf{r})$ may be assumed orthogonal to all the $\phi_i(\mathbf{r})$ with no loss of generality. In fact, if the overlap terms are dropped from Eq. (110), the resulting solution $F(\mathbf{r})$ is indeed constrained to exhibit this orthogonality. Equation (110) is then written in abbreviated form

$$(-\tfrac{1}{2}\nabla_r^2+V_{sx}(\mathbf{r})-\tfrac{1}{2}k^2)F(\mathbf{r})=0\,, \tag{113}$$

where

$$V_{sx}(\mathbf{r})=-\frac{Z_a}{r_a}-\frac{Z_b}{r_b}+2\hat{J}-\hat{K}\,, \tag{114}$$

and where the definition of the Coulomb and exchange operators $\hat{J}$ and $\hat{K}$, respectively, is clear from Eqs. (110) and (111).

The numerical solution of Eq. (113) is complicated by the strong dependence of V_{sx} on r near the nuclei. If direct numerical solution of the partial differential equation is attempted, a tight mesh in θ as well as r is required (see, for example, Tully and Berry, 1969). If a single-center partial-wave expansion of the form of Eq. (23) is invoked, many terms are often required to accurately represent the wave function near the nuclei. For the diatomic case, the use of two-center spheroidal coordinates can be helpful (Nagahara, 1953; Takayanagi, 1967; Hara, 1969a). However, the resulting equations are more difficult to solve, and the coupling does not disappear completely. (For a model calculation comparing the two approaches see Darewych, Baille, and Hara, 1974). We have already discussed the R-matrix and T-matrix expansion methods as attractive alternative techniques to handle these complexities near the nuclei.

In spite of the concerns just expressed, the single-center and two-center partial-wave expansions have been employed in a number of applications, so we will describe briefly how the general (one-center) development of Sec. II.C simplifies for this special level of approximation. The partial-wave expansion (23) is (suppressing the parameter R)

$$F_m(\mathbf{r}) = r^{-1} \sum_l u_{lm}(r) Y_{lm}(\hat{r}) , \tag{115}$$

where the radial functions satisfy the coupled integro-differential equations

$$\left[\frac{d^2}{dr^2} + k^2 - \frac{l(l+1)}{r^2}\right] u_{lm}(r) = 2 \sum_{l'} [V_{lm,l'm}(r) + W_{lm,l'm}(r)] \times u_{l'm}(r) , \tag{116}$$

where the "direct" matrix elements are

$$V_{lm,l'm}(r) = \langle lm | V_S(\mathbf{r}) | l'm \rangle = \sum_{\lambda=0}^{\infty} v_\lambda^{(S)}(r) \left(\frac{2l'+1}{2l+1}\right)^{1/2} \times C(l'\lambda l; m0) C(l'\lambda l; 00) , \tag{117}$$

where the radial functions $v_\lambda^{(S)}(r)$ are the coefficients in a single-center expansion of the static potential energy

$$V_S(\mathbf{r}) = \sum_{\lambda=0}^{\infty} v_\lambda^{(S)}(r) P_\lambda(\cos\theta) , \tag{118}$$

where $\cos\theta = \hat{r} \cdot \hat{R}$.

The "exchange" matrix elements (assuming F is orthogonal to the φ_i) are defined by

$$W_{lm,l'm}(r) u_{l'm}(r) = -\sum_i \langle lm | \int d\mathbf{r}' \phi_i(\mathbf{r}') \frac{1}{|\mathbf{r}-\mathbf{r}'|} (r')^{-1} \times u_{l'm}(r') Y_{l'm}(\hat{r}') \phi_i(\mathbf{r}) \rangle , \tag{119}$$

where the brackets imply integration over $\hat{r}$. The diagonality in m results from the axial symmetry of the (assumed) Σ target-state wave function. The spectroscopic notation $\sigma, \pi, \delta, \ldots$ is commonly used for $m = 0, 1, 2, \ldots$, respectively. The coupled equations written in matrix form are identical to Eq. (30), where the matrix $\mathbf{k}^2$ is diagonal in this case, and the channel index becomes $p = (l, m)$. Solution of these coupled integro-differential equations may be carried out using a variety of numerical methods. Sinfailam (1970) has published a computer program, based on the noniterative procedure of Marriott (1958) and Omidvar (1961) and discussed by several authors in connection with electron–atom (or ion) scattering (see Smith, Henry, and Burke, 1966; Thomas, 1973; and Omidvar, 1974).

If the fixed-nuclei approximation is continued into the asymptotic region (adiabatic nuclei approximation), then the boundary conditions are those given in Eqs. (34)–(36) with relations (37) between the K^B, S^B, and T^B matrices. The equations for the scattering amplitude, and differential and integral cross sections developed in Secs. II.C–II.E, apply here, but with the appropriate simplification $\alpha = \alpha_0$ and $\Lambda_{\alpha_0} = 0$. In particular, the fixed-nuclei elastic differential cross section averaged over nuclear orientation is

$$\overline{\frac{d\sigma}{d\Omega}} = \frac{1}{4k^2} \sum_\mu \sum_{L=0}^{\infty} A_{\mu L} T^B(lm, l_0 m) T^B(\bar{l}\bar{m}, \bar{l}_0 \bar{m})^* P_L(\cos\theta') , \tag{120}$$

where θ' is the LAB-frame scattering angle, $\mu = (l, m, l_0, \bar{l}, \bar{m}, \bar{l}_0)$, and the summation includes all allowed values of these indices. The coefficients are given by

$$A_{\mu L} = (2L+1)^{-1} [(2l+1)(2l_0+1)(2\bar{l}+1)(2\bar{l}_0+1)]^{1/2} i^{l-l_0-\bar{l}+\bar{l}_0} \times C(l_0 \bar{l}_0 L; 00) C(l\bar{l}L; 00) C(l_0 \bar{l}_0 L; -m\bar{m}) C(l\bar{l}L; -m\bar{m}) . \tag{121}$$

The integral cross section averaged over nuclear orientation is simply

$$\bar{\sigma} = \frac{\pi}{k^2} \sum_{l, l_0, m} |T^B(lm, l_0 m)|^2 . \tag{122}$$

This cross section can also be expressed in terms of the eigenphase shifts η_{im}, defined by the elements of the diagonalized S matrix

$$\exp(2i\eta) = \mathbf{U}\mathbf{S}^B\mathbf{U}^{-1} , \tag{123}$$

where $\mathbf{U}$ is the unitary transformation matrix that accomplishes the diagonalization. Since $\mathbf{S}^B$ is block diagonal in m, the eigenphase shifts may be characterized as Σ, Π, Δ, etc. (Note this is for the special case of a Σ target.) By direct substitution of Eq. (123), with $\mathbf{T}^B = 1 - \mathbf{S}^B$, into Eq. (122), one obtains

$$\bar{\sigma} = \frac{4\pi}{k^2} \sum_{i,m} \sin^2(\eta_{im}) . \tag{124}$$

Unlike the integral cross section, the differential cross section cannot be expressed in terms of the η_{im} alone. The sum of the eigenphase shifts, though not directly related to a measurable cross section, is often studied in theoretical applications as one measure of convergence and as an indicator of numerical accuracy. (For an interesting discussion of the behavior of the eigenphase sum near a resonance, see Hazi, 1979a.) In Eqs. (120)–(124) the cross sections are parametric functions of R, held fixed throughout. In the adiabatic nuclear vibration approximation, the cross section for a transition $v_0 \to v$ is determined simply by replacing the T^B matrices in Eqs. (120)–(122) by the matrix element $\langle v | \mathbf{T}^B(R) | v_0 \rangle$ as described in general in Sec. II.D.

The LAB-frame formulation of the static-exchange (SE) approximation follows in similar manner by making the simplification $\alpha = \alpha_0$ and $\Lambda_{\alpha_0} = 0$ (for the case of a closed-shell $^1\Sigma$ target state) in Sec. II.E. The coupled radial equations are those given in Eq. (62), but with the channel index defined by $p = (l, j, v; J)$, or $p = (lj; J)$ if R is kept fixed. These can be solved for all $r \geq 0$, or the frame transformation procedure can be used to match BODY solutions and LAB solutions at the FT boundary. In any case the cross sections are given by Eqs. (52) and (53) with the appropriate simplification. The differential cross section for transitions $j_0, v_0 \to j, v$, averaged over initial m_{j_0} and summed over final m_j, is

$$\left(\frac{d\sigma}{d\Omega}\right)_{vj, v_0 j_0} = \left(\frac{k}{k_0}\right) (2j_0+1)^{-1} \sum_{m_j, m_{j_0}} |f_{vjm_j, v_0 j_0 m_{j_0}}(\mathbf{k}', \mathbf{k}_0)|^2 , \tag{125}$$

which can be expressed in terms of the T matrix, via a little Racah algebra (Arthurs and Dalgarno, 1960) by

$$\left(\frac{d\sigma}{d\Omega}\right)_{vj, v_0 j_0} = \frac{(-1)^{j-j_0}}{4k_0^2(2j_0+1)} \sum_{\lambda=0}^{\infty} A_\lambda P_\lambda(\cos\theta') , \tag{126}$$

where the coefficients are

$$A_\lambda = \sum_\mu Z(l_1 J_1 l_2 J_2; j_0 \lambda) Z(l_1' J_1 l_2' J_2; j\lambda) T(vjl_1', v_0 j_0 l_1; J_1) \times T(vjl_2', v_0 j_0 l_2; J_2)^* . \tag{127}$$

The summation in Eq. (127) includes all values of $\mu = (l_1 l_2 l_1' l_2' J_1 J_2)$. The Z coefficients are expressed in terms of Clebsch–Gordan and Racah coefficients by

$$Z(abcd; ef) = (-1)^{(f-a+c)/2}[(2a+1)(2b+1)(2c+1)(2d+1)]^{1/2} \times C(acf; 00) W(abcd; ef) . \tag{128}$$

Chandra (1975a) has pointed out that the computation of the A_λ can be simplified by making use of an angular momentum recoupling method of Fano and Dill (1972).

The integral cross section corresponding to Eqs. (125)–(127) is simply

$$\sigma_{jv, j_0 v_0} = \frac{\pi}{k_0^2 (2j_0 + 1)} \sum_{J l l_0} (2J+1) |T(vjl, v_0 j_0 l_0; J)|^2 . \tag{129}$$

If the internuclear separation R is frozen throughout the calculation, then the quantum numbers v_0 and v do not appear, and the cross sections depend parametrically on R.

The static-exchange approximation has been applied to electron–H_2 scattering by Massey and Ridley (1956), Wilkins and Taylor (1967), Ardill and Davison (1968), Tully and Berry (1969), Hara (1969a), Henry and Lane (1969, 1971), Morrison and Collins (1978), and Collins, Robb, and Morrison (1979), and via the R-matrix and T-matrix expansion methods by Schneider (1975a, b), Rescigno, McCurdy, and McKoy (1975b), and Fliflet and McKoy (1978a), respectively. Applications to electron–N_2 scattering include the calculations of Buckley and Burke (1977), and via the R-matrix and T-matrix expansion methods, those of Morrison and Schneider (1977) and Fliflet, Levin, Ma, and McKoy (1978). Applications to electron–F_2 scattering include the R-matrix calculation of Schneider and Hay (1976) and a "low-l spoiling" angular-momentum-decoupled approximation via the T-matrix expansion method by Rescigno, Bender, McCurdy, and McKoy (1976). Similar angular-momentum-decoupling approximations have been applied to electron–H_2 scattering by Morrison and Lane (1975) and McCurdy, Rescigno, and McKoy (1976).

2. Model exchange

A number of approximate models have been developed to simplify the treatment of exchange. What the models have in common is the removal of nonlocality. The exchange operator in Eqs. (116) and (119) is replaced by a simple "local exchange" potential energy function

$$W_{lm, l'm}(r) u_{l'm}(r) \cong V^{\text{ex}}_{lm, l'm}(r) u_{l'm}(r) . \tag{130}$$

This is equivalent to representing the electron–molecule "static-exchange" interaction by an approximate local potential

$$V_{\text{SE}}(\mathbf{r}) = V_S(\mathbf{r}) + V_{\text{ex}}(\mathbf{r}) \tag{131}$$

made up of static and exchange contributions. Recent applications have focused on either the free-electron-gas (FEG) or the semiclassical (SC) exchange models. Only these will be outlined here.

a. Free-electron-gas exchange

The free-electron-gas exchange model is based on the picture of a Fermi gas of noninteracting electrons (Slater, 1960a, b), where the total wave function, made up of plane-wave parts, is antisymmetrized in accordance with the Pauli exclusion principle, and the exchange energy calculated by summing over all momentum states up to the Fermi level. [For discussions of this model applied to electron–molecule scattering, see Hara (1967), Riley and Truhlar (1975), Baille and Darewych (1977a), and Morrison and Collins (1978). The latter authors discuss the connection with the ordinary Hartree–Fock theory and give a concise derivation of the FEG result.] By allowing the density of the electron gas, and thereby the Fermi momentum, to vary with position $\mathbf{r}$, an exchange potential energy is obtained of the form

$$V^{\text{FEG}}_{\text{ex}}(\mathbf{r}) = -(2/\pi) k_F(\mathbf{r}) F[\eta(\mathbf{r})] , \tag{132}$$

where the Fermi momentum is related to the charge density of the unperturbed molecule $\rho(\mathbf{r})$ by

$$k_F(\mathbf{r}) = [3\pi^2 \rho(\mathbf{r})]^{1/3} , \tag{133}$$

and where

$$F[\eta] = \frac{1}{2} + \left(\frac{1-\eta^2}{4\eta}\right) \ln \left|\frac{1+\eta}{1-\eta}\right| \tag{134}$$

with

$$\eta = [K(\mathbf{r})/k_F(\mathbf{r})] . \tag{135}$$

In Eq. (135), Hara (1967) has suggested that the momentum $K(\mathbf{r})$ of the scattered electron should be referred to the same energy base as that of the bound electrons in the gas. Thus the $\mathbf{r}$ variation of $K(\mathbf{r})$ arises from $k_F(\mathbf{r})$ according to

$$[K(\mathbf{r})]^2 = k^2 + [k_F(\mathbf{r})]^2 + 2I , \tag{136}$$

where I is the ionization potential energy of the molecule (in a.u.).

This version of the FEG exchange potential, i.e., Eq. (132), depends on the incident electron energy through Eq. (136). A much simpler exchange potential, viz., that used in standard $X\alpha$ applications (see, for example, Dill and Dehmer, 1977), is derived by averaging the function $F[\eta(\mathbf{r})]$ in some manner over energy, and in the present case, $\mathbf{r}$. One obtains the simple result

$$V^{X\alpha}_{\text{ex}}(\mathbf{r}) = -(3/2\pi)\alpha_x [3\pi^2 \rho(\mathbf{r})]^{1/3} , \tag{137}$$

where for bound-state applications the value $\alpha_x = 1$ was suggested by Slater (1951, 1960b). The value $\alpha_x = \frac{2}{3}$ was obtained in a somewhat different manner by Gaspar (1954), Kohn and Sham (1965), and Cowan *et al.* (1966). (See the review by Lindgren and Rosen, 1974.) In electron scattering there is no "correct" value for the parameter α_x. The procedure leading to Eq. (132) is already based on a rather crude approximation to the exchange interaction, and the averaging that leads to Eq. (137) is inappropriate for the continuum (Hara, 1967; and Riley and Truhlar, 1975). In Eq. (137) the parameter α_x should properly be considered an "adjustable parameter."

b. Semiclassical exchange

A semiclassical exchange approximation has been derived by Riley and Truhlar (1975) similar in spirit to the work of Furness and McCarthy (1973). (See also Lewis *et al.*, 1974.) By assuming that the exchange integral in Eq. (110) can be written

$$\int d\mathbf{r}'\phi_i(\mathbf{r}')\frac{1}{|\mathbf{r}-\mathbf{r}'|}F(\mathbf{r}')=A(\mathbf{r})F(\mathbf{r}), \tag{138}$$

where $A(\mathbf{r})$ is local and slowly varying in $\mathbf{r}$, and that the "local kinetic energy"

$$\tfrac{1}{2}[k(\mathbf{r})]^2 \equiv [\tfrac{1}{2}k^2 - V_S(\mathbf{r}) - V_{\mathrm{ex}}(\mathbf{r})] \tag{139}$$

is large so that an expansion of $A(\mathbf{r})$ in inverse powers of $[k(\mathbf{r})]^2$ can be truncated at the first term, the authors obtain

$$V_{\mathrm{ex}}^{\mathrm{SC}}(\mathbf{r}) = \tfrac{1}{2}[k^2/2 - V_S(\mathbf{r})] - \tfrac{1}{2}\{[k^2/2 - V_S(\mathbf{r})]^2 + \beta^2\}^{1/2}, \tag{140}$$

where (for closed-shell targets)

$$\beta^2 = 4\pi\rho(\mathbf{r}). \tag{141}$$

A high-energy exchange (HE) approximation is derived from Eq. (140) by dividing through by the first term, expanding the radical and truncating at the first term, viz.,

$$V_{\mathrm{ex}}^{\mathrm{HE}}(\mathbf{r}) = -\frac{2\pi\rho(\mathbf{r})}{k^2 - 2V_S(\mathbf{r})}. \tag{142}$$

Riley and Truhlar (1975) also suggest exchange approximations for open shells and inelastic scattering [see also Riley and Truhlar (1976) and Truhlar and Mullaney (1978)] as well as a number of other approximations linking their exchange treatment with those of Bonham (1962), Ochkur (1964), Rudge (1965a, b and 1973) and others. The authors give detailed comparisons for electron–He and Ar scattering where both the SC and the FEG potentials give phase shifts accurate to a few percent over a wide energy range (see related study by Baille and Darewych, 1977a).

An assessment of the accuracy of the exchange approximations described here is difficult; it requires careful comparison between model results and the results of accurate static-exchange calculations. Examples of application to electron–molecule scattering will be given in the applications sections.

3. Polarization

An electron correlation effect found to be particularly important in low-energy electron scattering is polarization. When an electron (or any charged particle for for that matter) slowly approaches the target atom or molecule, the bound electrons are influenced by the electric field of the external charge, and an adiabatic redistribution of bound electronic charge density occurs, resulting in an (induced) dipole moment on the target molecule. The adiabatic change in energy due to the slow approach of the electron exhibits the asymptotic form

$$V_p(\mathbf{r}) \underset{r\to\infty}{\simeq} -\frac{\alpha(\hat{r})}{2r^4}, \tag{143}$$

where the polarizability $\alpha(\hat{r})$ depends on the direction of the external electric field and hence the position vector of the electron. Equation (143) represents a dipole approximation and breaks down as the electron closely approaches the molecule. Moreover, the adiabatic picture breaks down at high energies and near the nuclei, where the electron has a large "local kinetic energy."

From the point of view of a close-coupling description, e.g., the fixed-nuclei expansion (24) and coupled equations (26), this polarization effect is manifested in the *virtual* excitation of excited electronic states that are energetically inaccessible at low energies, i.e., energies below the first electronic threshold (Castillejo, Percival, and Seaton, 1960). While it is not possible to include all these important channels directly, it is possible to handle them indirectly by including *pseudostates* in the close-coupling expansion, specifically chosen as to allow for polarization. This technique is commonly employed in electron–atom scattering (see discussion by Bransden and McDowell, 1977). Correlation effects may be systematically included in the R-matrix method by using a sufficiently flexible basis set, although to accomplish this inside the R-matrix boundary $r = a_c$ could require an uncomfortably large value of a_c (Schneider, 1977b). In the T-matrix expansion method correlation effects are included by choosing a suitably modified optical potential which may be corrected by means of perturbation theory (Kaldor and Klonover, 1977; Klonover and Kaldor, 1978 and 1979a, b, c).

The polarized orbital (PO) method of Temkin (1957) and Temkin and Lamkin (1961) is particularly appealing for slow collisions since it involves forming the adiabatic wave function for the perturbed target system [see review of Drachman and Temkin (1972) and Duxler *et al.* (1971)] by a perturbation or variational approach. The elastic scattering then is determined with respect to this perturbed target state. Only a brief description of this approach will be given here. Consider the fixed-nuclei Schrödinger equation for the target electronic state given by Eq. (20), where the target electronic Hamiltonian is given by Eq. (15). As the starting point in the PO method, we assume that the ground-state target molecule is perturbed by an external stationary electron located at $\mathbf{r}$. We obtain for the perturbed ("polarized") target states, the equation (suppressing R for the moment)

$$[H_m^{(e)} + V_{em}(\mathbf{r},\mathbf{r}_m) - E_0^{(p)}(\mathbf{r})]\psi_0^{(p)}(\mathbf{r}_m;\mathbf{r}) = 0, \tag{144}$$

where a parametric dependence on $\mathbf{r}$ occurs in the perturbed energy $E_0^{(p)}$ and the wave function $\psi_0^{(p)}$ of the target. Asymptotically, the perturbed energy exhibits the expected behavior, and a "polarization potential" energy can be defined such that

$$V_0^{(p)}(\mathbf{r}) \equiv E_0^{(p)}(\mathbf{r}) - E_0^{(e)} - V_S(\mathbf{r}) \underset{r\to\infty}{\simeq} -\frac{\alpha(\hat{r})}{2r^4} \tag{145}$$

where $\alpha(\hat{r})$ is the polarizability of the molecule, $E_0^{(e)}$

is the unperturbed ground-state energy, and V_S is the static potential. In order to partially correct for nonadiabatic behavior when the electron closely approaches the nuclei, Temkin (1957) suggested for the electron–atom problem that the interaction V_{em} be set to zero, via a step function, whenever the scattered electron is inside the bound electron. This weakens the polarization potential at small r, as a rigorous nonadiabatic correction would be expected to do. If this device is *not* employed, then it is important to calculate the correction energy, given to first order by

$$\Delta V_0^{(p)}(\mathbf{r}) = -\tfrac{1}{2}\langle \psi_0^{(p)}(\mathbf{r}_m;\mathbf{r})|\nabla_r^2|\psi_0^{(p)}(\mathbf{r}_m;\mathbf{r})\rangle\,, \tag{146}$$

where the integration is taken over all target electronic coordinates $\mathbf{r}_m$. The correction $\Delta V_0^{(p)}$, which is added to $V_0^{(p)}(\mathbf{r})$, is positive and falls off as r^{-6} asymptotically (Dalgarno and Lewis, 1956). Callaway *et al.* (1968) have shown the correction to be large in electron-He scattering. There have been a few applications of the PO method to electron–H_2 scattering (Hara 1969a, b; Lane and Henry, 1968; and Henry and Lane, 1969, 1971) where Temkin's cutoff procedure is used. However, the first application of the PO method to electron–molecule scattering was the calculation of the electron–H_2^+ differential cross section by Temkin and Vasavada (1967), followed by the extended calculations of Temkin, Vasavada, Chang, and Silver (1969). (See the discussion in Golden, Lane, Temkin, and Gerjuoy, 1971.) Adiabatic polarization potentials for N_2 have been calculated by Morrison and Hay (1979) and by Eades, Truhlar, and Dixon (1979); for N_2 and CO by Truhlar and Van-Catledge (1978); and for Li_2 by Dixon, Eades, and Truhlar (1979).

A polarization model often employed entails the use of a parametrized cutoff polarization potential. One form frequently used is (in a.u.)

$$V_{\rm POL}(\mathbf{r}) = -\frac{\alpha(\hat{r})}{2r^4}\left[1-\exp\left(-\frac{r}{r_p}\right)^n\right], \tag{147}$$

where the popular choice $n=6$ provides a rather steep cutoff for $r<r_p$. For a linear molecule, the polarizability may be expressed as

$$\alpha(\theta) = \alpha_0 + \alpha_2 P_2(\cos\theta)\,, \tag{148}$$

where, in terms of the polarizabilities parallel ($\alpha_\parallel$) and perpendicular ($\alpha_\perp$) to the internuclear axis, the "spherical" and "nonspherical" polarizabilities are given by

$$\alpha_0 = \tfrac{1}{3}(\alpha_\parallel + 2\alpha_\perp)\,, \tag{149}$$

and

$$\alpha_2 = \tfrac{2}{3}(\alpha_\parallel - \alpha_\perp)\,, \tag{150}$$

in atomic units (a_0^3). The cutoff parameter r_p in Eq. (147) is usually varied to examine sensitivity, and then either determined semiempirically (e.g., to "tune" the position of a resonance) or arbitrarily assigned some "reasonable" value. It should be noted that, in contrast to this model procedure, Temkin's polarized orbital method does not involve an adjustable parameter. A number of examples of both methods will be given in the applications sections.

4. Pseudopotential methods

In the pseudopotential method, one usually replaces the short-range static, exchange, and correlation effects by an "effective potential" (often repulsive for ground-state targets) that includes some contribution from kinetic as well as potential energy. The pseudowave function that satisfies this "effective" Schrödinger equation tends to be small at small r, but has the correct asymptotic behavior. Following Tully (1969) we write the fixed-nuclei Schrödinger equation for the electron-plus-target system as

$$(T+V-E)\Psi = 0\,, \tag{151}$$

where T and V represent the sum of kinetic-energy operators, and the full electrostatic potential energy of the system, respectively. (Note: In the one-electron approximation, $T=-\frac{1}{2}\nabla_r^2$, and V represents the one-electron static-exchange interaction.) Let us assume that bound-state solutions exist for Eq. (151), described by eigenfunctions Ψ_j of the same symmetry as Ψ and corresponding to eigenenergies E_j. According to Phillips and Kleinman (1959), a pseudowave function $\tilde{\Psi}$ can be defined by

$$\tilde{\Psi} = \Psi + \sum_{j=1}^{c} \beta_j \Psi_j\,, \tag{152}$$

which satisfies

$$(T+V+V_R-E)\tilde{\Psi} = 0\,, \tag{153}$$

where $V+V_R$ is called the "effective potential," and the "pseudopotential" V_R is defined by

$$V_R\Psi = \sum_{j=1} \beta_j (E-E_j)\Psi_j\,. \tag{154}$$

Tully (1969) suggests that in Eq. (154) the core energies E_j be replaced by H since only approximate Ψ_j are normally available. Since the correct Ψ is orthogonal to the Ψ_j, the β_j are just the overlaps $\langle\tilde{\Psi},\Psi_j\rangle$, and are completely arbitrary. Usually, the β_j are chosen so that $\tilde{\Psi}$ is small close to the target. With this choice, approximations made there in treating correlation and, perhaps, exchange effects in the solution of Eq. (153) will not give rise to large errors. Once $\tilde{\Psi}$ is obtained, then if Ψ is required for all space, it can be determined by orthogonalizing $\tilde{\Psi}$ to all of the Ψ_j. Of course, $\tilde{\Psi}\to\Psi$ as $r\to\infty$. The assumption in Tully's generalization of pseudopotential theory to the multielectron problem is that bound states of the full Hamiltonian do indeed exist. If there are no bound states, then other alternatives are possible including: (1) Eqs. (151)–(154) may be applied in the one-electron approximation, where V becomes an optical potential, or in the static-exchange approximation, the Hartree–Fock potential; or (2) the Ψ_j in the many-electron problem may be chosen as the variational eigenfunctions that result in an ordinary configuration interaction (or other equivalent linear variational) calculation applied to the electron-plus-target system. The first alternative is the traditional one-electron pseudopotential method [see, for example, Schneider and Berry (1969) and Schneider, Weinberg, Tully, and Berry (1969)]. The second alternative is the "generalized pseudopotential method" proposed by Zarlingo, Ishihara, and Poe (1972) and applied to electron–H scattering. These authors suggest that this method may be particularly effective in applications to inelastic scattering.

Tully's multielectron extension of the pseudopotential method is based on the assumption that near the target atom or molecule the electron's motion is rather independent of the type of state it is in. Therefore, the Ψ_j in Eq. (152) can be expected to account for complicated short-range correlation effects, provided E is not appreciably larger than $|E_j|$ for the higher-energy states included in Eq. (152). Zarlingo *et al.* (1972) adopt the same point of view, but suggest that variational "quasibound-state" approximations to the continuum also qualify as appropriate choices for Ψ_j. Moreover, these authors propose generalization to inelastic processes and higher energies. These and related methods still hold promise for electron–molecule scattering and molecular photodetachment and photoionization processes, but applications are slow in coming.

Burke and Chandra (1972) have applied a modified version of one-electron pseudopotential theory to electron–N_2 elastic scattering and rotational excitation (Chandra and Burke, 1973). Chandra and Temkin (1976a, b, c) have applied the same technique to vibrational excitation in electron–N_2 collisions. Briefly, the idea is to replace the exchange interaction by an orthogonalization constraint. If we rewrite Eq. (153), here considered as a one-electron equation for an electron in the field of a *closed-shell target* as

$$\begin{aligned}(T+V-E)\tilde{\Psi} &= -V_R\tilde{\Psi}\\ &= -\sum_j^c \beta_j(E-E_j)\Psi_j\\ &= -\sum_j^c \lambda_j\Psi_j\,, \end{aligned} \tag{155}$$

and treat the λ_j as Lagrangian multipliers, solutions $\tilde{\Psi}$ may be obtained that are constrained to be orthogonal to all the Ψ_j in Eq. (155). If one assumes, then, that the exchange interaction $V_{\text{ex}}=V-V_S$, where V_S is the static potential, primarily influences the wave function by forcing this orthogonality, then a reasonable approximation would be the replacement of V by V_S in Eq. (154). The pseudowave function obtained in this way is then an approximation to Ψ. This is the method suggested by Burke and Chandra (1972). The authors admit that this is likely to be a crude approximation. Indeed, Riley and Truhlar (1976), in a model study, find the method to be inaccurate. It should also be noted that this procedure is *not* in the spirit of the pseudopotential method discussed in the first part of the section. There the pseudowave function $\tilde{\Psi}$ was *not* constrained to be orthogonal to the Ψ_j; in fact, the philosophy was to choose the β_j in Eqs. (152) and (154) so that $\tilde{\Psi}$ remains small close to the target. The true wave function Ψ and the Burke–Chandra wave function are *not* particularly small near the target. It is appropriate to consider the Burke–Chandra method an exchange "model." It does take into account an important feature (orthogonalization) of the exchange orbital of the same symmetry as the scattering orbital of interest. Lippmann and Schey (1961) have discussed this approximation in connection with electron–atom scattering and have emphasized that the orthogonality constraint does ensure that the elastic-scattering phase shifts (eigenphase shifts for the electron–molecule problem) have the correct low-energy behavior, as specified by an extension of Levinson's theorem. Swan (1955) has shown (for the case of spherical symmetry) that the phase shifts approach $(n+m)\pi$ in the zero-energy limit, where for a given symmetry n is the number of true bound states of the electron-plus-target system and m is the number of (one-electron) states from which the scattered electron is excluded by the Pauli exclusion principle. For a discussion of nonspherical potentials see Newton (1977) and Osborn and Bollé (1977).

Recent calculations by Collins, Robb, and Morrison (1979) and Collins, Robb, and Norcross (1979) indicate that the best results are obtained when both orthogonalization constraints and a local exchange potential are employed.

H. Weak-scattering approximations

1. Method of distorted waves

The method of distorted waves (DW) is basically a "weak coupling" approximation. It is useful when real and "virtual" transitions between different states of the molecule are improbable. In that case, the coupled equations (11) arising from the "coupled-states" expansion (10) can be solved by perturbation methods. Consider the transition $0\rightarrow n$. If the coupling is weak, a reasonable zeroth-order assumption is to ignore all terms on the right-hand side of Eq. (11) except the single term $n'=0$. Thus the initial-state scattering function satisfies

$$\{\nabla_{\mathbf{r}}^2+k_0^2-2[V_{00}(\mathbf{r})+W_{00}(\mathbf{r})]\}F_0(\mathbf{r})=0\,, \tag{156}$$

where from Eq. (13)

$$F_0(\mathbf{r})\underset{r\to\infty}{\simeq}\exp(i\mathbf{k}_0\cdot\mathbf{r})+\frac{1}{r}\exp(ik_0r)f_{00}(\mathbf{k}_0',\mathbf{k}_0)\,, \tag{157}$$

and each of the possible final-state scattering functions satisfy inhomogeneous, but uncoupled, equations

$$\begin{aligned}&\{\nabla_{\mathbf{r}}^2+k_n^2-2[V_{nn}(\mathbf{r})+W_{nn}(\mathbf{r})]\}F_n(\mathbf{r})\\ &\quad=2[V_{n0}(\mathbf{r})+W_{n0}(\mathbf{r})]F_0(\mathbf{r})\,,\end{aligned} \tag{158}$$

where from Eq. (13)

$$F_n(\mathbf{r})\underset{r\to\infty}{\simeq}\frac{1}{r}\exp(ik_nr)f_{n0}(\mathbf{k}_n,\mathbf{k}_0)\,. \tag{159}$$

The formal solution to Eq. (158) is

$$F_n(\mathbf{r})=2\int d\mathbf{r}'G_n(\mathbf{r},\mathbf{r}')[V_{n0}(\mathbf{r}')+W_{n0}(\mathbf{r}')]F_0(\mathbf{r}')\,, \tag{160}$$

where $G_n(\mathbf{r},\mathbf{r}')$ is the final-state Green function, defined by the equation

$$\{\nabla_{\mathbf{r}}^2+k_n^2-2[V_{nn}(\mathbf{r})+W_{nn}(\mathbf{r})]\}G_n(\mathbf{r},\mathbf{r}')=\delta(\mathbf{r}-\mathbf{r}') \tag{161}$$

and the asymptotic condition

$$G_n(\mathbf{r},\mathbf{r}')\underset{r\to\infty}{\simeq}\frac{1}{r}\exp(ik_nr)\mathfrak{F}_n(\mathbf{k}_n,\mathbf{k}_0;\mathbf{r}') \tag{162}$$

where $\mathfrak{F}_n$ is a well-behaved function in $\mathbf{r}'$ (Mott and Massey, 1965). The scattering amplitude for the $0 \to n$ transition, therefore [from Eqs. (159), (160), and (162)], becomes

$$f_{n0}^{\mathrm{DW}}(\mathbf{k}_n, \mathbf{k}_0) = 2 \int d\mathbf{r}' \mathfrak{F}_n(\mathbf{k}_n, \mathbf{k}_0; \mathbf{r}')[V_{n0}(\mathbf{r}') + W_{n0}(\mathbf{r}')]F_0(\mathbf{r}') . \tag{163}$$

The formulation leading to Eq. (163) is based on a three-dimensional description of the "distorted-wave" functions $F_0(\mathbf{r})$ and $\mathfrak{F}_n(\mathbf{k}_n, \mathbf{k}_0; \mathbf{r}')$. A partial-wave DW approximation can also be formulated in which weak coupling of different partial waves as well as molecular states is assumed. This is a much more severe approximation, and one that is valid in only very special circumstances (Arthurs and Dalgarno, 1960). An important application of the partial-wave DW approximation to rotational excitation in electron–H_2 scattering by Ardill and Davison (1968) first demonstrated the importance of exchange for this process.

A somewhat more sophisticated version of the DW approximation than that described here has been applied to electronic excitation of H_2 by Rescigno, McCurdy, and McKoy (1975b), and Rescigno, McCurdy, McKoy, and Bender (1976), and of N_2 by Fliflet, McKoy, and Rescigno (1979a) and to dissociation of F_2 by Fliflet, McKoy, and Rescigno (1979b). This prescription for the DW approximation is equivalent to first-order many-body theory (Csanak, Taylor, and Yaris, 1971; and Csanak, Taylor, and Tripanthy 1973) and can be derived from the two-potential formula (Taylor, 1972). It is still a weak-coupling theory, however, and fails when the coupling is strong.

2. Born approximation

If in addition to the approximation of "weak coupling" it is reasonable to ignore the "distortion potentials" $V_{00}(\mathbf{r}) + W_{00}(\mathbf{r})$ in Eq. (156) and $V_{nn}(\mathbf{r}) + W_{nn}(\mathbf{r})$ in Eq. (158), the DW approximation reduces to the (first) Born approximation (Mott and Massey, 1965; Massey, 1969). The Green function of Eqs. (161) and (162) reduces, then, to the free-particle form

$$G_n(\mathbf{r}, \mathbf{r}') = -\frac{1}{4\pi} \frac{\exp(ik_n|\mathbf{r} - \mathbf{r}'|)}{|\mathbf{r} - \mathbf{r}'|} \tag{164}$$

$$\underset{r \to \infty}{\simeq} -\frac{1}{4\pi r} \exp(ik_n r) \exp(-i\mathbf{k}_n \cdot \mathbf{r}') . \tag{165}$$

Identifying the function $\mathfrak{F}_n$ from Eqs. (162) and (165) and approximating $F_0(\mathbf{r}')$ by a plane-wave function, we obtain for the scattering amplitude the familiar expression (ignoring the exchange term)

$$f_{n0}^{B}(\mathbf{k}_n, \mathbf{k}_0) = -\frac{1}{2\pi} \int d\mathbf{r}' \exp(-i\mathbf{K} \cdot \mathbf{r}') V_{n0}(\mathbf{r}') , \tag{166}$$

where the momentum-transfer vector is defined by

$$\mathbf{K} = \mathbf{k}_n - \mathbf{k}_0 . \tag{167}$$

The Born approximation is usually considered to be a high-energy approximation, valid only when the energies k_0^2 and k_n^2 in Eqs. (156) and (158) are much larger than the potentials, and there have been many applications to electronic excitation, dissociation, and ionization of molecules by fast electrons (Massey, 1969). Exchange effects can be included via the Born–Oppenheimer (BO) approximation, which corresponds to including the exchange operator $W_{n0}(\mathbf{r}')$ in Eq. (166), or the simpler approximations of Ochkur (1964) and Rudge (1965a, b) [Mott and Massey (1965); see also Rudge (1973), and Bransden and McDowell (1977)]. The Born approximation may also be formulated in terms of partial waves, by simply expanding each of the plane-wave functions $\exp(-i\mathbf{k}_n \cdot \mathbf{r}')$ from Eq. (165) and $F_0(\mathbf{r}') = \exp(i\mathbf{k}_0 \cdot \mathbf{r}')$ in terms of spherical harmonics. The Born T-matrix elements for higher-order partial waves are often accurate even at relatively low energies since the centrifugal barriers prevent penetration into the region of configuration space where the interactions are strong. Use of the Born results for large values of l is an efficient procedure and one that is widely used in applications.

a. Rotational excitation

Rotational excitation of molecules near threshold is dominated by long-range electron–molecule interactions. Massey (1931) argued that for low-energy electron scattering from a polar molecule the long-range interaction will dominate so that the electron will be only weakly perturbed during the collision and, therefore, that the Born approximation should be valid in the threshold region. We will restrict the discussion here to linear molecules in Σ electronic states. Taking the electron–molecule interaction to be approximated by the dipole term

$$V_{em}(\mathbf{r}) \cong -\frac{d}{r^2} \cos\theta , \tag{168}$$

where d is the dipole moment (in a.u.) and θ is the angle between $\mathbf{r}$ and the internuclear axis $\mathbf{R}$, the differential cross section for a rotational transition $j_0 \to j$, summed over final m_j and averaged over initial m_{j_0}, is (Crawford, Dalgarno, and Hayes, 1967)

$$\left(\frac{d\sigma}{d\Omega}\right)^{B}_{j_0 \to j} = \left(\frac{4}{3} d^2\right) (2j_0 + 1)^{-1} \begin{Bmatrix} j_0 + 1 \\ j_0 \end{Bmatrix} \left(\frac{k_j}{k_0}\right) K^{-2} , \tag{169}$$

where the upper (lower) factor in curly brackets refers to the case $j_0 \to j_0 + 1$ $(j_0 - 1)$, and where K is related to the (LAB-frame) scattering angle θ' by

$$K^2 = k_j^2 + k_0^2 - 2k_j k_0 \cos\theta' . \tag{170}$$

The selection rule $j_0 \to j_0 \pm 1$ applies in this approximation. The corresponding integral cross section is

$$\sigma^{B}_{j_0 \to j} = \left(\frac{8\pi d^2}{3k_0^2}\right) (2j_0 + 1)^{-1} \begin{Bmatrix} j_0 + 1 \\ j_0 \end{Bmatrix} \ln\left[\frac{k_0 + k_j}{|k_0 - k_j|}\right] , \tag{171}$$

and the momentum-transfer cross section is

$$\sigma^{(m)B}_{j_0 \to j} = \left(\frac{8\pi d^2}{3k_0^2}\right) (2j_0 + 1)^{-1} \begin{Bmatrix} j_0 + 1 \\ j_0 \end{Bmatrix} \times \left(1 - \frac{(k_j - k_0)^2}{2k_j k_0} \ln\left[\frac{k_0 + k_j}{|k_0 - k_j|}\right]\right) . \tag{172}$$

We note that the differential cross section given by Eq. (169) is well behaved at all scattering angles and the integral and momentum-transfer cross sections, given by Eqs. (171) and (172), respectively, are finite at all energies. However, in the (mathematical) limit where the moment of inertia of the molecule I approaches infinity (fixed nuclear rotation limit), the rotational energy-level separation vanishes so that $k_j \to k_0$. In this limit, the differential cross section of Eq. (169) diverges in the "forward direction" $\theta' \to 0$, and the integral cross section given by Eq. (171) is undefined. These results are not artifacts of the Born approximation; they occur in the exact fixed-nuclei treatment as well (Garrett, 1971c). The momentum-transfer cross section given by Eq. (172) remains finite. These observations suggest that the validity of a fixed-nuclei (in particular, fixed-nuclear-rotation) approach to electron scattering from *polar* molecules is questionable [see reviews by Garrett (1972) and Itikawa (1978)].

For the case of electron scattering from nonpolar molecules, such problems do not occur. Taking the electron–molecule interaction to be approximated by the quadrupole term

$$V_{em}(\mathbf{r}) \cong -\frac{Q}{r^3}P_2(\cos\theta), \tag{173}$$

where Q is the quadrupole moment and θ is defined as before, the Born approximation to the integral cross section for transitions $j_0 \to j_0 \pm 2$ is (Gerjuoy and Stein 1955a, b)

$$\sigma^B_{j_0\to j} = \left(\frac{8\pi Q^2}{15}\right)\left(\frac{k_j}{k_0}\right)B_{j_0\to j} \tag{174}$$

where

$$\left.\begin{aligned} B_{j_0\to j_0+2} &= \frac{(j_0+2)(j_0+1)}{(2j_0+3)(2j_0+1)} \\ B_{j_0\to j_0-2} &= \frac{j_0(j_0-1)}{(2j_0-1)(2j_0+1)} \end{aligned}\right\}, \tag{175}$$

where the selection rules $j_0 \to j_0 \pm 2$ apply. Dalgarno and Moffett (1963) have extended this treatment to include the nonspherical polarization interaction. Rahman, Gianturco, and Lamanna (1978) give results for the amplitude obtained by applying the Glauber approximation to the pure quadrupole interaction.

b. Vibrational excitation

The validity of the Born approximation for low-energy vibrational excitation is less clear. However, when the cross section near threshold is dominated by long-range dipole or quadrupole interactions, such an approach may be reasonable (see Takayanagi, 1965a, b, 1966, and 1972). The expressions for the differential and integral cross sections for transitions $v_0, j_0 \to v, j$ are obtained by making the replacements

$$d \to \langle v|d(R)|v_0\rangle, \tag{176}$$

and

$$Q \to \langle v|Q(R)|v_0\rangle, \tag{177}$$

and

$$k_j^2 \to k_{vj}^2 \tag{178}$$

in Eqs. (169)–(175), where the dependence of the dipole and quadrupole moments on internuclear separation is explicit in Eqs. (176) and (177). Since the vibrational energy-level separation is so much larger than that for rotational states, it is a very good approximation to ignore the j dependence of k_{vj}^2 (corresponding to the fixed-nuclear-rotation limit $I \to \infty$). Then, summing Eq. (169) over final rotational states, we see that cross sections for transitions $v_0 \to v$ can be defined by

$$\left(\frac{d\sigma}{d\Omega}\right)^B_{v_0\to v} = \frac{4}{3}|\langle v|d|v_0\rangle|^2\left(\frac{k_v}{k_0}\right)K^{-2}, \tag{179}$$

where $K^2 = k_v^2 + k_0^2 - 2k_vk_0\cos\theta'$,

$$\sigma^B_{v_0\to v} = \frac{8\pi}{3k_0^2}|\langle v|d|v_0\rangle|^2 \ln\left[\frac{k_0+k_v}{|k_0-k_v|}\right], \tag{180}$$

and

$$\sigma^{(m)B}_{v_0\to v} = \frac{8\pi}{3k_0^2}|\langle v|d|v_0\rangle|^2\left(1-\frac{(k_v-k_0)^2}{2k_vk_0}\ln\left[\frac{k_0+k_v}{|k_0-k_v|}\right]\right). \tag{181}$$

We note that the differential cross section given by Eq. (179) does not diverge in the "forward direction" $\theta' \to 0$ since K remains finite, and the integral and momentum-transfer cross sections, given by Eqs. (180) and (181), respectively, are both well defined.

III. APPLICATIONS

A. Introduction

The ultimate test of a theory, of course, is how well it describes the physical phenomena. In principle, this is determined by comparison with experimental measurement. However, measurements always contain some error, and often the amount of error is not well known. So, progress in understanding requires that theory and experiment proceed hand in hand. Error in theoretical calculation usually arises from approximations made in solution of the Schrödinger equation. The approximations are of two basic types: (1) An approximate Hamiltonian is formed by replacing terms in the true Hamiltonian by approximate representations, or (2) an approximate (e.g., variational) solution is sought using the true Hamiltonian. In most actual applications there are elements of both. For example, the frame transformation procedure assumes that H_{ROT} and H_{VIB} can be neglected entirely in the inner region. Then, in the inner region a (fixed-nuclei) calculation, say of the R matrix, is carried out using a limited basis set of some variety. In the exterior region, the transformed (BODY to LAB) R matrix is then propagated into the asymptotic region. However, only a finite number of channels, hence target states, can be considered, so that some truncation is necessary. The resulting errors are not always easy to estimate.

In order to help organize the discussion in the following sections, it is useful to rather arbitrarily divide theory into two areas: *ab initio* calculations and model studies. There is a good deal of overlap between these so that the distinctions are not clearly drawn. However, most theoretical investigations do possess a primary focus that will roughly characterize a particular study. It is important to recognize that the immediate objectives of all studies are not the same. If one judges a careful *ab initio* calculation of elastic electron–N_2 scattering in the static-exchange approximation by how well the cross section agrees with experiment, the value of the work will be totally missed.

In a true *ab initio* treatment one attacks the full Schrödinger equation (containing the true Hamiltonian) using approximate methods of solution that can be systematically tested for accuracy and improved to obtain convergence to the exact result. The lack of convenient bound principles in the continuum explains to a considerable extent the difficulty of carrying out accurate *ab initio* calculations of electron–molecule scattering wave functions and observable cross sections. At the current stage of development of this field, it is common practice to "loosely" describe as *ab initio* any treatment that does not involve adjustable parameters, even though it may be based on the neglect of a portion of the true Hamiltonian, or an approximate treatment of correlation, e.g., the polarized-orbital method (see Drachman and Temkin, 1972).

In model studies, complicated exchange and correlation effects are sometimes mocked by simpler "effective interactions," which usually contain one or more adjustable parameters. Then, in solving the simpler (usually one-electron) Schrödinger equation, one is still faced with a need to truncate the number of channels retained. However, the error in truncation of the one-electron problem can be made as small as desired by merely raising the level of computing. Some justifications for a model study (as opposed to *ab initio*) are: (1) the system is too complex for an *ab initio* approach, and a qualitative description is felt to be useful; (2) novel "effective interactions" are being developed and tested on simpler systems for possible application to more complex problems; (3) one wishes to illustrate the dominance of a particular feature such as the long-range dipole interaction in electron–polar-molecule scattering; (4) a simple model is used to help organize, and perhaps interpret, experimental data. The responsibility of members of the theoretical community is to actively participate in this effort to better describe and understand the phenomena. This requires that *ab initio* calculations be performed where they can be reasonably done, and that the phenomenological model studies be pursued in other cases.

B. Electron-H_2 scattering

1. Elastic scattering (H_2)

Hydrogen, with only two electrons, is the simplest neutral molecule, and therefore has received the most theoretical attention. Because the nuclear charges are small and the nuclei rather close together ($R_0 \sim 0.7$ Å) in the ground electronic state, the H_2 molecule is "atomlike," resembling He in terms of the overall "strength" of the electron interaction.

Early theoretical studies by Fisk (1936) showed that only qualitative results could be obtained by representing the electron–molecule interaction by a simple (parametrized) potential energy function. Nagahara (1953, 1954) formulated the electron–molecule elastic scattering problem in the fixed-nuclei approximation and calculated the elastic cross section for H_2, using a realistic static potential energy based on the ground-state charge density. While the results were encouraging, it appears now that the equations were not solved accurately. Massey and Ridley (1956) recognized that exchange effects, known to be important in elastic electron–helium scattering, should play an important role in H_2 as well. They applied the Hulthên and Kohn variational methods (see Moiseiwitsch, 1966; Mott and Massey, 1965) in both the static and static-exchange approximations and showed that the static cross section is much too large at low energies. Just as in the case of electron–helium scattering, the effect of exchange is to lower the elastic cross section at low energies, thereby improving the agreement with experiment (Ramsauer and Kollath, 1930a, b, 1931, and 1932). Since Massey and Ridley (1956) included only the $s\sigma$ partial wave, their cross section is too small at the higher energies. Their results will be discussed later in relation to other early theoretical studies. In a model calculation, Carter, March, and Vincent (1958) also determined that exchange was likely to be important in elastic scattering, although their model was not capable of quantitative accuracy.

a. Static-exchange

In the static-exchange (SE) approximation, the theory incorporates only static and exchange interactions of the electron with the molecule in its *unperturbed* ground electronic state $^1\Sigma_g^+$. There is no allowance for polarization or other correlation effects. Most applications are based on the fixed-nuclei approximation, with the internuclear separation R frozen at its equilibrium value. The elastic cross section calculated in the BODY frame is usually averaged over molecular orientation. [We have seen in Sec. II.D that under conditions such that the adiabatic nuclei approximation is valid, this averaged BODY-frame elastic cross section is equal to the total (elastic plus rotational excitation) cross section in the LAB frame.] Generally, elastic static-exchange cross sections agree only qualitatively with the measurements or with more sophisticated theory. The agreement with experiment tends to be best for the differential cross sections at *large* angles, where short-range interaction dominates.

In the first effort to numerically solve the continuum Hartree–Fock (static-exchange) equations (116) for the electron–H_2 system, Wilkins and Taylor (1967) did verify that including exchange had a large effect on the cross section. However, numerical inaccuracies in results led to the incorrect conclusion that polarization effects, which were neglected in their calculation, were unimportant.

Tully and Berry (1969) solved the two-dimensional static-exchange Schrödinger equation (110) directly, i.e., without introducing the usual partial-wave expansion. The elliptic partial integro-differential equation was solved by finite difference methods. The exchange terms were handled iteratively, and various pseudopotential approximations were tested as starting points in the iterative scheme. It was concluded that the simple Slater free-electron-gas exchange potential given by Eq. (137) was a particularly poor choice. The unperturbed H_2 ground state was represented by the Weinbaum (1933) function. Probable sources of numerical error in this static-exchange calculation are: (1) use of rather large radial step size $\Delta r = 0.2a_0$ and angular step size $\Delta\theta = \pi/30$ in the numerical solution of the Schrödinger equation; (2) error in the self-consistency iteration; and (3) the assumption that at $r \geq 10a_0$, the individual partial waves $s\sigma$, $p\sigma$, $p\pi$, $d\sigma$, and $d\pi$ are fully uncoupled (thus, $s\sigma$-$d\sigma$ coupling is ignored there). The phase shifts and integral (fixed-nuclei) cross sections were calculated at several energies in the range $0.034 \leq E \leq 6.667$ eV. Differential cross sections are presented at $k = 0.3(1.22$ eV), 0.4(2.18 eV), and 0.6(4.90eV), where comparison with early measurements (Ramsauer and Kollath, 1930a, b, 1931, and 1932) showed good agreement at large angles (i.e., $\theta \gtrsim 90°$). At small angles, the static-exchange cross section falls significantly below the measurements. Results will be given later in comparison with other work. In addition to the historical significance of this work, Tully and Berry's results often have been used as a calibration point for testing new methods. However, more accurate static-exchange results are now available [for example, see Collins, Robb, and Morrison (1979), and the Appendix].

In a recent systematic study of various exchange models of possible use in more complicated electron–molecule scattering problems, Morrison and Collins (1978) compared "exact" static-exchange eigenphase shifts and total cross sections for electron–H_2 scattering with the results of several versions of the free-electron-gas (FEG) exchange model. The "exact" static-exchange calculations correspond to the converged self-consistent solutions of Eqs. (113) and (114), or more specifically the coupled integro-differential Eqs. (116) (see the Appendix). The unperturbed H_2 ground state was represented by the Hartree–Fock wave function of Fraga and Ransil (1961) which gives an equilibrium separation of $1.402a_0$ and a quadrupole moment of $0.48ea_0^2$ [the more accurate value obtained by Wolniewicz (1966) is $0.484ea_0^2$]. The numerical solution of the integro-differential equations was accomplished using the computer code of Sinfailam (1970) which treats exchange noniteratively (see Sec. II.G.1). Only $\Sigma_g(m = 0$ and l even) symmetry was considered and partial waves $l = 0$, 2, and 4 were retained in Eq. (115). The static potential was adequately represented by terms $\lambda = 0$, 2, and 4 in the expansion (118) and in the exchange kernel of Eq. (119) reduced by retaining terms $\lambda = 0$ and 2 in an expansion of the bound orbital $\phi_i(\mathbf{r}')$ in spherical harmonics. A set of 20 coupled equations was solved and the K matrix extracted at $r = 10a_0$. Elastic (fixed-nuclei) Σ_g cross sections are compared in Fig. 6. The model-exchange calculations include studies of: (1) the Hara (1967) modification of the FEG local potential "HFEGE" given by Eqs. (132)–(136); (2) a different ("asymptotically adjusted") version of this potential (Riley and Truhlar, 1975) with the ionization potential I in Eq. (136) set to zero so that $K(r) \sim k$ as $r \to \infty$ ("AAFEGE"); and (3) a semiempirical version where I is adjusted so that the cross sections are in agreement with "exact" static-exchange results ("TFEG"). The conclusion for H_2 is that Hara's potential is too weak and the "asymptotically adjusted potential" is too strong. A choice of $I = 0.071$ a.u. in Eq. (136) gives very good agreement with the Σ_g static-exchange results at all energies considered. However, this may not be true for other symmetries. Applications to electron–N_2 and electron–CO_2 scattering will be discussed in the appropriate sections.

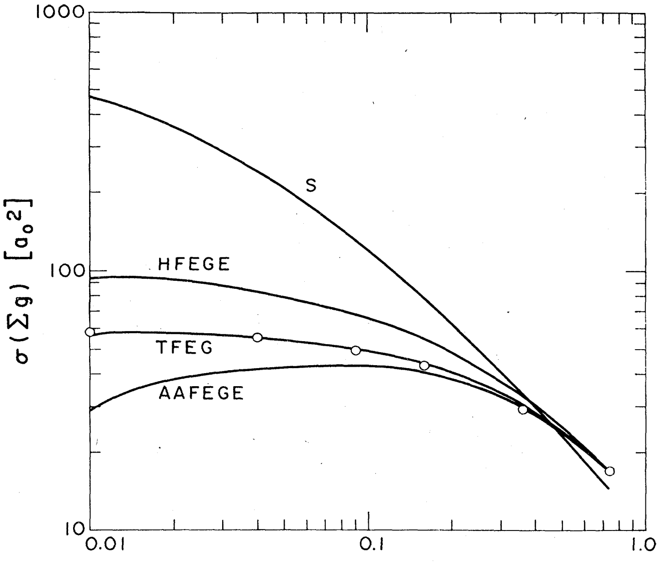

FIG. 6. Cross sections for e–H_2 scattering in the static approximation S and three model exchange calculations (solid curves). The open circles are converged exact static-exchange cross sections. The three FEG exchange potentials were recalculated at each scattering energy using $I(H) = 0.564$ a.u., $I(A) = 0.0$ a.u., and $I(T) = 0.071$ a.u. (Reprinted from Morrison and Collins, 1978.)

Baille and Darewych (1977b), in a similar study of model-exchange approximations in electron–H_2 scattering, also include the effects of polarization via the polarization potential of Lane and Henry (1968). In addition to the FEG potentials they consider the semiclassical exchange (SCE) approximation of Riley and Truhlar (1975). They conclude that the SCE model is superior to the various versions of the FEG model, but that even this potential fails for energies $E \lesssim 6$ eV. They note an apparent discrepancy between their "HFEGE" cross sections and those of Morrison and Collins (1978). However, the differences are quite consistent with the fact that the latter authors consider only Σ_g symmetry and do not include polarization. The effect of adding in the polarization potential is to decrease the low-energy Σ_g cross sections and increase the Σ_u cross sections. The semiempirical adjustment of Morrison and Collins (1978) could well bring the total cross section of Baille and Darewych (1977b) into agreement with the adiabatic–exchange result.

Before describing the early efforts to go beyond the static-exchange approximation by including polarization corrections, it is appropriate here to review recent applications of new methods of treating the electron–molecule scattering problem. The pilot calculations are always carried out in the static-exchange approximation, so that comparison can be made with accurate static-exchange results. In discussing these recent studies, it is important to keep in mind that the immediate goal is development of new methods that *eventually* will lead to more accurate or more efficient calculations (or both) of scattering cross sections for more complicated processes involving more complex molecules.

Schneider (1975a, b) was the first to apply R-matrix theory (see Sec. II.F) to an electron–molecule scattering problem. He calculated elastic fixed-nuclei cross sections for electron–H_2 scattering in the static-exchange approximation. The general R-matrix theory is discussed in Sec. II.F.1. Since Schneider chose to work in two-center spheroidal coordinates, his equations are somewhat different from those discussed in Sec. II.F.1 but the theory is essentially the same (Schneider, 1974). In these early calculations, the Hamiltonian was approximated by the one-electron static-exchange Hamiltonian of Eqs. (113) and (114), and a Gaussian basis set was used for the diagonalization of $H^{(e)}+L_b$ and the representation of the amplitudes in Eq. (99). The evaluation of integrals over the finite region of space within the R-matrix boundary is the most time-consuming part of the calculation. This step was streamlined by introducing an auxiliary basis set of ordinary Gaussians $\langle\alpha|$ that, in principle, span all of space. The matrix elements $\langle\alpha|V|\beta\rangle$, etc., are then identical to those encountered in an ordinary molecular structure calculation and are evaluated by standard optimized techniques. In all, Schneider used 60 ordinary and 60 floating Gaussians in the static-exchange calculation. He found that the inclusion of p as well as s orbitals centered on the two nuclei was necessary in order to accurately describe the d-wave contributions to Σ_g and Π_g symmetries and the p-wave contributions to Σ_u and Π_u symmetries, especially at the higher energies of the range studied ($0 \lesssim E \lesssim 13.6$ eV). The effects of the Buttle correction (see Sec. II.F.1) were found to be small, but were included except near a pole of the unperturbed Hamiltonian (chosen as $-\frac{1}{2}\nabla_r^2$), where they were judged to be inaccurate. In the outer region, outside the R-matrix boundary, the phase shifts were obtained by matching the R-matrix to a set of single-channel solutions numerically integrated inward from infinity, by means of the Numerov method. Coupling of partial waves due to the electron–quadrupole interaction was ignored in the outer region. Integral elastic cross sections (in the static-exchange approximation) were given for energies in the range $0 \lesssim E \lesssim 13.6$ eV. Differential cross sections were calculated for $k=0.2(0.54$ eV), 0.3(1.22 eV), 0.5(3.4 eV), 0.6(4.9 eV), and 0.7(6.66 eV). Probable sources of error are: (1) incompleteness of the basis set within the R-matrix boundary; (2) numerical error in the transformation of basis set: (3) neglect of partial-wave coupling in the outer region; and (4) errors in treating the coordinate transformation from spheroidal to spherical at the boundary. A detailed comparison of phase shifts with Tully and Berry (1969) indicates differences in $\eta_{s\sigma}$ ranging from 0.003 rad, at $k=0.05$, to 0.056 rad at $k=0.6$, Schneider's phase shifts being *smaller* at each energy. Differences in $\eta_{p\sigma}$ range from 0.001 rad at $k=0.2$ to 0.024 at $k=0.6$, Schneider's phase shifts being larger at each energy. (See the Appendix.) A comparison of integral (*fixed nuclei*) elastic cross sections is given in Fig. 7. Also shown there are static-exchange results of Hara (1969a), to be discussed, and the measurements of Linder and Schmidt (1971a). The small differences in calculated low-energy phase shifts show up as rather large differences in cross sections. The figure also reminds us that the static-exchange approximation is not even a qualitatively correct physical description of the scattering at low energies. Differential cross sections are compared in Fig. 8 for $k=0.5(3.4$ eV) with the measurements of Linder and Schmidt (1971a). Theoretical static-exchange results of Rescigno, McCurdy, and McKoy (1975a), to be discussed, are also given. The results of Tully and Berry (1969) lie below those of Schneider (1975) as expected from Fig. 7 (see the Appendix). The comparison with experiment shows clearly that while the static-exchange interaction tends to dominate large-angle scattering, it is not sufficient at small angles. Here polarization effects play an important role.

Rescigno, McCurdy, and McKoy (1975a) applied their T-matrix expansion method (Rescigno, McCurdy, and McKoy, 1974a, b) to a *fixed-nuclei* calculation of elastic electron–H_2 scattering in the static-exchange approximation. The purpose of this study was to demonstrate the usefulness of this new method by making comparisons with other static-exchange calculations. The theory has been discussed in Sec. II.F.2. The essential

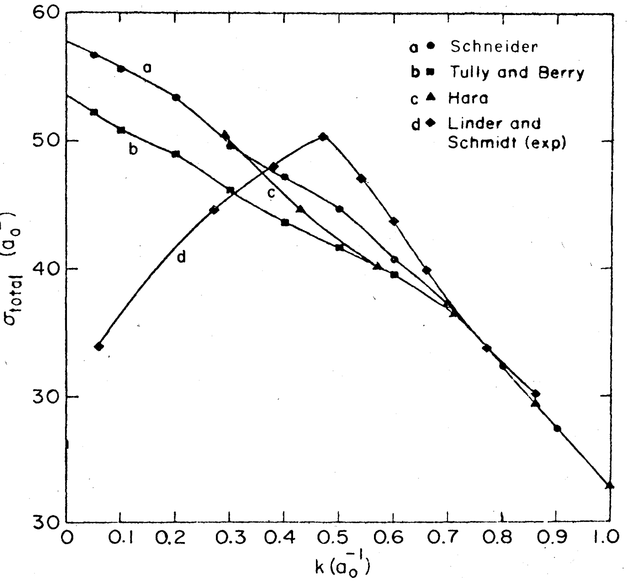

FIG. 7. Cross sections for e–H_2 scattering in the static-exchange approximation: (a) Schneider (1975b); (b) Tully and Berry (1969); (c) Hara (1969a); and (d) experimental; Linder and Schmidt (1971a). (Reprinted from Schneider, 1975b.)

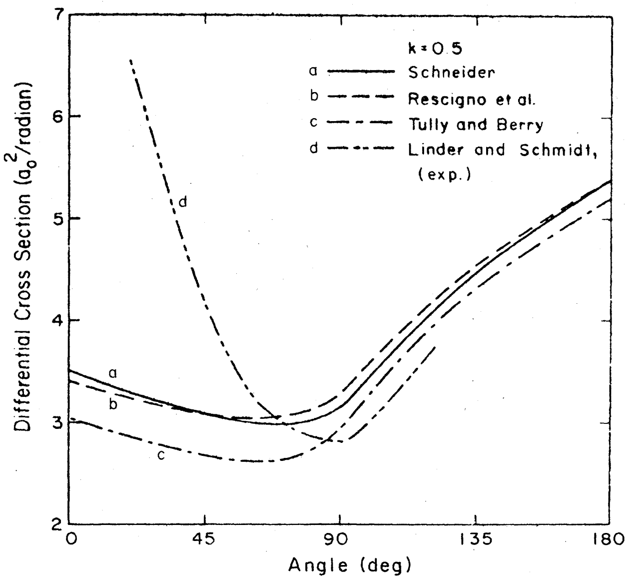

FIG. 8. Differential cross sections for e–H_2 scattering in the static-exchange approximation: (a) Schneider (1975b); (b) Rescigno *et al.* (1975a); (c) Tully and Berry (1969); and (d) experimental; Linder and Schmidt (1971a). (Reprinted from Schneider, 1975b.)

ingredients in the calculation are the choice of optical potential in Eq. (103) and the basis set to be used in forming the "truncated" T matrix of Eq. (106). In this study V was approximated by the Hartree–Fock (static-exchange) potential V_{sx}, defined in Eq. (114). The H_2 ground state was represented by the Hartree–Fock wave function. The basis set chosen for the continuum orbital consists of 22 Cartesian Gaussian functions of the form

$$G_\alpha(\mathbf{r}-\mathbf{A}) = x^l y^m (z-A)^n \exp\{-\alpha[x^2+y^2+(z-A)^2]\}, \tag{182}$$

centered on the two nuclei and properly symmetrized. In the present application only s-type Gaussians ($l=m=n=0$) were used. The nonlinear parameters α were chosen by combining Huzinaga's results for a 10-Gaussian representation of the 1s hydrogen atom (Huzinaga, 1965) with more diffuse functions with α chosen in a geometric series of ratio 1.6 (Schneider, 1974). If the T operator from Eq. (103) is substituted into the expression (101) for $f^B(\mathbf{k},\mathbf{k}_0)$, the leading term in U is just the first Born approximation. The authors found that this term should be included exactly (i.e., not truncated by representation in the finite basis set), by simply replacing T in Eq. (101) by

$$T \cong U + T^t - U^t. \tag{183}$$

Calculations of $T^t - U^t$ were carried out for Σ_g and Σ_u symmetries; all other symmetries were included in the first Born approximation by means of Eq. (183). Elastic (fixed-nuclei) differential cross sections, averaged over nuclear orientation, were calculated at energies $k=0.3$(1.22 eV), 0.4(2.18 eV), 0.5(3.4 eV), 0.6(4.9 eV), and 0.7(6.66 eV), and compared with other theoretical static-exchange calculations of Tully and Berry (1969) and Hara (1969a). The agreement with the static-exchange results of Schneider is very good, as illustrated by the differential cross section at $k=0.5$(3.4 eV) in Fig. 8. Probable sources of error in this calculation are: (1) incompleteness in the basis set, and (2) neglect of partial-wave coupling in the asymptotic region. [See also Levin, Rescigno, and McKoy (1977) and Fliflet and McKoy (1978a,b).] (See the Appendix.)

Morrison and Lane (1975) proposed a "pseudobound-state" method based on the assumption that an ordinary (bound-state) variational approximation to the wave function of the H_2^- system will resemble the true scattering wave function near the molecule (see, for example, Hazi and Fels, 1971). The variational wave function can then be joined onto a continuum function just outside the region where exchange and other short-range effects are important. (See related discussion of pseudopotential methods in Sec. II.G.4.) Only Σ_g symmetry is considered in this study. An N-configuration, three-electron variational function Ψ_v is constructed as a linear combination of functions $\Phi_i(\mathbf{r}_1,\mathbf{r}_2,\mathbf{r}_3)$, where the Φ_i are symmetrized Slater determinants of the form $|1s^a\overline{1s}^b\Phi_i^a|$, etc., and where the $1s^a$, $1s^b$ orbitals are obtained from a single-configuration calculation of the ground-state energy of H_2 (and held frozen) and the Φ_i^a are Slater-type orbitals (STO), characterized by a nonlinear parameter α_i and power of r, n_i. A convenient choice of STO is obtained by holding α_i fixed and including powers of r up to N. The Hamiltonian matrix is diagonalized and an approximate "continuum orbital" projected out (Σ_g symmetry) of a low-energy eigenfunction

$$\phi(\mathbf{r}) = \langle\psi_0^{(e)}(\mathbf{r}_1,\mathbf{r}_2)|\Psi_v(\mathbf{r}_1,\mathbf{r}_2,\mathbf{r}_3)\rangle$$
$$= \sum_{l\ \mathrm{even}} r^{-1}u_{l0}^{(v)}(r)Y_{l0}(\hat{r}). \tag{184}$$

If $\phi(\mathbf{r})$ is orthogonalized to the core orbital $1s^a(\mathbf{r}) + 1s^b(\mathbf{r})$, a node occurs at $r \cong 2a_0$. The $s\sigma$ phase shift is then calculated by using the $s\sigma$ orbital of Eq. (184) at some two adjacent points near $r=r_0$ to start an outward integration (Numerov) of the static radial equation into the asymptotic region. Calculations were also performed using the static and polarization (Lane and Henry, 1968) potentials in the outer region. The logarithmic derivative of the variation orbital was taken to be independent of the scattering energy. Phase shifts were then calculated for a range of energies $0.05 < E < 10.0$ eV for various choices of basis set (i.e., number of basis functions N), nonlinear parameters α, and starting radius (i.e., R-matrix boundary). The results for all energies were found to be insensitive to different choices of α and r_0 (in the range 1.5–2.5a_0), and were well converged for a choice of 14 basis functions ($N=14$). The static-exchange phase shifts calculated in this way are in good agreement with Tully and Berry (1969) and excellent agreement (i.e., phase shift differences $\lesssim 0.005$) with Henry and Lane (1969) and Schneider (1975b) for energies up to 1.0 eV. Above 1.0 eV the static-exchange phase shifts deteriorate, probably due to the assumption that the short-range variational orbital is independent of energy. When polarization is included in the outer region the resulting $s\sigma$ phase shifts and partial cross sections are in excellent agreement with the approximate adiabatic-exchange results of Henry and Lane (1969). The major drawbacks in the present method are: (1) limitation to cases where the asymptotic partial-wave coupling is weak, i.e., "low-l spoiling"; (2) linear dependence problems in the STO basis set; (3) restriction to low energies; and (4) generalization of the method not straightforward.

Winter and Lane (1975) applied the Fredholm method to elastic (fixed-nuclei) electron–H_2 scattering in the static-exchange approximation using the same type of basis set as Morrison and Lane (1975), and based on the L^2 procedures developed by Murtaugh and Reinhardt (1972, 1973) for electron–atom scattering. Assuming that the partial waves are asymptotically decoupled (i.e., low-l spoiling), the phase shift, modπ, can be expressed in terms of the Fredholm determinant by [see, for example, Bransden (1970), or Gottfried (1966)]

$$\delta_l(E) = -\lim_{\varepsilon\to 0} \arg[D_l(E+i\varepsilon)], \qquad (185)$$

where at a complex energy z above the positive real axis, D is expressible approximately as (see, also Reinhardt, Oxtoby, and Rescigno, 1972)

$$D(z) \cong \prod_{k=1}^{K} \left[\frac{z-E_k}{z-E_k^0}\right]. \qquad (186)$$

The E_k and E_k^0 are, respectively, the eigenvalues of the full (electronic) Hamiltonian and that of the initial noninteracting system, where in both cases a discrete representation in terms of K L^2 basis functions is assumed. (In the molecular case, the E_k, E_{k_0}, $D(z)$, and phase shift δ_l depend on m as well as l.) Analytic continuation is then employed from a point near the real axis to the real axis (Reinhardt, Oxtoby, and Rescigno, 1972). The $s\sigma$ phase shifts were found to be in good agreement with the results of Tully and Berry (1969) and in excellent agreement with the static-exchange results of Henry and Lane (1969). The major drawbacks in the method are similar to those found in all "low-l spoiling" procedures, viz., errors in neglecting asymptotic partial-wave coupling and difficulty in generalization. In this particular application, the analytic continuation procedure was found to be somewhat awkward and tedious.

McCurdy, Rescigno, and McKoy (1976) independently developed a "low-l spoiling" method very similar to the pseudobound-state method of Morrison and Lane (1975) and applied it to H_2, N_2, and F_2 (Rescigno, Bender, McCurdy, and McKoy, 1976). In their application to (fixed-nuclei) elastic electron–H_2 scattering, the Hartree–Fock Hamiltonian, Eqs. (113) and (114), for the H_2 system is first diagonalized in a discrete basis set [22 s-type Gaussians on each H (Rescigno, McCurdy, and McKoy, 1975a)]. The approximate continuum orbital is then projected out of a positive-energy eigenfunction $\Psi_{HF}(\mathbf{r})$ by forming

$$u_{lm}(r) = \langle Y_{lm} | \Psi_{HF}\rangle. \qquad (187)$$

The phase shifts η_{lm} are then obtained by matching u_{lm} and its first derivative at some large value of r to the single-channel version of the asymptotic form given in Eqs. (34)–(36), where $\tan\eta_{lm} = K_{lm}$. The $s\sigma$ and $p\sigma$ phase shifts calculated for energies in the range $0 \leq E \leq 13.6$ eV were found to be in apparent good agreement with Schneider (1975b), although only graphical comparisons are given. The sources of error in this method include those described for Morrison and Lane (1975). In addition, long-range interactions are neglected in the present method. However, the use of Gaussian basis functions (rather than STO) seems to significantly reduce the linear-dependence problem.

b. Static-exchange polarization

The adiabatic-exchange (AE) approximation was given a specific meaning by Temkin (1957). (See also Drachman and Temkin, 1972.) However, we will sometimes use the term to refer to calculations where some reasonable account of both exchange and polarization has been taken. As described in Sec. II.G.3, the term "polarization" describes a long-range correlation effect which arises from the adiabatic response of the target electrons to the presence of the scattered electron. Generally, the adiabatic-exchange approximation results in marked improvement over the static-exchange model. The calculated elastic differential cross section is much improved in the forward direction (small-angle scattering) and the integral cross section usually exhibits the correct energy dependence, and is often quantitatively accurate as well.

Hara (1969a) calculated (fixed-nuclei) elastic cross sections for electron–H_2 scattering in the static, static-exchange, and adiabatic-exchange approximation. These results were then used with the adiabatic nuclear rotation approximation to calculate rotational excitation cross sections (Hara, 1969b). Hara's approach is to solve numerically the static-exchange equations (110) (with and without the polarization potential added to V_s), in two-center spheroidal coordinates. The exchange terms are handled in an iterative fashion starting with the static case. The ground-state $^1\Sigma_g^+$ target molecular wave function is represented by a single Slater determinant constructed from a five-term SCF (self-consistent field) molecular orbital of Kolos and Roothaan (1960). The polarization potential used is that of Hara (1969c) based on a variational-perturbation approximation to the adiabatic polarization energy of Eqs. (144) and (145), evaluated in two-center spheroidal coordinates. A standard linear variational approach is used, where the perturbed-target wave function is expanded in a set of two-center two-electron basis functions of the form used by James and Coolidge (1933) in their 16-term representation of the ground state of H_2. The coefficients in this expansion depend parametrically on $\mathbf{r}$, the position of the perturbing electron. The secular equation is then expanded in orders of the electron-molecule interaction V_{em}, and only first- and second-order terms are retained. The first-order energy is the static potential V_s, and the second-order term is the polarization potential $V_0^{(p)}$ of Eq. (145). Hara retains only the dipole contribution to $V_0^{(p)}$, but that should be the dominant contribution at least for large r. The short-range step-function cutoff procedure of Temkin (1957) is employed as a partial nonadiabatic correction. However, this does *not* introduce an adjustable parameter into the calculations. The polarizabilities obtained in this calculation are $\alpha_0 = 4.52a_0^3$ and $\alpha_2 = 0.33\,a_0^3$ (i.e., $\alpha_{\parallel} = 4.851\,a_0^3$ and $\alpha_{\perp} = 4.359\,a_0^3$), so that an overall scaling of $V_0^{(p)}$ is required to ensure the correct asymptotic form [corresponding to $\alpha_0 = 5.50\,a_0^3$ and $\alpha_2 = 1.38\,a_0^3$ (Kolos and Wolniewicz, 1967)]. The need for scaling, of course, gives rise to uncertainty in the accuracy of the polarization potential. The resulting $V_0^{(p)}$ is similar to that of Lane and Henry (1968), but somewhat weaker. Hara has calculated integral elastic and momentum-transfer cross sections at a number of energies in the range ($0 \leq E \leq 28$ eV) and differential elastic cross sections at 2.49, 4.44, 6.996, and 9.99 eV. His results for the integral (fixed-nuclei) elastic cross section are given in Fig. 9 for both the static-exchange ("Hara, No Polarization") and approximate adiabatic-exchange ("Hara, Including Polarization") calculations. Also shown in this figure are the static-exchange results of Massey and Ridley (1956), Wilkins and Taylor (1967), Tully and Berry (1969), and the static-exchange and adiabatic-exchange results of Henry and Lane (1969), to be discussed. Comparison with the measurements (Ramsauer and Kollath 1930a, b, 1931, 1932; and Golden, Bandel, and Salerno, 1966) shows the importance of including polarization in the integral cross section, at least for energies below 10 eV. Not shown in the figure are the experimental elastic cross sections of Linder and Schmidt (1971a) and Srivastava *et al.* (1975). All of the experimental cross sections appear to be consistent with the exception of those of Srivastava *et al.* (1975), which are significantly smaller below 6 eV. The importance of polarization at small angles is apparent in Fig. 10, where the theoretical adiabatic-exchange (Hara, 1969a; Henry and Lane, 1969) differential elastic cross sections are compared with the measurements of Linder and Schmidt (1971a) and Trajmar *et al.* (1970a, b); all curves are normalized at 90°. The effect of the long-range attractive polarization interaction is to increase the small-angle cross sections, bringing them into better agreement with experiment. (Compare the static-exchange results of Fig. 8.) It should be noted in connection with Fig. 10 that Hara's cross sections are really total (elastic plus rotational excitation) since they were obtained in a fixed-nuclei calculation and averaged over nuclear orientation.

The greatest source of error in Hara's calculation is probably his treatment of polarization. The accuracy of the calculated cross sections is as good as one is likely to obtain without considerable improvement in the treatment of electron correlation effects.

Henry and Lane (1969) calculated elastic and rotational-excitation cross sections for electron–H_2 scattering in the static, static-exchange, and adiabatic-exchange (including polarization) approximations. The internuclear separation was fixed at $R = 1.4a_0$. The LAB-frame equivalent of the coupled equations (116)–(119) were solved numerically. Equations (62) simplify for the case of a single ${}^1\Sigma_g^+$ electronic state and fixed internuclear separation, so that the channels are defined by $p = (jl; J)$. In the exchange matrix elements, orthogonality of the "continuum orbital" to the target orbital was assumed, as in Eq. (119). The static potential V_s was taken to be that calculated by Lane and Geltman (1967) using the ground-state function of Wang (1928). The static potential was corrected at large distances by smoothly joining the $v_2^{(s)}$ term in the expansion (118) to the asymptotic form $-Q/r^3$, where Q was chosen to be $0.49\,ea_0^2$ (Kolos and Wolniewicz, 1967). The exchange terms were calculated using the single-center H_2 wave function of Huzinaga (1957). The coupled equations were solved using outward and inward integration by

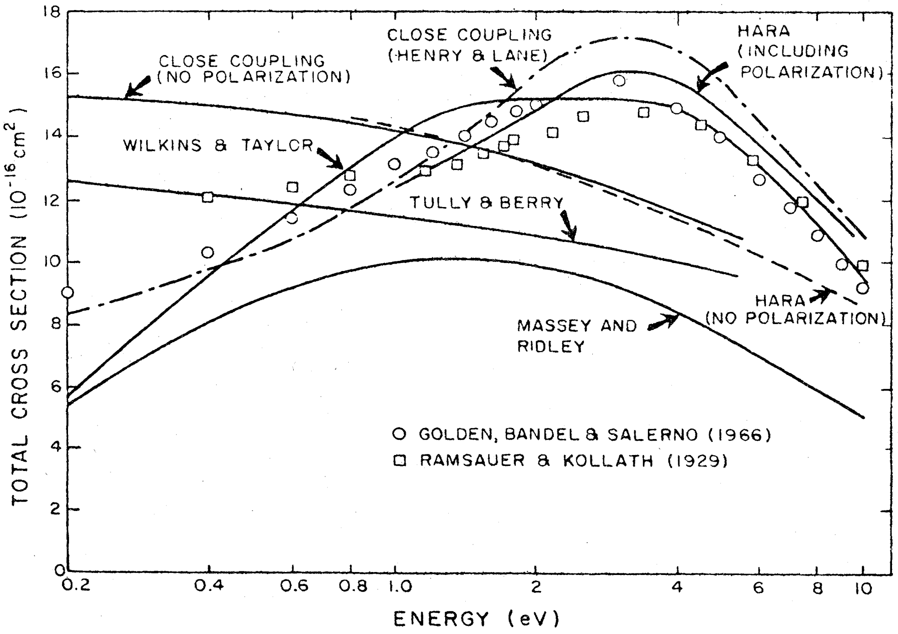

FIG. 9. Comparison of total e^-–H_2 cross sections. All theoretical curves include exchange in one form or another. Theoretical calculations plotted: Henry and Lane (1969) close coupling, with polarization (dot-dash), and without (solid); Hara (1969a) two-center, with polarization (solid), and without (dash); Wilkins and Taylor (1967); Massey and Ridley (1956); Tully and Berry (1969). Experimental data of Ramsauer and Kollath (1930a, b, 1931, 1932) and Golden *et al.* (1966). (Reprinted from Golden *et al.*, 1971.)

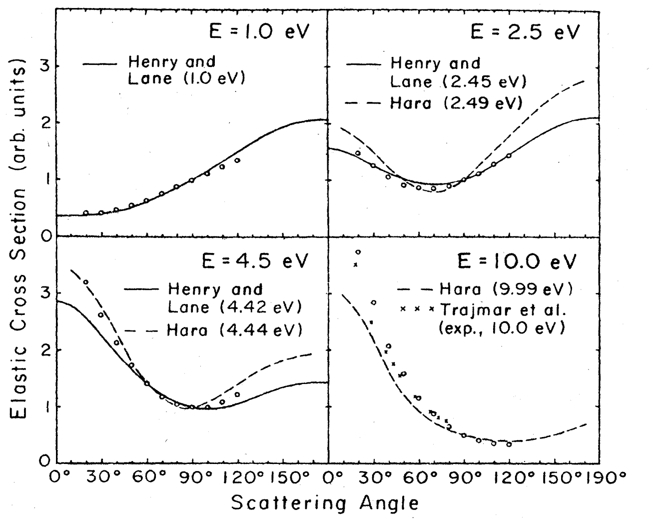

FIG. 10. Differential cross sections for elastic e–H_2 scattering. Comparison of theory including polarization with experiment. Theory: (solid curve) Henry and Lane (1969), (dashed curve) Hara (1969a). Experiment: (open circles) Linder and Schmidt (1971a), (×) Trajmar *et al.* (1970a, b). (Reprinted from Linder and Schmidt, 1971a.)

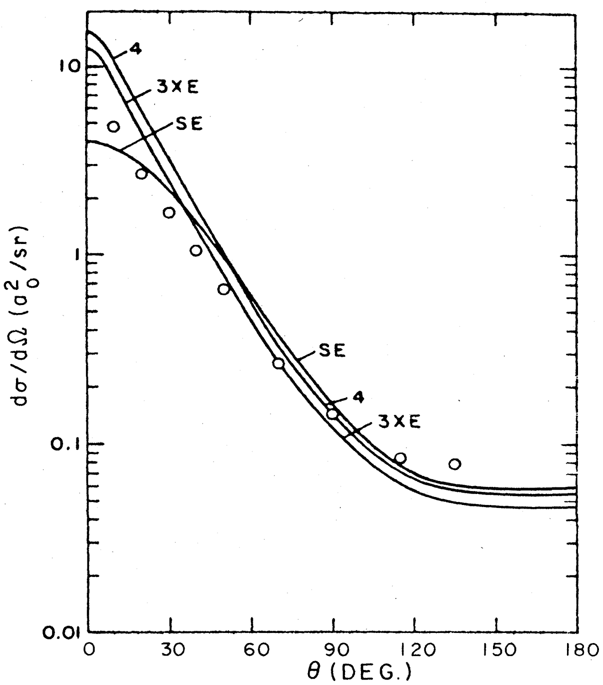

FIG. 11. Differential total (elastic plus rotational excitation) cross sections for e–H_2 scattering at 40 eV. Theory: Truhlar and Brandt (1976), (curve SE) static exchange, (curves 3XE and 4) models without exchange. Experiment: (open circles) Srivastava *et al.* (1975). (Reprinted from Truhlar and Brandt, 1976.)

Numerov's method and the asymptotic expansion method of Burke and Schey (1962). Exchange was treated using the noniterative method of Marriot (1958) and Omidvar (1961, 1974). [See Smith, Henry, and Burke (1966) for a general discussion of these methods.] Closed as well as open rotational channels were included. The polarization potential used was that calculated by Lane and Henry (1968), who employed a linear variational treatment in which the lowest energy of the system ($e+H_2$) was minimized with respect to the parameters $C_{\alpha\beta}$ in a trial function of the form

$$\psi_0^{(p)}(\mathbf{r}_1, \mathbf{r}_2; \mathbf{r}) = \psi_0^{(e)}(\mathbf{r}_1, \mathbf{r}_2) \sum_{\alpha,\beta} C_{\alpha,\beta}(x_1+x_2)^{\alpha}(z_1+z_2)^{\beta}, \qquad (188)$$

where the unperturbed H_2 wave function $\psi_0^{(e)}$ was approximated by the one-center function of Joy and Parr (1958). The Temkin (1957) step-function cutoff procedure was employed as a rough nonadiabatic correction. The numerically determined $V_0^{(p)}(\mathbf{r})$ was expanded as

$$V_0^{(p)}(\mathbf{r}) = v_0^{(p)}(r) + v_2^{p}(r)P_2(\cos\theta), \qquad (189)$$

and $v_0^{(p)}$ and $v_2^{(p)}$ were fit to convenient analytic functions, and scaled so that the r^{-4} asymptotic form was consistent with the polarizabilities $\alpha_0 = 5.50a_0^3$ and $\alpha_2 = 1.38a_0^3$ (Kolos and Wolniewicz, 1967). This scaling gives rise to considerable uncertainty in the accuracy of the polarization potential. Elastic (LAB-frame elastic) and rotational-excitation, integral cross sections were calculated for a number of energies in the range $0 \leq E \leq 13.6$ eV. Differential elastic cross sections are shown in Fig. 10 for energies 1.0, 2.45, and 4.42 eV. Total (elastic $j = 0 \rightarrow 0$ plus $j = 0 \rightarrow 2, 4$, etc., rotational-excitation) integral cross sections are shown in Fig. 9.

The greatest source of error in these calculations is the treatment of polarization. It is encouraging that the cross sections calculated by Hara (1969a, b) are similar to those of Henry and Lane (1969), a fact that reflects that the polarization potentials are not in serious disagreement. Nevertheless, the approximate manner in which polarization is treated in both these studies is an obvious source of error, particularly at the higher energies.

Truhlar and Brandt (1976) have focused on the role of exchange and polarization in elastic scattering and rotational excitation at somewhat higher energies. They have performed a two-state ($j = 1, 3$) LAB-frame rotational close-coupling calculation including exchange via the local semiclassical (SC) approximation of Riley and Truhlar (1975) and polarization by constructing a polarization potential similar to that of Lane and Henry (1968), but modified so as to vanish at the nuclei. In Fig. 11 total (elastic plus rotational-excitation) differential cross sections are compared with the measurements of Srivastava *et al.* (1975) at 40 eV. The "semiclassical" static exchange ("SE") cross section falls below experiment at small angles, as might be expected. Including polarization (curve "4" with exchange and curve "$3\times E$" without exchange) raises the small-angle cross section, but does not alter the large-angle scattering appreciably. The major uncertainties in this calculation are: (1) the semiclassical exchange model; (2) the approximate polarization potential; and (3) the question of numerical convergence of the close-coupling expansion, truncated at the two-state level. Considering all of these factors, the agreement with experiment is remarkably good. Truhlar, Dixon, and Eades (1979) have recently reinvestigated the question of how the adiabatic polarization potential should be calculated and give new results for the electron–H_2 interaction.

At somewhat higher energies, Bhattacharyya, Goswami, and Ghosh (1978), obtain qualitative agreement with measured differential cross sections by applying the adiabatic nuclear rotation approximation, using the eikonal theory based on model static-exchange-polarization interactions (see Bhattacharyya and Ghosh, 1975, 1976).

Schneider (1977a, b) has extended his R-matrix study (Schneider, 1975a, b) to include polarization by incorporating in the basis set pseudo-orbitals obtained by carrying out a configuration-interaction variational calculation for the H_2 molecule in the field of a distant charge. The polarizabilities obtained in this way are $\alpha_{\parallel} = 6.3860a_0^3$ and $\alpha_{\perp} = 4.5460a_0^3$, in very good agreement with the respective values 6.3805 and $4.5777a_0^3$ of Kolos and Wolniewicz (1967). The R-matrix calculations, with the expanded ("polarized") basis, are then performed essentially as before to obtain the cross sections. Integral (fixed-nuclei) cross sections are compared in Fig. 12 with other theoretical work of Kaldor and Klonover (1977) and Klonover and Kaldor (1978) and the experimental *elastic* cross sections of Linder and Schmidt (1971a). The agreement with the measurements is good. It should be noted that Schneider's cross sections include rotational excitation implicitly (since the fixed-nuclei elastic cross sections are averaged over nuclear orientation) and may exceed the pure elastic cross section by as much as 1×10^{-16} cm^2 at 2 eV. Nevertheless, there still appears to be a substantial discrepancy at the lowest energies compared.

Kaldor and Klonover (1977) and Klonover and Kaldor (1978) have applied the T-matrix expansion method of Rescigno, McCurdy, and McKoy (1974a, b), including polarization effects, to a (fixed-nuclei) calculation of elastic and (adiabatic nuclei) rotational-excitation cross sections for electron–H_2 scattering. The basic equation is Eq. (101), where a "truncated" approximation to the T matrix is obtained by solving Eq. (106). The optical potential was approximated by

$$V = V_{sx} + V^{(2)}_{op} , \tag{190}$$

where V_{sx} is the static-exchange potential (operator) of Eq. (114) and $V^{(2)}_{op}$ is the *second-order* approximation to the perturbation series represented by all linked, proper diagrams (see, for example, Csanak, Taylor, and Yaris, 1971). This approximation is expected to incorporate the most important polarization effects in a systematic and rigorous manner. Elastic (fixed-nuclei) cross sections were calculated both in the static-exchange approximation and with polarization included via the optical potential. The calculated elastic cross sections (adiabatic nuclear rotation) are compared in Fig. 12 with the R-matrix results of Schneider (1977a, b), also including polarization, and the experimental elastic cross sections of Linder and Schmidt (1971a). The agreement with Schneider (1977a, b) and with experiment is good over most of the energy range. At the lower end, say $1 < E < 3$ eV, the theoretical cross sections lie below experiment. The fact that the energy dependence of the theoretical cross section is not very smooth suggests a source of numerical error that varies with energy.

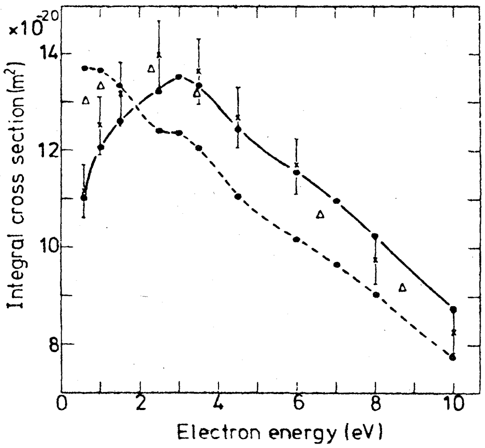

FIG. 12. Integral cross sections for e–H_2 scattering. Theory: (dashed curve) static exchange, (solid curve) exchange polarization; Klonover and Kaldor (1978); (open triangles) exchange polarization, Schneider (1977a, b). Experiment: (×) Linder and Schmidt (1971a). (Reprinted from Klonover and Kaldor, 1978.)

2. Rotational excitation (H_2)

Rotational excitation in electron-molecule scattering occurs as the result of a torque acting on the molecule which arises from the field of the scattered electron. [See early reviews by Craggs and Massey (1956), Takayanagi (1967, 1973, and 1975a, b), Phelps (1968), Takayanagi and Itikawa (1970b), and Golden *et al.* (1971).] Since the anisotropic electron–molecule interaction is long range (varying asymptotically as r^{-2} for polars, r^{-3} for molecules with quadrupole moments) the influence can be felt when the electron is still rather far from the molecule. Massey (1931) argued that for polar molecules the major contribution to the rotational-excitation cross section should arise from such large electron–molecule separations that the initial electronic wave function of the incident electrons would be only weakly perturbed, and the first Born approximation applied only to the long-range static interaction should be valid. The dominant transition would be $j \to j \pm 1$. Gerjuoy and Stein (1955a, b) extended this argument to nonpolar molecules where the quadrupole interaction determines the cross section, and the dominant transition is $j \to j \pm 2$. Dalgarno and Henry (1965) showed that a distorted-wave treatment including static short-range, as well as the long-range quadrupole, interactions agrees with the Born result. [Chang (1970, 1974a, b) has made a critical study of the Born–quadrupole approximation near threshold and suggested rotational-excitation measurements as a method of accurately determining quadrupole moments for nonpolar molecules.]

The importance of polarization, especially the anisotropic contribution, to rotational excitation of nonpolar molecules was stressed by Dalgarno and Moffett (1963), who extended the first Born approximation to include this effect. They argued that the long-range r^{-4} polarization potential of Eq. (143) is still sufficiently weak so that the scattered electron will be perturbed only slightly. Indeed, the influence of the α_2 term in Eqs. (143) and (148) gives rise to a much steeper rise in the cross section above threshold, in better agreement with the available measurements [Engelhardt and Phelps (1963); see Phelps (1968)]. Sampson and Mjolsness (1965) and Geltman and Takayanagi (1966) performed distorted-wave calculations using a variety of semiempirical model interaction potentials including the long-range quadrupole and polarization effects. They concluded that the cross sections would continue to increase above threshold, perhaps peaking somewhere between 1 and 10 eV; the short-range static interactions play an important role at these energies. However, near threshold (say within 0.1 eV or so) the quadrupole and polarization contributions were still dominant, and the Born results appeared to be good. Both the Born and distorted-wave approximations are based on the "weak-coupling" assumption (i.e., first-order perturbation treatment of the parts of the electron–molecule interaction that directly couple different rotational states). If the coupling is sufficiently strong, "feedback" (or "backcoupling") can influence both the elastic and rotational-excitation cross sections. Moreover, $j \to j+4$ cross sections can be enhanced, for example, by a step process $j \to (j+2) \to j+4$, occurring in a single collision.

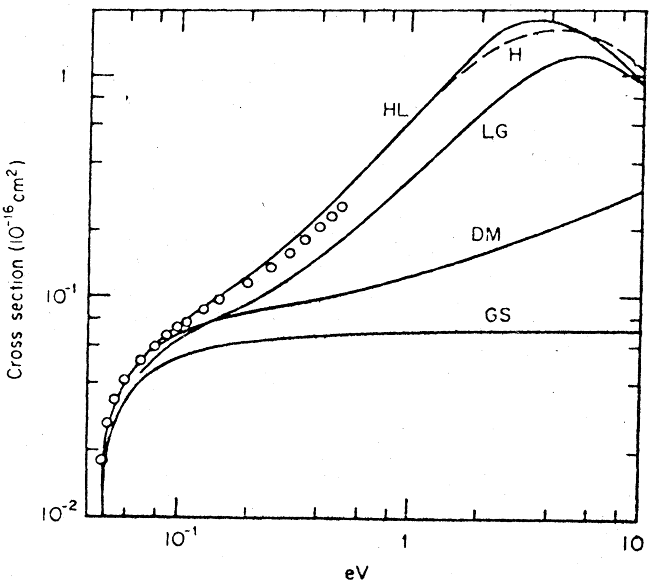

FIG. 13. Rotational-excitation cross sections for $j = 0 \to 2$ transition in e–H_2 scattering. Theory: (HL) Henry and Lane (1969), (H) Hara (1969b), (LG) and Lane and Geltman (1967), (DM) Dalgarno and Moffett (1963), (GS) Gerjuoy and Stein (1955a, b). Experiment: Crompton *et al.* (1969). (Reprinted from Takayanagi and Itikawa, 1970b.)

Lane and Geltman (1967, 1969) examined the "weak-coupling" assumption in electron–H_2 scattering by performing a LAB-frame rotational close-coupling calculation including long-range quadrupole and polarization interactions and short-range static- and model-exchange interactions. The adjustable parameters in the model potentials were determined semiempirically by fitting the experimental total cross section data of Golden, Bandel, and Salerno (1966). Rotational-excitation cross sections were then obtained for: $j = 0 \to 2, 4; j = 1 \to 3, 5; j = 2 \to 4; j = 3 \to 5$; and the inverse processes, over an energy range of threshold to 13.6 eV. The conclusions reached in this work (some of which represent confirmation of the insights of previous workers) include: (1) rotational coupling and coupling of different partial waves is *weak* for H_2 because of the small nuclear charge and near-spherical electronic charge distribution of the ground-state molecule; (2) the $\Delta j = \pm 2$ cross sections exceed those for $\Delta j = \pm 4$ by about 10^3 for the same reasons; (3) the $\Delta j = \pm 2$ cross section is dominated by electron partial waves $d \to s$ at threshold, and $p \to p$ above threshold [see Chang (1970) for further discussion of this point]; (4) short-range interactions strongly influence $|\Delta j| > 2$ cross sections at all energies, and $\Delta j = \pm 2$ cross sections for energies above about 0.1 eV; (5) the rotational-excitation cross section summed over all final states $\sum_{j'} \sigma(j \to j')$ is independent of initial state j [as expected according to the adiabatic approximation (Oksyuk, 1966)]; and (6) the differential rotational-excitation cross section for $\Delta j = \pm 2$ transitions is much more isotropic than the corresponding elastic (or total) cross section except at the lower energies. Cross sections for $j = 0 \to 2$ and $j = 1 \to 3$ transitions are included in Figs. 13 and 14, respectively, along with the experimental measurements of Crompton, Gibson, and McIntosh (1969) and Linder and Schmidt (1971a) and other theoretical results to be discussed. [Recently, Varracchio (1979) has used the same model electron–H_2 interaction potential in an interesting illustration of the field-theoretic "effective potential" formulation, obtaining reasonably good

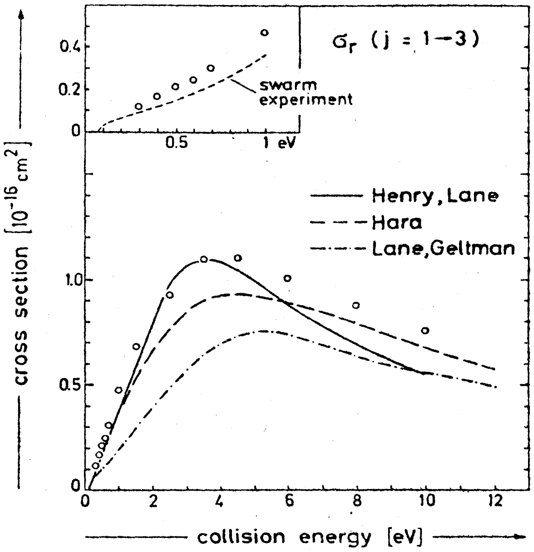

FIG. 14. Rotational-excitation cross sections for $j = 1 \to 3$ transition in e–H_2 scattering. Theory: (solid curve) Henry and Lane (1969), (dashed curve) Hara (1969b), (dot-dashed curve) Lane and Geltman (1967). Experiment: (open circles) Linder and Schmidt (1971a), (inset, dashed curve) transformed data from $j = 0 \to 2$ measurements of Crompton *et al.* (1969). (Reprinted from Linder and Schmidt, 1971a.)

agreement with Lane and Geltman (1967). See also Csanak, Taylor, and Varracchio (1974) and Varracchio (1977).]

Abram and Herzenberg (1969), Chang and Temkin (1969, 1970), and Hara (1969b) pointed out that the adiabatic nuclear rotation (ANR) approximation (see Sec. II.D) should be good except very near threshold. But near threshold the Born approximation is valid. The quantitative reliability of this approximation was studied by Chang and Temkin (1969), who showed that the predicted proportionality (for $j'=j\pm 2$) to a single Clebsch–Gordan coefficient

$$\sigma_{j\to j'}\propto[C(j2j',00)]^2, \tag{191}$$

was well satisfied by the close-coupling cross sections of Lane and Geltman (1967) over a wide range of energies including higher energies ($E\gtrsim 0.5$ eV) where the Born (quadrupole) approximation, which also satisfies this proportionality, clearly fails. (This, of course, does not imply that the cross sections of Lane and Geltman are "physically correct." It does argue that they are "numerically accurate," for the particular model chosen, and more importantly, that the adiabatic nuclear rotation approximation is valid here.) As an independent check, Chang and Temkin (1969, 1970) infer values for the fixed-nuclei phase shifts, actually the difference $\Delta\eta=\eta_{10}-\eta_{11}$, from the measured integral $j=0\to 2$ cross sections of Crompton, Gibson, and McIntosh (1969). Using these semiempirical phase differences in the ANR expression for the *differential* $j=0\to 2$ cross sections, the latter were found to compare well with the measurements of Ehrhardt and Linder (1968). This result was also found to agree very closely with the adiabatic exchange calculation of Hara (1969a) (see Golden *et al.*, 1971). The validity of the ANR approximation in electron–molecule scattering was well established by this important work.

The importance of exchange in electron–H_2 scattering was first examined by Ardill and Davison (1968) in a distorted-wave calculation including only static and exchange interactions. They found that at $E\simeq 0.5$ eV, including exchange results in a ~70% increase in the rotational-excitation cross section. Since polarization was not included their cross sections were not in good agreement with experiment.

Hara (1969a, b) and Henry and Lane (1969) calculated elastic and rotational-excitation cross sections for electron–H_2 scattering, including the effects of both exchange and polarization [see also Henry and Lane (1971) and Chang and Wong (1977) for D_2, and Hara (1971) and Takayanagi (1971) for HD targets]. These calculations were briefly described in Sec. III.B.1.b. Both theories agree on the $j=0\to 2$ and $j=1\to 3$ cross sections at low energies ($E\lesssim 2$ eV) and theory and experiment are in good agreement over this same range, as illustrated in Figs. 13 and 14. In Fig. 14 it is apparent that above 2 eV, the two theoretical cross sections begin to diverge, the results of Hara remaining in better agreement with experiment. At this point it is not possible to choose one calculation over the other. The major uncertainty in both is the treatment of polarization, which is not really correct in either calculation. Pande and Singh (1977), using a static-plus-polarization model potential in a LAB-frame rotational close-coupling calculation, obtain reasonable agreement with the $j=0\to 2$ results of Hara (1969a, b) and Henry and Lane (1969), except, curiously, near threshold. It is likely that the model polarization potential employed in this study mocks the missing exchange effects.

The recent application of the T-matrix-expansion method to electron–H_2 scattering by Kaldor and Klonover (1977) and Klonover and Kaldor (1978) (described in Sec. III.B.1.b) represents an attempt to include polarization effects in a systematic way. Applying the adiabatic nuclear rotation (ANR) approximation, as described in Sec. II.D, these authors calculated $j=1\to 3$ cross sections for energies $E\leqslant 10$ eV. Their results for the integral $j=1\to 3$ cross section calculated in the static-exchange and adiabatic-exchange (second-order polarization) approximations are compared in Fig. 15 with the measurements of Linder and Schmidt (1971a). The agreement with experiment is particularly good above 4 eV. At lower energies the theoretical cross section drops off rather sharply. The authors suggest that higher-order terms in the perturbation expansion may be required. However, the static-exchange cross section also shows this sharp drop at low energies suggesting that the source of this feature may actually be in that part of the calculation, perhaps reflecting incompleteness in the basis (Kaldor 1979b). More recently, Klonover and Kaldor (1979a) have shown that the ANR elastic and rotational-excitation cross sections increase sharply with internuclear separation R. Averaging the calculated scattering amplitude over the ground vibrational state distribution in R (in the sense of the adiabatic nuclear vibration approximation)

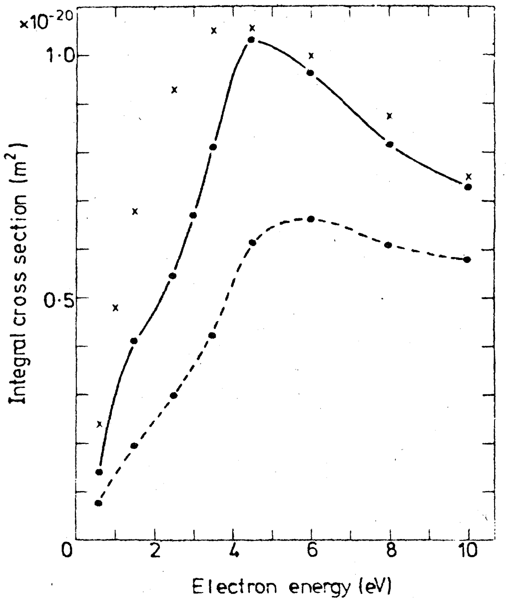

FIG. 15. Rotational-excitation cross sections for $j=1\to 3$ transition in e–H_2 scattering. Theory: (solid curve) exchange polarization; (dashed curve) static exchange, Kaldor and Klonover (1977), Klonover and Kaldor (1978). Experiment: (×) Linder and Schmidt (1971a). (Reprinted from Klonover and Kaldor, 1978.)

they obtain improved agreement with the measurements of Linder and Schmidt (1971a) for the elastic and $j=1 \rightarrow 3$ rotational-excitation integral and differential cross sections at all energies.

At higher energies the agreement of theory with experiment is still only qualitative. The model two-rotational-state close-coupling studies of Truhlar and Brandt (1976) at 10 and 40 eV (see brief discussion in Sec. III.B.1.b) show that qualitative agreement of the differential cross sections may be obtained using the semiclassical exchange model of Riley and Truhlar (1975) and a variety of model polarization potentials. Similar results, at somewhat higher energies, were obtained by Bhattacharyya, Goswami, and Ghosh (1978) in their application of the adiabatic nuclear rotation approximation using eikonal theory (see Bhattacharyya and Ghosh, 1975, 1976).

At very low energies (i.e., $E \lesssim 0.1$ eV), the density dependence of carefully measured drift velocities of electrons in dense H_2 and D_2 was interpreted to imply the existence of "rotational resonances" (Frommhold, 1968; Kouri, 1968a, b; Sams, Frommhold, and Kouri, 1972). The "rotational resonance" complex would correspond to an electron temporarily attached to a rotating H_2 (D_2) molecule. However, the calculations of Henry and Lane (1969) strongly implied that such resonances could not exist in a single electron–H_2 encounter. Crompton and Robertson (1971) and Bartels (1972) in separate and quite different experiments confirmed that there is definitely some mechanism present at high densities that acts like electron trapping. Garrett (1977) has suggested that the trapping may be a collective effect involving many H_2 (D_2) molecules, and using a reasonable model for the interaction, he is able to show that temporary binding can indeed occur. Garrett concludes that a more rigorous treatment will be required in order to settle the question.

3. Vibrational excitation (H_2)

Vibrational excitation in electron–molecule scattering, classically speaking, occurs as a result of the force exerted on the nucleus due to the field of the scattered electron. Unlike rotational excitation, it is the component along the internuclear axis, rather than that perpendicular to it, that is most important to this process. Because of the unfavorable electron-to-nuclei mass ratio, an efficient transfer of energy (hence, large vibrational-excitation cross section) requires a long interaction time. This may result from a strong long-range interaction that depends sensitively on the internuclear separation, or a temporary attachment (resonance) of the electron for a time comparable to, or exceeding the vibrational period. In H_2, the long-range interactions are not strong, and low-energy ($E \lesssim 10$ eV) long-lived resonances do not occur. (There are, of course, series of sharp Feshbach resonances starting at about 11 eV.) Therefore the low-energy vibrational-excitation cross sections in electron–H_2 collisions tend to be smoothly varying in energy and not particularly large (i.e., $\lesssim 10^{-16}$ cm^2).

Early theoretical studies of vibrational excitation of molecules by electron impact [Morse (1929, 1953); Massey (1935); Wu (1947); Carson (1954); reviewed by Craggs and Massey (1956) and Massey (1969)] were based on the weak-coupling Born and distorted-wave approximations. In most of these calculations, only short-range electron–molecule interactions were considered [Wu (1947) considered a dipole interaction], and the resulting cross sections were found to be much too small to be consistent with early experimental measurements such as those of Ramien (1931). The swarm measurements of Frost and Phelps (1962) and Englehardt and Phelps (1963) and the electron-beam studies of Schulz (1964) made it clear that there was something missing in the early calculations. Schulz (1964) suggested that vibrational excitation in H_2 might proceed via temporary formation of a resonant H_2^- complex in much the same way as in N_2 (Schulz, 1962) and CO where resonances were clearly observed at energies $\cong 2.3$ eV and 1.7 eV, respectively. Chen and Magee (1962) had proposed a mechanism for vibrational excitation in electron–H_2 collisions which involved the explicit intermediate compound $^2\Sigma_u^+ H_2^-$ state. They used the real $^2\Sigma_u^+$ potential curve calculated by Dalgarno and McDowell (1956) to represent the nuclear potential energy for the compound state, and predicted vibrational-excitation cross sections $\cong 10^{-16}$ cm^2 in the range 6–8 eV (see Chen, 1969).

Bardsley, Herzenberg, and Mandl (1966a, b) applied the previously developed method of Herzenberg and Mandl (1962) to the "resonant scattering" of electrons by H_2. Their general approach was to calculate a resonant H_2^- state with complex potential energy $W(R) = V(R) - \frac{1}{2} i\Gamma(R)$ by expanding the wave function in Kapur–Peierls states. Thus, explicit account was taken of the outgoing-wave boundary condition, unlike the standard Rayleigh–Ritz variational calculations of H_2^- states which suffered from instability problems as explained by Davidson (1962) and further confirmed by Taylor and Harris (1963a, b, c). It was assumed that the relevant $^2\Sigma_u^+$ resonant state at low energies arose simply from a p-wave electron temporarily trapped inside the $l=1$ centrifugal "barrier." The authors found that for internuclear separations $R \gtrsim 3a_0$ a bound H_2^- state exists and $\Gamma(R)=0$. For $R \lesssim 3a_0$ the H_2^- state was found to be unstable with respect to autodetachment resulting in $H_2 + e$. The nuclear motion in this complex potential was then determined by solving the appropriate (modified) nuclear Schrödinger equation. Then, taking advantage of the small electron to nuclear mass ratio, the adiabatic (Born–Oppenheimer) approximation was employed and the "resonant" vibrational-excitation cross section calculated by a simple quadrature in R. The cross sections were also averaged over all orientations of the internuclear axis (adiabatic nuclear rotation approximation). The $v=0 \rightarrow 1$ and $0 \rightarrow 2$ cross sections obtained in this way were found to be in qualitative agreement with the experimental data available at the time (Englehardt and Phelps, 1963; Schulz, 1964). Qualitative agreement was considered satisfactory considering the approximations made in the calculations and the uncertainties in the measurements. It seemed to suggest that vibrational excitation of H_2 proceeds via a broad $^2\Sigma_u^+ H_2^-$ resonance state, although the lifetime $\tau(R_0) \equiv \hbar/\Gamma(R_0)$ evaluated at the ground-state equilibrium separation of

$R_0 \cong 1.4a_0$ is about 10^{-16} sec. This is comparable to a nonresonant collision time and shorter than a vibrational period. Subsequent development of the "stabilization method" (Taylor and Williams, 1965; Taylor, Nazaroff, and Golebiewski, 1966; Taylor, 1967; and Eliezer, Taylor, and Williams, 1967) has led to improved calculations of the real part of the H_2^- potential energy curve. However, the essence of the resonant-scattering picture given by Bardsley, Herzenberg, and Mandl (1966a, b) for low-energy electron–H_2 collisions remains valid.

Takayanagi (1965a, b) argued that one ought to be able to understand vibrational excitation in H_2 without relying on a purely resonant-scattering picture. If indeed the enhancement in the cross section arises from temporary, albeit very brief, trapping of a p-wave electron, then a simple distorted-wave calculation based on a physically reasonable electron–H_2 interaction potential should exhibit the effect. Takayanagi chose rather simple forms for the electron–molecule interaction, just to see what order of magnitude could be obtained. First, he showed that a Born–quadrupole calculation gives extremely small vibrational-rotational excitation cross sections—below 10^{-19} cm^2 in all cases. In addition, he demonstrated that allowing for the R dependence of the anisotropic polarizability $\alpha_2(R)$ results in an increase of the cross sections by less than a factor of 4. Next, allowance was made for the R dependence in the isotropic (average) polarizability $\alpha_0(R)$ by appropriately modifying the Born formulae. With this change, the $v=0\to 1$ cross section jumped to values in the range 3×10^{-17} cm^2 to 3×10^{-16} cm^2, depending on how the long-range polarization potential was cut off [see corrections to the Born results (Takayanagi, 1965b)]. Finally, distorted-wave calculations were carried out using the semiempirical distortion potential of Takayanagi and Geltman (1964, 1965). The shape of the $v=0\to 1$ cross section was different, exhibiting a somewhat sharper peak shifted to higher energies; however, the magnitude was about the same. Thus, Takayanagi (1965a, b) concluded that the long-range polarization interaction can be important to vibrational excitation and should be included in any realistic treatment of the problem.

Almost simultaneously, Breig and Lin (1965) carried out a similar study in which they applied the Born approximation to a number of model electron–molecule interactions for H_2, N_2, and CO. Raman data were used to estimate the important matrix elements, the quadrupole matrix element being chosen in the same way as Takayanagi (1965a). For reasonable choices of short-range cutoff functions, $v=0\to 1$ cross sections in the range 1 to 6×10^{-17} cm^2 were obtained, in essential agreement with the measurements. The authors concluded that the polarization interaction was important to vibrational excitation.

Motivated by the impressive measurements of simultaneous rotational and vibrational excitation of H_2 by Ehrhardt and Linder (1968), Abram and Herzenberg (1969) applied the adiabatic nuclear rotation (ANR) approximation (or impulse approximation, as they describe it) to the problem. They assumed that the $^2\Sigma_u^+ H_2^-$ resonance state was entirely responsible for the transitions and, noting that the estimated lifetime of this resonance was much less than a rotational period, assumed that the adiabatic approximation applied to rotational motion was valid. Moreover, they argued that because of the Σ_u symmetry of the resonance state, the angular dependence of the intermediate wave function would be given by $\cos(\hat{k}_0\cdot\hat{R})$, and that of the final state (continuum) wave function would be given by $\cos(\hat{k}\cdot\hat{R})$, where $\mathbf{k}_0$ and $\mathbf{k}$ are, respectively, the initial and final electron momentum. The authors showed that the scattering amplitude corresponding to $\mathbf{k}_0, v_0 \to \mathbf{k}, v$ with a fixed orientation of the internuclear axis $\hat{R}$ could be written

$$f(\mathbf{k}_0, v_0\to \mathbf{k}, v;\hat{R}) = \cos(\hat{k}_0\cdot\hat{R})\cos(\hat{k}\cdot\hat{R}) f(\hat{k}_0, v_0\to\hat{k}, v)\ , \tag{192}$$

where the last factor is an $\hat{R}$-independent resonant amplitude for $v_0\to v$ transitions; it is independent of the scattering angle $\theta' = \cos^{-1}(\hat{k}\cdot\hat{k}_0)$ as well. The authors did not attempt to calculate this factor, but concentrated on the angular dependence of various rotational-vibrational cross sections obtained by using Eq. (192) in the formula (see Sec. II.D)

$$f(\theta',\phi')_{vjm_j,\,v_0j_0m_{j_0}} \cong \int d\hat{R}\, Y_{jm_j}(\theta_R,\phi_R)^* f(\mathbf{k}_0, v_0\to\mathbf{k}, v;\hat{R}) \times Y_{j_0m_{j_0}}(\theta_R,\phi_R)\ . \tag{193}$$

Since the experiments did not isolate $m_{j_0}\to m_j$ transitions, comparisons were made of the cross sections averaged over m_{j_0} and summed over m_j. The theoretical results were in essential agreement with the following observations of Ehrhardt and Linder (1968): (i) the pure vibrational-excitation cross sections show pronounced p-wave character; (ii) the cross sections for $v=0\to 1$ and $j_0\to j_0+2$, for $j_0 = 1$, 2, and 3, are observed to be relatively independent of angle; and (iii) the cross section for $v=0\to 1$ and $j=1\to 3$ is about half that for $v=0\to 1$ and $j=3\to 5$. They also agree that the "total" cross section for all transitions $v=0\to 1$ and $j_0\to j$, for all possible j is proportional to $1+2\cos^2\theta'$ (O'Malley and Taylor, 1968; Bardsley and Read, 1968). [See comments of Chang (1974c) and Takayanagi (1975a, b).]

A comprehensive study of weak-scattering methods based on a variety of approximate electron–molecule interactions, and applied to elastic scattering and vibrational excitation, was begun by Truhlar and Rice (1970), to be referred to in this section as Paper I. A coordinated experimental–theoretical investigation of electron–molecule scattering was carried out over a period of several years and results were reported in a series of papers (Trajmar, Truhlar, and Rice, 1970a, Paper II; Trajmar, Truhlar, Rice, and Kupperman, 1970b, Paper III; Truhlar, Trajmar, and Williams, 1972, Paper IV; Truhlar, 1972, Paper V; Truhlar, Williams, and Trajmar, 1972, Paper VI; Chutjian, Truhlar, Williams, and Trajmar, 1972, Paper VII; and Truhlar, 1973, Paper VIII). In this series, Papers I–III and VIII deal with electron–H_2 scattering. Much of this work was carried out at higher energies than we are primarily concerned with in this review. The principal conclusions may be summarized very briefly: (1) the long-range quadrupole and polarization interactions are very important for integral $v = 0 \to 1$ cross sections; polarization completely dominates the small-angle ($\theta \lesssim 60°$) scattering. The smaller $v = 0 \to 2, 3$ cross sections are much more sensitive to short-range interactions [see related comments by Ritchie (1972) and Truhlar (1973)]; (2) the studies of exchange effects via the simple polarized–Born–Ochkur–Rudge approximation (Ochkur, 1964; Rudge 1965a, b; Morrison and Rudge, 1967) indicate that this type of approximation is poor for vibrational excitation of H_2 at energies as high as 60 eV. The nature of the agreement at 10 eV is illustrated in Fig. 16.

The first close-coupling calculation of vibrational excitation was carried out by Henry (1970) for electron–H_2 scattering. The laboratory-frame theory of Sec. II.E.1 was used, and the procedure was similar to that employed in the rotational-excitation studies of Henry and Lane (1969). The short-range static interaction potential was constructed using the simple H_2 charge distribution of Wang (1928). The long-range contributions including both the quadrupole and polarization interactions were identical to those of Henry and Lane (1969). However, the quadrupole moment $Q(R)$ and polarizabilities $\alpha_0(R)$ and $\alpha_2(R)$ were allowed to vary with internuclear separation R. The exchange terms were included in precisely the same manner as Henry and Lane (1969). There was no allowance for variation of the exchange kernel with internuclear separation. Vibrational matrix elements of the electron–H_2 interaction potential were evaluated by numerical quadrature using accurate vibrational wave functions based on the ground-state nuclear potential energy of Kolos and Wolniewicz (1967). Comparison of the most important matrix elements with those of Truhlar and Rice (1970) shows essential agreement. The coupled radial equations, including exchange, were solved in precisely the same way as in the rotational-excitation studies of Henry and Lane (1969), described in Sec. III.B.2. The close-coupling expansion was truncated to include only the ground ${}^1\Sigma_g^+$ electronic state, and at most vibrational states $v = 0$, 1, and 2 and rotational states $j = 1$ and 3 (ortho-H_2). In order to illustrate the sensitivities of the cross sections to various features of the interaction, Henry (1970) carried out a number of studies, leaving out one or another characteristic feature. He concludes that short-range coupling alone (i.e., ignoring all coupling matrix elements involving the quadrupole and polarization terms) accounts for less than one-half of the integral $v = 0 \to 1(\Delta j = 0)$ cross section for all energies studied ($E \lesssim 10$ eV). The importance of rotational coupling was examined by studying the effect of dropping the $j = 3$ channels from the calculation. This caused a reduction in the integral $v = 0 \to 1(\Delta j = 0)$ cross section of about ~40% for $E \lesssim 4$ eV. The large effect is presumably due to important p-wave coupling via the anisotropic part of the electron–molecule interaction potential. (In a LAB-frame treatment, the coupling of partial waves is tied to the coupling of rotational states. In this example, when the $j = 3$ state is removed, the p-wave coupling disappears as well.) The effect of neglecting the $v = 2$ vibrational state in the calculation of the $v = 0 \to 1$ cross section was found to be much less serious. These sensitivity studies, and others carried out previously (Henry and Lane, 1969) suggest that the retention of only the $j = 1, 3$ rotational states should not result in serious error. However, the convergence in vibrational states may be slow, and the neglect of higher vibrational states could be a source of significant error (Henry and Chang, 1972). Probably the most serious source of error is the "scaled" polarization potential. Henry and Lane (1969) speculated that the polarization potential of Lane and Henry (1968), obtained only at $R_0 = 1.4a_0$, might be too strong. If this is the case, then the overall scaling of the potential according to the variation of the polarizabilities $\alpha_0(R)$ and $\alpha_2(R)$ with R would likely result in too strong a vibrational coupling, causing the vibrational excitation cross sections to be too large. Indeed, the calculated integral cross sections for $v = 0 \to 1(\Delta j = 0)$, $v = 0 \to 2(\Delta j = 0)$, and $v = 0 \to 1(j = 0 \to 3)$ transitions were found to exceed the observed cross sections by as much as a factor of 2 in some cases.

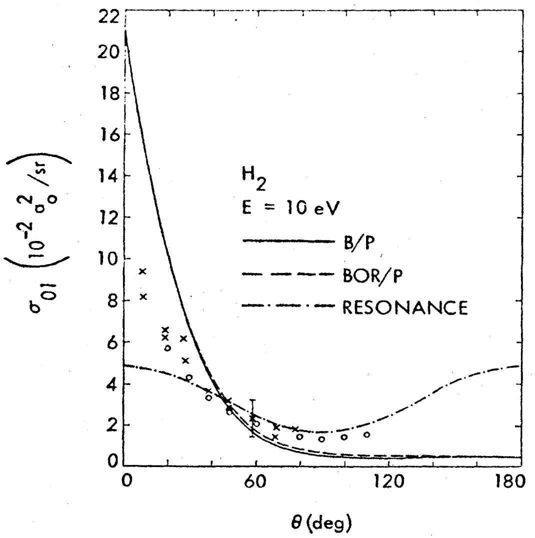

FIG. 16. Differential cross sections for $v = 0 \to 1$ vibrational transition in e–H_2 scattering at 10 eV. Theory: (solid curve) Born polarization; (dashed curve) Born–Ochkur–Rudge polarization; (dot-dashed curve) pure p-wave resonance form, Trajmar *et al.* (1970b). Experiment, (open circles) Ehrhardt *et al.* (1968); (crosses) Trajmar *et al.* (1970b). (Reprinted from Trajmar *et al.*, 1970b.)

Henry and Chang (1972), using the frame-transformation approach of Chang and Fano (1972), carried out an adiabatic nuclei calculation of cross sections for vibrational and rotational-vibrational excitation in electron–H_2 scattering. In this calculation the adiabatic approximation was applied to both rotational and vibrational motion of the molecule. The electron–molecule interaction potential, including the static and polarization contributions, was approximated by precisely the same form as that used by Henry (1970) with one exception. In the present work, the long-range terms in the single-center expansion were cut off sharply for all $r \le r_c(R)$, where the cutoff radius $r_c(R)$, in general a function of internuclear separation R, was chosen so that

$$\int_0^{r_c(R)} d\mathbf{r}_m |\psi_0^{(e)}(\mathbf{r}_m;R)|^2 = x\,, \tag{194}$$

where $\psi_0^{(e)}$ is the ground-state electronic wave function, the integral runs over all values of electronic coordinates $\mathbf{r}_1$ and $\mathbf{r}_2$, and where x is a parameter usually taken to be 0.25. This cutoff procedure was an attempt to correct the adiabatic polarization potential of Lane and Henry (1968), which was evaluated only at $R = R_0 \cong 1.4a_0$. The long-range tail of this potential could be corrected by simply using the R-dependent polarizabilities $\alpha_0(R)$ and $\alpha_2(R)$ to appropriately scale the functions v_0^P and v_2^P; however, the cutoff inherent in the Lane and Henry (1968) interaction should vary somehow with internuclear separation R. The procedure used by Henry and Chang (1972) is reasonable, but unfortunately admits a new parameter x. The exchange terms were handled in the same manner as Henry (1970) and Henry and Lane (1969) and were taken to be independent of R. The scattering equations were solved in the BODY frame for several appropriate values of R. The operator H_{ROT} of Eq. (68) was ignored so that there was no coupling between different m_l, and $\Sigma_{g,u}, \Pi_{g,u}$, etc., scattering states could be treated separately. In addition, the approximation was made of ignoring coupling between different l so that single-channel radial equations could be solved for the $s_\sigma, p_\sigma, p_\pi$, etc., phase shifts independently. [This is a fairly good approximation for a small molecule like H_2 at low energies since the channels p_σ and s_σ do not couple (they are of u and g parity, respectively) and d_σ, f_σ, etc., radial functions do not penetrate the respective centrifugal barriers very much at low energies. In heavier molecules, e.g., N_2, CO, CO_2, $l \geq 2$ partial waves are quite important near the nuclei where they are "generated" from incoming s and p waves due to the strong attractive electron–nuclear interaction (this is true even in the zero-energy limit).] The frame transformation was carried out at $r = 5a_0$ and the LAB-frame K and T matrices immediately determined, with no further integration in the outer region. The authors argued that substantially all the important (i.e., R-dependent) phase had accumulated by $r = 5a_0$ so that further integration in the BODY frame would have little effect. The choice not to continue integration in the LAB frame, after the frame transformation, followed from the expectation that the vibrational-coupling matrix elements would be small for $r > r_0$. Essentially, the justification was the assumed validity of the adiabatic approximation applied to nuclear vibration. The s_σ, p_σ, and p_π phase shifts resulting from this BODY-frame calculation, and determined at $r = 5a_0$, all depend on R, as illustrated in Fig. 17. However, the p_σ phase shift exhibits the strongest variation with R in the important region $1.0a_0 \lesssim R \lesssim 2.0a_0$. While the p_σ phase shift does not pass through $\pi/2$ for R in this region, as it would if a *long-lived* compound state were formed, there is no ambiguity in attributing this rapid rise in the p_σ phase shift to a *short-lived* compound state, i.e., a "broad" resonance feature, as did Bardsley, Herzenberg, and Mandl (1966a, b). In order to better interpret the results obtained by Henry (1970), Henry and Chang (1972) calculated the $v = 0 \rightarrow 1$ cross section with exactly the same interaction as Henry (1970), i.e., with $x = 0$, or $r_c(R) = 0$, in Eq. (194). In Fig. 18 the pure $v = 0 \rightarrow 1$ vibrational-excitation cross sections of Henry (1970), curve B, and Henry and Chang (1972), curve A, are compared with the experimental results of Linder (1969) and Linder and Schmidt (1971a). The authors attributed the large bump in the cross section determined by Henry (1970) to improper truncation of the close-coupling expansion in vibrational states, implying that had more states been retained the consequent redistribution of flux, for example via virtual mechanisms like $v = 0 \rightarrow 1 \rightarrow 2$, would have resulted in a smaller $v = 0 \rightarrow 1$ cross section, more like that of Henry and Chang (1972). Henry (1970) did carry out a few checks of this kind though not with the full interaction nor with a sufficiently large number of channels to be conclusive. Another possible explanation is that the choice of $r = 5a_0$ as a transformation *and* K matrix (i.e., phase shift) matching radius underestimates the p_σ phase shifts and their R variation, so that the Henry and Chang (1972) cross section should be larger. The p_σ scattering tends to depend more on long-range interactions than does s_σ, and the R-dependent $\alpha_0(R)$ and $\alpha_2(R)$ may still be effective beyond $5a_0$. This question could be resolved with a slightly more refined calculation. The authors also concluded that the r_c cutoff was necessary, and they felt that $x = 0.25$ was a reasonable choice. Their integral $v = 0 \rightarrow 1$ cross section is shown in Fig. 19 along with the experimental results:

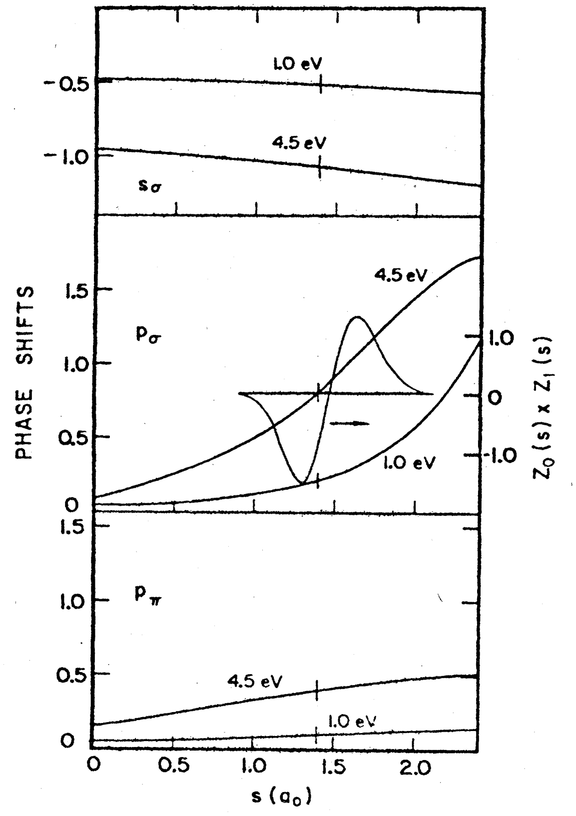

FIG. 17. Electron–H_2 scattering phase shifts for s_σ, p_σ, and p_π partial waves; and product of $v = 0$ and $v = 1$ vibrational wave functions as a function of internuclear separation $s = R$. (Reprinted from Henry and Chang, 1972.)

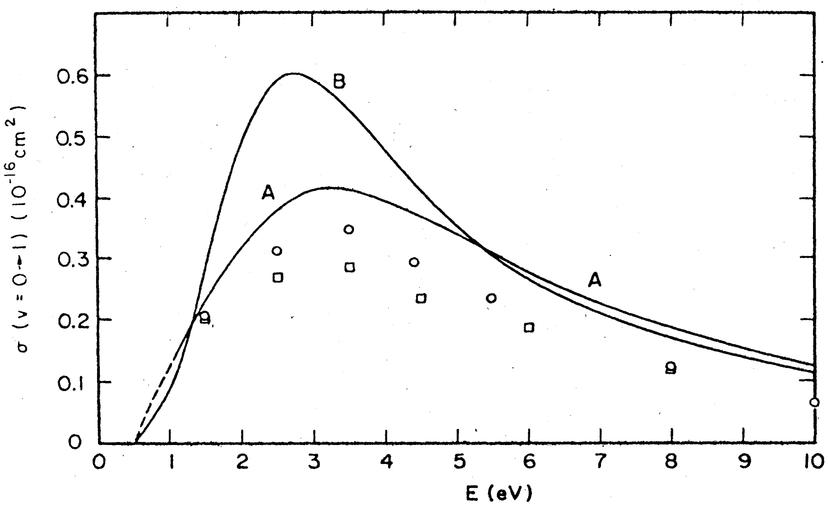

FIG. 18. Cross sections for $v=0\rightarrow1$ vibrational excitation in e–H_2 scattering. Theory: (curve A) adiabatic nuclear vibration, Henry and Chang (1972); (curve B) vibrational close coupling, Henry (1970). Experiment: (open circles), Linder (1969); (open boxes) Linder and Schmidt (1971a). (Reprinted from Henry and Chang, 1972.)

Linder and Schmidt (1971a); Ehrhardt, Langhans, Linder, and Taylor (1968); Trajmar *et al.* (1970a,b); Schulz (1964); Englehardt and Phelps (1963); Crompton *et al.* (1970); and Burrow and Schulz (1969). Agreement with most of the data is satisfactory. (The authors caution that their procedure is not appropriate near threshold.) In Fig. 20 the calculated ($x=0.25$) and observed $v=0\rightarrow1(\Delta j=0)$ and $v=0\rightarrow1(j=1\rightarrow3)$ cross sections are compared; the measurements are those of Linder and Schmidt (1971a). Again, the agreement is good. The corresponding differential cross sections are illustrated in Fig. 21, where the notation is the same as in Fig. 20. The calculated ratio of cross sections $v=0\rightarrow1(\Delta j=0)$ to $v=0\rightarrow1(j=1\rightarrow3)$ also was found to be in excellent agreement with the observed ratio (Ehrhardt and Linder, 1968; and Linder and Schmidt, 1971a). (See clarifying comments regarding this ratio given by Chang, 1974c.) Henry and Chang (1972), in concluding remarks, are careful to point out that their approximation of neglecting all contributions to the scattering for $r\geqslant5a_0$ will certainly fail at low energies, and that of ignoring partial waves with $l\geqslant2$ will fail at higher energies, say $E\gtrsim10$ eV. Finally, the authors caution that the fixed-nuclei approximation will fail for applications where long-lived compound states are involved.

Faisal and Temkin (1972) also applied the adiabatic approximation to vibrational excitation in electron–H_2 scattering. They did not actually solve the scattering equations, but rather "pieced together" R-dependent phase shifts using the results of other calculations. Working in the fixed-nuclei approximation they assumed linear variation of the BODY-frame phase shifts with respect to R, i.e.,

$$\eta_{lm}(R)\cong\eta_{lm}(R_e)+\eta'_{lm}(R_e)(R-R_e)\,, \tag{195}$$

where the derivative was estimated by the simple expression

$$\eta'_{lm}(R_e)\cong\left[\frac{\eta_{lm}(R_e)-\eta_{lm}(0)}{R_e}\right]\times\begin{cases}1 & l,m\neq1,0\\ g(E) & l,m=1,0\end{cases} \tag{196}$$

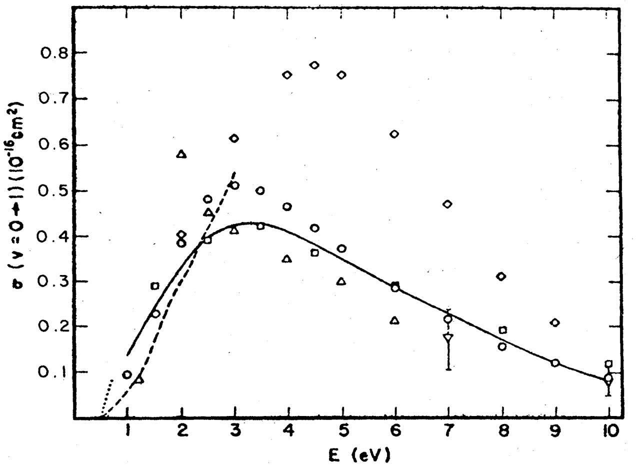

FIG. 19. Cross sections for $v=0\rightarrow1$ vibrational excitation in e–H_2 scattering. Theory: (solid curve) adiabatic nuclear vibration with parameter $x=0.25$ in Eq. (194). Experiment (□) Linder and Schmidt (1971a); (○) Ehrhardt *et al.* (1968); (▽) Trajmar *et al.* (1970b); (△) Schulz (1964); (◇) Englehardt and Phelps (1963); (dashed line) Crompton *et al.* (1970); (dotted line) Burrow and Schulz (1969). (Reprinted from Henry and Chang, 1972.)

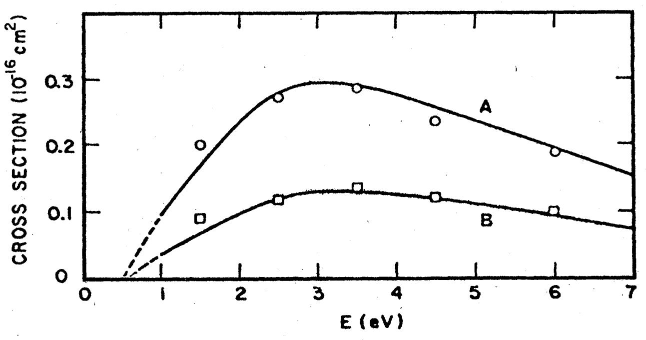

FIG. 20. Cross sections for $v=0\rightarrow1$ ($\Delta j=0$) vibrational excitation and $v=0\rightarrow1$ ($j=1\rightarrow3$) rotational–vibrational excitation in e–H_2 scattering. Theory: (solid curves) adiabatic nuclear vibration with parameter $x=0.25$ in Eq. (194), Henry and Chang (1972). Experiment: (open circles and squares), Linder and Schmidt (1971a). (Curve A and open circles) $v=0\rightarrow1$, $\Delta j=0$; (curves B and open squares) $v=0\rightarrow1, j=1\rightarrow3$. (Reprinted from Henry and Chang, 1972.)

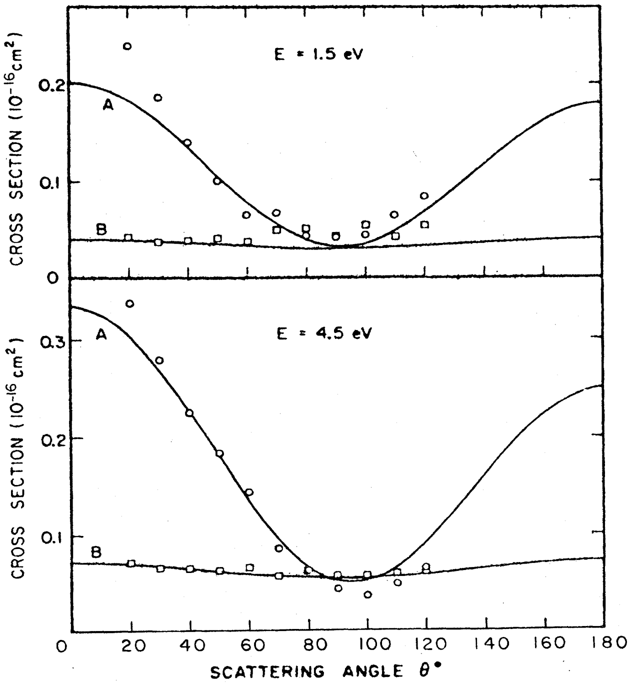

FIG. 21. Differential $v = 0 \rightarrow 1$ ($\Delta j = 0$) vibrational and $v = 0 \rightarrow 1$ ($j = 1 \rightarrow 3$) rotational-vibrational cross sections in e–H_2 scattering at 1.5 and 4.5 eV. (Curves A and B and ○ and □ as in Fig. 20.) (Reprinted from Henry and Chang, 1972.)

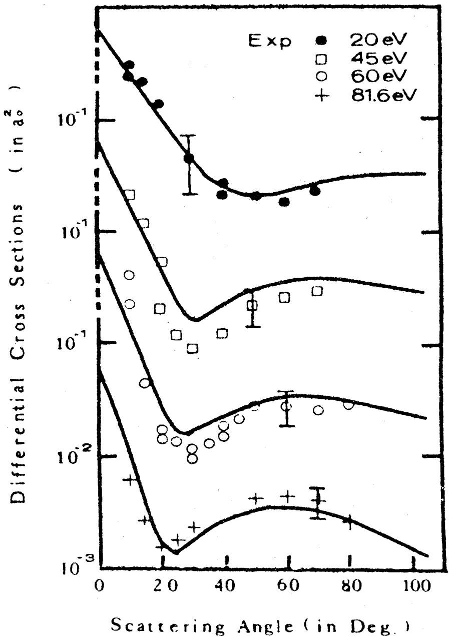

FIG. 22. Differential cross sections for $v = 0 \rightarrow 1$ ($\Delta j = 0$) vibrational excitation in e–H_2 scattering at 20, 45, 60, and 81.6 eV. Theory: (solid curves) Glauber approximation, Chang *et al.* (1973). Experiment: (●, □, ○, +) as given in Trajmar *et al.* (1970b). (Reprinted from Chang *et al.*, 1973.)

where $\eta_{lm}(R_e)$ was taken from the calculations of Tully and Berry (1969), with Born-approximation corrections added to $l > 0$ phase shifts to account for polarization effects. The $R = 0$ phase shift $\eta_{lm}(0)$ was identified with the electron–helium phase shifts, including exchange and polarization, of Duxler, Poe, and LaBahn (1971). The factor $g(E)$ is an energy-dependent parameter which was adjusted to fit the measured total $v = 0 \rightarrow 1(\Delta j = 0)$ cross section. Note that $g(E)$ does not depend on R, and therefore is simply an energy-dependent scaling factor. It does not affect the angular dependence of the differential cross sections, but simply scales the overall magnitude, at a given energy, by a constant factor. By fitting to the total $v = 0 \rightarrow 1$ (all Δj), taken as the sum of the observed cross sections for $v = 0 \rightarrow 1(\Delta j = 0)$ and $v = 0 \rightarrow 1(j = 1 \rightarrow 3)$ cross sections the factor $g(E)$ was assigned the values ranging from 3.7 to 1.2 for energies in the range 1.224–8.704 eV. The semiempirical, integral, and differential cross sections for transitions $v = 0 \rightarrow 1(\Delta j = 0)$ and $v = 0 \rightarrow 1(j = 1 \rightarrow 3)$ were found to be in very good agreement with the measurements and the results of Henry and Chang (1972) shown in Figs. 19–21, providing evidence for the validity of the adiabatic approximation applied to vibrational excitation.

Chang, Poe, and Ray (1973) applied the Glauber approximation to $v = 0 \rightarrow 1$ excitation in H_2. In this work a model electron–H_2 potential is constructed consisting of a (cutoff) long-range R-dependent polarization potential and a short-range superposition of screened H atom potentials (Wang, 1928) separated by variable distance R. The vibrational wave functions are approximated by Morse functions. Within the framework of Glauber theory (Glauber, 1959; Franco and Glauber, 1966) calculation of the differential vibrational excitation cross sections is straightforward. The calculated $v = 0 \rightarrow 1$ differential cross sections at several energies are compared in Fig. 22 with the observations of Trajmar *et al.* (1970a, b). The agreement is surprisingly good not only at small angles where the long-range polarization interaction dominates the scattering but also at intermediate and large angles where one would expect exchange and other molecular effects to be important. The authors do show that the "double scattering" correction is small at 81.6 eV. They remark that this correction is likely to be more important for $v = 0 \rightarrow 2, 3$, etc., transitions and at low energies for all transitions.

Wong and Schulz (1974), in a measurement of differential cross sections for rotational, vibrational, and rotational–vibrational excitation in electron–H_2 scattering, observed that the ratio of the $v = 0 \rightarrow v'(\Delta j = 0)$ to $v = 0 \rightarrow v'(j = 1 \rightarrow 3)$ cross sections decreases as v' increases, i.e., in going from $v = 0 \rightarrow 1$ to $0 \rightarrow 2$ and $0 \rightarrow 3$ transitions. The effect has not been predicted by earlier theoretical studies. Temkin and Sullivan (1974) and Chang (1974c) stress different mechanisms as an explanation of this behavior. Temkin and Sullivan (1974) pointed out that the vibrational wave functions used in the adiabatic nuclei approximation (Faisal and Temkin 1972) should depend on the rotational quantum number because of the centrifugal "effective" barrier tending to push the vibrational wave function outward for increasing j. This mechanism as well as partial-wave interference was felt to be important. The authors numerically determined the j-dependent vibrational wave functions and energies, obtaining good agreement with the accurate results of Kolos and Wolniewicz (1965), and then repeated the adiabatic nuclei calculations in the manner of Faisal and Temkin (1972). By choosing a somewhat different value of the scaling parameter $g(E)$ in Eq. (196), viz., 2.0 instead of 2.4 for $E \cong 4.9$ eV, they obtained an appreciable dependence of the ratio of $v=0 \rightarrow v'(\Delta j=0)$ to $v=0 \rightarrow v'(j=1 \rightarrow 3)$ cross sections on the final vibrational quantum number v'. The angular dependence of the ratios was found to be in good agreement with the observations for $v'=1$, 2, and 3. The effect of incorporating j-dependent vibrational functions is to raise the $v=0 \rightarrow 1$ ratio considerably and lower the $v=0 \rightarrow 2$ ratio slightly, while leaving the $v=0 \rightarrow 3$ ratio essentially unchanged. The angular dependence of the $v=0 \rightarrow 3$ ratio is, in fact, reproduced quite well by the $^2\Sigma_u^+$ resonance theory of Abram and Herzenberg (1969).

Chang (1974c) took the alternative point of view that the important effect was simply interference of the p_σ with other partial waves and, therefore, that the theory of Henry and Chang (1972) was sufficient to describe the phenomenon. Using their R-dependent phase shifts $\eta_{lm}(R)$ at 4.5 eV, he evaluated the appropriate S-matrix elements from the expression

$$S^{m}_{v'l,vl} \cong \int_0^\infty \psi^{(v)}_{v'}(R) \exp[2i\eta_{lm}(R)]\psi^{(v)}_{v}(R)R^2 dR \qquad (197)$$

by expanding the exponential in Hermite polynomials, with coefficients which involved the derivatives of $\eta_{lm}(R)$ evaluated at $R_e \cong 1.4a_0$, and by approximating the vibrational wave functions by harmonic oscillator functions. The calculated ratios of $v=0 \rightarrow v'(\Delta j=0)$ to $v=0 \rightarrow v'(j=1 \rightarrow 3)$ cross sections were found to be in fair agreement with the observations for $v'=1$ and 3, but rather poor agreement was obtained for $v'=2$. Chang (1974c) shows in general that the ratio of $v=0 \rightarrow v'+1(j=1 \rightarrow 3)$ to $v=0 \rightarrow v'(j=1 \rightarrow 3)$ cross sections is approximately equal to 0.1, independent of the value of v'; this result is in agreement with the observations of Wong and Schulz (1974). The author disagrees with Temkin and Sullivan (1974) and argues that centrifugal distortion of the vibrational wave function is important; however, he did not test this assertion by comparative calculations. It is probable that neither of the models is sufficiently accurate to decide the question.

Chang and Wong (1977) report experimental measurements and theoretical interpretation of the isotope effect in rotational, vibrational, and rotational-vibrational excitation as evidenced in the ratios of the respective D_2 to H_2 cross sections. Using arguments based on frame-transformation theory, the authors interpret the observations in terms of the dependence of the various cross sections on nuclear (reduced) mass and on nuclear statistics. Predictions are made for HD, HT, DT, and T_2 targets.

Klonover and Kaldor (1979b) have applied their *ab initio* method of including both exchange and polarization effects (Kaldor and Klonover, 1977; Klonover and Kaldor, 1978) to vibrational excitation of H_2. (See description in Sec. III.B.2). This is the first true *ab initio* calculation of vibrational excitation in molecules. The procedure is based on the T-matrix-expansion method (Rescigno, McCurdy, and McKoy, 1974a, b; 1975a) in which correlation effects are included systematically via a diagrammatic perturbation series. The procedure is similar to that of Klonover and Kaldor (1978), where here the adiabatic approximation is applied to the vibrational as well as rotational degrees of freedom of the molecule (adiabatic nuclei approximation). It is important to note that there are no adjustable parameters in this approach. Nonadiabatic corrections to the polarization interaction are automatically included. On the other hand, a great deal of intuition and good judgment based on experience goes into selection of an adequate basis set for the discretization of the scattering problem (see Sec. II.F.2). The calculated integral cross sections for $v=0 \rightarrow 1(\Delta j=0)$ and $v=0 \rightarrow 1(j=1 \rightarrow 3)$ transitions are compared in Figs. 23 and 24, respectively, with the measurements of Linder and Schmidt (1971a). The agreement is very encouraging, especially considering that no semiempirical adjustment has been made. The somewhat irregular energy variation evident in the elastic and rotational-excitation cross sections (Kaldor and Klonover, 1977; Kaldor and Klonover, 1978; see Sec. III.B) is not present here. Differential cross sections have been calculated for the same transitions. The agreement with experiment (Linder and Schmidt, 1971a) is also good except at small angles ($\theta \lesssim 50°$) where the theoretical cross sections lie below experiment, as shown in Fig. 25. This difference is consistent with the integral cross section in Fig. 23. Recent extensions of these calculations (Klonover and Kaldor, 1979c) obtain somewhat improved $v=0 \rightarrow 1(\Delta j=0$ and $j=1 \rightarrow 3)$ results and differential cross sections for $v=0 \rightarrow 1, 2, 3(\Delta j=0$ and $j=1 \rightarrow 3)$ transitions in good agree-

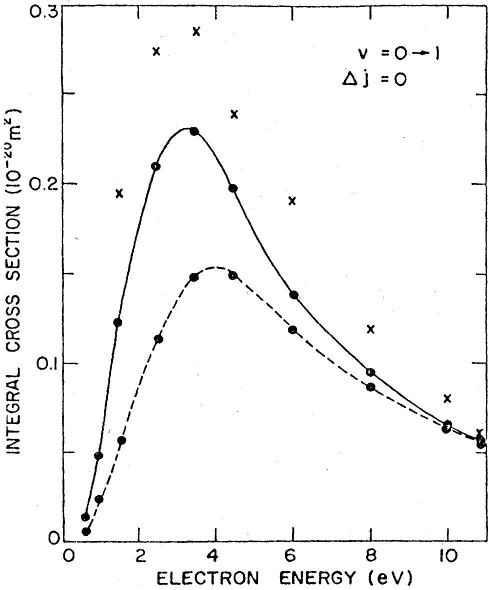

FIG. 23. Cross sections for $v=0 \rightarrow 1(\Delta j=0)$ vibrational excitation in e–H_2 scattering. Theory: (solid curve) exchange polarization, (dashed curve) static exchange, adiabatic nuclear vibration, Klonover and Kaldor (1979). Experiment: (×) Linder and Schmidt (1971a). (Reprinted from Klonover and Kaldor, 1979.)

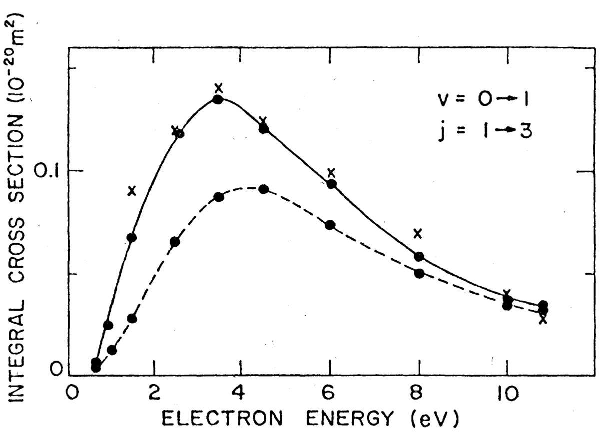

FIG. 24. Cross sections for $v=0\rightarrow 1$ ($j=1\rightarrow 3$) rotational–vibrational excitation in e–H_2 scattering (curves and × as in Fig. 23). (Reprinted from Klonover and Kaldor, 1979.)

ment with the measurements of Wong and Schulz (1974).

Kaldor (1979a) has recently shown that the T-matrix-expansion method may also be used to carry out a full vibrational close-coupling calculation. However, the adiabatic nuclei approximation still leads to considerable simplification.

C. ELECTRON-N_2 SCATTERING

1. Elastic scattering (N_2)

The nitrogen molecule with its 14 electrons contrasts with H_2 as a scattering target. Because of the appreciable nuclear charge, the molecule is not very "atomlike." The static electron–molecule interaction potential energy is strong and highly asymmetric. The observed *total* cross section illustrated in Fig. 26 [Brüche (1927); Golden (1966); see also Mathur and Hasted (1977), and Potter, Steph, Dwivedi, and Golden (1977)] is characterized by a large shape resonance, centered at about 2 eV and carrying a fine structure. [Also shown in the figure is the early theoretical cross section obtained by Fisk (1936) using a simple semi-empirical model.] At low energies, well below the resonance, the cross section falls to a value not much different from that of H_2. The structure superimposed on the broad resonance is known to result from transient vibrational states associated with the N_2^- negative complex [see reviews by Bardsley and Mandl (1968), Chen (1969), Golden (1978), and Schulz (1973, 1976), and discussion in Massey (1969)]. Since the lifetime of the N_2^- complex is comparable to a vibrational period, the picture of a vibrating N_2^- molecule is not appropriate. The intuitive "boomerang" model of Herzenberg (1968) and Birtwistle and Herzenberg (1971) was invented to describe this intermediate case. The adiabatic approximation to *vibrational excitation* clearly breaks down for energies in the vicinity of this resonance structure (the adiabatic nuclear rotation approximation is still valid). The fixed-nuclei calculations described in this section are of course *not* expected to reproduce the structure. The structure results from subtle vibrational effects that must be explicitly included in the theory (Birtwistle and Herzenberg, 1971; Chandra and Temkin, 1976a, b, c).

a. Static exchange

The first theoretical treatment of electron–N_2 scattering that included a proper approach to exchange was that of Burke and Sinfailam (1970). They adopted the fixed-nuclei static-exchange approximation (see Sec. II.G) in which the N_2 molecule is assumed to remain in its unperturbed $^1\Sigma_g^+$ ground state (single configuration description: $1\sigma_g^2 2\sigma_g^2 3\sigma_g^2 1\sigma_u^2 2\sigma_u^2 1\pi_u^4$). A single-center partial-wave expansion [Eq. (115)] was used, leading to the coupled integro-differential equation (116). The ground-state LCAO–MO–SCF orbitals of Nesbet (1964) were used in both the static potential energy, Eq. (117), including terms $\lambda \leq 4$, and the exchange term, Eq. (119).

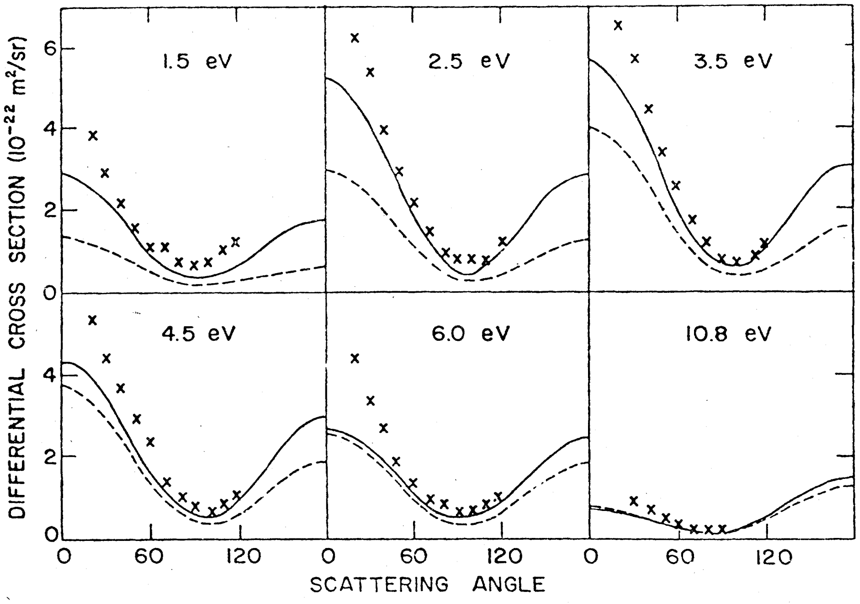

FIG. 25. Differential cross sections for $v=0\rightarrow 1$ ($\Delta j=0$) vibrational excitation in e–H_2 scattering (curves and × as in Fig. 23). (Reprinted from Klonover and Kaldor, 1979.)

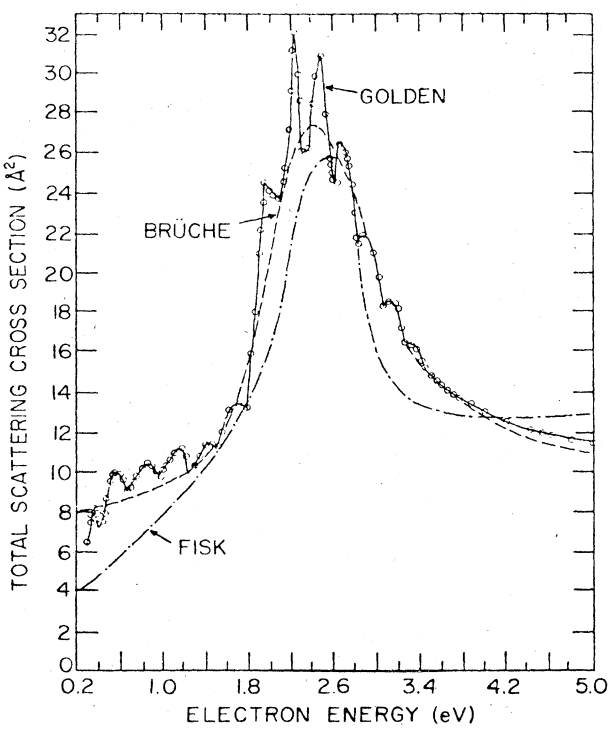

FIG. 26. Total cross sections for $e-N_2$ scattering. Experiment: (solid curve) Golden (1966); (dashed curve) Brüche (1927). Early theoretical model (chain curve) Fisk (1936). (Reprinted from Golden *et al.*, 1971.)

The procedure of Faisal (1970) as coded by Faisal and Temkin (1972) was used for the former. The coupled equations (116) were solved by the noniterative technique [Marriott (1958), Omidvar (1961, 1974); see Smith *et al.* (1966)]. A series of convergence studies performed for each "symmetry" (i.e., value of m), in which different numbers of partial waves were retained in Eqs. (115) and (116), strongly indicated that convergence in l was slow. Even though values of $l \leqslant 8$ were included for some of the symmetries, the "eigenphase sums" [see Eq. (123) and related discussion] and the elastic cross sections were clearly not converged. These high-l partial waves do *not* contribute directly to the T matrix; the corresponding radial functions $u_{lm}(r)$ are vanishingly small in the asymptotic region due to the large centrifugal barriers that are present. However, near the nuclei, the strong nonspherical interaction mixes ("couples") a large number of high-l partial waves. At larger r, only the low-l partial waves can penetrate the corresponding centrifugal barriers and, in so doing, survive in the asymptotic region. However, these important low-l partial waves are strongly influenced by the mixing that has occurred near the nuclei, and that influence is reflected in their asymptotic form and, thus, in the T matrix. (See discussion of Fano, 1970b.) Because the region near the nuclei is so important, early truncation of the static potential energy $V_s(\mathbf{r})$, [Eq. (118)], can also give rise to large errors in the calculation. Although the static and static-exchange calculations of Burke and Sinfailam (1970) were not fully converged with respect to the expansion of $V_s(\mathbf{r})$ and the partial-wave expansion (115), a number of important features were evident: (1) the effect of including exchange is to *increase* the eigenphase sums, removing a false Σ_g ($m = 0$, even $l \geqslant 0$) resonance present in the static calculation and introducing a Π_g ($m = \pm 1$, even $l \geqslant 2$) resonance in qualitative agreement with experiment; (2) in the low-energy limit, the contributions of various symmetries are dominated by the lowest-order partial wave present, i.e., $\Sigma_g(m=0)$, by s waves, $\Sigma_u(m=0)$ by p waves, $\Pi_g(m=\pm 1)$ by d waves, $\Pi_u(m=\pm 1)$ by p waves, etc.; and (3) exchange is less important for higher-order partial waves, hence for symmetries corresponding to large m; however, even the $\Delta_g(m=\pm 2$, even $l \geqslant 2)$ and $\Delta_u(m=\pm 2$, odd $l \geqslant 3)$ eigenphase-shift sums showed substantial increases when exchange was included.

Burke and Chandra (1972) pursued the question of convergence in the single-center-expansion approach. However, in order to include significantly more partial waves, it was necessary to adopt an approximate "modified pseudopotential" (MPS) approach to treating exchange. (See Sec. II.G.4 for discussion of this method.) The procedure is to replace the exchange terms in Eq. (116) by inhomogeneous terms of the form

$$\sum_j^{\text{occ}} \lambda_j \phi_j(\mathbf{r}), \tag{198}$$

where the ϕ_j are occupied molecular orbitals (Nesbet, 1964) and the λ_j are Lagrange multipliers, chosen self-consistently so that the scattering orbital, Eq. (115), for each symmetry (i.e., $\sigma_g, \sigma_u, \pi_g, \pi_u, \ldots$) is orthogonal to every occupied orbital of the same symmetry. The authors argue that this orthogonality constraint is the most important effect of exchange for a closed-shell target molecule. An obvious limitation of the MPS method is its failure to include *any* contribution of exchange for symmetries that are not found among the occupied orbitals, e.g., π_g. A rough check of the MPS method was made by comparing MPS results, obtained with the same truncation of static-potential-energy and partial-wave expansions as Burke and Sinfailam (1970) with the static-exchange results of the latter. The eigenphase sums were found to be similar, and based on this agreement a systematic study of convergence was carried out. In the static approximation, convergence both in λ and l was found to be slow. For Σ_g, it was felt necessary to retain all terms $\lambda \leqslant 12$ in $V_s(\mathbf{r})$ and $l \leqslant 12$ in the partial-wave expansion. With the orthogonalization constraint imposed (i.e., the MPS approximation to static exchange) convergence was faster in both λ and l, and only $l \leqslant 10$ were retained. Their experience with the Σ_u and Π_u symmetries was similar. No exchange contribution was included for Π_g symmetry, since there are no occupied π_g orbitals in the ground state of N_2. Convergence was therefore very slow for this symmetry. These calculations confirmed the features noted by Burke and Sinfailam (1970), viz., the disappearance of a false Σ_g resonance (in the static calculation) and the overall increase of all eigenphase sums when exchange is included. Burke and Chandra (1972) also calculated model-polarization cross sections, which will be discussed in the next section.

Crees and Moores (1975, 1977) emphasized that the slow convergence could be reduced by simply solving the scattering equations in the two-center prolate spheroidal coordinates (Nagahara, 1953; Hara, 1969a). In this study, exchange was *not* included. The static interaction potential energy was calculated using the same N_2 ground-state wave function as Burke and Chandra (1972), but expanded in Legendre polynomials of argument $\eta = (r_a - r_b)/R$ rather than $\cos\theta$. The coupled ordinary differential equations [i.e., the counterparts of Eq. (116) in variable $\xi = (r_a + r_b)/R$, but somewhat different in form] were solved by the linear-algebraic method of Seaton (1974). The eigenphase sums for $^2\Sigma_g$ and $^2\Pi_g$ symmetries resulting from this calculation are not in good agreement with the "converged" one-center static calculations of Burke and Chandra (1972).

Morrison and Collins (1977) in an attempt to resolve this discrepancy, carried out carefully controlled convergence studies of the single-center expansion method [i.e., the approach of Burke and Chandra (1972)] applied to electron–N_2 scattering in the static approximation. They used ground-state N_2 wave functions (Cade, Sales, and Wahl 1966) of similar quality to the previous studies. The coupled equations (116) were solved with the exchange terms omitted, using the integral equations method [Sams and Kouri (1969a, b), including the stabilization features of White and Hayes 1972]. Using the same truncation as Burke and Chandra (1972), i.e., $\lambda \leq 14$ and $l \leq 12$, the authors obtained eigenphase sums in essential agreement with those of Burke and Chandra (1972). Extending the calculation to include more terms in the expansion of $V_s(\mathbf{r})$ in Eq. (118) ($\lambda \leq 14$ for the electron–electron repulsion terms and $\lambda \leq 28$ for the electron–nuclear attraction terms), the authors conclude that their own cross sections are converged to 1% and that the calculations of Crees and Moores (1975) are in error. [This was independently suggested by Buckley and Burke (1977) and has been confirmed by Crees and Moores (1977), who give corrected results in better agreement with other authors.]

Buckley and Burke (1977) extended the earlier fixed-nuclei ($R = R_0 = 2.068a_0$) static-exchange calculations of Burke and Sinfailam (1970) to include additional terms in the expansions of the static and exchange interactions and higher-order partial waves as needed for convergence. (Polarization effects were also included via a model potential; these will be discussed in the next section.) The static and exchange terms were evaluated using the LCAO–MO–SCF N_2 ground-state wave function of Nesbet (1964) as described by Burke and Sinfailam (1970). It was concluded by the authors, but not shown, that convergence of the static-exchange cross section was satisfactory with $\lambda \leq 14$ in the expansion of $V_s(\mathbf{r})$ of Eq. (118) and $l \leq 13$ in the partial-wave expansion (115). Convergence was found to be better for the larger values of m. Partial cross sections were calculated for symmetries Σ_g, Σ_u, Π_g, Π_u, Δ_g, and Δ_u. Channels corresponding to larger values of m were found to be unimportant for energies considered ($E \leq 13.6$ eV). Eigenphase sums for $\Sigma_g (m = 0$, even $l \geq 0)$ channels are illustrated (modπ) in Fig. 27 for the static, static-exchange, and static-exchange-polarization (to be discussed) approximations. The effect of exchange is to remove the strong energy dependence of the eigenphase sum (dominated by the s_σ wave at low energies) and, though not apparent in the figure, constrain the eigenphase sum to approach 3π in the $k \to 0$ limit, since there are three σ_g occupied orbitals in N_2 (Swan, 1955). The Π_g comparison is given in Fig. 28. In this case the effect of exchange is to "pull" the Π_g resonance to a lower energy ($\cong$4 eV) and to reduce the width. [The observed resonance, averaged over fine structure, is located at about 2.4 eV; Golden (1966).] Polarization effects were then included via a semiempirical model potential. These calculations will be discussed in the next section.

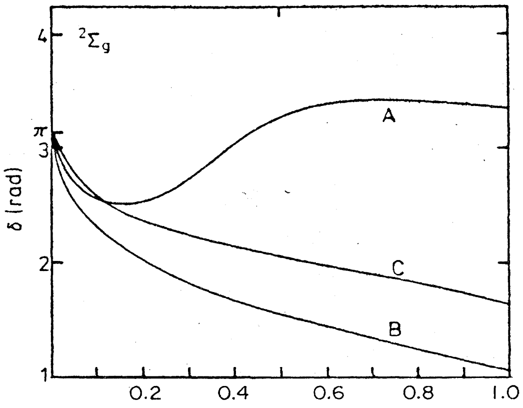

FIG. 27. Scattering Σ_g eigenphase-shift sums for e–N_2 scattering (curve A) static, (curve B) static exchange, (curve C) static-exchange polarization. (Reprinted from Buckley and Burke, 1977.)

Morrison and Schneider (1977) applied R-matrix theory as formulated for electron–molecule scattering by Schneider (1974, 1975a, b, 1977a, b; see Sec. II.F.1) to the fixed-nuclei static-exchange treatment of electron–N_2 scattering. Particular emphasis was placed on choosing the basis set so as to: (1) accurately represent (near Hartree–Fock) the unperturbed N_2 ground-

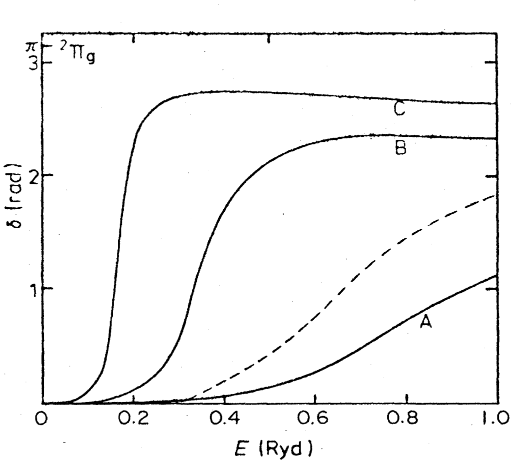

FIG. 28. Scattering Π_g eigenphase shift sums for e–N_2 scattering (curves A, B, C) as in Fig. 27 and (dashed curve) static-field calculations of Crees and Moores (1975). (Reprinted from Buckley and Burke, 1977.)

state wave function; (2) span configuration space within the R-matrix boundary [in spheroidal coordinates $\xi = (r_a + r_b)/R = 7a_0$, i.e., $r \cong 10a_0$]; and (3) avoid linear dependence problems. A detailed description of the basis sets chosen is given by the authors and will not be repeated here. Outside the R-matrix boundary, coupling between different partial waves is ignored, and single-channel radial equations are solved with the electron–molecule interaction approximated by the *diagonal* terms of the electron–quadrupole interaction. Eigenphase sums and integral total (BODY-frame elastic) cross sections are given for several choices of basis sets. The eigenphase sums are in fair agreement (i.e., $\simeq 10\%$) with the "low-l-spoiling" results of McCurdy, Rescigno, and McKoy (1976). The agreement with Buckley and Burke (1977) is at least qualitative; however, there are significant differences. For example, Buckley and Burke (1977) find the Π_g resonance at $E_r \cong 4.5$ eV in their static-exchange calculation, whereas Morrison and Schneider (1977) locate the resonance at $E_r \cong 5.4$ eV.

Fliflet, Levin, Ma, and McKoy (1978) have applied the T-matrix expansion method of Rescigno *et al.* (1974a, b, 1975a; see Sec. II.F.2) to a fixed-nuclei static-exchange treatment of electron–N_2 scattering. The procedure is similar to that for electron–H_2 scattering, as described in Sec. III.B.1. As in the R-matrix method, the critical step in the calculation is the choice of basis set. This is where the uncertainty creeps into both methods. A discussion of the choice of basis set is given by the authors. Integral elastic cross sections are included in Fig. 29. Significant improvement in the static-exchange results may require a variational correction for first-order errors due to truncation of the static-exchange potential and such corrections are expected to be time consuming and expensive (Fliflet and McKoy, 1978a). As in the R-matrix calculation of Morrison and Schneider (1977) disagreement with experiment is due primarily to the neglect of polarization.

Morrison and Collins (1978) included elastic electron–N_2 scattering in their study of free-electron-gas model-exchange potentials. The FEG models are discussed in Sec. II.G.2 and the procedures used in this study have been described in connection with elastic electron–H_2 scattering in Sec. III.B.1. The ground-state N_2 molecule was represented by the analytic near-Hartree-Fock SCF function of Cade, Sales, and Wahl (1966) at $R = R_0 = 2.068a_0$. [The authors estimate that the effect of choosing a different ground-state wave function (see, e.g., Nesbet, 1964), would be at most 15% in the elastic cross sections.] In the model-exchange potential given by Eq. (132), $2I = 1.146$ Ry was used for the Hara version (HFEG) and $I = 0$ for the so-called "asymptotically adjusted" version (AAFEG). Based on the earlier convergence study of Morrison and Collins (1977), it was felt necessary to include: (1) all terms $\lambda \leq 14$ (electron–electron repulsion) and $\lambda \leq 28$ (electron–nuclear attraction) in the expansion of the static potential, Eq. (118); (2) all terms $\lambda \leq 14$ in the model-exchange potentials; and (3) $l \leq 26(\Sigma_g, \Pi_g)$ and $l \leq 25(\Sigma_u, \Pi_u)$ in the partial-wave expansion (115). In practice, it was possible to truncate the partial-wave expansion to $l \leq 8$ beyond $r = 3a_0$. The coupled radial equations (116) were solved in the same manner as Morrison, Lane, and Collins (1977). In Fig. 30, calculated elastic cross sections are compared for the HFEG and AAFEG model-exchange potentials. The AAFEG results are inconsistent with all other static-exchange results; this model exchange is apparently much too strong. The HFEG results are surprisingly consistent with other static-exchange results. For example, the position of the Π_g resonance is very close to that obtained by Morrison and Schneider (1977) in their static-exchange R-matrix calculation, which bears no relation to the present calculation in any detail. In a similar study of these model-exchange potentials on electron–H_2 scattering (see Sec. III.B.1) the authors also found that AAFEG was much too strong, but HFEG was much too weak so that an adjustment of I was required to bring the cross sections into agreement with static-exchange results. It may be the case that the FEG models are simply too crude and that the "necessary" adjustment varies with the molecule under study. Optimistically, one would hope to see a trend, by studying a number of different systems, that could be understood on physical grounds, and used to construct more realistic exchange models for more complex systems. [See also a recent study by Rumble and Truhlar (1979) of electron–N_2 elastic scattering at 13.6 eV using various approximations to the static and exchange potentials with some allowance for polarization.]

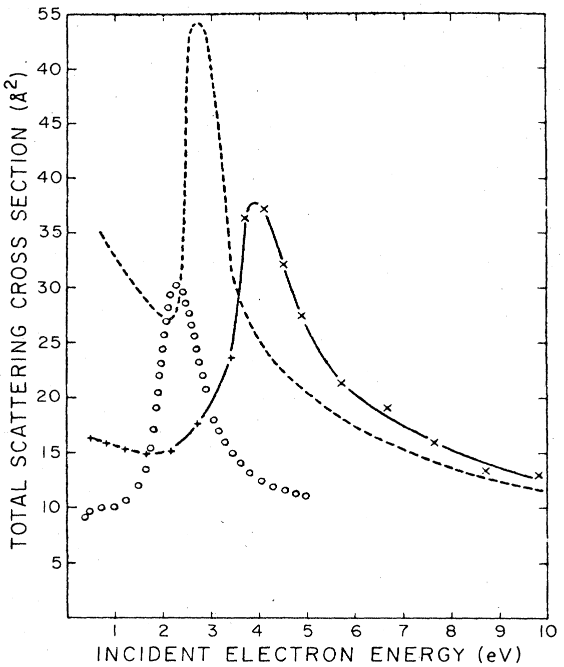

FIG. 29. Total cross sections for e–N_2 scattering. Theory: (solid curve and ×, +) T-matrix static exchange, Fliflet *et al.* (1978); (dashed curve) unconverged static exchange, Burke and Sinfailam (1970). Experiment: (open circles) Golden (1966); observed vibrational structure not shown here. (Reprinted from Fliflet *et al.*, 1978.)

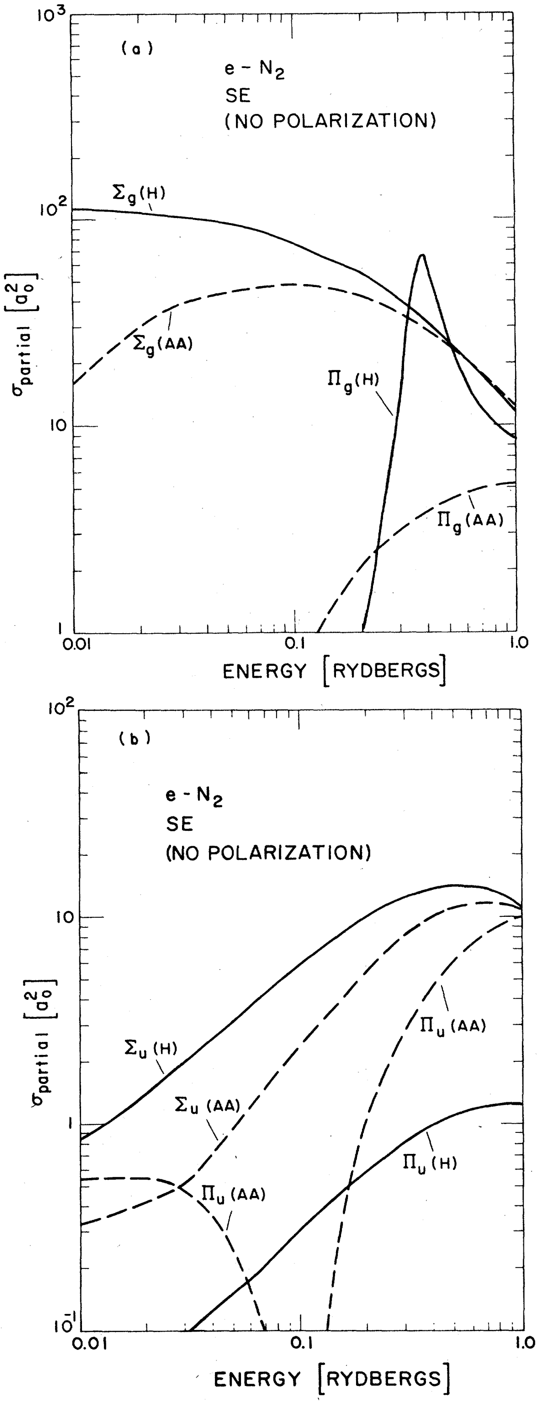

FIG. 30. Theoretical partial cross sections for e–N_2 scattering in the static-exchange approximation. Two approximate exchange potentials, (H) HFEG and (A) AAFEG, are compared for symmetries (a) Σ_g, Π_g, and (b) Σ_u, Π_u. (Reprinted from Morrison and Collins, 1978.)

b. Static-exchange polarization

Burke and Chandra (1972) included polarization in their "modified pseudopotential" (MPS) fixed-nuclei calculation of electron–N_2 scattering by means of a model polarization potential of the form of Eq. (147) with $\alpha_0 = 12.0a_0^3$, $\alpha_2 = 4.2a_0^3$, and the cutoff radius r_p determined by "tuning" the position of the Π_g resonance to $E_r \simeq 2.4$ eV. The choice $r_p = 1.592a_0$ placed the resonance at 2.394 eV. Including polarization in this manner had no apparent effect on convergence criteria; the expansion of $V_s(\mathbf{r})$ was represented by terms $\lambda \leq 14$ in Eq. (118) and the partial-wave expansion included terms $l \leq 10(\Sigma_g)$, $12(\Pi_g)$, and $13(\Sigma_u, \Pi_u)$. It is important to realize that the MPS method provides no exchange contribution for Π_g symmetry, since the ground state of N_2 has no π_g occupied orbitals (see Secs. II.G.4 and III.C.1.a). Therefore, in selecting the polarization cutoff radius r_p by "tuning" the Π_g resonance, one is forcing the model polarization potential to represent exchange effects as well, at least for Π_g symmetry. Then, in the other symmetries Σ_g, Σ_u, and Π_u where the MPS method does account for exchange effects via the orthogonalization constraint, some artificial contribution of exchange will unavoidably be included in the model polarization potential. The net results of all this is likely to be a polarization potential that is somewhat too strong. The eigenphase sums are illustrated in Fig. 31 for the most important symmetries. In Fig. 32 the integral elastic cross section is compared with those of other theoretical studies of Buckley and Burke (1977) and Morrison and Collins (1978), and the measurements of Golden (1966). Differential cross sections are compared in Figs. 33(a), 33(b), and 34. The extent of agreement between different theoretical calculations will be discussed below.

Buckley and Burke (1977) have included polarization in their fixed-nuclei static-exchange calculation of electron–N_2 scattering in precisely the same manner as did Burke and Chandra (1972). However, since exchange is properly treated by solving the coupled radial integro-differential equations (116) there is no longer the ambiguity in interpreting the role of the model polarization potential. The cutoff radius r_p in Eq. (147) was again chosen by "tuning" the position of the Π_g resonance. The value $r_p = 2.308a_0$ places the resonance of $E_r = 2.39$ eV. Eigenphase sums are included in Figs.

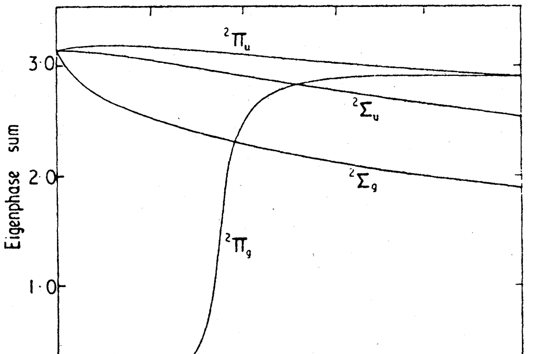

FIG. 31. Scattering eigenphase-shift sums for important symmetries in e–N_2 scattering. Static-exchange-polarization calculations of Burke and Chandra (1972). (Reprinted from Burke and Chandra, 1972.)

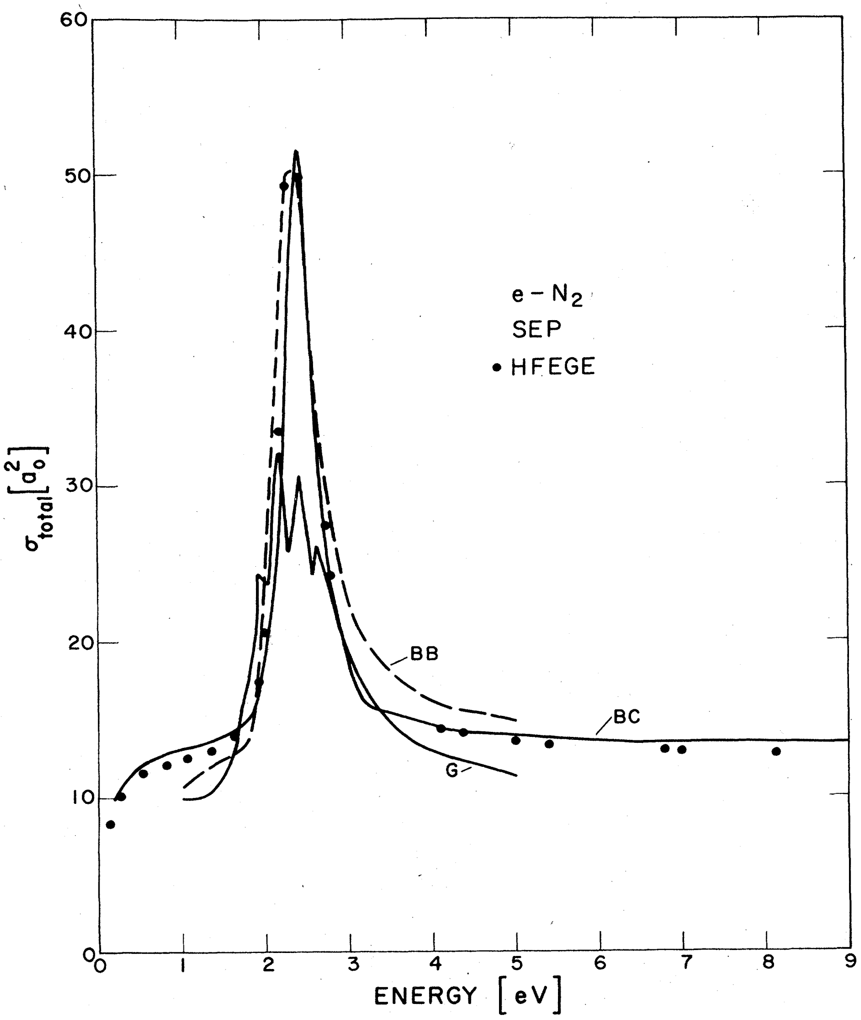

FIG. 32. Total cross section for e–N_2 scattering. Theory: static-exchange-polarization calculations; (dashed curve BB) Buckley and Burke (1977), (solid curve BC), Burke and Chandra (1972); (closed circles), Morrison and Collins (1978). Experiment: (solid curve G) Golden (1966). (Reprinted from Morrison and Collins, 1978.)

27 and 28. The integral elastic cross sections are shown in Figs. 32. Differential cross sections are illustrated in Fig. 33(a) in comparison with relative measurements of Ehrhardt and Willmann (1967). The results of Burke and Chandra (1972) are given in Fig. 33(b) for comparison. The authors examined the Π_g resonance in detail, fitting the Π_g eigenphase sum to the Breit–Wigner expression

$$\sum_l \eta_{lm} = \sum_l \eta^{(0)}_{lm} + \tan^{-1}\left[\frac{(1/2)\Gamma}{k_r^2 - k^2}\right], \tag{199}$$

where Γ and k_r^2 are the width and position (in Ry) of a resonance characterized by a partial wave l, m, and the $\eta^{(0)}_{lm}$ are the corresponding "background phase shifts." In this way the Π_g width was calculated to be $\Gamma = 0.64 \pm 0.02$ eV. The values obtained by other workers are: 0.8 ± 0.3 eV (Krauss and Mies, 1970); 0.57 ± 0.02 eV (Birtwistle and Herzenberg, 1971); and 0.40 (Burke and Chandra, 1972). [The authors note that Krauss and Mies (1970) calculated the width at $R = 2.0a_0$, rather than the value $2.068a_0$ used by the others.] Examination of the individual eigenphase shifts (or T-matrix elements) confirmed that the Π_g resonance was primarily d wave in character (i.e., asymptotic) in agreement with Burke and Chandra (1972), and as predicted by Bardsley, Mandl, and Wood (1967) and Krauss and Mies (1970).

Morrison and Collins (1978) also included polarization effects in their model free-electron-gas exchange study of electron–H_2 and –N_2 scattering. (See previous section and Sec. II.G.) They used the same model polarization potential, Eq. (147), with $\alpha_0 = 11.89a_0^3$ and $\alpha_2 = 4.19a_0^3$ as Burke and Chandra (1972) and Buckley and Burke (1977), determining the cutoff radius r_p by "tuning" the position of the Π_g resonance to agree with experiment. The two exchange models HFEG and AAFEG (see previous section) were studied separately. "Tuning" the resonance to $E_r = 2.39$ eV resulted in values $r_p = 2.341a_0$ (HFEG) and $r_p = 0.753a_0$ (AAFEG). Again, the conclusion was reached that the AAFEG model potential is much too strong, apparently binding the $1\pi_g$ orbital that should give the resonance. The HFEG model, including polarization, appears to provide a reasonable *local* representation of the electron–N_2 interaction. The HFEG polarization cutoff radius $r_p = 2.341a_0$ is very close to the value $2.308a_0$ obtained by Buckley and Burke (1977), lending further support to the usefulness of this model. [In an application of the HFEG model to electron–CO_2 scattering, Morrison *et al.* (1976, 1977) arrive at a similar conclusion.]

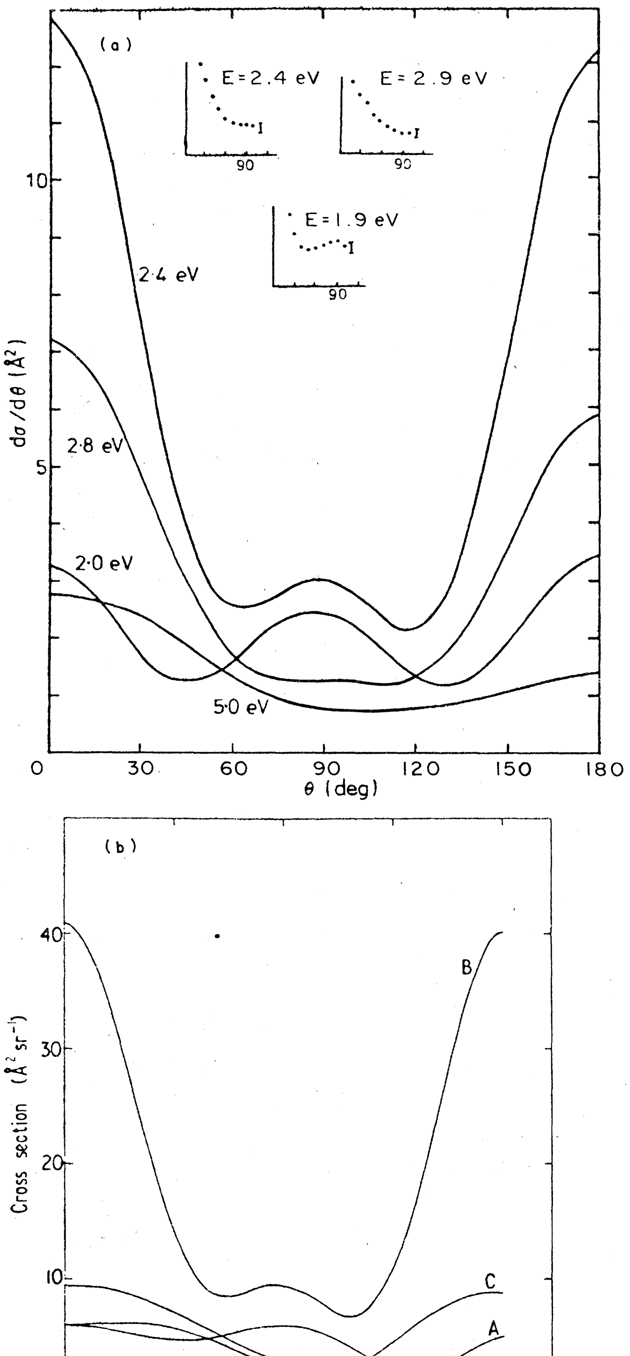

FIG. 33. Differential cross sections for e—N_2 scattering (a) static-exchange polarization, Buckley and Burke (1977); (inset) measurements of Ehrhardt and Willmann (1967); (b) static-exchange polarization, Burke and Chandra (1972), (A) 2.0 eV, (B) 2.4 eV, (C) 3.0 eV, and (D) 5.0 eV. (Reprinted from Buckley and Burke, 1977; and Burke and Chandra, 1972.)

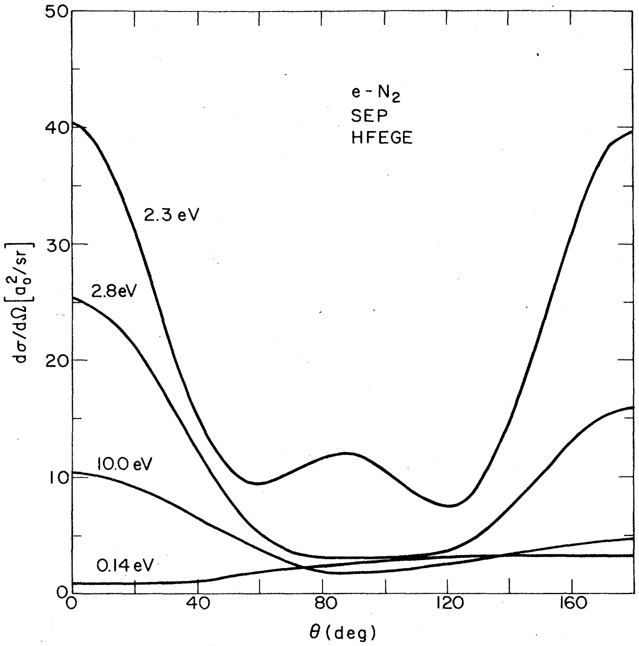

FIG. 34. Differential cross sections for e—N_2 scattering. Static-exchange polarization including symmetries $\Sigma_{g,u}$, $\Pi_{g,u}$ and $\Delta_{g,u}$. (Reprinted from Morrison and Collins, 1978.)

Nevertheless, it should be stressed that exchange is intrinsically a nonlocal effect and a truly accurate representation by any local model is not expected. The authors estimate the width of the calculated Π_g resonance to be $\Gamma \cong 0.48$ eV. The integral elastic and momentum-transfer cross sections are given, respectively, in Figs. 32 and 35. Differential cross sections ("SEP") at several energies are shown in Fig. 34. In Fig. 36, the calculated differential cross section ("SEP") at 7.0 eV is illustrated for two cases, one in which only Σ and Π (g and u) contributions are included, and a second, in which the Δ_g and Δ_u contributions are

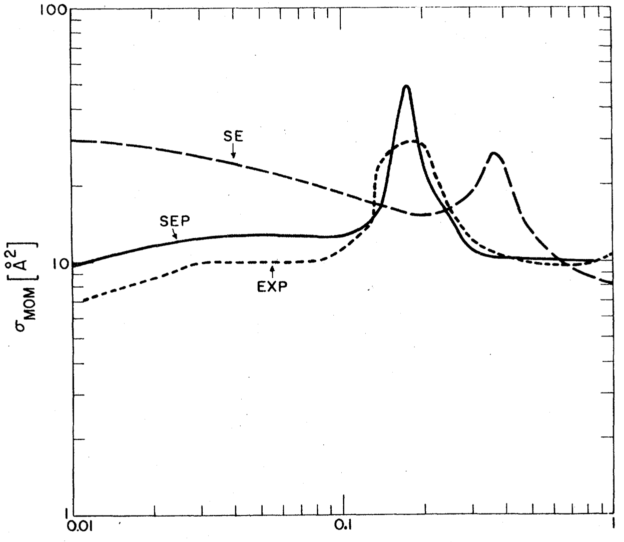

FIG. 35. Momentum-transfer cross section for e—N_2 scattering. Theory: (dashed curve SE) static exchange, (solid curve SEP), static-exchange polarization, Morrison and Collins (1978). Experiment: (dashed curve EXP) Englehardt and Phelps (1963). (Reprinted from Morrison and Collins, 1978.)

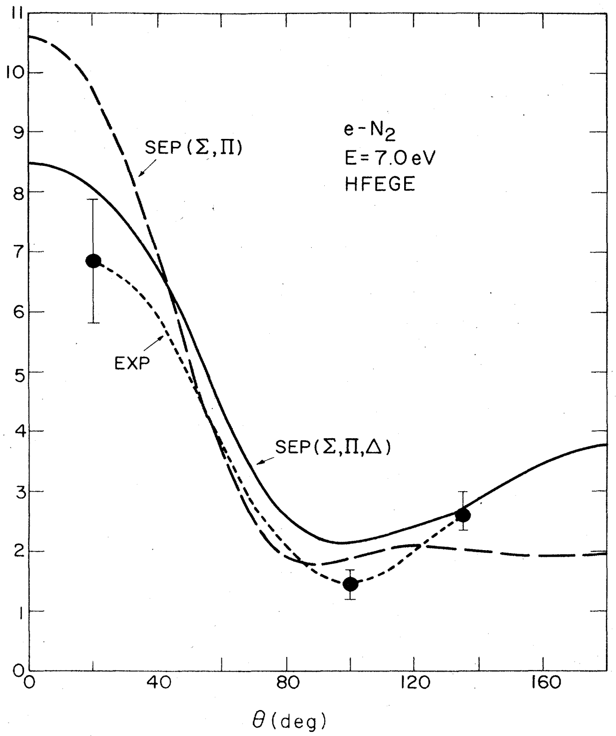

FIG. 36. Differential cross sections for e—N_2 scattering at 7.0 eV. Theory: static-exchange polarization, [solid curve SEP (Σ,Π,Δ)] including symmetries $\Sigma_{g,u}, \Pi_{g,u}, \Delta_{g,u}$; [dashed curve SEP (Σ,Π)] including symmetries $\Sigma_{g,u}$ and $\Pi_{g,u}$. Experiment: (dashed curve EXP) absolute measurements of Srivastava *et al.* (1976). (Reprinted from Morrison and Collins, 1978.)

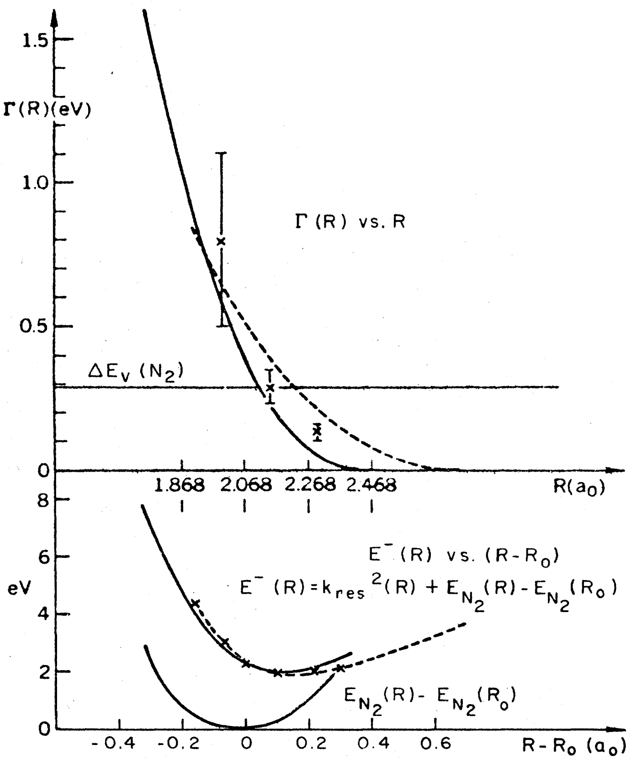

FIG. 37. Width $\Gamma(R)$ and position $E^-(R)$ of Π_g resonance in e—N_2 scattering as functions of R. (Solid curves) Chandra and Temkin (1976a); (dashed curve) Birtwistle and Herzenberg (1971); (×) Krauss and Mies (1970). The lowest curve is the ground-state potential energy curve of N_2 with equilibrium separation R_0, and vibrational spacing $\Delta E_v(N_2)$. (Reprinted from Chandra and Temkin, 1976a.)

added; the latter are small contributors to the integral cross section, but clearly influence the angular distribution. The *absolute* measurements of Srivastava *et al.* (1976) are included for comparison. The authors note similar agreement for energies 5.0 and 10.0 eV.

Chandra and Temkin (1976a, b, c) were among the first to include vibrational states explicitly in a close-coupling e—N_2 calculation. Recognizing that the Π_g resonance invalidated the adiabatic approximation for nuclear vibration, they proposed a so-called "hybrid theory" (see also Choi and Poe, 1977a, b) in which a vibrational close-coupling approach is used for the Π_g channels, and an ordinary adiabatic nuclear vibration calculation is performed for the other (nonresonant) symmetries. (The adiabatic nuclear rotation approximation was used throughout.) The fixed-nuclei calculations were very similar to the modified pseudopotential calculations of Burke and Chandra (1972), discussed earlier in this section. Target N_2 wave functions of Nesbet (1964) were used to calculate the static potential $V_s(\mathbf{r})$ and to impose the orthogonality constraints (see Sec. II.G.4) at several internuclear separations R. The model polarization potential, Eq. (147), was chosen in the same manner as by Burke and Chandra (1972), and all dependence on R was ascribed to variation in $\alpha_0(R)$ and $\alpha_2(R)$, estimated by means of a simple semiempirical model. (We note as a reminder that the MPS method fails to include any exchange in the resonant Π_g symmetry.) By performing calculations at several values or R, the variation in the position $E^-(R)$ and width $\Gamma(R)$ of the resonance is obtained. These quantities are compared in Fig. 37 with other theoretical results. [For comparison, recall that other theoretical values reported for $\Gamma(R)$ at the equilibrium separation $2.068a_0$ are: Burke and Chandra (1972), $\Gamma \cong 0.40$ eV; Buckley and Burke (1977), $\Gamma = 0.64 \pm 0.02$ eV; and Morrison and Collins (1978), $\Gamma \cong 0.48$ eV.] In Fig. 37, the vibrational spacing $\Delta E_v(N_2)$ is also indicated, showing that for $R \gtrsim R_0 = 2.068a_0$, the lifetime of the N_2^- complex is comparable with the vibrational period, and the adiabatic nuclear vibration approximation fails. It should be emphasized that the Born–Oppenheimer approximation is still valid, i.e., the electrons still respond "adiabatically" to changes in the internuclear separation. However, the impulse picture no longer applies, in that the vibrational wave function of Eq. (18) is not the unperturbed initial-state vibrational wave function of the N_2 molecule. The nuclei respond to the potential of a transient N_2^- ion, and the form of the vibrational wave function is strongly influenced by the variation of the N_2^- lifetime $[1/\Gamma(R)]$ with internuclear separation (see Bardsley and Mandl, 1968; Birtwistle and Herzenberg, 1971; Schulz, 1973, 1976; and Temkin, 1976). Chandra and Temkin (1976a) approach this problem by employing a vibrational close-coupling procedure in which the vibrational response to the transient N_2^- complex is represented by "virtual" transitions among different unperturbed vibrational states of the N_2 system. In the vibrational close-coupling calculation of the Π_g channels, only channels corresponding to $l \leq 6$ were retained, so that the final cross sections were not converged in partial waves. (The polarization potential was adjusted so that even for the nonconverged calculation, the position of the $^2\Pi_g$ resonance was "tuned" to 2.4 eV. Values of $r_p = 1.496a_0$ and $1.554a_0$ accomplished this for the truncations $l \leq 4$ and $l \leq 6$, respectively.) By limiting the number of partial waves, it was then possible to study the convergence in vibrational states more thoroughly. This study for elastic ($v = 0 \rightarrow 0$) scattering is illustrated in Fig. 38 where calculated integral cross sections are compared for different truncations of the expansion in vibrational states $v = 0, 1, \ldots, N_{\max}$ for $N_{\max}$ up to 10, and the two different truncations in partial waves. The development of structure in the resonance as more vibrational "flexibility" is allowed is beautifully illustrated in this study. The calculated integral elastic cross sections, including all symmetries, are compared with the measurements of Potter, Steph, Dwivedi, and Golden (1977) in Fig. 39. The agreement is only qualitative, in that the positions and magnitudes of the peaks and valleys do not agree, and the theoretical cross section lies above that observed by about 15%–20%. [The apparent structure in the experimental cross section below $\cong 1.75$ eV is an artifact of the measurement and not a genuine feature of the cross section (Potter *et al.*, 1977).] Differential elastic cross sections at several angles are compared in Fig. 40 with the relative measurements of Ehrhardt and Willmann (1967). Again, there is qualitative agreement only. (The comparisons are similar for vibrational excitation to be discussed in Sec. III.C.3.) The principal sources of error in the calculation are: (1) use of model-exchange and model polarization potentials; (2) truncation of the partial-wave expansion before convergence is obtained; and (3) truncation of the expansion in vibrational states. The latter does not seem to be the major problem, as can be seen in Fig. 38, where the convergence in $N_{\max}$ appears to be very good. However, there are substantial qualitative changes evident in going from $l \leq 4$ to $l \leq 6$; this suggests that the details would be very different in a fully converged (in partial waves) calculation. The comparison of position $E^-(R)$ with width $\Gamma(R)$ of the resonance with the semiempirical curves of Birtwistle and Herzenberg (1971) in Fig. 37 strongly suggests that the detailed structure of the calculated cross sections will not be in agreement with the measurements. The width $\Gamma(R)$ is likely to be sensitive both to the model potentials chosen and to the truncation of the partial-wave expansion. Below the resonance, the calculated differential cross sections are similar to those of Burke and Chandra (1972) illustrated in Fig. 33(b) and in good agreement with the relative measurements of Ehrhardt and Willmann (1967). The calculated differential elastic cross sections at 5.0 and 10.0 eV (Chandra and Temkin, 1976b) are compared in Fig. 41 with the calculations of Truhlar *et al.* (1976), to be discussed in Sec. III.C.3, and the absolute measurements of Srivistava *et al.* (1976). The shape of the angular distribution is in good agreement with the measurements of both energies, and the magnitude agrees well at 10.0 eV. At 5.0 eV, the calculated cross section lies above the experimental curve by an amount that is consistent with the high-energy trend evident in Fig. 39. Chandra and Temkin also calculated rotational- and vibrational-excitation cross sections, which will be discussed in the next two sections.

In a very recent application of R-matrix theory, extended to include vibrational excitation, Schneider, Le Dourneuf, and Lan (1979) report good agreement with experiment for the shapes of the resonance peaks in the elastic and vibrational-excitation cross sections. These calculations allow for exchange and polarization effects in a nonempirical manner.

Dill and Dehmer (1977) have applied the "multiple-scattering method" (MSM) to the calculation of integral elastic cross sections for electron–N_2 scattering at energies $0 < E < 1$ keV. Siegel, Dill, and Dehmer (1978) have reported the corresponding elastic differential cross sections at lower energies $0 \leq E \leq 30$ eV. The MSM is particularly useful in treating complicated molecules, surfaces, or solids where there are many scattering centers. The authors chose N_2 as a test case since this molecule has received so much theoretical attention. The method is straightforward. [See, for example, Dill and Dehmer (1974), Siegel and Dill (1976), and the review of Johnson (1973).] In the fixed-nuclei approximation, the electron–molecule interaction (see Fig. 42) is approximated by a local "muffin-tin" potential that consists of: finite-range spherically symmetric potentials centered on each nuclei (Regions I_1 and I_2), a constant potential in the intermediate Region II, and an outer Region III where long-range interactions (e.g., polarization) can be included. The one-electron Schrödinger equation is solved, with appropriate boundary conditions imposed at the nuclei and in the asymptotic region. Since the potential energy is constant in Region II, the wave function (partial-wave expansion) is that of a free particle. The only complication is the proper boundary matching at the Region I/Region II interface, and that is an algebraic problem. The potential in Region III is spherically symmetric and further integration of the wave function in that region is not difficult.

In the present application to N_2, the authors chose Hartree–Slater atomic potentials (see, for example, Herman and Skillman, 1963) with a large-r cutoff to ensure proper asymptotic behavior (Latter, 1955). The most satisfactory choice of potential was obtained by modifying that used in earlier photoionization calculations of N_2 by adding an extra electronic charge evenly distributed over both nuclei. Thus a "configuration" $1s^2 2s^2 2p^{3.5}$ was assigned to each atom (i.e., Regions I_1 and I_2). Exchange was approximated by the Slater ("$X\alpha$") form given in Eq. (137). Two model potentials "A" and "B" were studied. Potential "A" is the most attractive, with $\alpha = 1$ in the Slater exchange potential, $V_{\mathrm{II}} = -1.8$ Ry in Region II, and a polarization potential $-12\, r^{-4}$ Ry applied in the outer region ($r > 2.109a_0$). This choice of potential reproduces the Π_g resonance at $E_r \cong 2.4$ eV and the qualitative shape of the integral elastic cross section, as shown in Fig. 43. [The experimental data points correspond to the abso-

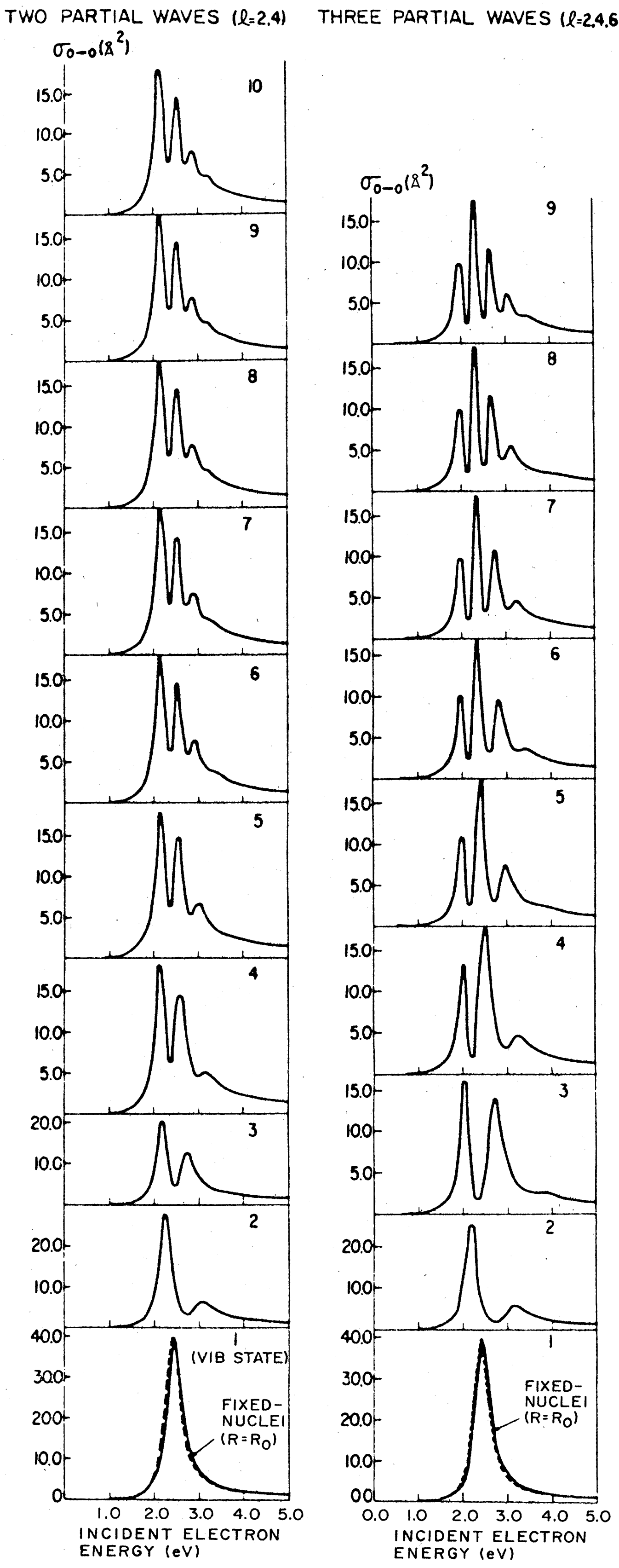

TWO PARTIAL WAVES (ℓ=2,4) THREE PARTIAL WAVES (ℓ=2,4,6)

FIG. 38. Calculated Π_g contribution to e—N_2 vibrationally elastic ($v = 0 \rightarrow 0$) cross section in hybrid theory. Comparison of two- and three-partial-wave calculations for increasing number of vibrational states retained in the close-coupling expansion ($N_{\max} = 1$ up to 10 shown in upper right hand curves for each curve). (Reprinted from Chandra and Temkin, 1976a.)

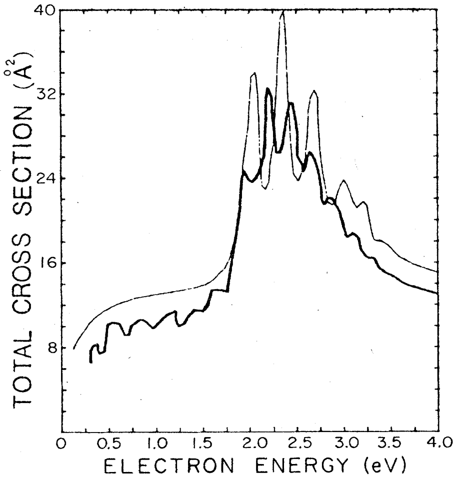

FIG. 39. Total cross section for e—N_2 scattering. Theory: (light solid curve) hybrid theory, Chandra and Temkin (1976a). Experiment: (heavy solid curve) Golden (1966); also see Potter *et al.* (1977). (Reprinted from Potter *et al.*, 1977.)

lute measurements of Golden (1966), Bromberg (1970), DuBois and Rudd (1976), and the *normalized* measurements of Srivastava *et al.* (1976) and Hermann, Jost, and Kessler (1976).] The structure in the calculated cross section on either side of 1 Ry is due to broad Δ_g and Σ_g resonances. Potential "*B*" is weaker, corresponding to $\alpha = \frac{2}{3}$ in the Slater exchange potential, $V_{\rm II} = -0.9$ Ry, and no polarization in Region III. The elastic cross sections resulting from this choice of potential are in better agreement with the high-energy cross section, as seen in Fig. 43, but produce the Π_g resonance at $E_r \simeq 0.5$ Ry. The authors argue on physical grounds that this is reasonable since both polarization and exchange effects are energy dependent and tend to be reduced at high energies. The failure of the potential "*A*" model to reproduce the low-energy integral elastic cross section (below the resonance) was traced to the Σ_g-symmetry channels. In an extension of these calculations to a study of the elastic differential cross sections, Siegel *et al.* (1978) have shown that this failure of the model at low energies is reflected in the large-scale scattering. Otherwise, the shapes of the angular distributions are surprisingly good over the energy range $0 \lesssim E \lesssim 30$ eV, as illustrated in Fig. 44. [The other results given for comparison in Fig. 44 are: theory: Chandra and Temkin (1976a, b), Buckley and Burke (1977), Davenport *et al.* (1978), Truhlar *et al.* (1976), and Brandt *et al.* (1976); experiment: Ehrhardt and Willmann (1967), Shyn *et al.* (1972), Srivastava *et al.* (1976), and Finn and Doering (1975).]

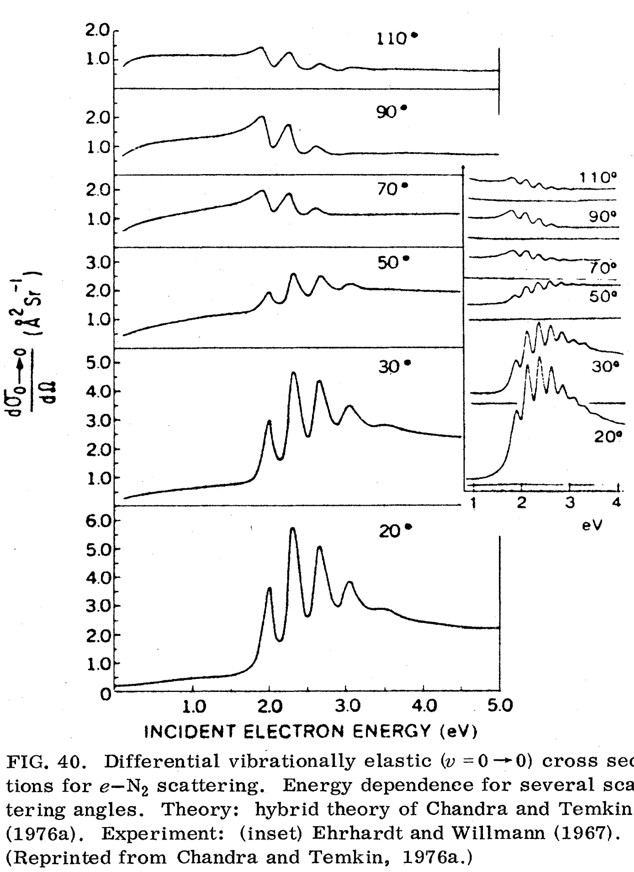

FIG. 40. Differential vibrationally elastic ($v = 0 \to 0$) cross sections for e—N_2 scattering. Energy dependence for several scattering angles. Theory: hybrid theory of Chandra and Temkin (1976a). Experiment: (inset) Ehrhardt and Willmann (1967). (Reprinted from Chandra and Temkin, 1976a.)

The multiple-scattering method clearly has promise for complex systems, where even the qualitative features of the electron scattering are unknown. Dill and Dehmer (1977) suggest improvements in the model [e.g., the use of an energy-dependent exchange potential, allowing overlap of the atomic spheres (Regions I_1 and I_2), etc.] that may lead to a more predictive theory for large systems. The important advantage the MSM has over other model approaches (e.g., Sawada, Ganas, and Green, 1974) is the degree to which the strong anisotropic interaction near the nuclei is included in the former. The accurate characterization of features such as the Π_g resonance in N_2 requires that the region near the nuclei be treated in a realistic manner.

A somewhat different "multiple-scattering" approach to electron–molecule scattering has been applied to vibrational–rotational excitation in electron collisions with H_2, Li_2, Na_2, and K_2 by Drukarev and Yurova (1977). In these calculations, the electron–molecule interaction is represented by "zero-range potentials" of the two atomic scattering centers; this leads to considerable simplification in handling the multiple scattering (Demkov and Rudakov, 1970; Subramanian, 1968). All long-range interactions are ignored. In the case of electron–H_2 scattering the calculated cross section ratios of $v = 0 \to 1(\Delta_j = 0)$ to $v = 0 \to 1(j = 1 \to 3)$, at 2.5 and 3.0 eV, were found to agree well with the measurements of Linder and Schmidt (1971a) for angles $50° \lesssim \theta \lesssim 120°$. At smaller angles, the calculated ratios are similar to the theoretical results of Abram and Herzenberg (1969), but lie well below experiment, probably due to the neglect of polarization effects in both theories. The absolute $v = 0 \to 1(\Delta j = 0)$ calculated cross section differs significantly in shape (energy dependence) from that measured by Linder and Schmidt (1971a) and is larger by roughly a factor of 2. This simple approach should prove to be particularly useful in qualitative studies of very complex polyatomic molecules or clusters and

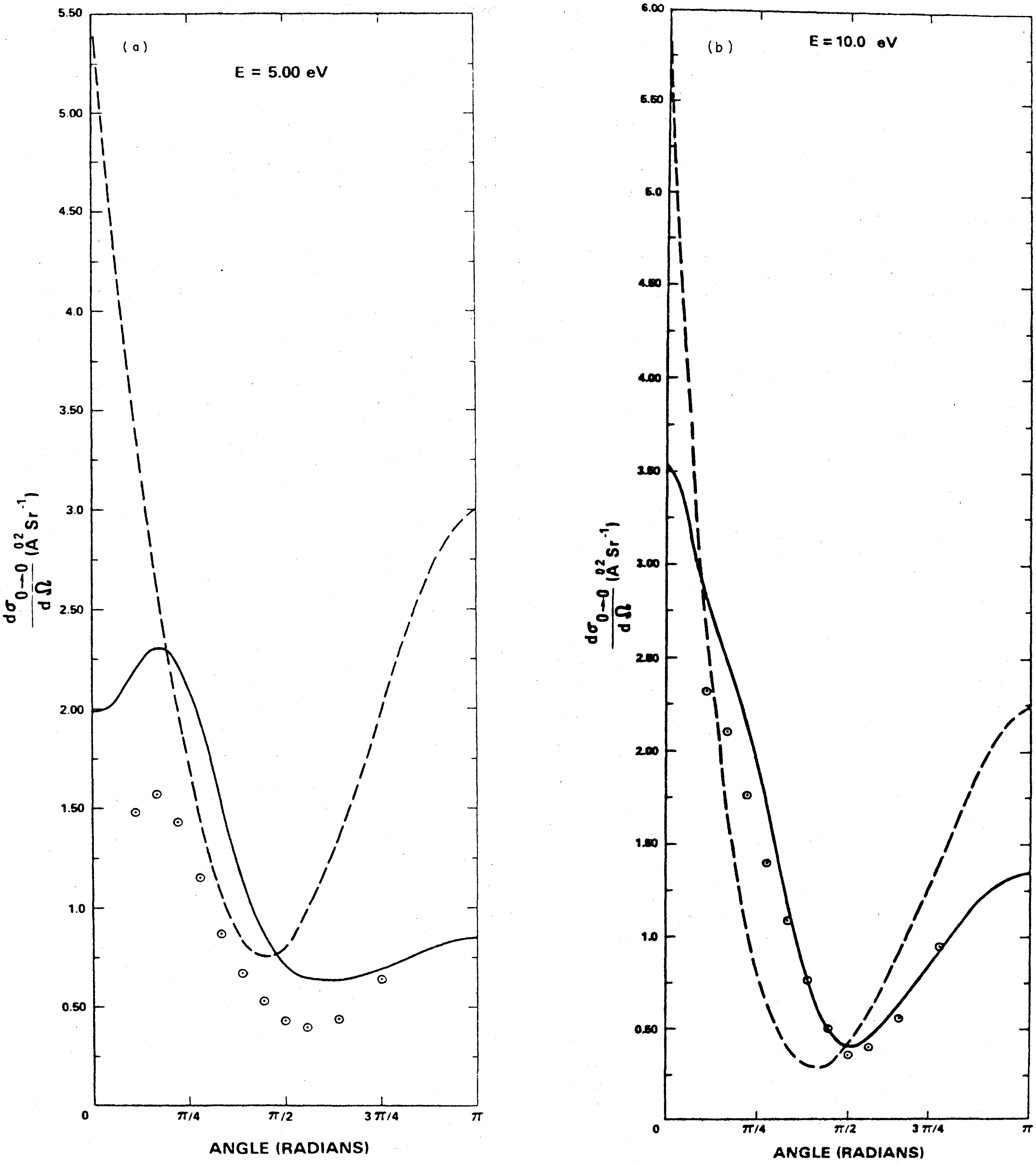

FIG. 41. Differential vibrationally elastic ($v = 0 \rightarrow 0$) cross sections for e–N$_2$ scattering at (a) 5.0 eV and (b) 10.0 eV. Theory: (solid curve) Chandra and Temkin 1976b); (dashed curve) Truhlar *et al*. (1976). Experiment: (circles) Srivastava *et al*. (1976). (Reprinted from Chandra and Temkin, 1976b.)

under conditions where long-range interactions are less important, i.e., high energies and large scattering angles. [See the somewhat related treatments of Huang and Chan (1977) and Choi, Poe, Sun, and Shan (1979).]

2. Rotational excitation (N$_2$ and O$_2$)

Near the threshold for a particular $j \rightarrow j'$ transition, the rotational-excitation cross section is dominated by

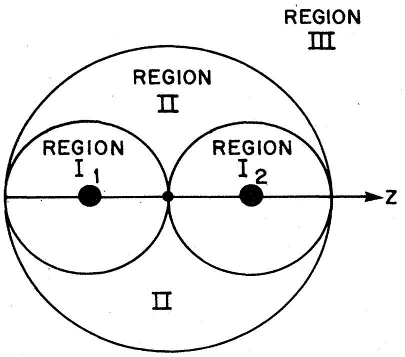

FIG. 42. "Muffin-tin" regions employed in multiple scattering method (MSM).

the electron–quadrupole interaction, and the Born (quadrupole) approximation is valid (Gerjuoy and Stein, 1955a, b; see Sec. II.H.2). However, there is no theoretical guideline that establishes how far above threshold this approach is useful. Dalgarno and Moffett (1963) have shown that because the quadrupole moment of N_2 is negative, the quadrupole and polarization (nonspherical α_2) contributions to the first Born approximation partially cancel, leading to a decrease in the $j \rightarrow j'$ cross section at higher energies. (This is in contrast with e–H_2 collisions where $Q>0$ so that the cross section increases monotonically.) Thus is illustrated for $j=0 \rightarrow 2$ in Fig. 45(a). Sampson and Mjolsness (1965), Takayanagi and Geltman (1965), and Geltman and Takayanagi (1966) studied the effects of including a certain amount of "distortion" in the wave function of the scattered electron. The relatively weak

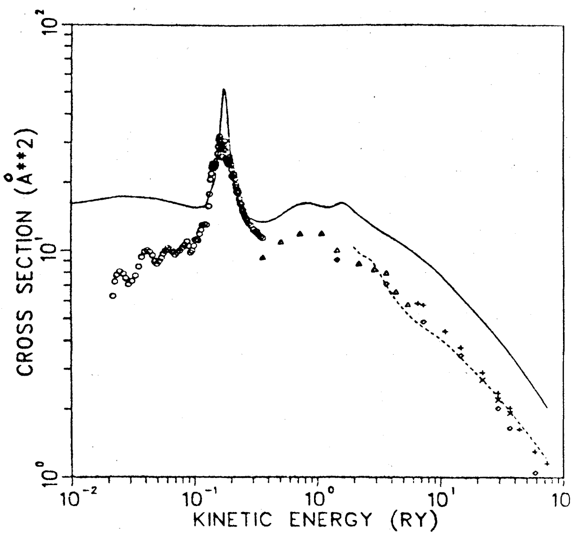

FIG. 43. Total cross sections for e–N_2 scattering. Theory: MSM theory (solid curve) low-energy potential A, (dashed curve) high-energy potential B, Dill and Dehmer (1977). Experiment: (○) Golden (1966); (×) Bromberg (1970); (◇) DuBois and Rudd (1976); (△) Srivastava *et al.* (1976); (+) Hermann *et al.* (1976). (Reprinted from Dill and Dehmer, 1977.)

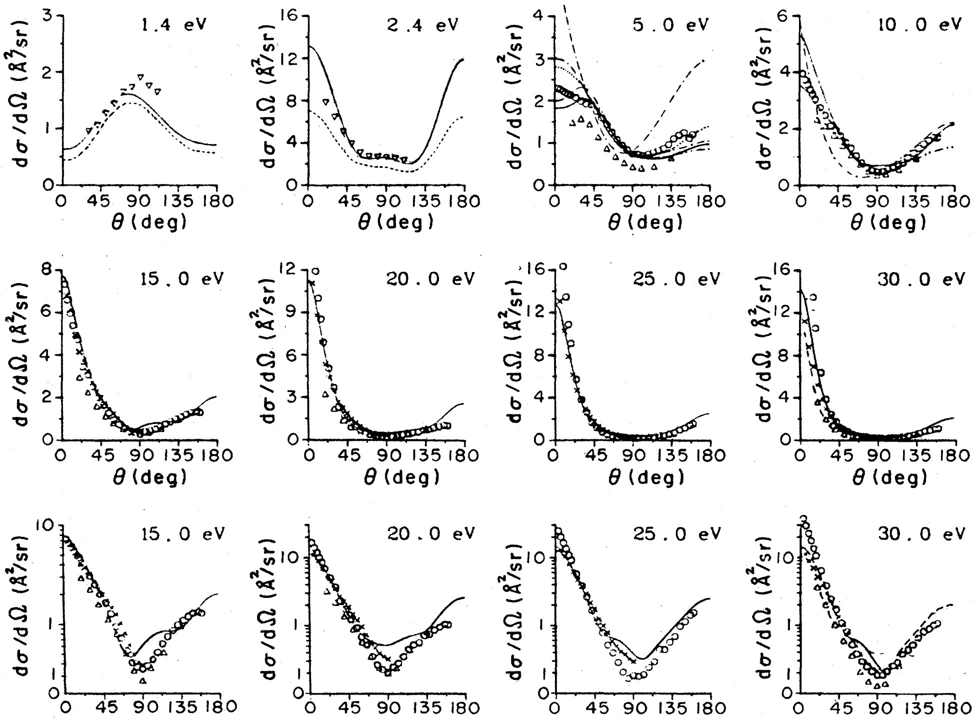

FIG. 44. Differential cross sections for e–N_2 scattering. Theory: (solid curve) Siegel *et al.* (1978); (other dashed, chain, etc., curves), Chandra and Temkin (1976a, b), Buckley and Burke (1977), Davenport *et al.* (1978), Truhlar *et al.* (1976), Brandt *et al.* (1976). Experiment: (∇, ○, △, ×) include Ehrhardt and Willmann (1967), Shyn *et al.* (1972), Srivastava *et al.* (1976), and Finn and Doering (1975). (Note: the figure is intended only to show overall qualitative agreement of most theories and experiment measurements.) (Reprinted from Siegel *et al.*, 1978.)

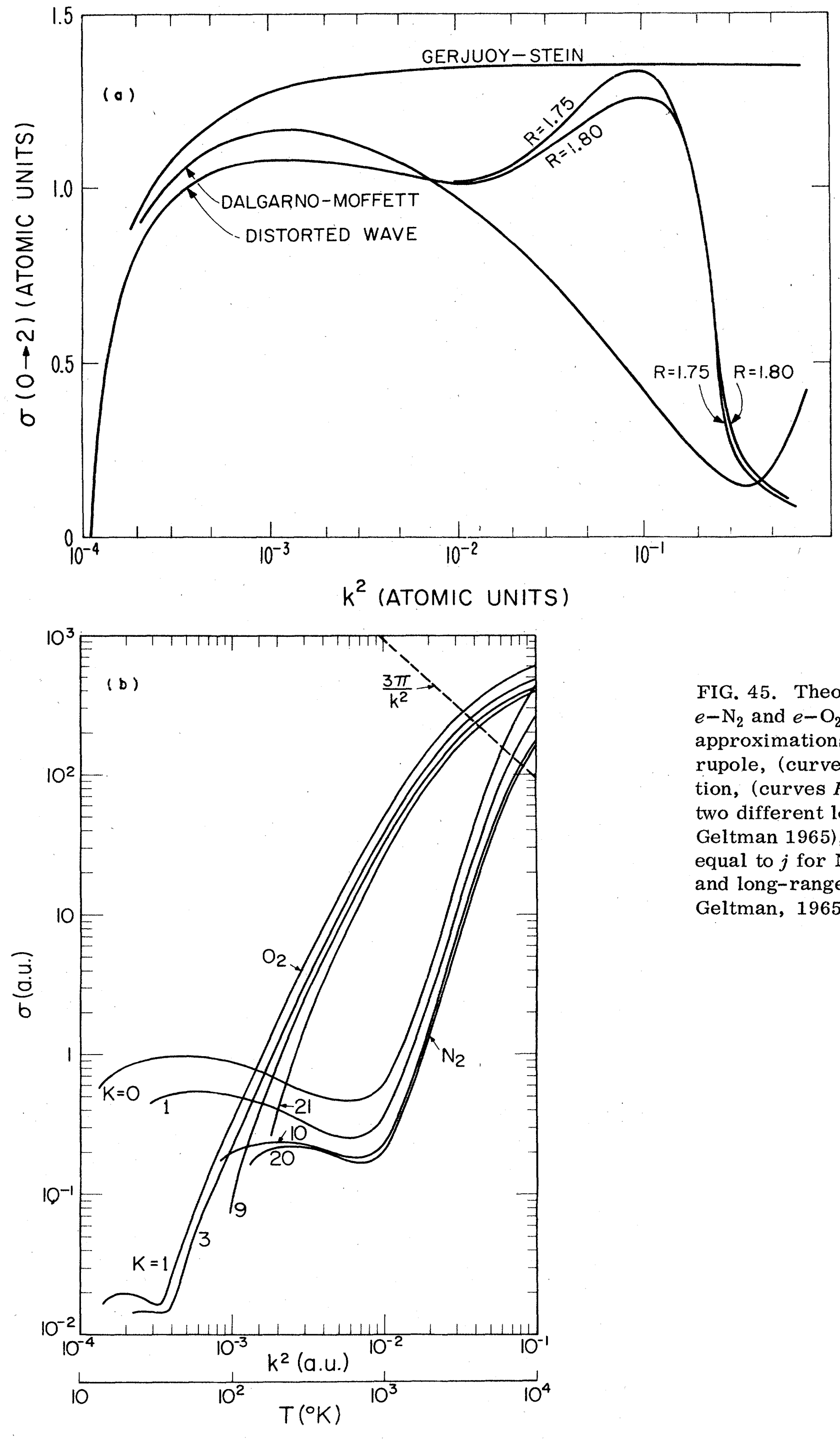

FIG. 45. Theoretical rotational-excitation cross sections for $e-N_2$ and $e-O_2$ scattering based on Born and distorted-wave approximations: (a) $j=0\rightarrow 2$, (curve Gerjuoy–Stein) Born quadrupole, (curve Dalgarno–Moffett) Born quadrupole polarization, (curves $R=1.75, 1.80$) distorted-wave calculations using two different long-range interactions (from Takayanagi and Geltman 1965); (b) $K\rightarrow K+2$ (K is total angular momentum, equal to j for N_2) in distorted-wave calculation including short- and long-range interactions. (Reprinted from Takayanagi and Geltman, 1965, and Geltman and Takayanagi, 1966.)

model potential chosen by Sampson and Mjolsness (1965) in their distorted-wave calculation resulted in a cross section very similar to the Born result for $Q=-1.10ea_0^2$ [see Eqs. (174) and (175)] and in good agreement with the swarm measurements of Englehardt, Phelps, and Risk (1964). Geltman and Takayanagi (1966) constructed a distortion potential based on an approximation to the full static potential with polarization. This strong attractive potential results in much greater cancellation at low energies and a steep increase of the cross section at higher energies [see Fig. 45(b)], where the distorted-wave approximation rapidly breaks down due to strong coupling effects and the consequent violation of unitarity (i.e., flux conservation). When only long-range (quadrupole and polarization) interactions are included the scattering is weaker, and the validity of the distorted-wave method is less in question [Fig. 45(a)]. However, the short-range interactions are undoubtedly important at the higher energies. In the case of O_2, the distorted-wave results of Sampson and Mjolsness (1966), who include only long-range interactions, are in marked contrast to the results of Geltman and Takayanagi (1966) illustrated in Fig. 45(b). At higher energies, the rotational excitation of N_2 is expected to be completely dominated by the Π_g resonance near 2 eV [Chen (1969); also see Schulz (1973)]. However, at present there are still no reliable theoretical estimates of the rotational excitation cross sections for N_2 below the resonance, or for O_2 at any energy.

The early (nonconverged) fixed-nuclei close-coupling calculations of Burke and Sinfailam (1970) (see Sec. III.C.1) established several important points: (1) exchange is important to rotational excitation as well as elastic scattering in N_2; (2) the Π_g resonance dominates the rotational excitation cross section for $E \cong E_r$; and (3) cross sections for $j \to j' \geq 4$ are appreciable near the resonances, but very small at other energies. Because of the lack of convergence in the expansion of $V_s(\mathbf{r})$ and in the partial-wave expansion as well as the neglect of polarization, the calculated cross sections are not quantitatively accurate.

Chandra and Burke (1973) and Chandra (1975a) applied the adiabatic nuclear rotation approximation to rotational excitation using the electron–N_2 T-matrix elements of Burke and Chandra (1972). In Fig. 46(a, b) rotational-excitation cross sections for transitions $j = 0 \to 2, 4$ and $j = 1 \to 3, 5$ are compared with the respective $j = 0 \to 0$ and $j = 1 \to 1$ elastic cross sections. The most notable feature is the fact that the cross sections for $j = 0 \to 4$ and $j = 1 \to 5$ exceed those for $j = 0 \to 2$ and $j = 1 \to 3$, respectively, for energies near the resonance peak. Similar results have been obtained by Buckley and Burke (1977) in their static-exchange-polarization study of electron–N_2 scattering. This is explained by the d-wave character of the resonance. A $d(l = 2)$ wave can directly couple rotational state $j = 0$ to both $j = 2$ and $j = 4$. The latter is favored by its statistical weight, and the cross section is correspondingly larger. [In contrast, electron–H_2 scattering exhibits only a very weak p-wave resonance, and d-wave scattering at energies $E \lesssim 10$ eV is very weak. A $p(l = 1)$ wave directly couples $j = 0$ to $j = 2$, but *not* to $j = 4$. Thus, in e–H_2 scattering, a $j = 0 \to 4$ transition requires a second-order coupling mechanism, and that is very weak.] The fixed-nuclei calculations on which these calculations were based were discussed in the previous section. Since the internuclear separation was held fixed at the equilibrium value in each case, the calculated rota-

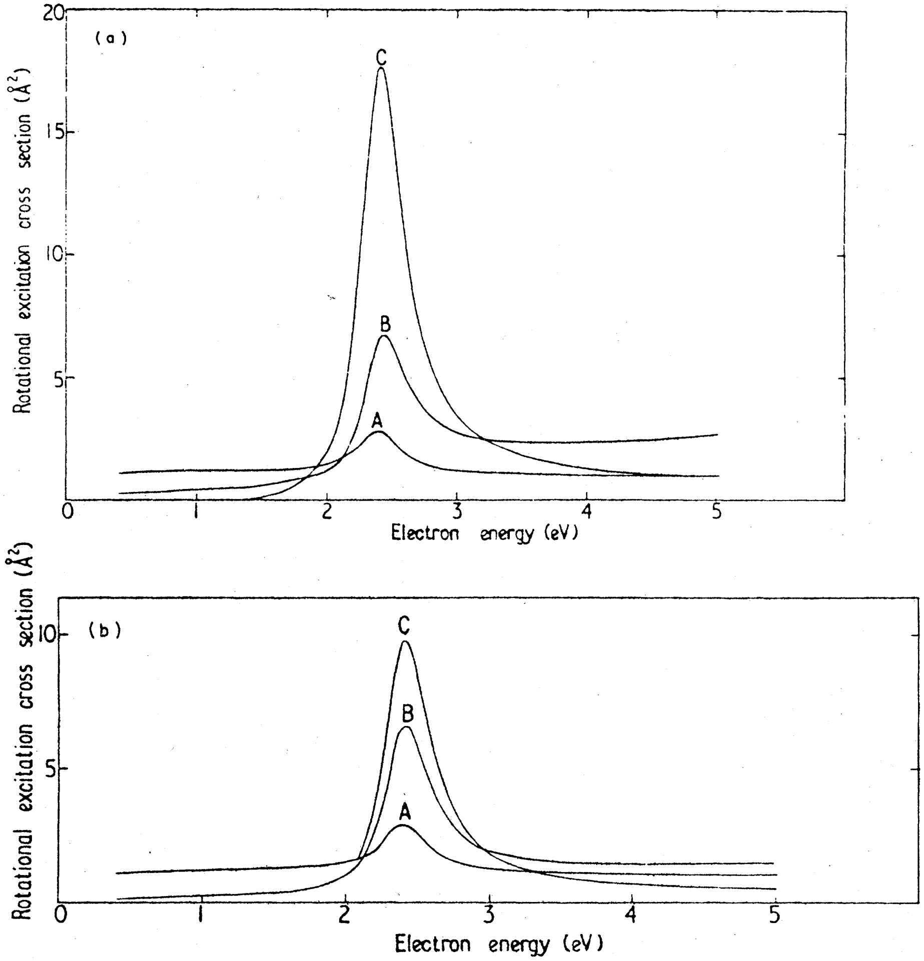

FIG. 46. Theoretical rotational-excitation cross sections for e–N_2 scattering: (a) (curve A) $j = 0 \to 0$, elastic reduced by 10; (curve B) $j = 0 \to 2$; (curve C) $j = 0 \to 4$. (b) (curve A) $j = 1 \to 1$ elastic reduced by 10; (curve B) $j = 1 \to 3$, (curve C) $j = 1 \to 5$. (Reprinted from Burke and Chandra, 1972.)

tional-excitation cross sections do not show fine structure on the resonance peak.

Chandra and Temkin (1976a, b) in their so-called "hybrid theory," allow for real and "virtual" vibrational excitation during the collision. Rotational-excitation cross sections, based on these calculations, were calculated by Chandra and Temkin (1976c) in the adiabatic nuclear rotation approximation. Cross sections for $j=0\rightarrow 0, 2, 4$ and $j=1\rightarrow 1, 3, 5$ are compared in Figs. 47(a) and 47(b), respectively, with the resonance-scattering model of Chen (1966a, b). At present there are no direct measurements of rotational excitation in N_2 at these energies. [Buckley (1977) suggests that the resonance envelope should be detectable with an energy resolution $\Delta E \lesssim 10$ meV.] The structure is expected to be present in rotational-excitation cross sections. However, the precise positions and magnitudes of the maxima and minima most likely will not agree with the calculations, for reasons discussed in the previous section.

3. Vibrational excitation (N_2)

The large hump in the total electron–N_2 cross section (see Fig. 26) was shown by Haas (1957) to be present in inelastic scattering as well. He suggested that a temporary N_2^- complex might somehow be involved. Schulz (1959), using a trapped-electron method, demonstrated that the cross section for vibrational excitation had a large peak at 2.3 eV. Schulz considered temporary formation of N_2^- to be the mechanism. Schulz (1962, 1964) went on to show the presence of a rich structure within the broad resonance profile; the presence of this structure was verified in elastic and inelastic scattering by several groups (Heideman, Kuyatt, and Chamberlain, 1966a, b; Schulz and Koons, 1966; Andrick and Ehrhardt, 1966; Boness and Hasted, 1966; Golden, 1966; Ehrhardt and Willmann, 1967; and Ehrhardt, Langhans, Linder, and Taylor, 1968).

Herzenberg and Mandl (1962) ascribed the observed resonance structure to the temporary excitation of different vibrational states of the N_2^- complex. Applying their modified version of the Kapur–Peierls resonant scattering theory they were able to choose the parameters $E^-(R_0)$, $\Gamma(R_0)$, and $v(R_0)$, where $v(R_0)$ is the slope of the N_2^- (real) potential energy curve $E^-(R)$ at $R=R_0$, so as to reproduce the qualitative features of the observations.

Chen (1964a, b, c) concluded that polarization, and other correlation effects neglected in the work of Herzenberg and Mandl (1962), could be important. Using the Feshbach projection-operator formalism, and assuming a single N_2^- electronic state was involved, he was able to parametrize his formal expressions for the vibrational-excitation cross sections so as to obtain fairly good agreement with the measurements. The improved agreement was primarily due to Chen's allowing the real part of the N_2^- potential energy curve to be different from that of N_2. He argued that the polarization interaction should depend on R and, consequently, that the N_2^- potential curve should differ in shape, and, therefore, in vibrational level spacing and equilibrium separation. Chen originally suggested that the N_2^- complex was a core-excited compound state, i.e., an electron temporarily bound to an *excited* configuration of N_2. Further analysis indicated that a better description of the state was that of an electron temporarily bound to a polarized ground state of N_2. The picture of a d-wave electron trapped within the centrifugal barrier is qualitatively correct, but it is important to realize that the ground state N_2 is rather strongly perturbed (i.e., polarized) by the extra electron. Chen also showed that structure should appear in the elastic cross section and in the rotational-excitation cross section. Schulz (1964) observed the former.

The early theoretical studies of resonant vibrational excitation in N_2 were semiempirical and qualitatively successful. They were not successful in reproducing more subtle features of the observed cross sections: (1) the fact that the peaks in the $v=0\rightarrow v'$ vibrational-excitation cross sections appear at slightly different energies, and with slightly different spacings, for different final vibrational states, and (2) that the peaks tend to shift toward higher energy and to spread farther apart as v' is increased. Herzenberg (1968) proposed an intuitive physical model to explain this phenomenon. The essential point made is that the lifetime of the electronic compound N_2^- state is too short to permit a large number of nuclear vibrations of the N_2^- to occur before the electron is ejected via "autodetachment." Thus, a description based on well-defined vibrational states of the N_2^- complex is inappropriate. In the "boomerang model" Herzenberg suggests that an outgoing nuclear wave (in R and t), generated from the initial electron–N_2 encounter and N_2^- formation at $R_0 \sim 1.09$ Å, propagates outward (toward larger R) and is reflected at the outer turning point of the N_2^- curve, as illustrated in Fig. 48 (Birtwistle and Herzenberg, 1971). The interference of outgoing and reflected waves results in a standing wave whose nodes tend to be shifted to the right for higher energies. Because the autodetachment width is so large near the left-hand turning point of the N_2^- curve, multiple reflections are removed. The oscillations of the cross section with respect to energy, in Herzenberg's formalism, occur in the expression

$$\sigma_{v'0} \propto \left| \int_0^\infty [R\psi_{v'}^{(v)}(R)]^* \xi_0(R,\varepsilon)\, dR \right|^2 , \tag{200}$$

where $\xi_0(R,\varepsilon)$ is simply the nuclear wave function for the N_2^- system and $\psi_{v'}^{(v)}(R)$ is the final N_2 vibrational wave function. These oscillations arise from the oscillatory R dependence of the N_2 and N_2^- nuclear functions. Since the R dependence of $\xi_0(R,\varepsilon)$ changes with energy, then so does the oscillatory behavior of $\sigma_{v'0}$. The authors point out that electron–N_2 scattering in the 2 eV region is really an intermediate physical case between the so-called "compound molecule limit" (small Γ) and the "impulse limit" (large Γ) discussed by Herzenberg and Mandl (1962). [See reviews by Bardsley and Mandl (1968) and Schulz (1973, 1976).] If the width were much smaller, multiple reflections would be important and cancellations would force $\xi_0(R,\varepsilon)$ to vanish except for special energies where phase matching occurs, viz., the vibrational energies of the N_2^- complex. In this case the resonance peaks would occur at the

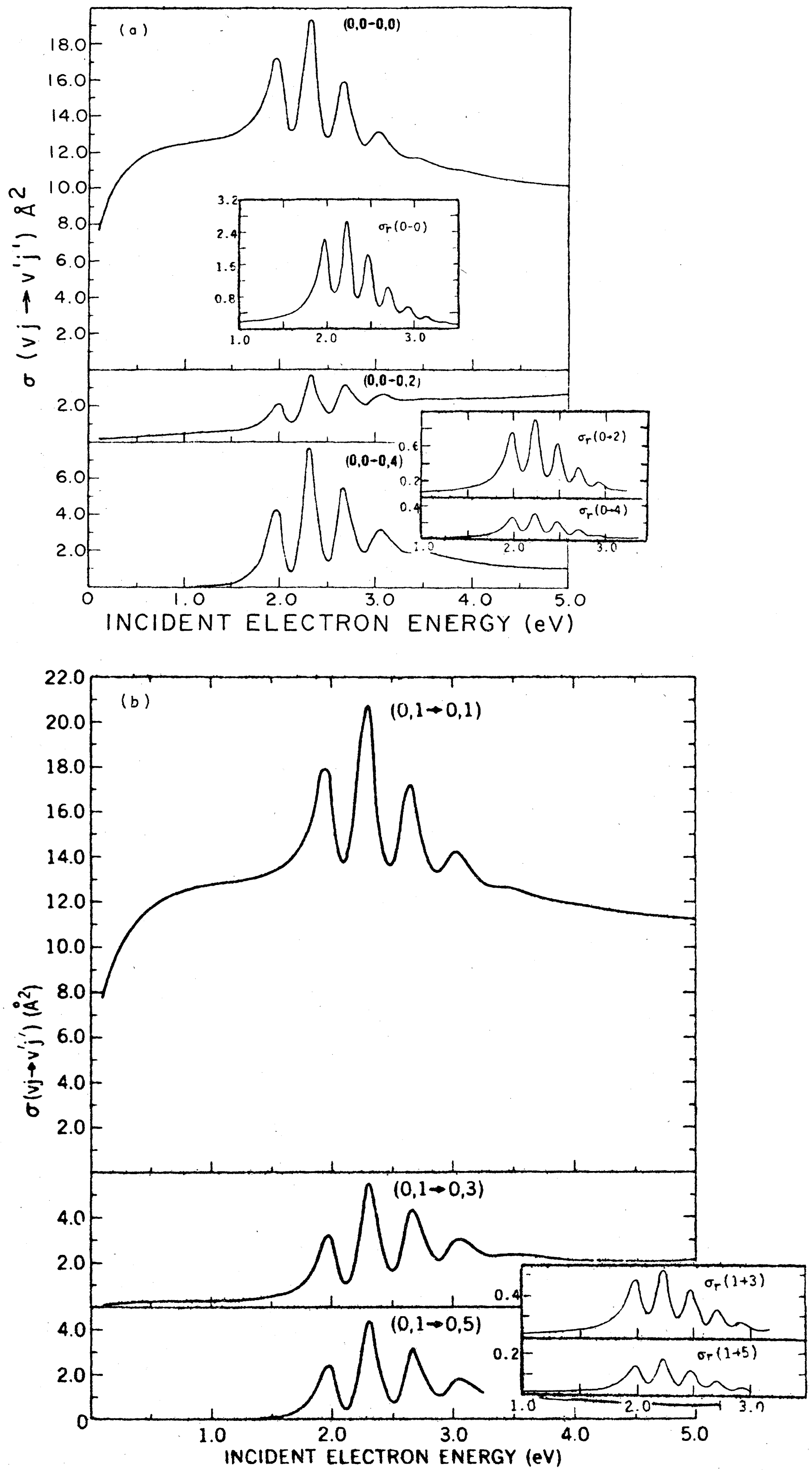

FIG. 47. Hybrid theory rotational-excitation cross sections for $(v=0, j\rightarrow v'=0, j')$ transitions in e–N_2 scattering, (insets) resonance model of Chen (1966a). (a) $j=0$; (b) $j=1$. (Reprinted from Chandra and Temkin, 1976c.)

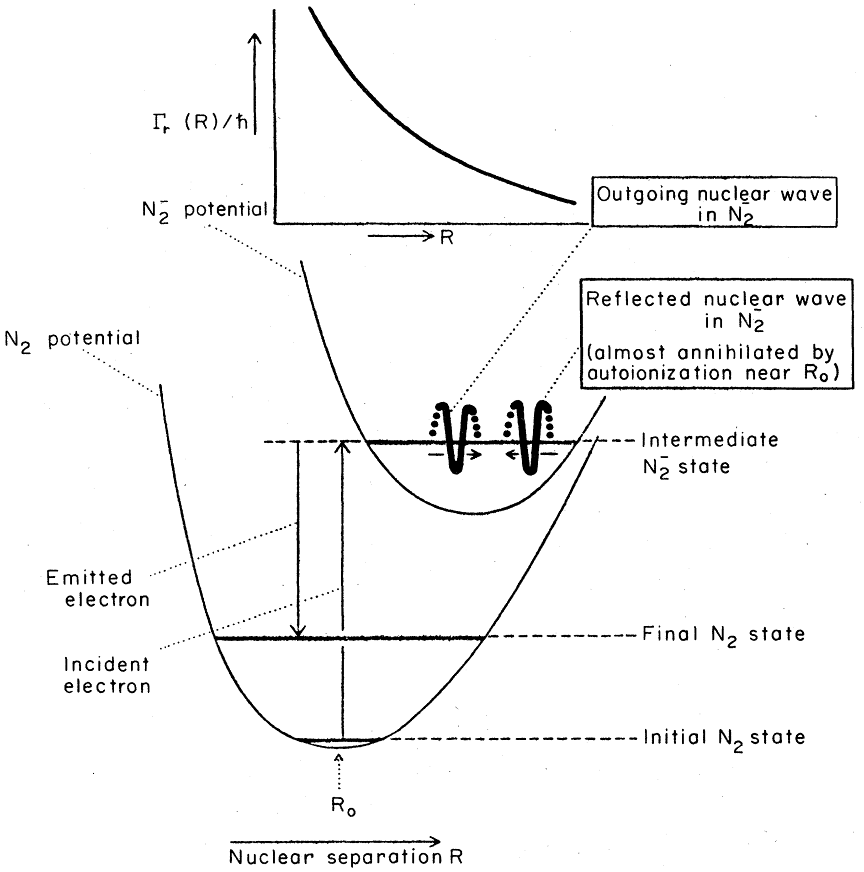

FIG. 48. The "boomerang" model of time evolution of the nuclear wave function in the transient N_2^- ion. (Reprinted from Birtwistle and Herzenberg, 1971.)

same energies for all final states v', and with the same spacings (e.g., e–O_2; see Linder and Schmidt, 1971b; Schulz, 1973; Koike, 1975). On the other hand, if the width were much larger, then the outgoing (in R and t) nuclear wave would decay before reflection at the outer turning point of the N_2^- curve could occur, and consequently no structure would result (e.g., e–H_2).

Insight into the structure of the N_2^- compound state was provided by Gilmore (1965), who proposed that based on molecular orbital theory the most likely assignment would be Π_g, arising from the configuration

$$KK(\sigma_g 2s)^2(\sigma_u 2s)^2(\sigma_g 2p)^2(\pi_u 2p)^4(\pi_g 2p)\,.$$

He deduced an N_2^- potential curve which resembled the semiempirical curve (see Chen, 1969) quite closely. The elastic angular distributions measured by Andrick and Ehrhardt (1966) were at least consistent with the Π_g assignment, but a large component of nonresonant scattering made a unique determination impossible. The differential vibrational-excitation cross sections measured by Ehrhardt and Willmann (1967) did, however, show distinctive maxima near $\theta = 90°$, providing more evidence for d-wave scattering and the Π_g characterization of the N_2^- state. Bardsley and Read (1968) and O'Malley and Taylor (1968) subsequently predicted the angular dependence

$$\sigma(\theta) \propto 1 - 3\cos^2\theta + \tfrac{14}{3}\cos^4\theta \tag{201}$$

for a scattering process dominated by a single d-wave Π_g compound state (see also Chang 1977a,b; Read 1968a,b, 1972); the expression agrees well with the observed vibrational-excitation angular distributions for $v = 0 \rightarrow 1$, 3, and 5 transitions over the energy range 1.9–3.1 eV. An *ab initio* calculation of the N_2^- electronic wave function and potential curve by Krauss and Mies (1970) was in essential agreement with the Gilmore (1965) assignment, but highlighted the importance of perturbations of the N_2 orbitals by the extra electron, an effect previously emphasized by Chen (1966 a,b). We will return to their results shortly.

Birtwistle and Herzenberg (1971) carried out a systematic semiempirical study of vibrational excitation in electron–N_2 scattering, using the phenomenological "boomerang" model of Herzenberg (1968). They gave careful attention to a precise determination of the R dependence of both the real part of the N_2^- potential curve and the autodetachment width. They represented the N_2^- potential curve by a Morse potential and the width by an expression due to Blatt and Weisskopf (1952, p. 390) which attributes most of the R dependence to an $l = 2$ "electron-penetration factor." A best fit, in the least-squares sense, to the data of Ehrhardt and Willmann (1967) for the $v = 0 \rightarrow 1$, 3, 5, and 7 cross sections at 15 energies is shown in Fig. 49 along with the experimental cross sections (arbitrary units). The N_2^- potential curve and width, determined in this manner, is shown in Fig. 37. Wong and Dubé (1978) also show that the "boomerang" model provides an adequate qualitative description of pure rotational and rotational–vibrational excitation in the 1–4 eV resonance region.

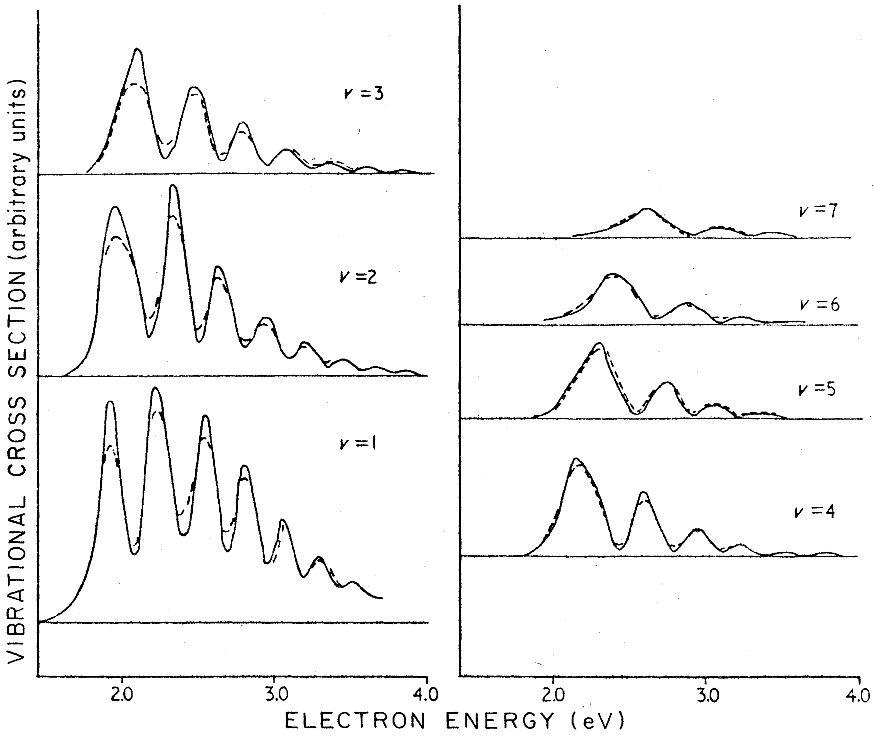

FIG. 49. Vibrational-excitation cross sections (relative) for 0 → v transition in e—N_2 scattering. Theory: (dashed curve) "boomerang" model. Experiment: (solid curve) Ehrhardt and Willmann (1967). (Reprinted from Birtwistle and Herzenberg, 1971.)

Chandra and Temkin (1976a) applied their "hybrid theory" to vibrational excitation and vibration–rotation excitation (Chandra and Temkin, 1976b,c). The "hybrid theory," as discussed in Sec. III.C.1, takes account of vibrational relaxation during the lifetime of the resonance by employing a vibrational close-coupling calculation for the Π_g symmetry (also see Choi and Poe, 1977a,b). The other symmetries are handled by the adiabatic nuclear vibration approximation. In Fig. 50, their calculated results for the $v=0\to1,2,3,4$ differential cross sections at $\theta=72°$ are compared with the measurements of Schulz (1964). The agreement is qualitative. The principal sources of error in the calculations are probably the lack of convergence in partial waves and the approximate treatment of exchange and polarization, as discussed in Sec. III.C.1. Differential $v=0\to1$ cross sections at 5.0 and 10.0 eV are compared in Figs. 51a,b, with the measurements of Srivastava *et al.* (1976) and the (nonconverged) close-coupling calculations of Truhlar *et al.* (1976), to be discussed. The effect of neglecting nonresonant contributions to the cross section is shown to be small, but significant. The calculated simultaneous vibration–rotation integral cross sections of Chandra and Temkin (1976c) for the transitions $(v,j)=(0,0)\to(1,0)$, $(1,2)$, and $(1,4)$ are compared in Fig. 52 with the results of Chen (1966a,b), who used a semiempirical resonance model to describe the process. The dominance of the $j=0\to4$ transition over that for $j=0\to2$ is apparent in the pure rotational-excitation (vibrationally elastic) cross sections as well. As noted earlier (Sec. III.C.1) this is a direct consequence of the d-wave character of the Π_g resonance.

In a very recent application of R-matrix theory, extended to include vibrational excitation, Schneider, Le Dourneuf, and Lan (1979) report good agreement with the measured elastic and vibrational-excitation electron–N_2 cross sections (all Δj) of Ehrhardt and Willmann (1967), Wong (unpublished), and Rohr (1977d) in the resonance region. These calculations allow for exchange and polarization effects in a nonempirical manner.

The vibrational-excitation cross sections fall off

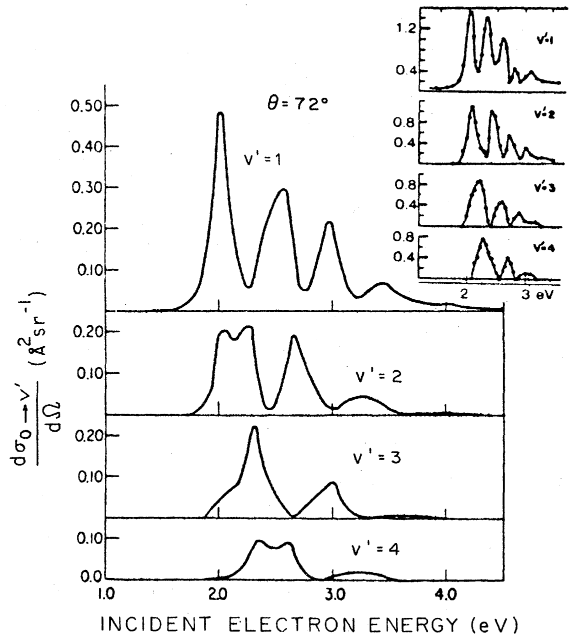

FIG. 50. Differential vibrational-excitation cross sections for 0 → v' transitions in e—N_2 scattering at $\theta=72°$. Theory: (solid curve) "hybrid theory." Experiment: (inset) Schulz (1964), renormalized. (Reprinted from Chandra and Temkin, 1976a.)

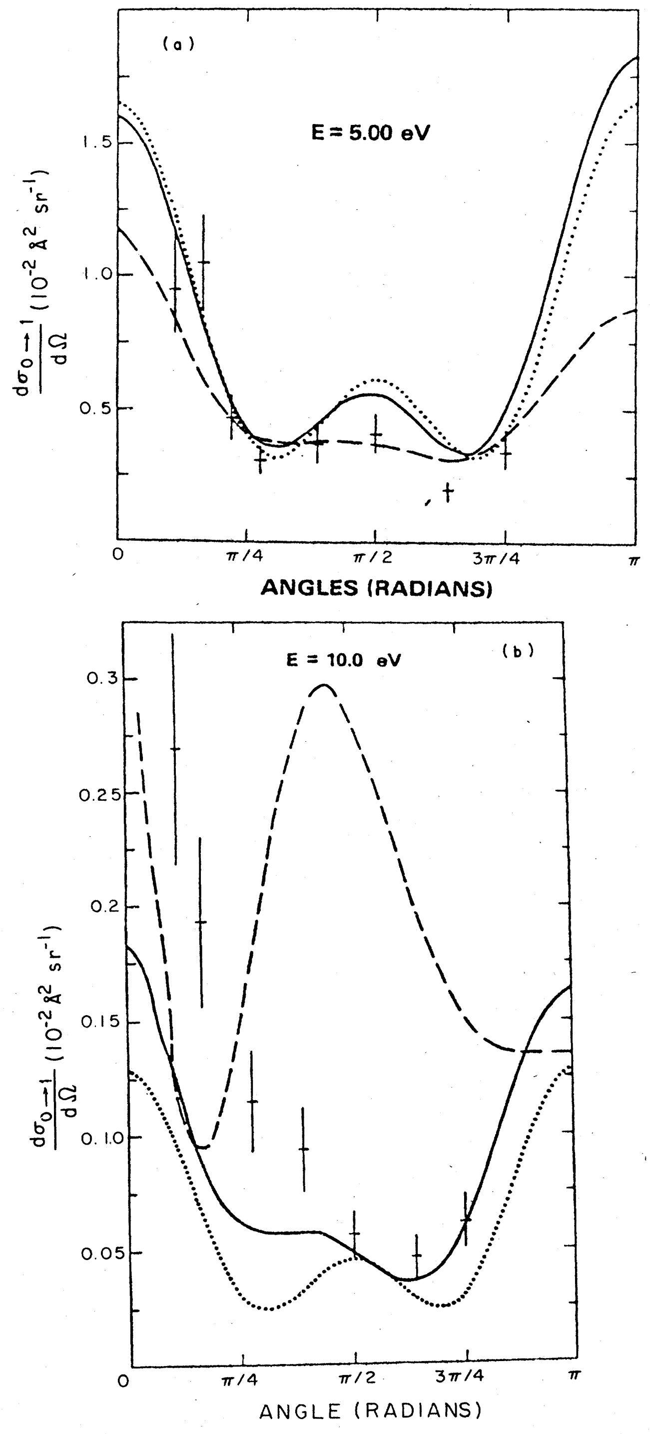

FIG. 51. Differential vibrational-excitation cross sections for $v=0\to1$ transition in e–N_2 scattering at (a) 5.0 eV, (b) 10.0 eV. Theory: (solid) "hybrid theory," (dotted) "hybrid theory" including only resonant Π_g symmetry, (dashed) Truhlar *et al.* (1976). Experiment: (+) Truhlar *et al.* (1976). (Reprinted from Chandra and Temkin, 1976b.)

rapidly both above and below the resonance region. This is particularly striking below the resonance in the swarm measurements of Englehardt, Phelps, and Risk (1964), as shown in Fig. 53. The measured $v=0\to1$ cross section is small near threshold, rising rather abruptly just above 1.0 eV. The beam data of Schulz (1964) and the theoretical results of Breig and Lin (1965) and Chen (1964a, b, c, 1966a, b) are also given for comparison. The discrepancy between the beam and swarm data is still not understood (Schulz, 1976; Phelps, 1968). The calculation of Breig and Lin (1965) is based on the Born approximation, including only the long-range interaction. (In the figure the two dashed lines are limiting cases.) These authors did not, of course, expect to reproduce the resonance. Their cross sections are too large just above threshold, probably indicating too small a cutoff radius for the long-range model interaction they chose. Chen's cross section was obtained by fitting a "Breit–Wigner" form to the experimental cross section at higher energies. The low-energy "tail" of this fit turns out to be in excellent agreement with the swarm measurements. Chandra and Temkin do not quote vibrational-excitation cross sections at these energies.

4. Scattering above the 2.3 eV resonance

Well above the Π_g resonance region (i.e., $E \gtrsim 20$ eV) Truhlar, Trajmar, and Williams (1972) and Truhlar (1972) report experimental and theoretical (polarized Born approximation) studies of elastic scattering and $v=0\to1$ vibrational-excitation in electron–N_2 scattering. Several model interaction potentials were examined. The calculated elastic-differential cross sections were found to be in qualitative agreement with experiment at 20, 30, and 83 eV for scattering angles $\theta \lesssim 60°$ to $75°$ for all of the model potentials studied, but tended to be too large at large angles. (The calculated $v=0\to1$ vibrational-excitation differential cross sections were found to agree with the measurements only at rather small angles where the long-range interactions are expected to dominate.) The authors were led to agree with Pavolvic, Boness, Herzenberg, and Schulz (1972), that the 20 eV vibrational-excitation cross section is also strongly influenced by resonance scattering.

Truhlar, Brandt, Chutjian, Srivastava and Trajmar (1976) report both the crossed-beam measurements of differential $v=0\to1$ vibrational-excitation cross sections at 5 and 10 eV and model close-coupling calculation of rotational–vibrational excitation cross sections at these energies. Finally Truhlar, Brandt, Srivastava, Trajmar, and Chutjian (1977) report similar studies at energies in the range 30–75 eV. The model electron–N_2 interaction potential used in the theoretical studies includes a static potential, calculated at a large number of internuclear separations by the semiempirical INDO/1s approximation (Truhlar, Van-Catledge, and Dunning, 1972), and a polarization potential of the form given in Eq. (147) where the cutoff radius $r_c=1.592\ a_0$ (Burke and Chandra, 1972) was adopted. Exchange effects were entirely ignored in these calculations. The values of $\alpha_0(R_0)$ and $[d\alpha_0(R)/dR]_{R_0}$ were estimated (Truhlar, 1973; Breig and Lin, 1965) based on experimental measurements. The values of $\alpha_2(R_0)$ and $[d\alpha_2(R)/dR]_{R_0}$, while more difficult to determine, were roughly estimated from experimental and theoretical considerations. The INDO/1s approximation to the static potential was found to be in reasonable agreement with accurate

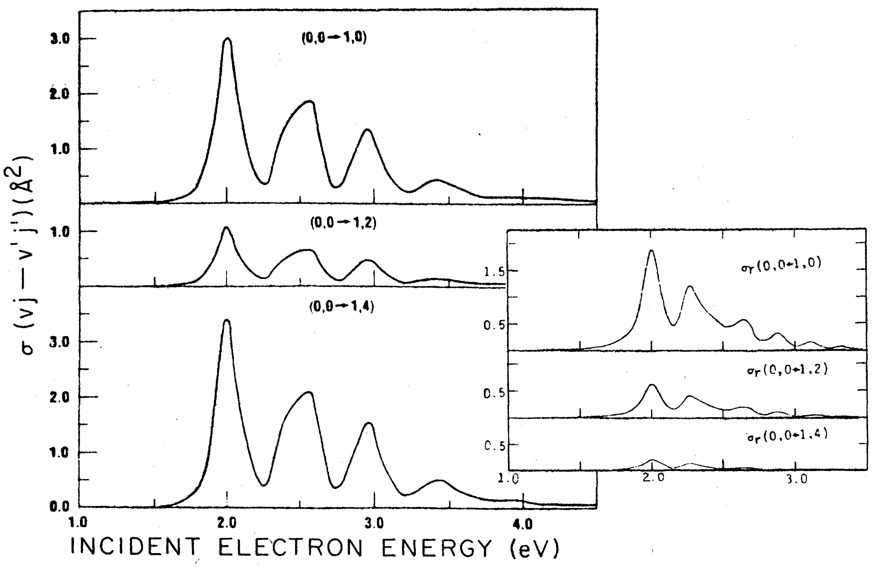

FIG. 52. Hybrid theory rotational–vibrational-excitation cross sections for transitions ($v=0, j=0\to v', j'$) in e–N$_2$ scattering: (inset) resonance model of Chen (1966a). (Reprinted from Chandra and Temkin, 1976c.)

ab initio results at small r but had to be corrected at large r where it predicted much too large a quadrupole moment. The static potential was *fit* to a single-center expansion, truncated to $\lambda_{\max}=16$. The close-coupling calculation was carried out in the LAB frame, coupled-angular-momentum framework, discussed in Sec. II.E.1. The close-coupling expansion was truncated in terms of both vibrational and rotational states. For values of total angular momentum $J\le J_1$ (J_1 ranged from 8 to 11 for energies of 30 and 75 eV, respectively) which contributed most to the $v=0\to1$ cross section, the four states $(v,j)=(0,0), (0,2), (1,0), (1,2)$ were retained. For larger values $J_1+1\le J\le 20$, still important to $j=0\to2$ ($v=0\to0$) rotational-excitation cross sections, only the two states $(v,j)=(0,0), (0,2)$ were retained, and for the remaining values $20\le J\le J_2$ (J_2 ranged from 67 to 105 for energies of 30 and 75 eV, respectively) only the single state $(v,j)=(0,0)$ was retained. In all cases, all values of l consistent with $j_{\max}=2$ and J were included. The coupled radial equations were solved using the Numerov method (Hartree, 1957; Hamming, 1962; Blatt, 1967; Sloan, 1968; Lane and Geltman, 1967; and Allison, 1970) with periodic reorthogonalization (Riley and Kuppermann, 1968) applied at small values of r to preserve linear independence of the solutions. Differential cross sections were calculated for pure elastic ($v=0\to0, j=0\to0$) scattering and pure rotational excitation ($v=0\to0, j=0\to2$), at the energies 30, 35, 45, 50, and 75 eV. Pure elastic and pure rotational-excitation integral and momentum-transfer cross sections were also determined at the same energies. In Fig. 54(a) the calculated $v=0\to0$ "vibrationally elastic" (includes $j=0\to0$ and $0\to2$ contributions) differential cross sections at 50 eV are compared with the experimental results of: Srivastava, Chutjian, and Trajmar (1976); DuBois and Rudd (1976) (corrected results); and Kambara and Kuchitsu (1972), the latter normalized at 30° to Srivastava *et al.* (1976). Comparisons given at 30 and 75 eV are similar. The agreement at small angles ($\theta\lesssim 30°$ to 45° is good, suggesting that the long-range interactions are adequately represented in the model. The failure of the model at larger angles is probably due to inadequate treatment of the short-range interactions (recall that exchange was entirely neglected) and the fact that so few rotational states were retained in the close-coupling expansion. The calculated integral and momentum-transfer elastic cross sections were found to be of the right order of magnitude as the measured values (Srivastava *et al.*, 1976). However, the integral cross sections exceed experiment by about 20%–30% over the range 30 to 75

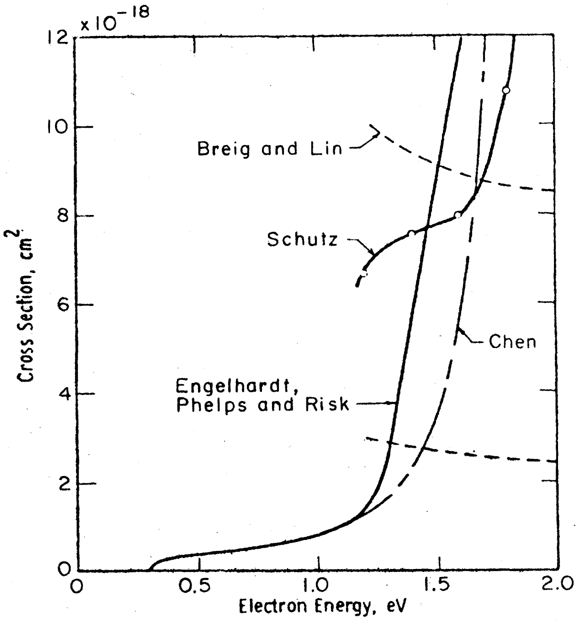

FIG. 53. Cross section for $v=0\to1$ vibrational-excitation in e–N$_2$ scattering near threshold. Theory: (chain curve) resonance model of Chen (1966a); (dashed curves) Born approximation based on different model interactions, Breig and Lin (1965). Experiment: (solid curve) Englehardt, *et al.* (1964); (solid curve and points) Schulz (1964). (Reprinted from Phelps, 1968.)

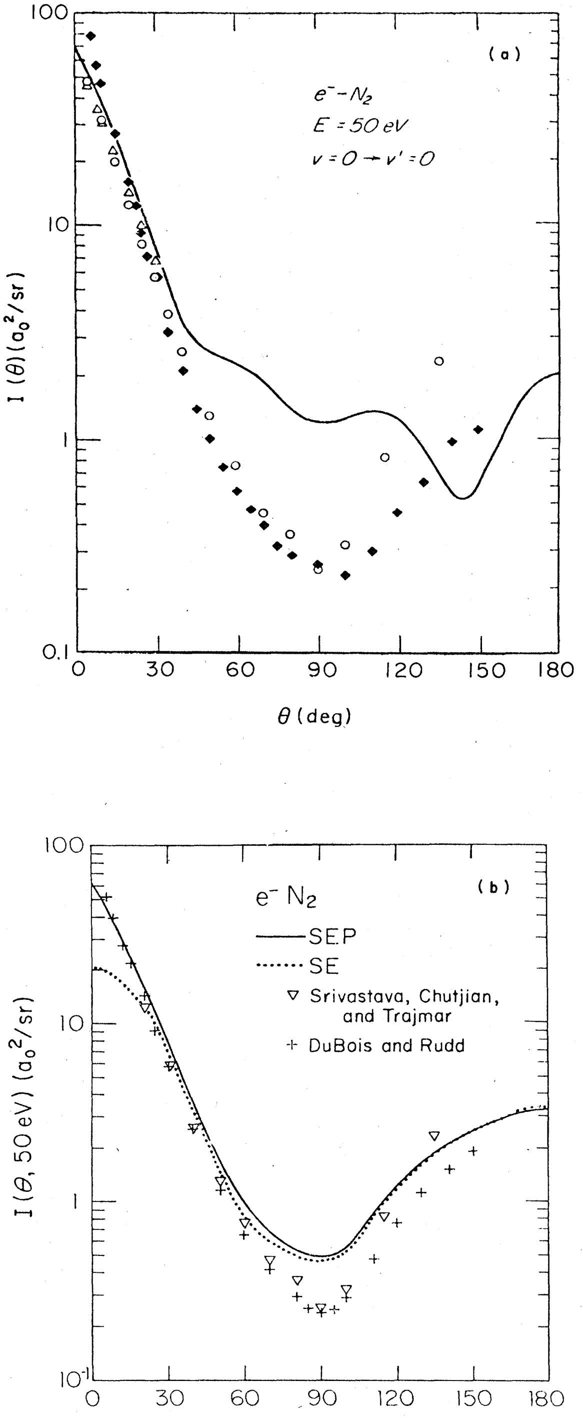

FIG. 54. Differential elastic ($v = 0 \rightarrow 0$) cross sections for e–N_2 scattering at 50 eV. Theory: (a) (solid curve) unconverged close-coupling results, Brandt *et al.* (1976); (b) converged close-coupling results of Onda and Truhlar (1978); (solid curve SEP) static-exchange polarization, [dotted curve (SE)] static exchange. Experiment: [diamonds in (a)], Kambara and Kuchitsu (1972), renormalized; [triangles △ in (a) and + in (b)], DuBois and Rudd (1976), [circles in (a) and triangles ▽ in (b)] Srivastava *et al.* (1976). (Reprinted from Brandt *et al.*, 1976, and Onda and Truhlar, 1978.)

eV and the momentum-transfer cross sections are about 10% larger at 30 eV, and 30% smaller at 75 eV, than the experimental values.

The importance of proper convergence of the close-coupling expansion is apparent in the recent calculations of elastic e–N_2 scattering cross sections at 30–50 eV by Onda and Truhlar (1978). In this calculation, the electron–N_2 interaction was represented by the sum of static (S), exchange (E), and polarization (P) contributions (see Sec. II.G). The static potential is calculated from the N_2 molecular charge density approximated by the INDOXI (1s) method (Truhlar, 1977; Truhlar, Van-Catledge, and Dunning, 1972; and Truhlar and Van-Catledge, 1973, 1976) and is properly corrected in the asymptotic region. Exchange is included via the semiclassical exchange approximation (see Sec. II.G.2.b) and polarization is modeled by the semiempirical cutoff form, Eq. (147), with the cutoff radius $r_p = 2.308 a_0$ chosen to agree with Buckley and Burke (1977). In the rotational close-coupling expansion, as many as 10 states were considered and a sufficient number of terms $\lambda \leq \lambda_{\max}$ were included in the expansions of the SEP e–N_2 potentials, at least for the size of rotational-state basis chosen. In Fig. 54(b) elastic ($v = 0 \rightarrow 0$) cross sections calculated in both the static-exchange and static-exchange-polarization approximations are compared with various experimental measurements. Of course, when polarization is neglected (SE), the small-angle scattering is underestimated. At larger angles there is little difference. The peculiar shape of the unconverged differential cross sections of Brandt *et al.* (1976) in Fig. 54(a) is most likely a numerical artifact of the lack of convergence of the expansions of the wave function and potential energy. Onda and Truhlar (1979a) have extended this numerical study to examine the sensitivity of the calculated e–N_2 cross sections at 30 eV to different choices of static, exchange, and polarization potentials.

The $v = 0 \rightarrow 1$ vibrational-excitation cross sections, calculated using essentially the same model and procedure as Brandt *et al.* (1976), are reported along with the crossed-beam measurements at energies in the range 30–75 eV by Truhlar *et al.* (1976). The calculated differential $v = 0 \rightarrow 1$ cross sections exceed the observed values by as much as an order of magnitude at $\theta \simeq 20°$ and by a factor of 2 or so at somewhat larger angles $\theta \approx 60°$. The integral cross sections are about twice the measured values. Although there are some areas of disagreement between different measurements, nevertheless it appears that the theoretical model is inadequate to describe vibrational excitation. Again, the problem is likely to be inaccurate treatment of the short-range interaction, especially the manner in which the polarization potential is cut off, and retention of too few rotational states in the close-coupling expansion. The latter is probably more serious. It has been suggested (Pavlovič *et al.*, 1972) that N_2-shape resonances are important at these energies, and the experimental integral $v = 0 \rightarrow 1$ cross sections do fall sharply in going from 30 to 35 eV.

Truhlar, Brandt, Chutjian, Srivastava, and Trajmar (1976) also report theoretical rotation–vibration excitation cross sections and crossed-beam measurements of $v=0\rightarrow 1$ vibrational excitation cross sections for electron–N_2 scattering at 5 and 10 eV. The theoretical model is the same as that described above. The calculated total integral and momentum transfer cross sections (dominated by elastic scattering and rotational excitation) at 5.0 eV exceed the measured values (Golden, 1966; Srivastava *et al.*, 1976; and Englehardt, Phelps, and Risk, 1964) by about a factor of 2, apparently due to an exceptionally large $j=0\rightarrow 2(v=0\rightarrow 0)$ rotational-excitation cross section. This $j=0\rightarrow 2$ $(v=0\rightarrow 0)$ theoretical cross section is slightly larger than the $j=0\rightarrow 0(v=0\rightarrow 0)$ elastic cross section and exceeds the theoretical results of Burke and Chandra (1972) and Chandra and Temkin (1976a) by about a factor of 4. The authors suggest the likely explanation that the lack of convergence in rotational states (only $j=0$ and 2 were included) is responsible, and that the large $j=0\rightarrow 2$ cross section is spurious. At 10 eV, the calculated total integral cross sections are in better agreement with Burke and Chandra (1972) and Chandra and Temkin (1976a), and the integral vibrationally elastic cross section is in excellent agreement with the experimental results of Srivastava *et al.* (1976). The momentum transfer cross sections lie about 25%–30% above the theoretical results of Burke and Chandra (1972) and Chandra and Temkin (1976a) and the measurements of Englehardt *et al.* (1964) and Srivastava *et al.* (1976). The calculated $v=0\rightarrow 1$(all Δj) vibrational-excitation cross sections (differential, integral, and momentum transfer) were also compared with the theoretical results of Chandra and Temkin (1976a) and the experimental measurements of the present authors (Truhlar *et al.*, 1976). At 5 eV, the calculated integral and momentum-transfer cross sections 0.195 and $0.190a_0^2$, respectively, are about 30% larger than the results of Chandra and Temkin (1976a) and lie within the range of experimental uncertainty (mainly due to 0° and 180° extrapolation) of the measurements. At 10 eV, the calculated integral and momentum transfer $v=0\rightarrow 1(\Delta j=0)$ cross sections, 0.092 and $0.091a_0^2$, respectively, exceed those of Chandra and Temkin (1976a) by about a factor of 4.6 and are about a factor of 2.5 larger than their measured values. The comparison of theoretical vibrational-excitation cross sections with the results of Chandra and Temkin (1976a) is complicated by several factors. Apparently, Chandra and Temkin (1976a) included only the Π_g partial waves in their original calculation of vibrational-excitation cross sections [see discussion by Truhlar *et al.* (1976) and their Footnote 9]. While this is indeed the dominant symmetry near the resonances, i.e., $2\lesssim E\lesssim 3$ eV, the Σ_g, Σ_u, and Π_u symmetries may take substantial (even dominant) contributions at energies $\gtrsim 5$ eV.

Chandra and Temkin (1976b) have reported differential elastic and vibrational-excitation cross sections at 5.0 and 10.0 eV, including both resonant and nonresonant contributions. The differential $v=0\rightarrow 1$ cross sections at 5.0 and 10.0 eV are compared in Fig. 51(a), 51(b) with the theoretical results of Truhlar *et al.* (1976) and the measurements of Srivastava *et al.* (1976). While both theoretical cross sections are similar at intermediate angles, that of Chandra and Temkin (1976b) is larger at large and small angles, and in the latter case is in better agreement with the measurements. At 10 eV, neither theory agrees very well with experiment; however, the results of Chandra and Temkin (1976b) are clearly superior here. An important uncertainty in the reliability of the theoretical results of Truhlar *et al.* (1976), as described previously, arises from the rather severe truncation of the close-coupling expansion to $j\leqslant 2$. The extent of the error introduced in this way is not known. At the same time, it must be noted that the calculations of Chandra and Temkin (1976b) also were not converged in the number of partial waves (l) included. One further point raised by Truhlar *et al.* (1976) is in regard to the accuracy of the vibrational matrix elements themselves. Convincing comparisons of theoretical and experimental vibrational-excitation cross sections must await theoretical results that are converged in the number of vibrational *and* rotational states and that take proper account of both exchange and polarization.

Choi, Poe, Sun, and Shan (1979) show that at fairly high energies $E\gtrsim 50$ eV, a reasonably good description of the differential cross section for elastic scattering and vibrational excitation may be obtained from a simple "two-potential" approach in which the scattering from two screened-Coulomb "atoms" and a long-range potential are added *incoherently*. The authors argue that totally neglecting the interference effects is superior to including them incorrectly due to inadequacies in approximate interaction potentials, convergence of coupled-states expansions, etc. [See related application of Huang and Chan (1977) to e–H_2 scattering.]

D. Electron-CO_2 scattering

Carbon dioxide is a closed-shell triatomic molecule and is linear in its ground $^1\Sigma_g^+$ state. Electron–CO_2 scattering is characterized by an unusually large momentum-transfer cross section at low energies and a broad "shape resonance" around 4.0 eV. The momentum-transfer cross section measured by Lowke, Phelps, and Irwin (1973) is compared in Fig. 55 with theoretical

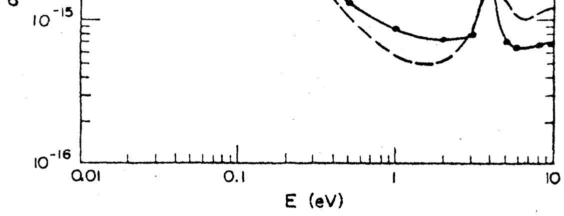

FIG. 55. Momentum-transfer cross sections for e–CO_2 scattering. Theory: (dashed curve) SEP model with HFEG exchange, Morrison *et al.* (1977). Experiment: (solid curve) Lowke *et al.* (1973). (Reprinted from Morrison *et al.*, 1977.)

results of Morrison, Lane and Collins (1977), to be discussed. Singh (1970) has estimated a scattering length of $-7.2a_0$ based on an "effective-range" analysis of the early momentum-transfer measurements of Hake and Phelps (1967). Tice and Kivelson (1967) reported that the electron–CO_2 collision frequency at $E \simeq 0.025$ eV, as determined from cyclotron-resonance linewidths, was much larger than that of other nonpolar molecules (e.g., N_2, O_2, CH_4, C_2F_6) and that it even exceeded the collision frequency for a number of "weakly" *polar* molecules (e.g., CO, N_2O). These authors suggested that the "transient dipole moment" associated with the "zero-point" bending of the molecule might be responsible for the unusually large low-energy cross section.

1. Elastic scattering and rotational excitation (CO_2)

Morrison, Lane, and Collins (1977) took the point of view that the large low-energy electron–CO_2 scattering momentum-transfer cross section could be explained without invoking nuclear motion. They performed a fixed-nuclei elastic-scattering (BODY-frame) calculation in which exchange and polarization effects were represented by the Hara (1967) free-electron-gas exchange potential of Eq. (132), with $I = 1.0135$ Ry (Franklin, 1969) and the parametrized polarization potential of Eq. (147), with $\alpha_0 = 17.90a_0^3$ and $\alpha_2 = 9.19a_0^3$ (Hirschfelder, Curtiss, and Bird, 1954). The cutoff parameter r_p in (147) was determined semiempirically by "tuning" the Π_u resonance to 3.8 eV (see Schulz, 1976) in the manner of Burke and Chandra (1972) in their study of electron–N_2 scattering. The value $r_p = 2.59a_0$ was obtained in this way. The coupled radial equations (116′), with the exchange terms of Eq. (119) replaced by the local-exchange approximation of Eqs. (130) and (132), were solved numerically using the integral equations method (Sams and Kouri, 1969a, b; White and Hayes, 1972). The static potential given by Eq. (118) and HFEG potential given by Eq. (132) were both expanded in single-center expansions, using the near-Hartree–Fock SCF/MO ground-state CO_2 charge densities of McLean and Yoshimine (1967, 1968) (see also Yoshimine and McLean, 1967). Because of the strong anisotropy in the electron–CO_2 static potential energy, largely due to the presence of two oxygen nuclei each at a distance $R_{CO} = 2.1944a_0$ from the center of mass (carbon atom), it was necessary to include a large number of terms $\lambda \le \lambda_{max}$ in these expansions, viz., $\lambda_{max} = 28$ for the exchange potential and the electron–electron (repulsive) part of $V_S(\mathbf{r})$, and $\lambda_{max} = 78$ for the electron–nuclear (attractive) contribution to $V_S(\mathbf{r})$. Convergence in the partial-wave expansion (115) was also found to be slow. In the region near the nuclei, $r \le 4.0a_0$, it was necessary to include 32 channels for Σ_g, 15 for Σ_u and Π_g, 23 for Π_u near the resonance, and 15 for Π_u far from the resonance in order to converge the cross sections to 1%. [We recall that the partial waves associated with each of these symmetries correspond to $l = 0, 2, \ldots (\Sigma_g)$; $l = 1, 3, \ldots (\Sigma_u)$; $l = 2, 4, \ldots (\Pi_g)$ and $l = 1, 3, \ldots (\Pi_u)$, etc.] At greater distances, $r \ge 4.0a_0$, the centrifugal barriers associated with the large-l partial waves suppress the corresponding radial functions, and the expansion (115) may be truncated further; the authors retained five partial waves for all symmetries except Π_g, and eight for the latter. In Fig. 56, calculated total (BODY-frame elastic) cross sections are compared in the static (S), static-exchange (SE), and static-exchange-polarization (SEP) approximations; the experimental data are those of Ramsauer and Kollath (1927), Kollath (1932), and Brüche (1927) [see also Brode (1933); recent measurements of Shyn, Sharp, and Carignan (1978); and Szmytkowski and Zubek (1978)]. The calculated resonance, which occurs in Π_u symmetry, is narrower than observed. The Π_u characterization of the resonances is in agreement with the assignment by Claydon, Segal, and Taylor (1970). However, the fine structure experimentally observed in elastic and vibrational-excitation cross sections is not present (Boness and Hasted, 1966; Andrick, Danner, and Ehrhardt, 1969; Danner, 1970; Burrow and Sanche, 1972; Sanche and Schulz, 1973; Čadež, Tronc, and Hall, 1974; Boness and Schulz, 1968, 1974; Čadež, Gresteau, Tronc, and Hall, 1977; see review of Schulz, 1976). The differential excitation function observed by Čadež *et al.* (1977) at 20° is shown in Fig. 57 for elastic scattering and vibrational excitation $(0,0,0) \to (\nu_1, \nu_2, \nu_3)$, where the quantum numbess ν_1, ν_2, and ν_3 refer to quanta of symmetric stretch, bending, and asymmetric stretch vibrations, respectively. [The data of Boness and Schulz (1974) are similar.] Boness and Schulz (1974) and Čadež *et al.* (1974) proposed that the structure arises from the "boomerang effect" (Herzenberg, 1968) and is therefore analogous to the shape resonances in electron–N_2 and –CO scattering discussed in Secs. III.C and III.E, respectively. Since the internuclear separation is held fixed in the calculation of Morrison, Lane, and Collins (1977), an accurate description of the resonance region is not expected. The "tuning" of the Π_u resonance to 3.8 eV, which determines the po-

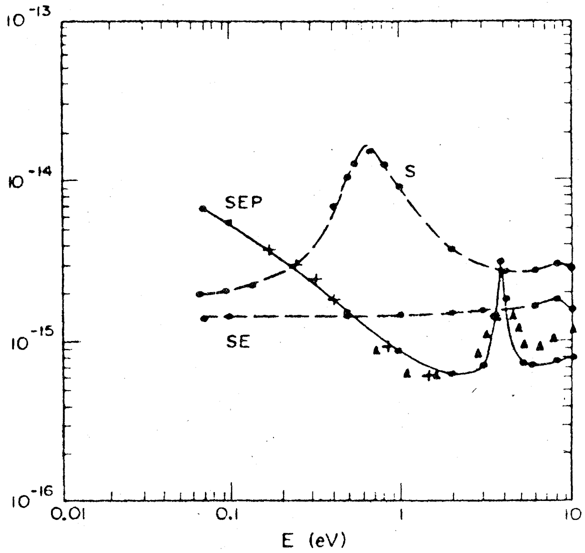

FIG. 56. Total cross sections for e–CO_2 scattering. Theory: (solid curve SEP) static-exchange polarization; (dashed curve SE) static exchange; (dashed curve S) static, Morrison *et al.* (1977). Experiment: (×) Ramsauer and Kollath (1927), Kollath (1932); (△) Brüche (1927); Brode (1933). (Reprinted from Morrison *et al.*, 1977.)

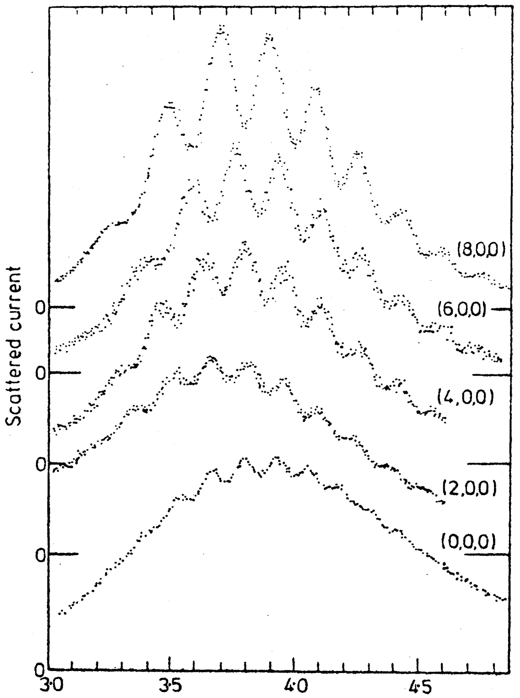

FIG. 57. Differential excitation functions at 20° for symmetric-stretch transition (0, 0, 0) → (v', 0, 0) in $e-CO_2$ scattering. (Reprinted from Cadez *et al.*, 1977.)

larization cutoff, is the only semiempirical adjustment made in the calculation. The large low-energy elastic and momentum-transfer cross section is a result of strong "enhancement" of the Σ_g partial cross section as illustrated in Fig. 58. Since the Σ_g wave function [i.e., Eq. (115) with $m = 0$ and *even* l] is dominated asymptotically by the s-wave component, it is tempting to associate this "enhancement" with the existence of a "virtual state" associated with the electron-CO_2 model potential (see Taylor, 1972). The possibility of a low-lying Σ_g resonance cannot be ruled out completely although it is not indicated in the CO_2^- study of Claydon, Segal, and Taylor (1970). In any case, this strong scattering of low-energy Σ_g partial waves may give rise to a near-threshold enhancement of vibrational-excitation cross sections, especially for symmetric-stretch transitions where the Σ_g partial waves dominate both the initial- and final-state scattering wave function. There is experimental evidence for such behavior in recent beam (Wong, 1978) measurements.

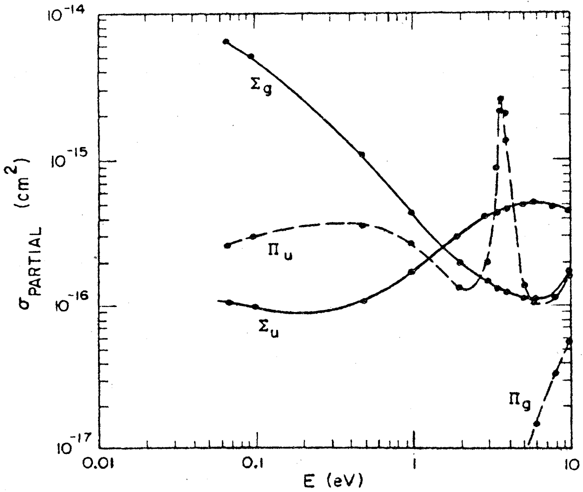

FIG. 58. Theoretical partial cross sections for $e-CO_2$ scattering. SEP model including HFEG exchange. (Reprinted from Morrison *et al.*, 1977.)

Morrison and Lane (1977) calculated rotational-excitation cross sections for electron-CO_2 scattering by applying the adiabatic nuclear rotation approximation (see sec. II.D), using the calculated T-matrix elements (SEP) of Morrison, Lane, and Collins (1977). The calculated $j = 0 \to 0$ elastic, $j = 0 \to 2, 4$ rotational-excitation, and total cross sections are shown in Fig. 59. The resonance dominates all cross sections for energies near the ("tuned") position of 3.8 eV. The $j = 0 \to 2$ cross section is also large at lower energies where it is strongly influenced by the large negative quadrupole moment of CO_2. [The value $q = -3.8598ea_0^2$ used in the calculation is comparable with the theoretical value $-3.9086ea_0^2$ of Vucelić *et al.* (1973), and the experimental value $-3.2014ea_0^2$ of Buckingham (1959).] It is interesting to compare the qualitative features of the $j = 0 \to 2$ cross section for H_2, N_2, and CO_2, as illustrated in Fig. 60 (we should keep in mind the missing fine structure that should appear on the N_2 and CO_2 resonances). The $j = 0 \to 4$ cross section is large near the resonance, but

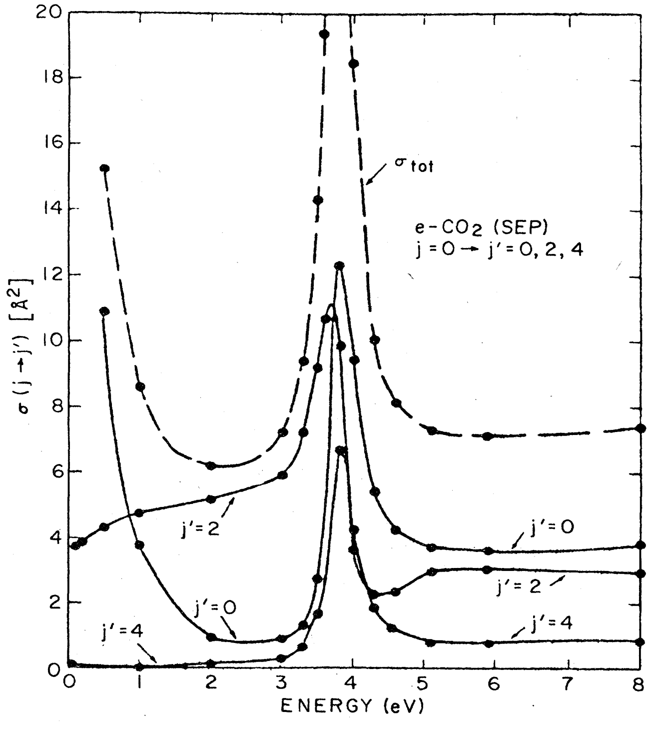

FIG. 59. Theoretical rotational-excitation cross sections for transitions $j = 0 \to j'$ in $e-CO_2$ scattering: (solid curves) rotational excitation and elastic; (dashed curve) total rotational excitation plus elastic. (Reprinted from Morrison and Lane, 1977.)

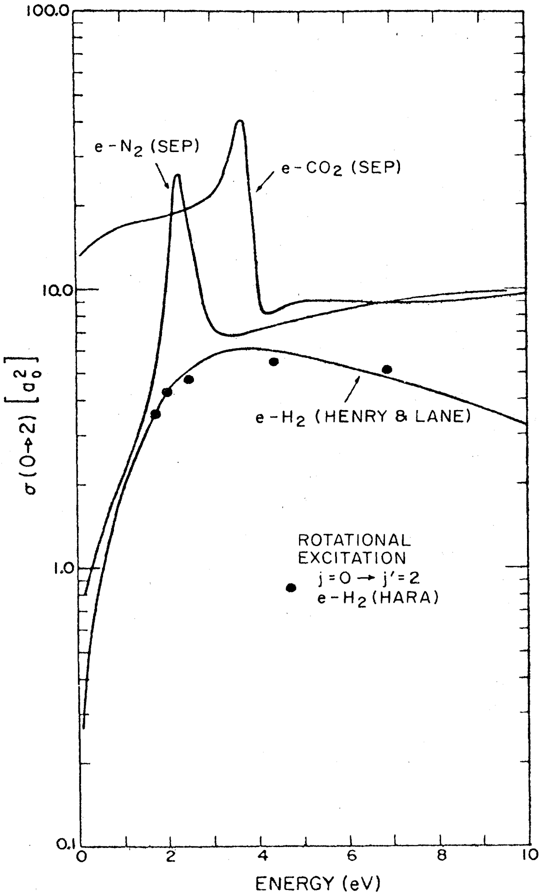

FIG. 60. Comparison of theoretical rotational-excitation cross sections for $j=0\to2$ transitions in e–H_2, N_2, and CO_2 scattering: (curves e–CO_2 SEP) Morrison and Lane (1977); (curve e–N_2 SEP) Morrison and Collins (1978); (curve e–H_2) Henry and Lane (1969); (closed circles) Hara (1969b). (Reprinted from Morrison and Lane, 1978.)

unlike the analogous case of electron–N_2 scattering, does *not* exceed the $j=0\to2$ cross section. The Π_u partial-wave function [i.e., Eq. (115) with $m=\pm1$ and *odd* l] is dominated asymptotically by p waves, which provide direct coupling for the $j=0\to2$ transition but not for $j=0\to4$. In contrast, in electron–N_2 scattering the Π_g resonance is asymptotically of "d-wave character." (See Sec. III.C.2) Finally, in Fig. 59, the $j=0\to0$ elastic cross section dominates the total for energies much below 1 eV. It then falls off very rapidly with energy and exhibits a "Ramsauer-like" minimum between 2.0 and 3.0 eV.

The calculations of Morrison, Lane, and Collins (1977) and Morrison and Lane (1977) are subject to the same criticism as the theoretical electron–N_2 studies described in Sec. III.C. The use of local model potentials for both exchange and polarization introduces uncertainty into the calculations. It is somewhat encouraging that Morrison and Collins (1978) found the HFEG exchange potential to be a good approximation in the case of electron–N_2 scattering. The qualitative features of the calculated elastic and rotational-excitation cross sections are probably correct, but the precise quantitative agreement of the calculated total and momentum-transfer cross sections with experiment (see Figs. 55 and 56) may be somewhat fortuitous.

Recently Onda and Truhlar (1979b) have reported LAB-frame close-coupling calculations of elastic scattering and rotational excitation in electron–CO_2 scattering. They also employ approximate exchange and polarization interactions.

2. Vibrational excitation (CO_2)

The vibrational states of CO_2 are defined by quantization of three normal modes. The corresponding set of quantum numbers ν_1, ν_2, and ν_3 describe quanta of symmetric stretch, bending, and asymmetric stretch, respectively. Of the three, only transitions $\Delta\nu_1$ involving changes in the symmetric-stretch vibration are optically (dipole) forbidden. At low energies (i.e., below the 3.8 eV shape resonance) there has been very little theoretical attention given to vibrational excitation (Itikawa, 1971c). Experimental cross sections extracted from the swarm measurements of Bulos and Phelps (1976) for the bending excitation 000 → 010 and the asymmetric-stretch excitation 000 → 001, and their rough estimate for the symmetric-stretch excitation in 000 → 100, are illustrated in Fig. 61. Also shown for comparison in Fig. 61 are Born(dipole)-approximation results for 000 → 010 and 000 → 001 transitions calculated from Eq. (180) by using dipole matrix elements obtained from the optical transition probabilities given by Penner and Olfe (1968). There is qualitative agreement between Born (dipole) theory and the swarm measurements; however, the shapes of the cross sections near threshold differ significantly. The resonance around 4 eV, of course, does not appear in the Born cross sections. The symmetric-stretch 000 → 100 cross section shown in Fig. 61 was inferred from the measurements of Stamatovic and Schulz (1973) near

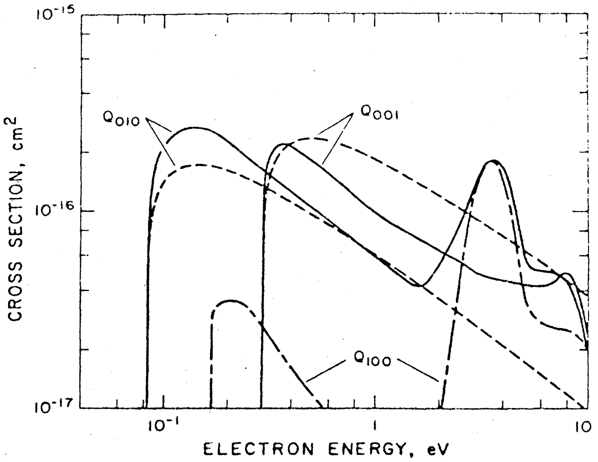

FIG. 61. Cross sections for vibrational excitation of the lowest symmetric-stretch (100), bending (010) and asymmetric-stretch (001) modes in e–CO_2 scattering. Theory: (dashed curves 010 and 001) Born approximation. Experiment: (solid curves 010 and 001) swarm measurements of Bulos and Phelps (1976); (chain curve 100) estimated. (Reprinted from Bulos and Phelps, 1976.)

threshold and Andrick, Danner, and Ehrhardt (1969) at $E \simeq 1$ eV. It exhibits a particularly steep energy dependence above threshold that could be related, via a "final-state" effect, to the large "enhancement" of the elastic-scattering cross section at low energies (Morrison, Lane, and Collins, 1977; and discussion in Sec. III.E.1). However, the true shape of this curve is by no means experimentally determined at the present time and further measurements are called for.

Morrison and Lane (1978) have applied the adiabatic-nuclear-vibration approximation to symmetric-stretch excitation $000 \rightarrow 100$ in e–CO_2 collisions near threshold. The calculations of the fixed-nuclei T matrix for a range of R_{CO} separations were of the same type as Morrison, Lane, and Collins (1977). A very strong resonance is present in the calculated cross section just above threshold. The precise shape of the resonance is not predicted by the theory because of the failure of the adiabatic approximation very near threshold. However, the presence of the resonance is established. It is likely that the responsible mechanism is strong "final-state" scattering, perhaps related to the existence of a virtual state in the e-CO_2 interaction.

At higher energies $E \simeq 4.0$ eV, the symmetric-stretch and bending mode cross sections for transitions $000 \rightarrow 100$ and $000 \rightarrow 010$, respectively, are dominated by a broad shape resonance that peaks at about $E_r \simeq 3.8$ eV. The optically active asymmetric-stretch transition $000 \rightarrow 001$ is observed to be nonresonant and is felt to be dominated by dipole coupling (Andrick, Danner, and Ehrhardt, 1969) as evidenced by strong forward scattering in the angular distribution. The resonance exhibits structure, as illustrated in Fig. 57, for the $000 \rightarrow \nu_1 00$ transitions. The positions of the peaks vary with transition (i.e., with final vibration quantum numbers) just as in the case of the 2.3 eV resonance in electron–N_2 scattering. Thus, the lifetime of the electron–CO_2 resonance, for nuclear geometries near equilibrium, is comparable with the vibrational periods, so that the positions of the peaks and valleys in the structure depend sensitively on the R dependence of the lifetime of the CO_2^- complex (Schulz, 1976). Čadež, Tronc, and Hall (1974) and Boness and Schulz (1974) proposed that the "boomerang effect" (Herzenberg, 1968), occurring in the symmetric-stretch mode, is responsible for the observed structure. In Fig. 62 the observed cross sections for transitions $000 \rightarrow \nu_1 00$, $\nu_1 = 1, 3, 5$, and 7 (Čadež, Gresteau, Tronc, and Hall, 1977) are compared with the results of the semiempirical "boomerang model" (Herzenberg, 1968; Birtwistle and Herzenberg, 1971) normalized by Čadež, Gresteau, Tronc, and Hall (1977) to their own data. The CO_2^- potential curve V^- and width Γ determined in this way are compared with Fig. 63 with the results of other authors (Claydon, Segal, and Taylor, 1970; Krauss and Neumann, 1972; Pacansky, Wahlgren, and Bagus, 1975; also Bardsley, 1969). (The symmetric-stretch coordinate S_1 in Fig. 63 is defined by $S_1 = (\Delta R_1 + \Delta R_2)/\sqrt{2}$.) A similar "boomerang model" calculation was performed by Szmytkowski and Zubek (1977) using the measurements of Boness and Schulz (1974) and Čadež, Tronc, and Hall (1974); their agreement is qualitatively similar to that of Čadež, Gresteau, Tronc, and Hall (1977) shown in Fig. 62 (see also Szmytkowski, Zubek, and Drewko, 1978). Domcke and Cederbaum (1977a, b) have also analyzed the CO_2^- resonance in the 4 eV region by applying a method based on a model Hamiltonian including explicit "bound-continuum" and electronic vibrational coupling via a many-body formulation. By treating the "bound-continuum" coupling as a perturbation and summing the S-matrix diagrams to infinite order, they obtain a simple expression for the differential cross section that requires only the specification of various resonance and coupling parameters which can be determined semiempirically. Their approach also accounts for all of the characteris-

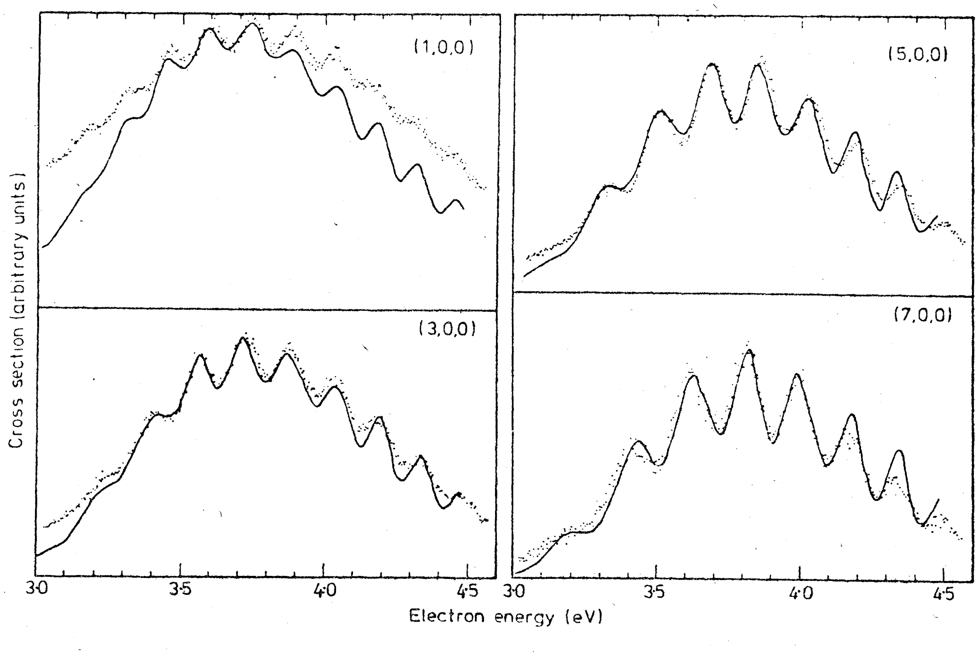

FIG. 62. Differential cross sections at 20° for vibrational excitation of symmetric-stretch transition ($000 \rightarrow v'00$) in e–CO_2 scattering: (points) measurements, (solid curves) "boomerang" model normalized to the data for each transition. (Reprinted from Cadez *et al.*, 1977.)

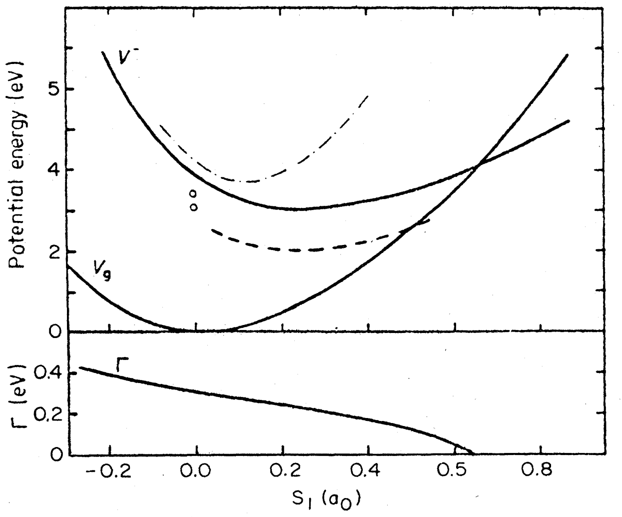

FIG. 63. Potential energy curves for the ground state of CO_2 (V_g) and the Π_u resonance state of $CO_2^-(V^-)$ for linear geometry. S_1 is proportional to the (symmetric) C–O separation. The curve V^- and the width Γ are determined (semiempirically) by the "boomerang" model (as illustrated in Fig. 62). Theoretical results include: (chain curve) Claydon *et al.* (1970); (dashed curve) Pacansky *et al.* (1975); (circles) Krauss and Neumann (1972), upper and lower calculated at 180° and 170° bond angles, respectively. (Reprinted from Cadez *et al.*, 1977.)

tic features of the resonant fine structure. Although consistent with the "boomerang model," the Domcke-Cederbaum approach is a convenient methodology for generalization and systematic improvement of the calculations.

E. Polar molecules

There has been a recent surge of activity in the theory of electron scattering by polar molecules. In part, this renewed interest has been stimulated by possible application to magnetohydrodynamic (MHD) power generation, where the electrical conductivity of the plasma is limited largely by momentum-transfer collisions of the electrons with polar molecules such as KOH, SO_2, and H_2O. Moreover, the first electron-beam measurements, made on CsF (Slater, Fickes, and Stern, 1972), and subsequent studies of CsF (Slater, Fickes, Becker, and Stern, 1974a), CsCl (Becker, Fickes, Slater, and Stern, 1974) and KI (Slater, Fickes, Becker, and Stern, 1974b) suggested that for strongly polar molecules the Born approximation greatly overestimates the differential scattering cross section (except at very small angles) and therefore the momentum-transfer cross section as well. Alternative theoretical approaches were clearly called for, and in response, a number of theoretical studies were carried out, ranging from sophisticated quantum-mechanical model calculations [for example, Itikawa (1978a), Collins and Norcross (1977, 1978) and references therein] to semiclassical treatments (Miller and Smith, 1978; Mukherjee and Smith, 1978; and Hickman and Smith, 1978).

In the vibrational excitation of polar molecules by electron impact, unexpected "threshold resonances" have been observed in recent high-resolution electron-beam experiments. A single narrow resonance has been observed just above each vibrational-excitation threshold in HF, HCl, HBr, and H_2O (Rohr and Linder, 1975, 1976; Seng and Linder, 1976; Rohr, 1977a, c, 1978; and Linder, 1977) and in the nonpolar case SF_6 (Rohr 1977b, 1979). The "threshold resonances" have been ascribed to strong final-state scattering, perhaps related to the existence of a "virtual state" in the electron–molecule system (Dubé and Herzenberg, 1977; Gianturco and Rahman, 1977a, b; and Taylor, Goldstein, and Segal, 1977). The precise nature of this resonance phenomenon still is not firmly established.

The early work on elastic and rotational-excitation electron–polar-molecule scattering has been summarized by Garrett (1972). A recent review by Itikawa (1978a) also emphasizes elastic scattering and rotational excitation at low energies ($E \lesssim 10$ eV), and provides an important update of the state of the theory. (See also Takayanagi, 1975a, b.)

1. Elastic scattering and rotational excitation

a. *The dipole interaction and "critical binding"*

Massey (1931) was the first to point out that because of the long-range nature of the electron–dipole interaction, the rotational-excitation and deexcitation cross sections for $\Delta j = \pm 1$ transitions in polar molecules are likely to be much larger than the elastic cross sections. He also showed that the Born approximation gives the correct $\Delta j = \pm 1$ cross section so long as the dipole moment is not too large.

Based partly on these findings, Altshuler (1957) argued that rotational excitation may be a large component in the momentum-transfer cross section so that the Born approximation could also be applied here. Using the adiabatic nuclear rotation approximation (see Sec. II.D) to describe rotational transitions and the Born approximation applied to the point-dipole interaction, Altshuler (1957) computed the momentum-transfer cross section for a range of dipole moments and energies (see also Maru and Desai, 1975). He obtained encouraging agreement with early measurements. However, subsequent experimental measurements began to uncover discrepancies, for example, in H_2O, D_2O, and H_2S, where measured momentum-transfer cross sections were found to be larger by a factor of 2 than the values predicted by Altshuler's theory (Hurst, Stockdale, and O'Kelley, 1963). This led Hurst *et al.* (1963) to speculate that in electron–polar-molecule scattering the electron might be temporarily captured by "virtually exciting" a rotational state, thus forming a "rotational resonance" complex that would subsequently decay with a characteristic lifetime. Turner (1966), using a "capture" theory of Bloch and Bradbury (1935), and keeping only the point-dipole electron–molecule interaction, showed that the rotational-resonance concept was viable (see also Garrett, 1975). Turner and Fox (1966), in their variational treatment of the minimum dipole moment, d_c, required to bind an electron to a *finite* dipole, concluded that the H_2O and D_2O data could be understood in terms of a rotational resonance, but that the H_2S dipole moment is simply too small to allow temporary binding [see Turner (1977) for an interesting history of the subject of "critical dipole moment"]. Since these early studies treated the conditions for binding in the framework of the fixed dipole, the results and interpretations are somewhat ambiguous (see also Shimizu, 1963; Mittleman and Von Holdt, 1965; Mittleman and Myerscough, 1966; Brown and Roberts, 1967; Crawford, 1967; Crawford and Dalgarno, 1967; Coulson and Walmsey, 1967; Fox, 1968; Levy-Leblond, 1967; and Levy-Leblond and Provost, 1967). Garrett (1971a, b, c, 1972, 1975) has shown that the critical dipole moment for binding of an electron to a *rotating* polar molecule is in general larger than d_c and depends on the charge separation of the finite dipole (or in general on short-range forces) and on the total angular momentum J (electron plus molecule) of the system (Itikawa, 1977). Garrett shows that the *fixed* finite-dipole results are obtained in the limit $I \rightarrow \infty$, where I is the moment of inertia of the molecule (also see Bottcher, 1971), and that the integral cross section diverges in this limit for any choice of the short-range interaction (Garrett, 1971c).

Takayanagi (1966) derived expressions for the rotational and vibrational excitation cross sections in the Born-dipole approximation and discussed validity conditions. It is not possible to establish firm criteria since short-range interactions can change the picture considerably, and in the case of a shape resonance can dominate the cross section over a wide range of energies (Schulz, 1973, 1976). A few general observations put forth by Takayanagi (1966) are as follows: (i) the weak coupling (i.e., first-order perturbation) approximation is likely to fail for dipole moments d such that $d \gtrsim 1(ea_0)$; (ii) distortion of the p-wave scattering orbital due to the polarization is likely to be important, say for $E \gtrsim 1$ eV, for (average) polarizabilities $\alpha_0 \gtrsim 20\ a_0^3$; (iii) once the polarization interaction becomes important, the electron will be "pulled" in, and the complicated short-range interactions will start to play a role; and (iv) in molecules with small (equilibrium) dipole moments, e.g., CO [$d = 0.044 ea_0$; Burrus (1958)] the quadrupole and anisotropic polarization interaction may dominate the coupling with the result that $\Delta j = \pm 2$ transitions may be favored over those with $\Delta j = \pm 1$. Takayanagi (1966) emphasizes that even when a few partial-wave contributions to the cross section are determined poorly by the Born-dipole approximation (e.g., due to α_0 being large) the total rotational-excitation cross section may still be good, simply because a large number of partial waves contribute. Recently, Clark (1977) has discussed the limitations of the Born approximation and its use in connection with frame-transformation theory (Chang and Fano, 1972; see Sec. II.E).

Crawford, Dalgarno, and Hays (1967) reexamined the experimental swarm data of Christophorou, Hurst, and Hadjiantoniou (1966) and made a convincing case that the Born fixed-dipole approximation to $\sigma^{(m)}$, originally given by Altshuler (1957), is superior to the exact (fixed-dipole) result (Mittleman and von Holdt, 1965) for all values of d. Recall that for small values $d \ll 0.5 ea_0$ the exact (fixed-dipole) and Born (fixed-dipole) cross sections are the same, but for $d > 0.5 ea_0$ the exact (fixed-dipole) cross section becomes much larger than Born, and at $d = d_c \simeq 0.64 ea_0$ the exact (fixed-dipole) $\sigma^{(m)}$ becomes infinite. This nonphysical divergence arises from the collapse of an infinite number of bound states "down the r^{-2} well," a reflection of the degeneracy of rotational energy levels in the $I \rightarrow \infty$ limit. (See discussion of Mittleman, Peacher, and Rozsnyai, 1968.) Crawford, Dalgarno, and Hayes (1967) argue that the Born fixed-dipole approximation is superior because it does not possess this mathematical anomaly. They do point out that the approximation will fail for sufficiently large values of d, since it is a weak-coupling (i.e., first-order perturbation) method. These authors conclude that aside from narrow rotational resonances which may occur in some cases [see Garrett (1975), and Fabrikant (1978)], discrepancies between the Born fixed-dipole approximation and experiment should be mainly due to the neglect of other interaction terms. They do not support the speculation (Levy-Leblond, 1967; Takayanagi and Itikawa, 1968) that a *physical* critical value of the dipole moment d_c exists such that momentum-transfer cross sections for molecules with $d = d_c$ are very different from those with values of d slightly less or slightly greater than d_c (see Garrett, 1972). Dalgarno, Caawford, and Allison (1968) examined this question of the existence of a "critical dipole moment" for electron scattering from a polar molecule by carrying out a model close-coupling calculation. The molecule was represented by a rigid rotator with rotational constant $B = 2.4 \times 10^{-4}$ eV, and the e–molecule interaction was modeled by a dipole term cut off at small r. The partial cross sections $\sigma_J(0 \rightarrow j')$ for $j' = 0$, 1, 2, and 3 were evaluated for total angular momentum $J = 0$, 1, and 2 and incident energy $E = 0.05$ eV. None of these cross sections exhibited any unusual behavior as the dipole moment was varied from 1.60 $\times 10^{-18}$ to 1.65×10^{-18} esu cm. Thus, it was demonstrated that the value $d_c = 1.625 \times 10^{-18}$ esu cm ($0.64 ea_0$) that corresponds to divergence of $\sigma^{(m)}$ for the fixed point dipole is of no special significance for the rotating dipole. Closed channels were not included in this calculation so it was not possible to search for rotational resonances that may have been present for this model system. Crawford (1968), using a similar model-interaction close-coupling procedure, calculated momentum-transfer cross sections for electron–H_2O scattering and obtained apparent improvement over the Born results. Itikawa (1971a, b, 1972), in similar Born-approximation studies of electron scattering by H_2O, NH_3, and H_2CO, emphasized that polarization effects can be important to the integral rotational-excitation cross sections, at least for transitions that are not dipole coupled.

Itikawa and Takayanagi (1969a) carried out a model close-coupling study of elastic and rotational-excitation cross sections for electron scattering from HCl and CN, the latter being of astrophysical interest. They employed the coupled-angular-momentum representation. Only the rotational states $j = 0$, 1, and 2 were included in the close-coupling calculation, and closed channels were apparently ignored. Born-approximation results were also calculated for comparison. The electron–molecule interaction was approximated by a model potential energy function expressed as a *truncated* series in Legendre polynomials in the form of Eq. (118), but keeping only the $\lambda = 0$ and 1 terms. The coefficient functions were approximated by employing a model of overlapping atomic charge distributions with allowance for the long-range dipole and polarization interactions. While the model interaction was not expected to yield accurate cross sections, some conclusions were possible: (1) the Born approximation works well for $\Delta j=\pm 1$ transitions because of the importance of large $-l$ contributions, and (2) the calculated cross sections for $\Delta j=0, \pm 2$ are much more sensitive to short-range interactions, while those for $\Delta j=\pm 1$ are dominated by the dipole term. The authors, working in the coupled-angular-momentum representation, noted that the Born results were accurate for partial cross sections corresponding to large total angular momentum J (more precisely large $|J-j|$ for the rotational states of interest) so that the close-coupling calculations need be performed only for a few values of J.

Itikawa (1969) calculated differential $j=0\rightarrow 1$ and $j=0\rightarrow 0$ cross sections for CN and HCl using the results of the close-coupling calculations of Itikawa and Takayanagi (1969a). He found that: (i) the $j=0\rightarrow 1$ scattering is strongly peaked in the forward direction due to the long-range r^{-2} dipole interaction; (ii) the Born approximation agrees well for $j=0\rightarrow 1$ with the CC results in the forward direction; (iii) many partial-wave contributions (i.e., many total angular momenta J) are necessary to describe the $j=0\rightarrow 1$ forward scattering accurately; and (iv) the *unitarized* Born approximation (usually labeled BII) can be used for "large-J" contributions to $\sigma(0\rightarrow 0)$ and the corresponding differential cross section. Extending these model calculations to a number of dipole moments on either side of the "critical" value, Itikawa (1969) noted that for an energy $E=0.03$ eV, the elastic contribution to the momentum-transfer cross section σ_m exhibited an enhancement causing a peak in σ_m (as a function of d) at about $d=1.1ea_0$, similar to that seen by Itikawa and Takayanagi (1969a) in the total integral cross section. This seemed to provide support for an observable effect of the "critical dipole moment."

However, Garrett (1972) showed that if one considers reasonable models for the short-range and polarization interactions, the "hump" in $\sigma^{(m)}$ versus d moves around depending on the details in the interaction. Moreover, the "hump" is sensitive to energy and the rotational state of the target molecule. [The latter observation contradicted the earlier assertion of Bottcher (1970), that "critical binding" is unaffected by molecular rotation.] Thus, in going from one molecule to another, the effect would be expected to wash out and no *physical* "critical" dipole moment would seem to exist. There is, however, some tendency for the measured $\sigma^{(m)}$ to exceed Born for small d and fall below Born for large d (Garrett, 1972). The latter is clearly due to unitarity violations in the Born approximation when the coupling is strong. For small values of d, σ_m is no longer dominated by rotational excitation and the dipole interaction, elastic scattering becomes important, and short-range interactions such as exchange play an important role (Takayanagi, 1975a, b).

Itikawa and Ashihara (1971) examined the effects of electron exchange on elastic and rotational-excitation e–HCl scattering by carrying out a model close-coupling calculation similar to that of Itikawa and Takayanagi (1969a) but with the exchange terms of Eqs. (116) and (119) included, but approximated by employing a very simple molecular wave function. They found that exchange effects were important for s and p partial waves, for integral $\Delta j=0$ (elastic) cross sections, and for the $j=0\rightarrow 1$ differential cross sections at large scattering angles, i.e., $\theta\geq 60°$. The integral $j=0\rightarrow 1$ cross section was found to be completely insensitive to exchange.

Crawford and Dalgarno (1971), in a model close-coupling treatment of electron–CO scattering, showed that because CO has such a small dipole moment ($d^{\mathrm{CO}}=0.044ea_0=0.112\times 10^{-18}$ esu cm), many aspects of the scattering are similar to the isoelectronic molecule N_2, in essential agreement with previous suggestions (Hake and Phelps, 1967). A model electron–CO interaction potential, including the long-range dipole and polarization interactions and an isotropic short-range contribution, was chosen by forcing agreement of the momentum-transfer cross section σ_m at a single energy $E=0.03$ eV with the measured value of Hake and Phelps (1967). The calculated σ_m were then found to reproduce the energy dependence of the measurements over the range $0.005\lesssim E\lesssim 0.10$ eV. Calculated $j=0\rightarrow 1$ differential cross sections were peaked in the forward direction as expected. However, the differential $j=0\rightarrow 2$ cross sections were found to be dominated by the electron–quadrupole interaction and were nearly isotropic at low energies, as occurs in electron–N_2 scattering. The integral $j=0\rightarrow 0$ (elastic) cross section was found to be rather insensitive to the presence of the dipole interaction. Ray and Barua (1974), applying the Born approximation to electron–CO and –NO scattering, showed that anisotropic short-range interactions make small, but nonnegligible, contributions to the rotational excitation cross sections for energies $E\lesssim 0.1$ eV. (See also Maru and Desai, 1975, 1976.)

The first attempt to include the full (anisotropic) static-exchange-polarization interaction in a multichannel calculation of elastic and rotational-excitation cross sections for electron scattering by a polar molecule is the application to CO by Chandra (1975b). Previous close-coupling calculations (e.g., Crawford and Dalgarno, 1971) were based on model interaction potentials that were correct asymptotically, but unrealistic near the molecule. Thus, one would not expect the model to reproduce the shape resonance in CO at $E\simeq 2$ eV, since the position and width of such a resonance is sensitive to short-range interaction, as we have seen in the discussion of electron–N_2 scattering (see Sec. III.C). In his fixed-nuclei calculation (with $R_{\mathrm{CO}}=2.132a_0$), Chandra (1975b) employed the "modified pseudopotential method" of Burke and Chandra (1972) in which exchange is approximated by explicitly forcing orthogonality of the scattering orbital to each occupied ground-state orbital of the same symmetry (see Secs. II.G.4 and III.C.1). The ground-state single-configuration representation of CO is $(1\sigma^2 2\sigma^2 3\sigma^2 4\sigma^2 1\pi^4)^1\Sigma$. Polarization was treated semiempirically by "tuning" the $^2\Pi$ resonance to $E=1.75$ eV, thereby fixing the polarization cutoff radius in Eq. (147) at $r_p=1.605a_0$. The polarizabilities of CO were chosen as $\alpha_0=13.3a_0^3$ and $\alpha_2=2.4a_0^3$ (Takayanagi and Itikawa, 1970b). The coefficients in the single-center expansion of the static potential given in Eq. (118) were calculated using the approach of Faisal (1970) and Faisal and Tench (1971), but correcting an error in their formulas and computer code. [The error occurred only for heteronuclear molecules. Unfortunately, the earlier application to electron–CO scattering by Burke, Chandra, and Gianturco (1972) was invalidated by this error in the static potential given by Gianturco and Tait (1972).] Terms up to $\lambda_{\max} = 24$ were retained in Eq. (118) and 15 partial waves were included in the expansion (115) for symmetries Σ, Π, and Δ. The momentum-transfer cross section was calculated for energies $0.1 \leq E \leq 10.0$ eV. Although the integral cross section diverges for a polar molecule in the fixed-nuclei approximation, the momentum-transfer cross section is finite. Agreement with the experimental momentum-transfer cross section of Hake and Phelps (1967) is fair, the calculated cross sections lying above the measured values by 20%–40%.

Chandra (1977) extended his earlier study of electron–CO scattering to take proper account of molecular rotation by incorporating a frame transformation applied to the R matrix at a suitable boundary (Chang and Fano, 1972). A description of the general procedure was given by Chandra and Gianturco (1974); however, the calculations given there were contaminated by the error in the static potential described above. Referring to Fig. 4 and the discussion in Sec. II.E.2, the inner region $r \leq a_F$ is treated by applying the "modified pseudopotential method," with a semiempirical polarization potential essentially as described by Chandra (1975b), in the fixed-nuclei approximation. The radial coupled equations are solved in the BODY frame and the R matrix constructed at $r = a_F$ from the radial functions and their first derivatives, according to Eq. (84). The frame transformation (85) for fixed internuclear separation is then performed and the LAB-frame radial functions are integrated into the asymptotic region. Exchange is ignored in the outer region $r > a_F$, and the static and polarization potentials are replaced by their asymptotic forms, scaled so as to be consistent with a dipole moment $d = 0.044ea_0$. The transformation radius $a_F = 11.774a_0$ was chosen by examining the sensitivity of the calculated cross sections to a_F and selecting a value in the "stabilized" region, roughly $10a_0 \lesssim a_F \lesssim 15a_0$, where the cross sections are least sensitive to the choice of a_F. Chandra reports elastic, rotational-excitation, and momentum-transfer cross sections for energies $E \leq 10$ eV. His calculated momentum-transfer cross sections for electron–CO scattering are compared in Fig. 64 with the experimental result of Hake and Phelps (1967) and the model calculations of Crawford and Dalgarno (1971). The agreement with experiment is similar to that obtained for electron–N_2 scattering (Burke and Chandra, 1972). We would expect the resonance to be broadened and reduced in magnitude by vibrational effects not included in this calculation. At lower energies $E \lesssim 1$ eV, the calculated cross section appears to be too large, probably reflecting the inadequacy of the approximate treatment of exchange and polarization.

Levin, Fliflet, and McKoy (1979) have applied the "T-matrix Expansion" method (see Sec. II.F.2) to electron–CO scattering in the static-exchange approximation. The procedure and results parallel the earlier electron–N_2 study of Fliflet, Levin, Ma, and McKoy (1978).

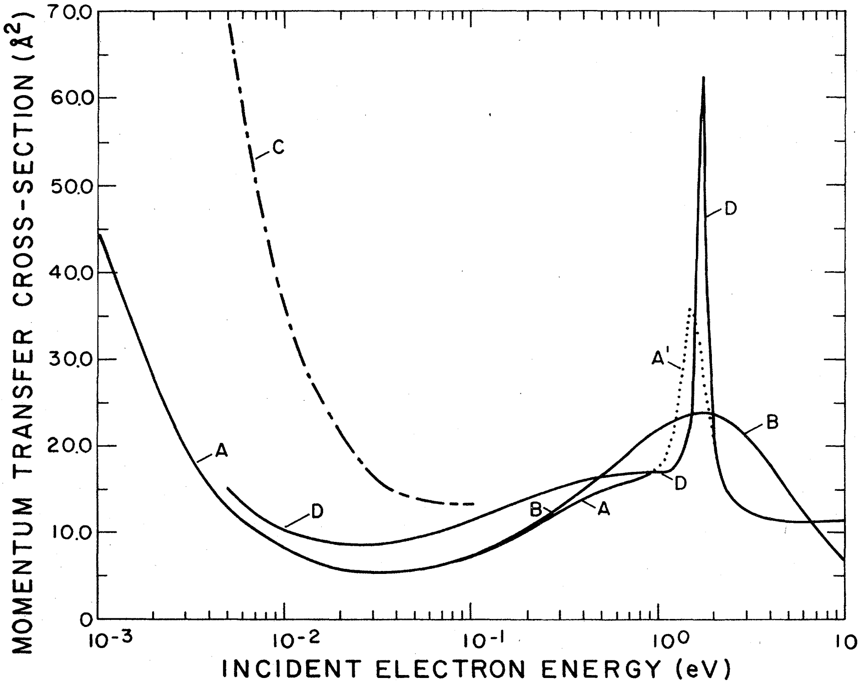

FIG. 64. Momentum-transfer cross sections for e–CO scattering. Theory: (curve B) rotational close coupling with the Crawford–Dalgarno model potential; (curves C and D) pseudopotential method by frame-transformation theory for two choices of the long-range dipole interaction. Experiment: (curve A) Hake and Phelps (1967); (curve A′) extrapolated from A. (Reprinted from Chandra, 1977.)

b. Strongly polar molecules

The electron beam measurements of Slater, Fickes, and Stern (1972); Slater, Fickes, Becker, and Stern (1974a,b); Becker, Fickes, Slater, and Stern (1974); and Stern and Becker (1975) generated a significant amount of interest and activity in the theory of electron scattering from molecules having large dipole moments ($d \gtrsim 1.5ea_0$). This work is described in some detail by Itikawa (1978a) and Collins and Norcross (1978). Only a very brief discussion will be given here. Several important fundamental questions have been raised and partially resolved by these efforts.

Rudge (1974), using a simple model "hard sphere plus dipole" interaction potential and a weak scattering approximation, calculated differential rotational-excitation cross sections for electron scattering from CsF($d = 3.10ea_0$), CsCl($d = 4.15ea_0$), and KI($d = 4.25ea_0$) at energies $0.5 \leq E \leq 10.0$ eV. The calculated cross sections are roughly an order of magnitude smaller than Born results, in qualitative agreement with the measurements; they exhibit oscillatory dependence on the scattering angle.

Allison (1975) in an ambitious model rotational-close-coupling calculation of electron–CsF scattering, adopted a "cutoff dipole" form for the interaction potential. The LAB-frame coupled equations (Arthurs and Dalgarno, 1960) were solved numerically, and differential $j = 41 \rightarrow 42$ rotational-excitation cross sections were calculated at energies $E = 1.0$ and 2.0 eV. The calculated cross sections are well below the Born results and show some structure above a scattering angle of $\theta \simeq 60°$. The calculated momentum-transfer cross section was found to be about one-third of the Born value.

Takayanagi (1974) and Ashihara, Shimamura, and Takayanagi (1975) pointed out that the Glauber approximation (Glauber, 1959) should offer improvement over the Born approximation since it does take some account of higher-order corrections. Moreover, the dipole interaction is favorable in that the major contributions to the cross sections come from distant encounters. Indeed, in the point-dipole approximation, the calculated differential cross sections for $j = 0 \rightarrow j'(j' \leq 3)$ in electron–CsCl scattering were found to be an order of magnitude smaller than the Born results. Structure was observed in the differential $j = 0 \rightarrow 1$ rotational-excitation cross section. The calculated momentum-transfer cross section σ_m was found to be about an order of magnitude smaller than the Born result for $E \leq 5$ eV and to vary as $1/E$ (true of the Born approximation as well) in qualitative agreement with the beam measurements. Detailed results and discussion of these calculations are given by Ashihara, Shimamura, and Takayanagi (1975). Calculated integral total and momentum-transfer cross sections for electron–CsCl scattering are compared with the measurements (Becker *et al.*, 1974) in Figs. 65(a) and 65(b). The authors emphasize that the validity of the Glauber approximation applied at such low energies is still questionable, in that it incorporates both the adiabatic nuclear rotation approximation (see Sec. II.D) and the use of the Glauber amplitude as an approximation to the $\hat{R}$-dependent elastic scattering amplitude. The latter is usually considered to be a reasonable high-energy approximation.

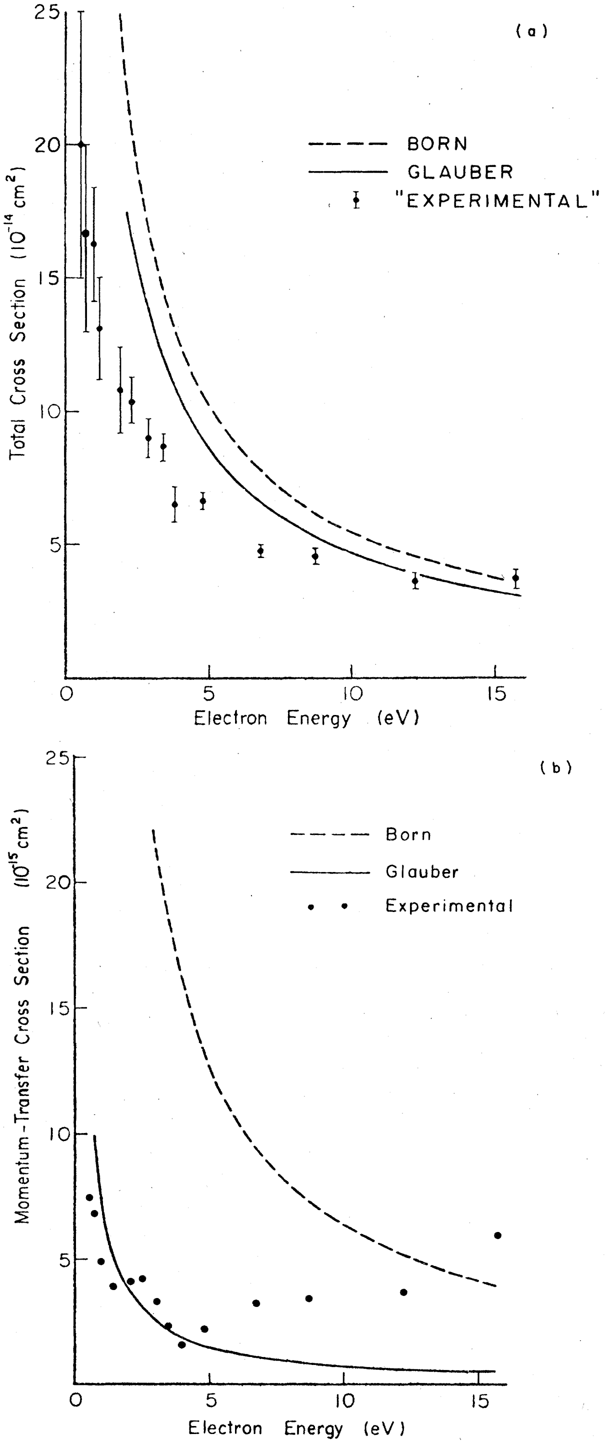

FIG. 65. Cross sections for e–CsCl scattering (a) total cross section (b) momentum-transfer cross section. Theory: (solid curves) Glauber approximation; (dashed curves) first Born approximation. Experiment: (closed circles) Becker *et al.* (1974). (Reprinted from Ashihara *et al.*, 1975.)

Onda (1976), still working within the framework of the adiabatic nuclear rotation approximation, showed that the Glauber amplitude works surprisingly well, at least for the differential cross sections at scattering angles $\theta \lesssim 50°$. A model "hard sphere plus dipole" potential was assumed for this study.

Itikawa (1976), in an effort to test further the accuracy of the Glauber and adiabatic nuclear rotation approximations, performed rotational-close-coupling calculations of $j=0 \to j'$ cross sections for electron–CsF scattering at energies $E \leqslant 5$ eV. The approach is very close to that of Itikawa and Takayanagi (1969a) and Itikawa (1969). The electron–CsF interaction was represented by cutoff dipole and quadrupole potentials [with $d=3.1ea_0$ and $q=-13.4ea_0^2$ (Stogryn and Stogryn, 1966)]. Generally, the Glauber and adiabatic nuclear rotation differential cross sections were found to agree well with the close-coupling results for angles $\theta \lesssim 60°$. At larger angles, the cross sections tend to be sensitive to the short-range interaction which was different in each of the three studies. Only qualitative agreement was found between the calculated differential and integral cross sections and the measurements (Slater *et al.*, 1974a; and Stern and Becker, 1975).

Itikawa (1977) extended this model close-coupling study to a range of dipole moments $d \lesssim 4.0ea_0$ in order to illustrate the variation of the integral elastic, rotational-excitation, and momentum-transfer cross sections with respect to d at energies $E=0.03$ and 1.0 eV. The most notable features of this study, also observed in the earlier work of Garrett (1972), are the strong saturation of the momentum-transfer cross sections for $d \gtrsim 1ea_0$, followed by an oscillation with respect to increasing d [see also Itikawa and Takayanagi (1969a) and Itikawa (1969)]. The detailed behavior is expected to be sensitive to short-range interactions, and therefore will not be accurately represented in such a model.

Gianturco and Rahman (1977b) have examined the possible occurrence of Wigner cusps in the electron–HF elastic and rotational-excitation cross sections at rotational thresholds. Ignoring exchange effects, the authors solved the LAB-frame coupled equations including some closed as well as open rotational channels. The expected cusps appeared at the opening of each new rotational channel.

Dickinson and Richards (1975) and Dickinson (1977) have constructed a particularly simple model to describe electron scattering from polar molecules. Recognizing the dominance of long-range scattering, they apply time-dependent perturbation theory to the scattering at large impact parameters [see Seaton (1962), and Seraph (1964)] and impose constraints on the small-impact parameter scattering to preserve unitarity. Combining the Born approximation with time-dependent perturbation theory, and using a hard-sphere short-range interaction to approximate the large-angle (small-impact) scattering, Dickinson (1977) calculates total integral cross sections for electron–CsF in excellent agreement with model close-coupling calculations. For electron–KI scattering, the calculated momentum-transfer cross section is qualitatively similar to that observed by Rudge, Trajmar, and Williams (1976).

A general semiclassical perturbation theory (SPS), applicable to a broad class of collision problems, is described by Miller and Smith (1978). Mukherjee and Smith (1978) describe in detail the application of this method to elastic scattering and rotational excitation in collisions of electrons with polar molecules. It is argued that the important assumptions of the theory, viz., the validity of first-order perturbation theory and a semiclassical approximation to the S matrix, are justified by the long-range nature of the dipole interaction and the large rotational quantum numbers that are usually important. The calculated (SPS) $\Delta j=\pm 1$ rotational-excitation and total integral cross sections are smaller than the Born results for molecules such as CsF and KI, where the Born approximation fails due to violation of unitarity. For small dipole moments, the SPS theory appropriately reduces to the Born approximation. Hickman and Smith (1978) extend the SPS theory to calculation of the momentum-transfer cross section. Since the momentum-transfer cross section emphasizes large-angle scattering, the validity of the basic assumptions of SPS theory is less clear. Nevertheless, the SPS cross sections do appear to be superior to the Born results for strongly polar molecules.

Rudge (1978b, c) has extended his earlier model calculations (Rudge, 1974) by incorporating a close-coupling solution of the coupled equations. The model electron–molecule interaction potential consists of a spherical *repulsive* core ("hard sphere") potential joined to a dipole potential at the hard-sphere radius $r_0=0.43d$ (where d = dipole moment), which was found to yield the observed electron affinity for LiF (Rudge, 1978a). Rudge finds that the calculated momentum-transfer cross sections for a range of dipole moments $2.0 \leqq d \leqq 4.5ea_0$ and energies $0.5 \leqslant E \leqslant 8.0$ eV vary between 45% and 20% of the Born-point-dipole results, the difference being greatest for large d and high energy. However, in comparing his results with other theoretical studies, Rudge concludes that a wide discrepancy exists between different theories and between experiment and theory.

The first effort to realistically account for short-range interactions and their importance in the determination of the momentum-transfer cross section was the theoretical study of electron–LiF scattering by Collins and Norcross (1977). An ambitious extension of this study to CsF, KI, LiF, NaF, and NaCl was also made by Collins and Norcross (1978). The electron-molecule interaction is represented by a "local-exchange" approximation (Hara, 1967; see Sec. II.G.2) to the full static-exchange interaction. (In the case of LiF, calculations were also performed using a model polarization potential.) The strong electron–nuclei attractive interactions, screened by the bound electrons, are therefore included along with the strong long-range dipole interaction that dominates at large electron–molecule separations. Several model interaction potentials used by other investigators also were studied for comparison. As an alternative to the frame transformation, the authors note that the rotational-impulse approximation is valid for "low-l" partial waves (hence, small total angular momentum J), in which case the ordinary fixed-nuclei, BODY-frame calculation is appropriate, even for strongly polar targets. [The authors refer to the adiabatic nuclear rotation approximation as the "adiabatic rotating molecule" (ARM) approximation.] For the "larger-l" partial waves, full LAB-frame (rotating-nuclei) close-coupling caclulations are performed. Since the radial functions corresponding to large l do not "penetrate" the short-range region, only the long-range interaction need be included in the LAB-frame calculation. For sufficiently large l, the partial-wave Born approximation is valid, and this combined with the full Born cross section [cf. Eqs. (169) and (172)] permits summation over $l \to \infty$ (see Crawford and Dalgarno, 1971). This approach was tested for the static approximation to electron–LiF scattering by performing fully converged calculations in the LAB frame for all partial waves. The coupled radial equations in both the BODY- and LAB-frame treatments were solved using the Green function approach (Sams and Kouri, 1969a, b) with stabilization (White and Hayes, 1972). A thorough discussion of the numerical procedure, convergence studies, and error limits is given by the authors. In most cases, it was necessary in the close-coupling calculations to consider partial waves $l \leq 26$ and $m_l \leq 2$. Detailed comparisons are made of partial, differential, integral, and momentum-transfer cross sections for elastic scattering and rotational excitation with the results of other theoretical studies and existing experimental measurements. A number of general conclusions appear to be well established for electron scattering from strongly polar molecules: (1) The adiabatic nuclear rotation approximation, applied as described by the authors, is valid, and the various cross sections summed over final rotational state are essentially independent to the initial value of j. (2) The total integral cross section is determined almost entirely by small-angle scattering, and hence by the dipole interaction. (3) The Born approximation to the differential cross section is valid for scattering angles $\theta \lesssim 15°$. (4) The large-angle differential cross section and the momentum-transfer cross section are very model dependent, sensitive to short-range interactions including exchange, and poorly determined by the Born and distorted-wave approximations. (5) The classical approximation of Hickman and Smith (1978) and the semiclassical approximation of Dickinson (1977) appear to bracket the momentum-transfer cross section, above and below, respectively (see Fig. 66). (6) The unitarized Born II and Born III approximations to the momentum-transfer cross section also appear to provide simple lower and upper limits, respectively (see Fig. 66). Certain of these conclusions, in particular

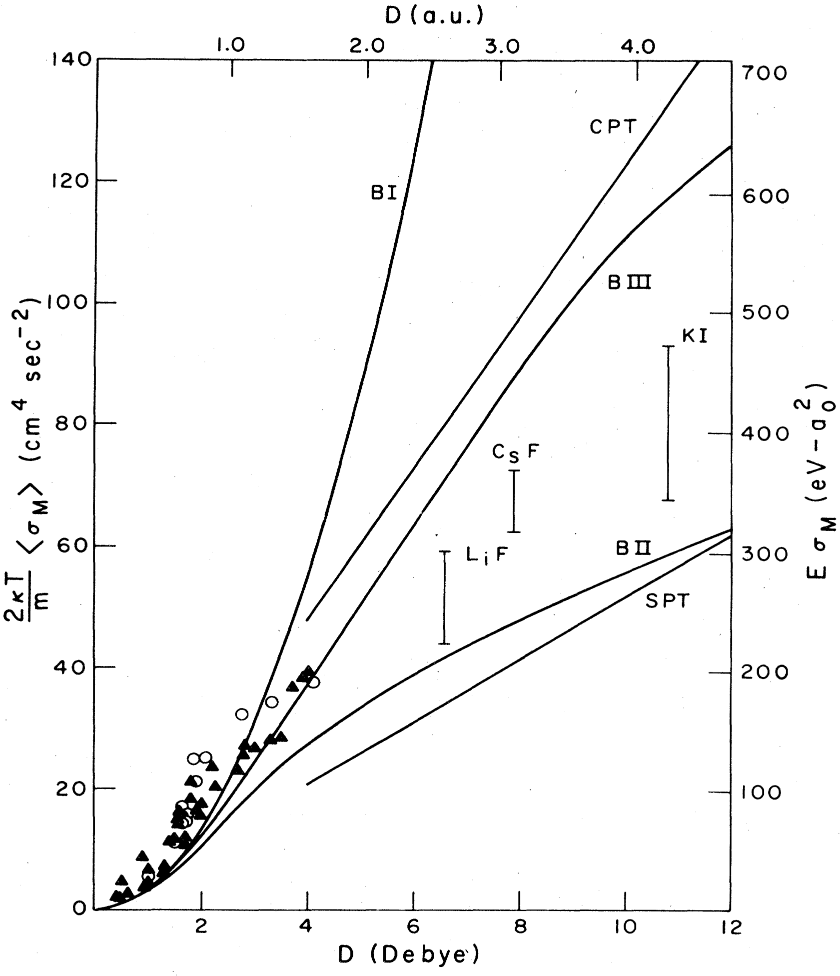

FIG. 66. Momentum-transfer cross sections at thermal energy as a function of dipole moment. Theory: (curves BI, II, III) Born and two versions of the unitarized Born approximation; (curve CPT) classical theory, Dickinson (1977); (SPT) semiclassical theory, Hickman and Smith (1978); (vertical bar for LiF, CsF, and KI) theoretical analysis of Collins and Norcross. Experiment: (△) Christophorou *et al.* (1967), Christophorou and Christodoulides (1969); (○) reanalysis of swarm data of Christophorou and Pittman (1970) by Fabrikant (1977). (Reprinted from Collins and Norcross, 1978.)

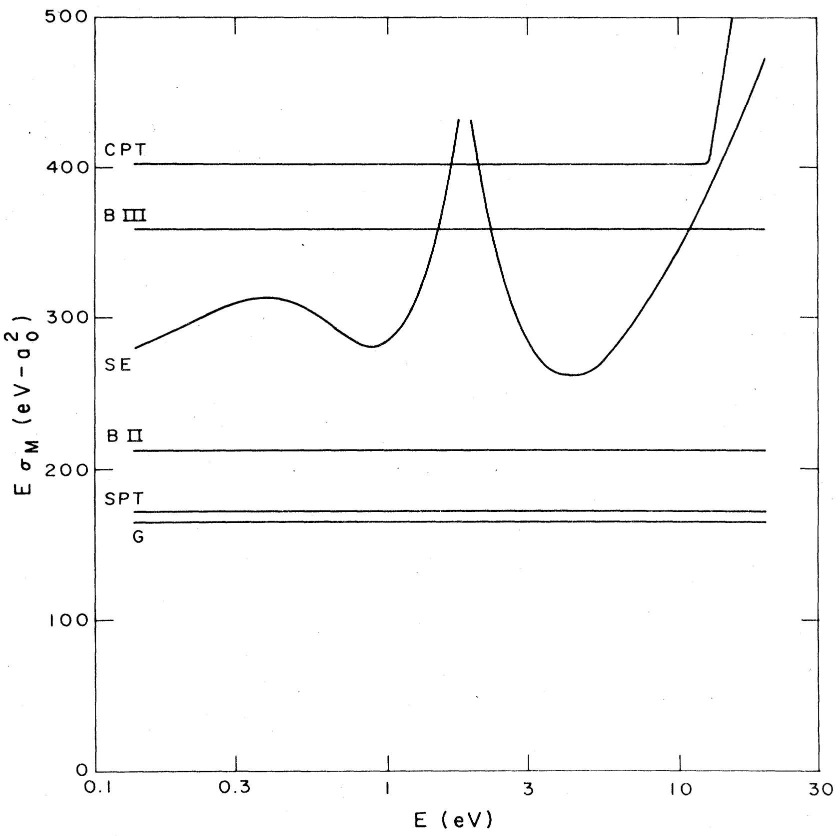

FIG. 67. Theoretical momentum-transfer cross sections for e–LiF scattering (curves BI, II, III, CPT, SPT) as in Fig. 66; (curve G) Glauber approximation, Shimamura (unpublished); (curve SE) static exchange, Collins and Norcross (1978). (Reprinted from Collins and Norcross, 1978.)

(2) and (3), were arrived at earlier by a number of investigators; they are included in the present discussion for completeness. One striking feature of the electron-LiF scattering cross sections is the occurrence of a shape resonance at $E \cong 2$ eV in both Σ and Π symmetries. The resonance was not found in the static approximation, where exchange is ignored completely, or with any of the dipole cutoff model potentials studied. In Fig. 67, the product $E\sigma_m$ is illustrated for various theoretical approximations. The Glauber (Shimamura 1977c) and semiclassical-perturbation (Hickman and Smith 1978) cross sections are considered to be too small due to the neglect of short-range interactions and the consequent underestimate of large-angle scattering. Collins and Norcross (1978) find similar resonances in NaF and NaCl, but not LiCl. Stabilization LiF$^-$ structure calculations of Jordan and Luken (1976) and Stevens (1977) suggest that the resonances in electron–LiF scattering are real. However, a recent study of electron–LiH and –LiF scattering by Collins, Robb, and Norcross (1979) casts serious doubt on the existence of these resonances. In this study both exact static-exchange (ESE) and approximate "orthogonalized static model exchange" (OSME) calculations were carried out and compared with one another and with other approximations. In the OSME approach, the "local-exchange" [the version of Hara (1967)] was employed; however, in addition, the continuum radial function was constrained to be orthogonal to the occupied core orbitals. The effect of this orthogonalization constraint was to remove the resonances in both the Σ and Π symmetries for electron–LiF scattering. Moreover, the OSME and the exact static-exchange calculations are in good agreement for both LiH and LiF. The other conclusions in the paper of Collins and Norcross (1977) remain unaffected by the results of the more recent study.

The calculated differential total (elastic plus rotational-excitation) cross sections at $E = 5.44$ eV are compared in Fig. 68 with the relative experimental cross section of Vušković, Srivastava, and Trajmar (1978) and with the results of the "dipole cutoff" model (DCO) and the Born approximation (BI); the experimental data are normalized to the static-exchange (SE) curve at $\theta = 40°$. Somewhat better agreement is obtained at $E = 20$ eV (not shown). The classical (Mukherjee and Smith, 1978) and Glauber (Shimamura, 1977c) differential cross sections (not shown) appear to be good for $\theta \lesssim 45°$.

Collins and Norcross (1978) performed several model close-coupling calculations of differential electron–KI scattering cross sections, comparing Born I and Born II with the results of different "dipole cutoff" potentials. They conclude that the experimental relative cross sections of Rudge, Trajmar, and Williams (1976), previously normalized to the distorted-wave calculation at $\theta = 15°$, should be renormalized downward. They argue that the good agreement with the Born I approximation implied by the original normalization is unrealistic, based on their other comparisons. In Fig. 69,

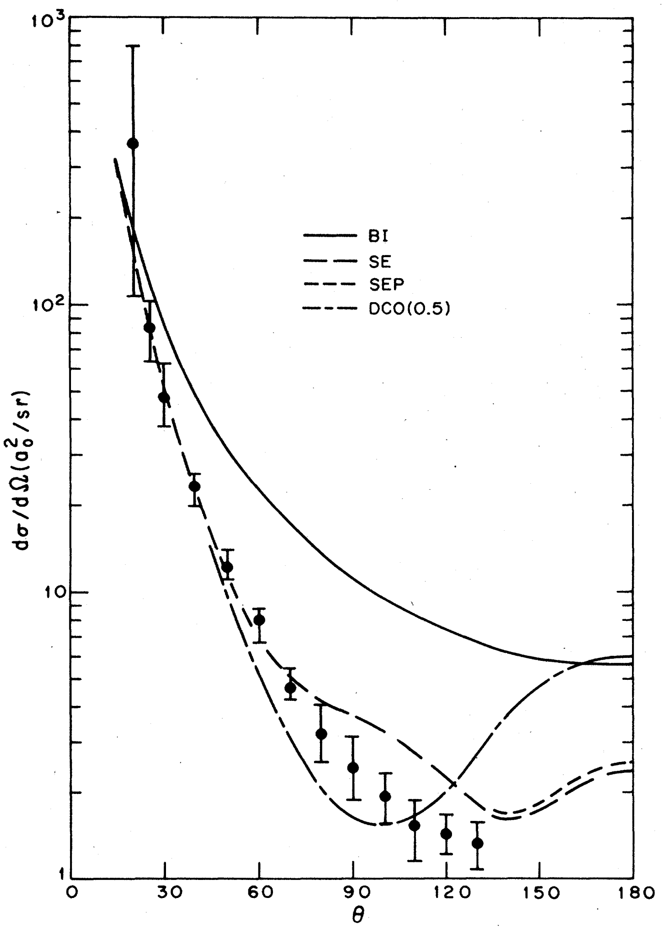

FIG. 68. Differential cross sections at 5.44 eV for e–LiF scattering. Theory: (curve BI) first Born approximation, (curves SE, SEP) static exchange and static-exchange polarization, respectively (curve DCO) dipole cutoff model potential, Collins and Norcross (1978). Experiments: Vušković *et al.* (1979) normalized to SEP theory at 40°. (Reprinted from Collins and Norcross, 1978.)

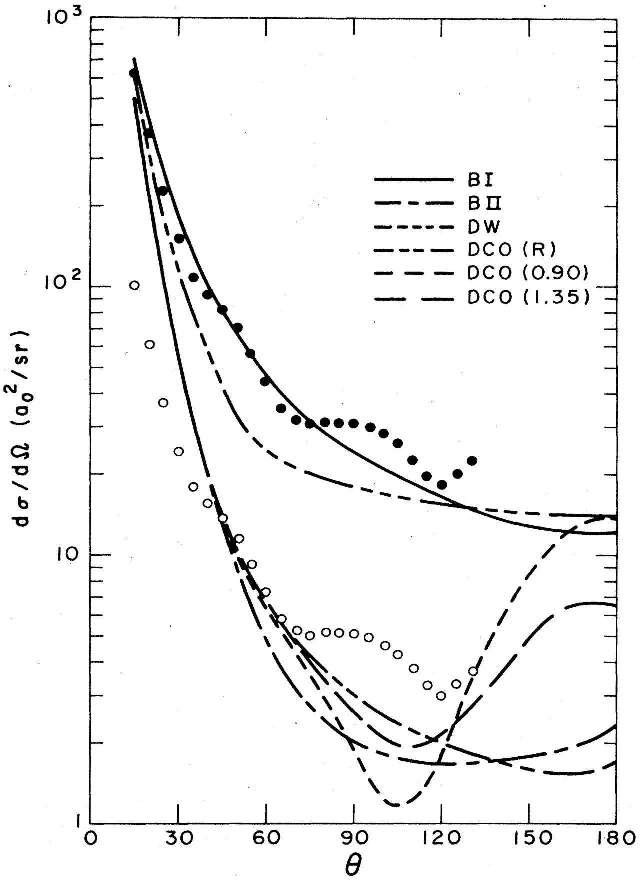

FIG. 69. Differential cross section at 6.74 eV for e–KI scattering. Theory: (curves BI, II) Born and unitarized Born approximation; (curve DW) distorted waves, Rudge *et al.* (1976); (curves DCO) various dipole cutoff model potentials, Collins and Norcross (1978). Experiment: (closed circles) original normalization, Rudge *et al.* (1976); (open circles) renormalized by Collins and Norcross (1978). (Reprinted from Collins and Norcross, 1978.)

both normalizations are shown along with the various theoretical curves. The model "dipole cutoff" studies included in this work and the later applications to electron–KOH and –CsOH scattering by Collins, Norcross, and Schmid (1979) provide examples of the applicability of Fabrikant's extension of effective-range theory to electron–polar-molecule scattering (Fabrikant, 1976, 1977). In this theory, the low-energy momentum-transfer cross section may be expressed simply as

$$\sigma_m = \pi k^{-2}[\alpha + \beta \sin(\gamma + \mu \ln k^2)],$$

where α, β, and μ are constants depending only on the dipole moment d, and where γ depends on d and short-range interactions. Thus, the product $E\sigma_m$ exhibits sinusoidal oscillation with respect to $\ln E$ (recall $E = k^2$ Ry). Fabrikant's simple result is particularly useful since only the *phase* of the oscillation, not its amplitude, is sensitive to short-range interactions.

When the target is a positive molecular ion, e.g., CH^+, the Coulomb field dominates the scattering. However, the dipole interaction still provides the long-range anisotropic term and can provide strong rotational coupling. Cross sections for rotational excitation of CH^+ have been calculated by Chu and Dalgarno (1974) using the Coulomb–Born approximation and by Mathur (1978) using the Glauber approximation. The Coulomb–Born results, which are expected to be the more reliable of the two near threshold, predict a finite cross section at threshold. The results of the two calculations agree at higher energies. Chu (1975) discusses the general case of electron scattering from a symmetric-top molecular ion in the Coulomb Born approximation, and gives results for $\mathrm{H_3O^+}$.

2. Vibrational excitation

In vibrational excitation, the existence of a finite dipole moment is less important in determining the cross sections than in elastic scattering and rotational excitation, although the dipole interaction may still be dominant at threshold for some molecules. Classically, large vibrational-excitation cross sections result from strong forces exerted on the nuclei by the scattered electron. Generally, short-range interactions are expected to be important even for polar molecules. As in the case of nonpolar molecules, the vibrational-excitation cross sections are strongly enhanced by resonant scattering.

a. CO, N_2O, H_2O, NO

The mechanism for vibrational excitation of CO is at least qualitatively understood (Schulz 1973, 1976). Being isoelectronic with N_2, CO might be expected to scatter electrons in a similar manner. Indeed, a shape resonance, shown to be of Π character, has long been a familiar feature of the total cross section (see Massey, 1969), and the momentum-transfer cross section (Hake and Phelps, 1967; Land, 1978). A hint of structure, presumably related to temporary formation of vibrational states of CO^-, is evident in the elastic cross section (Ehrhardt, Langhans, Linder, and Taylor, 1968). Finally, well-defined structure appears in the $v=0\rightarrow v'$ vibrational-excitation cross sections (Schulz, 1964; Ehrhardt *et al.*, 1968; and Boness and Schulz, 1973) very similar to that observed in electron–N_2 scattering, but somewhat broader in comparison. Boness and Schulz (1973) have shown, using a simple barrier penetration analysis, that the relative magnitudes of $v=0\rightarrow v'$ cross sections, for $v'=3,4,5$, etc., can be simply related to (centrifugal) barrier penetration probabilities for the dominant partial waves. The Π_g compound state in N_2 is associated with an incident and outgoing d wave, while the Π compound state in CO has some p-wave contribution as well (see discussion of Chang, 1977a,b). The more efficient penetration of the p relative to the d waves can account for the resonances in CO being broader than those in N_2. Zubek and Szmytkowski (1977) have applied the "boomerang model" (Birtwistle and Herzenberg, 1971) and obtained very good (semiempirical) agreement with the observed structure (Ehrhardt, Langhans, Linder, and Taylor, 1968). The $v=0\rightarrow 1$ cross section in the region between threshold ($E \gtrsim 0.26$ eV) and the onset of the resonance ($E \lesssim 0.9$ eV) is quite small and appears to be determined by nonresonant scattering. Figure 70 (Schulz, 1976) shows a comparison of the $v=0\rightarrow 1$ cross section measured by the swarm (Hake and Phelps, 1967) and beam (Ehrhardt *et al.*, 1968) methods and that calculated by Born and close-coupling methods using simple model electron–CO interaction potentials (Itikawa and Takayanagi, 1969b,c). The discrepancy between the beam and swarm results in not understood (Schulz, 1976). The "best" agreement with the swarm data is actually obtained by using the Born-dipole approximation (Takayanagi, 1966, 1967) with the vibrational matrix element of $d(R)$ extracted from the infrared intensity data (Phelps, 1968; Penner and Olfe, 1968). Itikawa and Takayanagi (1969b,c), carried out Born and limited close-coupling calculations of rotational–vibrational excitation ($v=0, j=0\rightarrow v'=1, j'=0,1$) cross sections using a model interaction potential which included a short-range static contribution (taken to be independent of R), and dipole and polarization terms, both cut off in the manner of Eq. (147). Assuming a "reasonable" value for the cutoff radius $r_c=1.5a_0$ and vibrational matrix elements, cross sections were calculated for $v=0\rightarrow 1$ ($j=0\rightarrow 0$ and $0\rightarrow 1$) transitions. In the close-coupling calculation truncation was rather severe, with only the states $v=0,1$ and $j=0,1$ being retained. The theoretical cross sections given in Fig. 70 correspond to the full electron–CO model interaction as described. In Fig. 71, theoretical Born and close-coupling cross sections for $v=0\rightarrow 1$ ($j=0\rightarrow 0$ and $0\rightarrow 1$) are compared for various choices of interaction and for

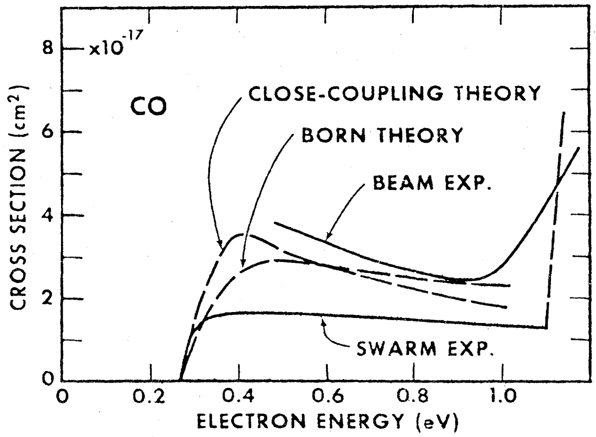

FIG. 70. Cross sections for $v=0\rightarrow 1$ vibrational excitation in e–CO collisions near threshold. Theory: (dashed curves) close coupling and Born, Itikawa and Takayanagi (1969b). Experiment: (solid curve, beam experiment), Ehrhardt *et al.* (1968); (solid curves, swarm experiment), Hake and Phelps (1967). (Reprinted from Schulz, 1976.)

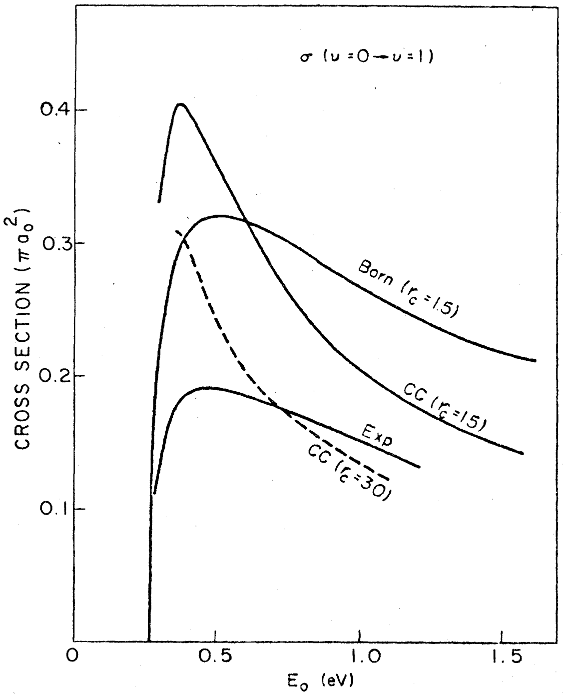

FIG. 71. Theoretical cross sections for $v=0\rightarrow 1$ vibrational excitation in e–CO scattering in the Born and close-coupling approximations. (Reprinted from Itikawa and Takayanagi, 1969b.)

a polarization cutoff radius of $r_c = 1.5a_0$. The conclusions are that the dipole and polarization interactions are of comparable importance, and that when both are included, the Born approximation fails. A quantitative comparison of these results with experiment suggests something is still missing in the theory. Itikawa (1970), using the T-matrix elements from this study, calculated differential rotational–vibrational-excitation cross sections. Generally, he found the Born and close-coupling results were in agreement at small angles, where the dipole interaction was most important, but were quite different at angles $\theta \gtrsim 60°$. Again, comparison with relative $v=0\rightarrow 1$ differential cross-section measurements (Ehrhardt *et al.*, 1968) at 0.74 eV suggested that the Born-dipole approximation was best. If indeed this turns out to be the case, a somewhat more elaborate calculation, close-coupling or otherwise, should exhibit the effective "cancellation" of other interactions.

Above the 1–7 eV resonance region, other resonances are observed (Schulz, 1973, 1976), some of which are very narrow and presumably of the Feshbach (or core-excited) type. Even in the ionization continuum, e.g., at 20 eV, there is evidence for resonant elastic scattering (Truhlar, Williams, and Trajmar, 1972) and vibrational excitation (Chutjian, Truhlar, Williams, and Trajmar, 1972). Theoretical polarized-Born calculations of the elastic differential cross sections in the energy range of 6–8 eV were found to be in fairly good agreement with the relative measurements (Truhlar, Williams, and Trajmar, 1972) at angles $\theta \lesssim 60°$ for several choices of model interaction potential. Similar model-interaction studies of $v=0\rightarrow 1$ vibrational excitation were less successful because of the strong resonance contribution around 20 eV (Chutjian *et al.*, 1972).

Broad shape resonances are observed in electron–N_2O scattering at $E \simeq 2.3$ eV and H_2O at $E \simeq 7$ eV, both in the elastic and vibrational-excitation cross sections (Schulz, 1976). Dubé and Herzenberg (1975) have applied the impulse approximation (here equivalent to the "adiabatic nuclear vibration" approximation) to vibrational excitation in N_2O near the 2.3 eV resonance. By fitting a few low-lying transitions, they obtain good agreement with the measured relative cross sections for higher members of the series (Azria, Wong, and Schulz, 1975). This short-lived resonance is estimated to have a width of approximately 0.7 eV.

In H_2O, Itikawa (1974b) has examined nonresonant contributions to the vibrational-excitation cross sections by performing Born-approximation calculations in which the electron–H_2O interaction was modeled by a sum of (long-range) dipole, quadrupole, and polarization potentials (also see Itikawa, 1974a). The calculated cross sections do not exhibit the sharp resonances observed just above threshold (to be discussed in the next section). This is certainly not surprising since these resonances are most likely tied to "final-state effects," totally neglected in the Born approximation. Short-range interactions are likely to be important from threshold to higher energies.

In the case of NO, there have been no theoretical calculations of vibrational-excitation cross sections to date. However, much has been learned from experimental investigations (Schulz, 1973, 1976). Narrow shape resonances dominate the vibrational-excitation cross sections from threshold up. As in the case of electron–O_2 scattering, the lifetimes of the resonant NO^- states exceed the vibrational periods so that rather well-defined vibrational states of NO^- exist and may be closely correlated with the positions of the resonant peaks. The electronic resonant "state" (Born–Oppenheimer) is characterized as $^3\Sigma^-$, and a semiempirical potential curve has been obtained by Spence and Schulz (1971). Only the $v=0$ vibrational state of NO^- is stable, with an electron affinity of 24(+10, −5) meV (Siegel, Celotta, Hall, Levine, and Bennett, 1972). The vibrational energy level spacing for the bound and resonant vibrational states is about 165 meV. Experimental evidence also has been found for resonance scattering via the higher-lying $^1\Delta$ and $^1\Sigma^+$ states of NO^- (Burrow, 1974). Tronc, Huetz, Landau, Pichon, and Reinhardt (1975) have concluded on the basis of their observed differential vibrational-excitation cross sections that the $^3\Sigma^-$ and $^1\Delta$ are long-lived states while the higher $^1\Sigma^+$ state is an intermediate case, i.e., more like the N_2 and CO "boomerang" resonances (Schulz, 1973, 1976). The observed branching ratios are consistent with a lower barrier height than that found in O_2^-. This is consistent with a strong mixing of p and d waves (Bardsley and Read, 1968). As in the case of O_2, very little is known about nonresonant contributions to the electron scattering cross sections.

b. Threshold resonances in the hydrides

Rohr and Linder (1975) in carrying out a high-resolution crossed-beam measurement of vibrational excitation in electron scattering from HCl discovered a remarkable feature that had not been predicted (see review by Linder, 1977). The $v=0\rightarrow 1$ cross section was found to exhibit a large, narrow resonance peak just above threshold and a very broad resonance at higher energies. The angular distribution near threshold was found to be isotropic, suggesting that asymptotically the scattering wave function was dominated by the s-wave contribution (see Chang, 1977c). Similar resonances were found in the cross sections for the higher transitions $v=0\rightarrow 2, 3$, etc., as well as in other polar molecules: HF (Rohr and Linder, 1976); H_2O (Seng and Linder, 1976; Rohr 1977c); HBr (Rohr 1977a, 1978); and even a nonpolar molecule SF_6 (Rohr 1977b, 1979). The $v=0\rightarrow 1$ differential cross sections at 120° for HF, HCl, and HBr are illustrated in Fig. 72 (Rohr, 1978).

Efforts to provide a theoretical explanation of the striking threshold resonances have met with some success. Gianturco and Rahman (1977a) have shown formally that such a resonance could be accounted for strictly in terms of a "final-state interaction" dominated by the long-range dipole potential energy. The authors conclude that sharp resonances should be present for HCl and HF, but not HI; they predicted only a broad feature for HBr.

Dubé and Herzenberg (1977) invoked the concept of a "virtual state" (Taylor, 1972) to explain the existence of the threshold resonances, and performed a model scattering calculation obtaining quite good qualitative

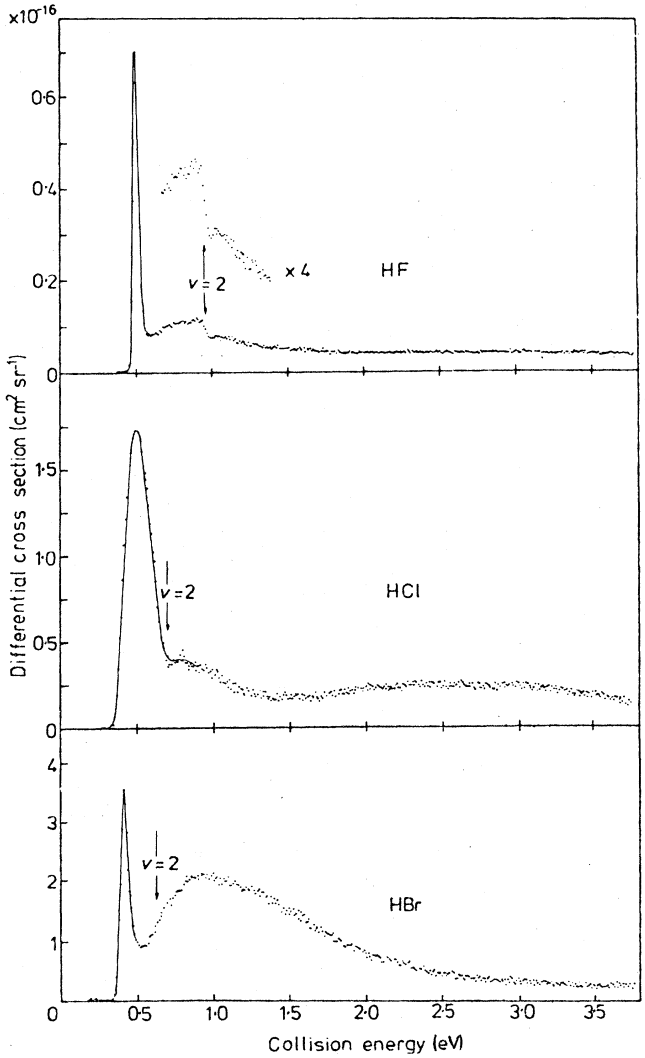

FIG. 72. Experimental differential cross sections at 120° for $v=0\rightarrow 1$ vibrational excitation in e—HF, e—HCl, and e—HBr scattering. (Reprinted from Rohr, 1978.)

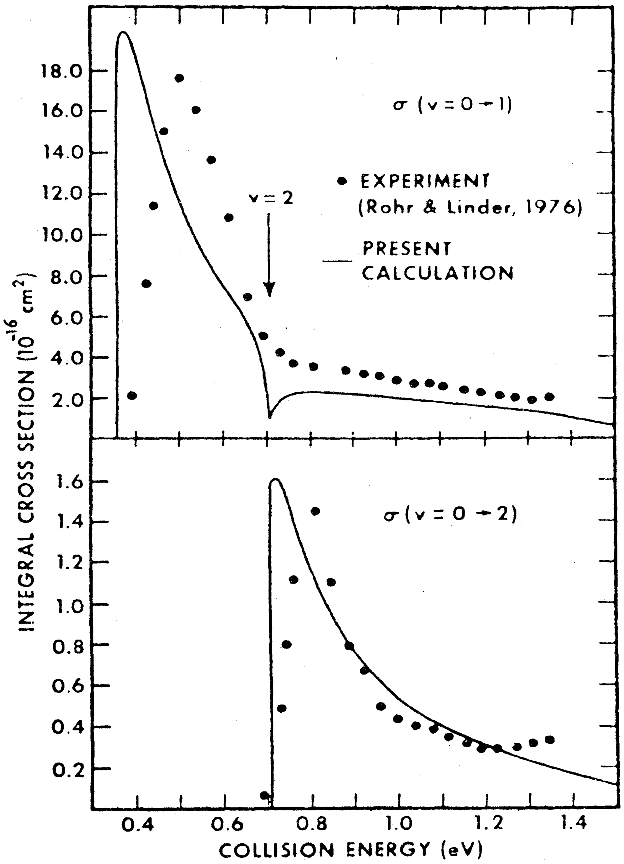

FIG. 73. Cross sections for $v=0\rightarrow 1$ and $0\rightarrow 2$ vibrational excitation in e—HCl scattering. Theory: (solid curves) model of Dubê and Herzenberg (1977). Experiment (closed circles), Rohr and Linder (1975, 1976). (Reprinted from Dubê and Herzenberg, 1977.)

agreement for the case of HCl studied. The electron–HCl interaction was represented by the dipole potential for $r \geqslant r_0$. The inner region $r<r_0$ was represented by means of a logarithmic derivative $f(R)$ at the boundary $r=r_0$. A range of parameters in $f(R)$, where R is the internuclear separation, was obtained by considering alternative physically reasonable charge distributions near the nuclei. Calculated cross sections for $v=0\rightarrow 1$ and $v=0\rightarrow 2$ transitions are compared with experiment (Rohr and Linder 1975) in Fig. 73. It is not really clear how much the dipole interaction influences the calculated cross sections since the existence of a "virtual state" is already implied by the value chosen for the logarithmic derivative $f(R)$ at $r=2a_0$. Nevertheless, the agreement is quite good. The calculated $v=0\rightarrow 1$ cross section also reveals a sharp cusp at the $v=0\rightarrow 2$ threshold. (The experimentally observed cusp is more striking in HF than in HCl. See Fig. 73.)

Taylor, Goldstein, and Segal (1977) applied the stabilization method (Taylor, 1970; Hazi and Taylor, 1970) to find potential energy curves of HCl⁻ resonance states. The authors are successful in correlating the qualitative shapes and positions of the theoretical HCl⁻ curves with a variety of experimental observations, including: dissociative attachment (Azria, Roussier, Paineau, and Tronc, 1974; Ziesel, Nenner, and Schulz, 1975; and Abouaf and Tiellet-Billy, 1977), associative detachment (Howard, Fehsenfeld, and McFarland, 1974), elastic scattering (Burrow 1974), and vibrational excitation (Rohr and Linder, 1976; Ziesel *et al.*, 1975). In regard to the vibrational-excitation threshold resonances, questions still remain regarding the true nature of these features, and to what extent the phenomenon is tied to particular classes of molecular targets. It is not clear that a stabilization calculation (Taylor *et al.*, 1977) can be expected to describe a "virtual state," if indeed that is responsible for the effects. [See Nesbet (1977), regarding this point.]

F. Electronic excitation

This review does not include electronic excitation. However, a brief mention of recent advances is appropriate. Early work is described by Massey (1969) and consists mainly of Born approximation calculations for H_2 and other simple molecules. Recent advances in describing e–H_2 electronic excitation have been along two lines: close coupling (CC) calculations using traditional methods (Chung and Lin, 1978), and calculations based on a version of the method of distorted waves (DW) using modern L^2-basis techniques (Rescigno, McCurdy, and McKoy, 1975b; Rescigno, McCurdy, McKoy, and Bender, 1976; Fliflet and McKoy, 1979). Both approaches are, in principle, superior to the Born–Ochkur–Rudge theory (Cartwright and Kuppermann, 1967; Chung, Lin, and Lee, 1975; Chung and Lin, 1972, 1974). However, there are cases of significant disagreement between the CC and DW results and the issue is not yet resolved.

Progress in the theoretical understanding and description of electronic excitation of N_2 and more complex molecules by electron impact is far less satisfying. The theoretical and experimental situation for N_2 is nicely described in three comprehensive papers by Cartwright, Chutjian, Trajmar, and Williams (1977a, b) and Chutjian, Cartwright, and Trajmar (1977). Born and Born–Ochkur–Rudge theories provide only qualitative descriptions except at high energies. The method of distorted waves, using L^2-basis techniques, has recently been applied to excitation of the $B\,^3\Pi_g$, $C\,^3\Pi_u$, and $E\,^3\Sigma_g^+$ states of N_2 by low-energy electron impact (Fliflet, McKoy, and Rescigno, 1979a) and to dissociation of F_2 (Fliflet, McKoy, and Rescigno, 1979b).

An interesting recent application of the semiclassical impact-parameter theory of electron scattering (Seaton, 1962; Stauffer and McDowell, 1966; and Hazi, 1979) to deexcitation of KrF and XeF excimers by Hazi, Rescigno, and Orel (1979) suggests that this simple method may have promise in dealing with spin-allowed electronic transitions in complex molecules, especially where highly excited states are involved.

IV. CONCLUDING REMARKS

In this review an attempt has been made to describe recent progress both in the application of traditional methods and in the development of new approaches to the electron–molecule collision problem. We have focused on low-energy elastic scattering and rotational and vibrational excitation since most of the recent theoretical progress in the field has been restricted to these processes. The molecule is a complex target, and an adequate theoretical description of electronic excitation will remain a challenging problem for some time. As in the atomic case, one expects a steady development of the art of applying variational theory to the electron–molecule continuum, perhaps with the use of pseudostates. However, unlike the atomic problem, here one must properly deal with the nuclear degrees of freedom.

The multicenter nature of the electron–molecule interaction introduces a degree of complexity not present in the atomic problem. Single-center (partial-wave) expansions of the scattering wave functions are slowly convergent so that large cumbersome multichannel scattering problems result even for the simple example of elastic scattering from a small molecule (fixed-nuclei) like N_2 or CO. In the strongly polar molecules one has in addition to this difficulty the strong coupling of partial waves due to the dipole interaction which persists out to very large electron–molecule separations. Much progress has been made in the use of so-called "L^2 integrable bases," thus taking advantage of the well developed technology of complex molecular structure calculations. In the applications to electron–molecule-scattering, large basis sets of these functions are required to represent the continuum wave function either inside a box (R-matrix method) or in all space (T-matrix expansion method). While these approaches have some very real potential advantages over more conventional (coupled-channel, etc.) methods, their implementation is nevertheless quite complicated. So far, no straightforward inexpensive procedure has been developed to handle such problems. There is still a clear need for workers in the field to push forward with complementary methods making sure that a significant overlap is maintained in the choice of systems and processes so that the relative advantages of the methods can be determined. At this stage in the development of the theory, a certain amount of duplication is necessary. The time is right for precise calculations of elastic scattering and rotational and vibrational and electronic excitation cross sections for simple molecules at low energies. Toward the other end of the scale, the continued development and application of more flexible but less precise approximate methods (e.g., multiple scattering theory) to complex molecules will continue to produce interesting results. Calculations of this type are particularly useful in providing the guidance often required for the proper interpretation of experimental data.

ACKNOWLEDGMENTS

Some of the background material for this review was developed when the author was a Visiting Fellow at the Joint Institute for Laboratory Astrophysics (JILA), 1975–1976. The bulk of the review was written in the summer of 1978 with the assistance of Dr. John Rumble and Dr. Jean Gallagher of the JILA Atomic Collisions Information Center and Mrs. Lorraine Volsky, Scientific Reports Editor, and her staff at JILA. The author gratefully acknowledges Dr. Michael Morrison for his critical reading of the manuscript and very helpful suggestions, and many other colleagues for illuminating conversations and for sharing their results prior to publication. The work was supported in part by the NBS Office of Standard Reference Data (through the JILA Atomic Collisions Information Center), the U. S. Department of Energy (Office of Basic Energy Sciences), and the Robert A. Welch Foundation.

APPENDIX: ACCURATE STATIC-EXCHANGE CALCULATIONS FOR ELECTRON–H_2 SCATTERING

In developing new methods or updating traditional methods of treating electron–molecule scattering it is important to have available accurate numerical results for purposes of testing and calibration. Recently Collins, Robb, and Morrison (1979) have performed a set of accurate static-exchange calculations for e–H_2 scattering in the fixed-nuclei approximation (BODY-

TABLE I. Static-exchange eigenphase sums (in radians) and cross sections (in a_0^2, in parentheses) for e—H_2 collisions. Results are converged to better than 1%; the values of the convergence parameters which ensure this criteron are shown for each symmetry.

k^2(Ry)	$^2\Sigma_g$	$^2\Sigma_u$	$^2\Pi_g$	$^2\Pi_u$	$^2\Delta_g$
0.01	2.9303(56.468)	0.0134 (0.2073)	0.0012(0.0048)	−0.0025(0.0316)	−0.0020(0.0116)
0.04	2.7246(53.034)	0.0493 (0.6763)	0.0038(0.0060)	0.0045(0.0095)	−0.0034(0.0131)
0.09	2.5267(47.896)	0.1233 (1.9397)	0.0070(0.0070)	0.0262(0.1396)	−0.0043(0.0122)
0.16	2.3399(41.823)	0.2459 (4.3867)	0.0110(0.0097)	0.0642(0.5360)	−0.0044(0.0094)
0.25	2.1679(35.483)	0.4084 (7.5826)	0.0169(0.0155)	0.1155(1.1592)	−0.0031(0.0058)
0.36	2.0114(29.467)	0.5797(10.096)	0.0252(0.0263)	0.1729(1.8432)	0.0001(0.0025)
0.49	1.8729(24.053)	0.7269(10.951)	0.0363(0.0436)	0.2289(2.3701)	0.0054(0.0012)
0.64	1.7509(19.427)	0.8361(10.453)	0.0501(0.0677)	0.2779(2.6449)	0.0128(0.0029)
1.00	1.5509(12.481)	0.9591 (8.092)	0.0840(0.1306)	0.3481(2.5535)	0.0324(0.0155)
$l_{\max}$	10	11	12	11	12
$\lambda_{\max}$	20	22	24	22	24
$l_{\max}^{\text{ex}}$	2	3	4	3	4
n_1^{ex}	2	2	2	2	2

frame) with just this purpose in mind. These authors solved the integral-equation counterparts of the BODY-frame coupled radial equations (116) treating the exchange term iteratively, in a manner similar to the earlier approach of Tully and Berry (1969). The $^1\Sigma_g^+$ ground state of H_2 was represented by the near-Hartree–Fock wave function of Fraga and Ransil (1961) at the equilibrium separation $R = 1.402a_0$. The total energy corresponding to this wave function is −1.1335 hartree and the permanent quadrupole moment is $q = 0.480ea_0^2$. In all cases, the integration mesh and the number of terms $\lambda \leq \lambda_{\max}$ and $l \leq l_{\max}$ retained in the expansions of the wave function and potentials, respectively, were chosen so as to ensure an accuracy of 1% in the eigenphase sums. The K matrix was determined at $50a_0$.

In Table I, the eigenphase sums are given for symmetries $^2\Sigma_g$, $^2\Sigma_u$, $^2\Pi_g$, $^2\Pi_u$, and $^2\Delta_g$ at nine energies between 0.01 and 1.00 Ry. The values of relevant convergence parameters are also given for reference, where $l_{\max}$ and $l_{\max}^{\text{ex}}$ are the maximum order partial waves retained in the expansions of the scattering function outside and inside the exchange kernel, respectively, $\lambda_{\max}$ is the maximum order term retained in the expansion of the static potential, and n_1^{ex} is the number of terms retained in the expansion of the bound mole-

TABLE II. Comparison of the dominant eigenphase shifts (in radians) of each symmetry for e—H_2 scattering from the iterative static-exchange calculations (CRM) with those obtained in other studies. Note that $1.0(-2) = 1.0 \times 10^{-2}$.

k^2(Ry)		$s\sigma$	$p\sigma$	$d\sigma$	$p\pi$	$d\pi$
0.01	CRM	2.928	1.28(−2)	2.3 (−3)	−3.42(−3)	1.37(−3)
	FM[a,d]	2.929		9.0 (−4)		
	S[b]	2.931	4.3 (−3)			
	TB[c]	2.939				
0.36	CRM	1.978	0.567	2.71(−2)	0.163	0.019
	FM	1.979	0.532	2.66(−2)	0.161	0.019
	S	1.949	0.561	1.83(−2)	0.163	0.018
	TB	2.006	0.537	2.0 (−2)	0.162	0.014
1.00	CRM	1.447	0.931	9.10(−2)	0.324	0.072
	FM	1.45		9.10(−2)		
	S	1.418	0.927	7.29(−2)	0.306	0.062
	TB					

[a] Fliflet and McKoy (1978a).

[b] Schneider (1975b).

[c] Tully and Berry (1969).

[d] The $s\sigma$ and $d\sigma$ eigenphases are the corrected values of Fliflet and McKoy (1978a).

TABLE III. Static-exchange eigenphase shifts (in radians) for selected energies. (Note: in forming the eigenphase sums for $^2\Sigma_g$ symmetry, π should be added.)

k^2(Ry)	$^2\Sigma_g$	$^2\Sigma_u$	$^2\Pi_g$	$^2\Pi_u$	$^2\Delta_g$
0.01	−0.213 59	0.012 83	0.001 37	−0.003 42	−0.002 14
	0.002 34	0.000 65	−0.000 17	0.000 95	0.000 18
	−0.000 05	−0.000 04	0.000 02	−0.000 01	
	0.000 05				
0.04	−0.423 37	0.046 35	0.002 95	0.003 71	−0.004 5
	0.004 97	0.002 28	−0.000 23	−0.000 49	0.000 95
	0.001 15	0.000 70	0.000 88	0.001 02	−0.000 21
	−0.000 17	−0.000 17	0.000 23	0.000 27	0.000 29
	0.000 36	0.000 12	0.000 01	−0.000 06	0.000 02
	0.000 02				
0.16	−0.817 78	0.238 53	0.007 48	0.058 31	−0.007 48
	0.012 09	0.004 73	0.002 08	0.003 68	0.001 85
	0.002 53	0.001 60	−0.000 13	0.001 39	−0.000 18
	−0.000 03	−0.000 07	0.000 96	−0.000 10	0.000 87
	0.001 08	0.000 77	0.000 50	0.000 69	0.000 44
	0.000 45	0.000 29	0.000 14	0.000 24	0.000 08
0.36	−1.163 94	0.567 76	0.019 02	0.163 07	−0.005 05
	0.027 12	0.007 73	0.003 49	0.006 12	0.002 91
	0.004 03	0.002 47	−0.000 03	0.002 18	−0.000 11
	0.001 68	0.000 04	0.001 54	0.000 00	0.001 36
	0.000 11	0.001 20	0.000 83	0.001 10	0.000 73
	0.000 77	0.000 54	0.000 34	0.000 47	0.000 25
1.00	1.447 26	0.930 97	0.071 71	0.323 90	0.024 32
	0.091 46	0.020 24	0.007 12	0.016 95	0.004 50
	0.007 53	0.004 56	0.002 82	0.004 17	−0.000 10
	0.002 95	0.000 22	0.000 11	0.000 17	0.002 13
	0.000 33	0.002 12	0.001 50	0.001 99	0.001 16
	0.001 39	0.001 03	0.000 70	0.000 95	0.000 43

cular target orbital. In Table II, the dominant eigenphase shifts (CRM) are compared with those of other calculations. Finally, individual static-exchange eigenphase shifts are given in Table III at selected energies.

REFERENCES

Abouaf, R., and D. Teillet-Billy, 1977, J. Phys. B **10**, 2261.

Abram, R. A., and A. Herzenberg, 1969, Chem. Phys. Lett. **3**, 187.

Allan, M., and S. F. Wong, 1978, Phys. Rev. Lett. **41**, 1791.

Allison, A. C., 1970, J. Comput. Phys. **6**, 378.

Allison, A. C., 1975, J. Phys. B **8**, 325.

Altshuler, S., 1957, Phys. Rev. **107**, 114.

Andrick, A., D. Danner, and H. Ehrhardt, 1969, Phys. Lett. A **29**, 346.

Andrick, D., and H. Ehrhardt, 1966, Z. Phys. **192**, 99.

Ardill, R. W. B., and W. D. Davison, 1968, Proc. R. Soc. London A **304**, 463.

Arthurs, A. M., and A. Dalgarno, 1960, Proc. R. Soc. London A **256**, 540.

Ashihara, O., I. Shimamura, and K. Takayanagi, 1975, J. Phys. Soc. Jpn. **38**, 1732.

Azria, R., L. Roussier, R. Paineau, and M. Tronc, 1974, Rev. Phys. Appl. **9**, 469.

Azria, R., S. F. Wong, and G. J. Schulz, 1975, Phys. Rev. A **11**, 1309.

Baille, P., and J. W. Darewych, 1977a, J. Chem. Phys. **67**, 3399.

Baille, P., and J. W. Darewych, 1977b, J. Phys. B **10**, L615.

Bardsley, J. N., 1969, J. Chem. Phys. **51**, 3384.

Bardsley, J. N., and M. Biondi, 1970, Adv. At. Mol. Phys. **6**, 1.

Bardsley, J. N., A. Herzenberg, and F. Mandl, 1966a, Proc. Phys. Soc. London **89**, 305.

Bardsley, J. N., A. Herzenberg, and F. Mandl, 1966b, Proc. Phys. Soc. London **89**, 321.

Bardsley, J. N., and F. Mandl, 1968, Rep. Prog. Phys. **31**, 471.

Bardsley, J. N., F. Mandl, and A. R. Wood, 1967, Chem. Phys. Lett. **1**, 359.

Bardsley, J. N., and F. H. Read, 1968, Chem. Phys. Lett. **2**, 333.

Bartels, A., 1972, Phys. Rev. Lett. **28**, 213.

Becker, W. G., N. G. Fickes, K. C. Slater, and R. C. Stern, 1974, J. Chem. Phys. **61**, 2283.

Bhattacharyya, P. K., and A. S. Ghosh, 1975, Phys. Rev. A **12**, 480.

Bhattacharyya, P. K., and A. S. Ghosh, 1976, Phys. Rev. A **14**, 1587.

Bhattacharyya, P. K., K. K. Goswami, and A. S. Ghosh, 1978, Phys. Rev. A **18**, 1865.

Birtwistle, D. J., and A. Herzenberg, 1971, J. Phys. B **4**, 53.

Blatt, J. M., 1967, J. Comput. Phys. **1**, 382.

Blatt, J. M., and V. F. Weisskopf, 1952, *Theoretical Nuclear Physics* (Wiley, New York).

Bloch, C., 1957, Nucl. Phys. **4**, 503.

Bloch, F., and N. E. Bradbury, 1935, Phys. Rev. **48**, 689.

Boness, M. J. W., and J. B. Hasted, 1966, Phys. Lett. **21**, 526.

Boness, M. J. W., and G. J. Schulz, 1968, Phys. Rev. Lett. **21**, 1031.

Boness, M. J. W., and G. J. Schulz, 1973, Phys. Rev. A **8**, 2883.

Boness, M. J. W., and G. J. Schulz, 1974, Phys. Rev. A **9**, 1969.

Bonham, R. A., 1962, J. Chem. Phys. **36**, 3260.

Bottcher, C., 1970, Mol. Phys. **19**, 193.

Bottcher, C., 1971, Chem. Phys. Lett. **9**, 57.

Brandt, M. A., D. G. Truhlar, and F. A. Van Catledge, 1976, J. Chem. Phys. **64**, 4957.

Bransden, B. H., 1970, *Atomic Collision Theory* (Benjamin, New York).

Bransden, B. H., and M. R. C. McDowell, 1977, Phys. Rep. **30**, 207.

Bransden, B. H., and M. R. C. McDowell, 1978, Phys. Rep. **46**, 249.

Breig, E. L., and C. C. Lin, 1965, J. Chem. Phys. **43**, 3839.

Brode, R. B., 1933, Rev. Mod. Phys. **5**, 257.

Bromberg, J. P., 1970, J. Chem. Phys. **52**, 1243.

Brown, S. C., 1979, Editor, *Electron Molecule Scattering* (Wiley, New York).

Brown, W. B., and R. E. Roberts, 1967, J. Chem. Phys. **46**, 2006.

Brüche, E., 1927, Ann. Phys. (Leipzig) **83**, 1065.

Buckingham, A. D., 1959, Q. Rev. Chem. Soc. London **13**, 183.

Buckley, B. D., 1977, J. Phys. B **10**, L351.

Buckley, B. D., and P. G. Burke, 1977, J. Phys. B **10**, 735.

Bulos, B. R., and A. V. Phelps, 1976, Phys. Rev. A **14**, 615.

Burke, P. G., 1968, Adv. Atom. Mol. Phys. **4**, 173.

Burke, P. G., 1974, Comput. Phys. Commun. **6**, 288.

Burke, P. G., 1977, in *X ICPEAC, Electronic and Atomic Collisions: Invited Papers and Progress Reports* edited by G. Watel (North-Holland, Amsterdam), p. 201.

Burke, P. G., and N. Chandra, 1972, J. Phys. B **5**, 1696.

Burke, P. G., N. Chandra, and F. A. Gianturco, 1972, J. Phys. B **5**, 2212.

Burke, P. G., I. Mackey, and I. Shimamura, 1977, J. Phys. B **10**, 2497.

Burke, P. G., and W. D. Robb, 1975, Adv. Atom. Mol. Phys. **11**, 144.

Burke, P. G., and H. M. Schey, 1962, Phys. Rev. **126**, 163.

Burke, P. G., and A. L. Sinfailam, 1970, J. Phys. B **3**, 641.

Burke, P. G., and J. F. Williams, 1977, Phys. Rep. **34**, 325.

Burrow, P. D., 1974, Chem. Phys. Lett. **26**, 265.

Burrow, P. D., and L. Sanche, 1972, Phys. Rev. Lett. **28**, 333.

Burrow, P. D., and G. J. Schulz, 1969, Phys. Rev. **187**, 97.

Burrus, C. A., 1958, J. Chem. Phys. **28**, 427.

Buttle, P. J. A., 1967, Phys. Rev. **160**, 719.

Cade, P. E., K. D. Sales, and A. C. Wahl, 1966, J. Chem. Phys. **44**, 1973.

Cadez, I. M., F. Gresteau, M. Tronc, and R. I. Hall, 1977, J. Phys. B **10**, 3821.

Cadez, I. M., M. Tronc, and R. I. Hall, 1974, J. Phys. B **7**, L132.

Callaway, J., R. W. LaBahn, R. T. Pu (Poe), and W. M. Duxler, 1968, Phys. Rev. **168**, 12.

Carson, T. R., 1954, Proc. Phys. Soc. London A **67**, 909.

Carter, C., N. H. March, and D. Vincent, 1958, Proc. Phys. Soc. London **71**, 2.

Cartwright, D. C., A. Chutjian, S. Trajmar, and W. Williams, 1977a, Phys. Rev. A **16**, 1013.

Cartwright, D. C., and A. Kuppermann, 1967, Phys. Rev. **163**, 86.

Cartwright, D. C., S. Trajmar, A. Chutjian, and W. Williams, 1977b, Phys. Rev. A **16**, 1041.

Castillejo, L., I. C. Percival and M. J. Seaton, 1960, Proc. R. Soc. London A **254**, 259.

Chandra, N., 1975a, J. Phys. B **8**, 1338.

Chandra, N., 1975b, Phys. Rev. A **12**, 2342.

Chandra, N., 1977, Phys. Rev. A **16**, 80.

Chandra, N., and P. G. Burke, 1973, J. Phys. B **6**, 2355.

Chandra, N., and F. A. Gianturco, 1974, Chem. Phys. Lett. **24**, 326.

Chandra, N., and S. K. Joshi, 1970, in *Advances in Astronomy and Astrophysics*, edited by Z. Kopal (Academic, London), Vol. 7, p. 1.

Chandra, N., and A. Temkin, 1976a, Phys. Rev. A **13**, 188.

Chandra, N., and A. Temkin, 1976b, J. Chem. Phys. **65**, 4537.

Chandra, N., and A. Temkin, 1976c, Phys. Rev. A **14**, 507.

Chang, E. S., 1970, Phys. Rev. A **2**, 1403.

Chang, E. S., 1974a, Phys. Rev. A **9**, 1644.

Chang, E. S., 1974b, Phys. Rev. A **10**, 1911.

Chang, E. S., 1974c, Phys. Rev. Lett. **33**, 1644.
Chang, E. S., 1977a, Phys. Rev. A **16**, 1841.
Chang, E. S., 1977b, Phys. Rev. A **16**, 1850.
Chang, E. S., 1977c, J. Phys. B **10**, L395.
Chang, E. S., and U. Fano, 1972, Phys. Rev. A **6**, 173.
Chang, E. S., and A. Temkin, 1969, Phys. Rev. Lett. **23**, 399.
Chang, E. S., and A. Temkin, 1970, J. Phys. Soc. Jpn. **29**, 172.
Chang, E. S., and S. Wong, 1977, Phys. Rev. Lett. **38**, 1327.
Chang, T. N., R. T. Poe, and R. Ray, 1973, Phys. Rev. Lett. **31**, 1097.
Chen, J. C. Y., 1964a, J. Chem. Phys. **40**, 3507.
Chen, J. C. Y., 1964b, J. Chem. Phys. **40**, 3513.
Chen, J. C. Y., 1964c, J. Chem. Phys. **41**, 3259.
Chen, J. C. Y., 1966a, Phys. Rev. **146**, 61.
Chen, J. C. Y., 1966b, J. Chem. Phys. **45**, 2710.
Chen, J. C. Y., 1969, Adv. Radiat. Chem. **1**, 245.
Chen, J. C. Y., and J. L. Magee, 1962, J. Chem. Phys. **36**, 1407.
Choi, B. H., and R. T. Poe, 1977a, Phys. Rev. A **16**, 1821.
Choi, B. H., and R. T. Poe, 1977b, Phys. Rev. A **16**, 1831.
Choi, B. H., R. T. Poe, J. C. Sun, and Y. Shan, 1979, Phys. Rev. A **19**, 116.
Christophorou, L. G., and A. A. Christodoulides, 1969, J. Phys. B **2**, 71.
Christophorou, L. G., G. S. Hurst, and A. Hadjiantoniou, 1966, J. Chem. Phys. **44**, 3506.
Christophorou, L. G., G. S. Hurst, and W. G. Hendrick, 1967, J. Chem. Phys. **45**, 1081.
Christophorou, L. G., and D. L. McCorkle, 1976, Chem. Phys. Lett. **42**, 533.
Christophorou, L. G., and D. Pittman, 1970, J. Phys. B **3**, 1252.
Chu, S. I., 1975, Phys. Rev. A **12**, 396.
Chu, S. I., and A. Dalgarno, 1974, Phys. Rev. A **10**, 788; **12**, 725 (E) 1975.
Chung, S., and C. C. Lin, 1972, Phys. Rev. A **6**, 988.
Chung, S., and C. C. Lin, 1974, Phys. Rev. A **9**, 1954.
Chung, S., and C. C. Lin, 1978, Phys. Rev. A **17**, 1874.
Chung, S., C. C. Lin, and E. T. P. Lee, 1975, Phys. Rev. A **12**, 1340.
Chutjian, A., D. C. Cartwright, and S. Trajmar, 1977, Phys. Rev. A **16**, 1052.
Chutjian, A., D. G. Truhlar, W. Williams, and S. Trajmar, 1972, Phys. Rev. Lett. **29**, 1580.
Clark, C. W., 1977, Phys. Rev. A **16**, 1419.
Claydon, C. R., G. A. Segal, and H. S. Taylor, 1970, J. Chem. Phys. **52**, 3387.
Collins, L. A., and D. W. Norcross, 1977, Phys. Rev. Lett. **38**, 1208.
Collins, L. A., and D. W. Norcross, 1978, Phys. Rev. A **18**, 467.
Collins, L. A., D. W. Norcross, and G. B. Schmid, 1979, J. Phys. B **12**, 1019.
Collins, L. A., W. D. Robb, and M. A. Morrison, 1978, J. Phys. B **11**, L777.
Collins, L. A., W. D. Robb, and M. A. Morrison, 1979, Phys. Rev. A (to be published).
Collins, L. A., W. D. Robb, and D. W. Norcross, 1979, Phys. Rev. A (to be published).
Coulson, C. A., and M. Walmsley, 1967, Proc. Phys. Soc. London, **91**, 31.
Cowan, R. D., A. C. Larson, D. Liberman, J. B. Mann, and J. Waber, 1966, Phys. Rev. **144**, 5.
Craggs, J. D., and H. S. W. Massey, 1956, in *Handbuch der Physik*, edited by S. Flügge (Springer, Berlin).
Crawford, O. H., 1967, Proc. Phys. Soc. London **91**, 279.
Crawford, O. H., 1968, Chem. Phys. Lett. **2**, 401.
Crawford, O. H., and A. Dalgarno, 1967, Chem. Phys. Lett. **1**, 23.
Crawford, O. H., and A. Dalgarno, 1971, J. Phys. B **4**, 494.
Crawford, O. H., A. Dalgarno, and P. B. Hayes, 1967, Mol. Phys. **13**, 181.
Crees, M. A., and D. L. Moores, 1975, J. Phys. B **8**, L195.
Crees, M. A., and D. L. Moores, 1977, J. Phys. B **10**, L225.
Crompton, R. W., D. K. Gibson, and A. I. McIntosh, 1969, Austr. J. Phys. **20**, 369.
Crompton, R. W., D. K. Gibson, and A. G. Robertson, 1970, Phys. Rev. A **2**, 1386.
Crompton, R. W., and A. G. Robertson, 1971, Austr. J. Phys. **24**, 543.
Csanak, G., H. S. Taylor, and D. N. Tripanthy, 1973, J. Phys. B **6**, 2040.
Csanak, G., H. S. Taylor, and E. F. Varracchio, 1974, J. Chem. Phys. **61**, 263.
Csanak, G., H. S. Taylor, and R. Yaris, 1971, Adv. Atom Mol. Phys. **7**, 287.
Dalgarno, A., 1968, Adv. Atom. Mol. Phys. **4**, 381.
Dalgarno, A., O. H. Crawford, and A. C. Allison, 1968, Chem. Phys. Lett. **2**, 381.
Dalgarno, A., and R. J. W. Henry, 1965, Proc. Phys. Soc. London **85**, 679.
Dalgarno, A., and J. T. Lewis, 1956, Proc. Phys. Soc. A **69**, 67.
Dalgarno, A., and R. A. McCray, 1972, Annu. Rev. Astron. Astrophys. **10**, 375.
Dalgarno, A., and M. R. C. McDowell, 1956, Proc. Phys. Soc. London A **69**, 615.
Dalgarno, A., and R. J. Moffett, 1963, Proc. Natl. Acad. Sci. India A **33**, 511.
Danner, D., 1970, Diplomarbeit, Physikalisches Institut der Universitat Freiburg.
Darewych, J. W., P. Baille, and S. Hara, 1974, J. Phys. B **7**, 2047.
Davenport, J. W., W. Ho, and J. R. Schrieffer, 1978, Phys. Rev. B **17**, 3115.
Davidson, E. R., 1962, J. Chem. Phys. **36**, 1080.
Demaria, A. J., 1973, Proc. IEEE **61**, 731.
Demkov, Y. N., and V. S. Rudakov, 1970, Zh. Eksp. Teor. Fiz. **59**, 2035, [Sov. Phys. JETP **32**, 1103 (1971)].
Dickinson, A. S., 1977, J. Phys. B **10**, 967.
Dickinson, A. S., T. G. Phillips, P. F. Goldsmith, I. C. Percival, and D. Richards, 1977, Astron. Astrophys. **54**, 645.
Dickinson, A. S., and D. Richards, 1975, J. Phys. B **8**, 2846.
Dill, D., and J. L. Dehmer, 1974, J. Chem. Phys. **61**, 692.
Dill, D., and J. L. Dehmer, 1977, Phys. Rev. A **16**, 1423.
Dixon, D. A., R. A. Eades, and D. G. Truhlar, 1979, J. Phys. B (to be published).
Domcke, W., and L. S. Cederbaum, 1977a, Phys. Rev. A **16**, 1465.
Domcke, W., and L. S. Cederbaum, 1977b, J. Phys. B **10**, L47.
Drachman, R. J., and A. Temkin, 1972, in *Case Studies in Atomic Physics II*, edited by E. W. McDaniel (North-Holland, Amsterdam).
Drukarev, G. F., and I. Y. Yurova, 1977, J. Phys. B **10**, 3551.
Dubé, L., and A. Herzenberg, 1975, Phys. Rev. A **11**, 1314.
Dubé, L., and A. Herzenberg, 1977, Phys. Rev. Lett. **38**, 820.
DuBois, R. D., J. B. Jeffries, and G. H. Dunn, 1978, Phys. Rev. A **17**, 1314.
DuBois, R. D., and M. E. Rudd, 1976, J. Phys. B **9**, 2657.
Duxler, W. M., R. T. Poe, and R. W. La Bahn, 1971, Phys. Rev. A **4**, 1935.
Eades, R. A., D. G. Truhlar, and D. A. Dixon, 1979, Phys. Rev. A (to be published).
Ehrhardt, H., L. Langhans, F. Linder, and H. S. Taylor, 1968, Phys. Rev. **173**, 222.
Ehrhardt, H., and F. Linder, 1968, Phys. Rev. Lett. **21**, 419.
Ehrhardt, H., and K. Willmann, 1967, Z. Phys. **204**, 462.
Eliezer, I., H. S. Taylor, and J. K. Williams, 1967, J. Chem. Phys. **47**, 2165.
Engelhardt, A. G., and A. V. Phelps, 1963, Phys. Rev. **131**, 2115.
Engelhardt, A. G., A. V. Phelps, and C. G. Risk, 1964, Phys. Rev. **135**, A 1566.
Fabrikant, I. I., 1976, Sov. Phys. JETP **44**, 77.

Fabrikant, I. I., 1977, J. Phys. B **10**, 1761.
Fabrikant, I. I., 1978, J. Phys. B **11**, 3621.
Faisal, F. H. M., 1970, J. Phys. B **3**, 636.
Faisal, F. H. M., and A. Temkin, 1972, Phys. Rev. Lett. **28**, 203.
Faisal, F. H. M., and A. L. V. Tench, 1971, Comput. Phys. Commun. **2**, 261.
Fano, U., 1970a, Phys. Rev. A **2**, 353.
Fano, U., 1970b, Comments At. Mol. Phys. **1**, 140.
Fano, U., 1977, in *X ICPEAC, Electronic and Atomic Collisions: Invited Papers and Progress Reports*, edited by G. Watel (North-Holland, Amsterdam), p. 271.
Fano, U., and D. Dill, 1972, Phys. Rev. A **6**, 185.
Fano, U., and C. M. Lee, 1973, Phys. Rev. Lett. **31**, 1573.
Finn, T. G., and J. P. Doering, 1975, J. Chem. Phys. **63**, 4399.
Fisk, J. B., 1936, Phys. Rev. **49**, 167.
Fliflet, A. W., D. A. Levin, M. Ma, and V. McKoy, 1978, Phys. Rev. A **17**, 160.
Fliflet, A. W., and V. McKoy, 1978a, Phys. Rev. A **18**, 1048.
Fliflet, A. W., and V. McKoy, 1978b, Phys. Rev. A **18**, 2107.
Fliflet, A. W., and V. McKoy, 1979, Phys. Rev. A (submitted).
Fliflet, A. W., and V. McKoy, and T. N. Rescigno, 1979a, J. Phys. B. (submitted).
Fliflet, A. W., V. McKoy, and T. N. Rescigno, 1979b, Phys. Rev. A (submitted).
Flygare, W. H., 1978, *Molecular Structure and Dynamics* (Prentice-Hall, Englewood Cliffs).
Fox, K., 1968, J. Phys. A **1**, 124.
Fraga, S., and B. J. Ransil, 1961, J. Chem. Phys. **35**, 1967.
Franco, V., and R. J. Glauber, 1966, Phys. Rev. **142**, 1195.
Franklin, J. L., 1969, Natl. Stand. Ref. Data Ser., Nat. Bur. Stand. **26**.
Frommhold, L., 1968, Phys. Rev. **172**, 118.
Frost, L. S., and A. V. Phelps, 1962, Phys. Rev. **127**, 1621.
Furness, J. B., and I. E. McCarthy, 1973, J. Phys. B **6**, 2280.
Garrett, W. R., 1971a, Mol. Phys. **20**, 751.
Garrett, W. R., 1971b, Phys. Rev. A **3**, 961.
Garrett, W. R., 1971c, Phys. Rev. A **4**, 2229.
Garrett, W. R., 1972, Mol. Phys. **24**, 465.
Garrett, W. R., 1975, Phys. Rev. A **11**, 509.
Garrett, W. R., 1977, Phys. Rev. A **16**, 2305.
Gaspar, R., 1954, Acta Phys. Acad. Sci. Hung. **3**, 263.
Geltman, S., and K. Takayanagi, 1966, Phys. Rev. **143**, 25.
Gerjuoy, E., and S. Stein, 1955a, Phys. Rev. **97**, 1671.
Gerjuoy, E., and S. Stein, 1955b, Phys. Rev. **98**, 1848.
Gianturco, F. A., and N. K. Rahman, 1977a, Chem. Phys. Lett. **48**, 380.
Gianturco, F. A., and N. K. Rahman, 1977b, J. Phys. B **10**, L219.
Gianturco, F. A., and J. H. Tait, 1972, Chem. Phys. Lett. **12**, 589.
Gianturco, F. A., and D. G. Thompson, 1976, J. Phys. B **9**, L383.
Gilmore, F. R., 1965, J. Quant. Spectrosc. Radiat. Transfer **5**, 369.
Glauber, R. J., 1959, in *Lectures in Theoretical Physics*, edited by W. E. Brittin and L. G. Dunham (Interscience, New York), Vol. I, p. 315.
Golden, D. E., 1966, Phys. Rev. Lett. **17**, 847.
Golden, D. E., 1978, Adv. Atom. Mol. Phys. **14**, 1.
Golden, D. E., H. W. Bandel, and J. A. Salerno, 1966, Phys. Rev. **146**, 40.
Golden, D. E., N. F. Lane, A. Temkin, and E. Gerjuoy, 1971, Rev. Mod. Phys. **43**, 642.
Gottfried, K., 1966, *Quantum Mechanics* (Benjamin, New York).
Haas, R., 1957, Z. Phys. **148**, 177.
Hake, R. D. Jr., and A. V. Phelps, 1967, Phys. Rev. **158**, 70.
Hall, R., 1977, in *X ICPEAC, Electronic and Atomic Collisions: Invited Papers and Progress Reports*, edited by G. Watel (North-Holland, Amsterdam), p. 25.
Hamming, R. W., 1962, *Numerical Methods for Scientists and Engineers* (McGraw-Hill, New York), p. 215.
Hara, S., 1967, J. Phys. Soc. Jpn. **22**, 710.
Hara, S., 1969a, J. Phys. Soc. Jpn. **27**, 1009.
Hara, S., 1969b, J. Phys. Soc. Jpn. **27**, 1592.
Hara, S., 1969c, J. Phys. Soc. Jpn. **27**, 1262.
Hara, S., 1971, J. Phys. Soc. Jpn. **30**, 819.
Hartree, D. R., 1957, *The Calculation of Atomic Structures* (Wiley, New York).
Hazi, A., 1979a, Phys. Rev. A **19**, 920.
Hazi, A., 1979b, Phys. Rev. A (to be published).
Hazi, A., and M. F. Fels, 1971, Chem. Phys. Lett. **8**, 582.
Hazi, A., T. N. Rescigno, and A. E. Orel, 1979, Appl. Phys. Lett. (submitted).
Hazi, A., and H. S. Taylor, 1970, Phys. Rev. A **1**, 1109.
Heideman, H. G. M., C. E. Kuyatt, and G. E. Chamberlain, 1966a, J. Chem. Phys. **44**, 355.
Heideman, H. G. M., C. E. Kuyatt, and G. E. Chamberlain, 1966b, J. Chem. Phys. **44**, 440.
Henry, R. J. W., 1970, Phys. Rev. A **2**, 1349.
Henry, R. J. W., and E. S. Chang, 1972, Phys. Rev. A **5**, 276.
Henry, R. J. W., and N. F. Lane, 1969, Phys. Rev. **183**, 221.
Henry, R. J. W., and N. F. Lane, 1971, Phys. Rev. A **4**, 410.
Herman, F., and S. Skillman, 1963, *Atomic Structure Calculations* (Prentice-Hall, Englewood Cliffs).
Hermann, D., K. Jost, and J. Kessler, 1976, J. Chem. Phys. **64**, 1.
Herzberg, G., 1950, *Spectra of Diatomic Molecules* (Van Nostrand, Princeton).
Herzenberg, A., 1968, J. Phys. B **1**, 548.
Herzenberg, A., and F. Mandl, 1962, Proc. R. Soc. London A **270**, 48.
Hickman, A. P., and F. T. Smith, 1978, Phys. Rev. A **17**, 968.
Hirschfelder, J. O., C. F. Curtiss, and R. B. Bird, 1954, *Molecular Theory of Gases and Liquids* (Wiley, New York).
Howard, C. J., F. C. Fehsenfeld, M. McFarland, 1974, J. Chem. Phys. **60**, 5068.
Huang, J. T. J., F. T. Chan, 1977, Phys. Rev. A **15**, 1782.
Hurst, G. S., J. A. Stockdale, and L. B. O'Kelly, 1963, J. Chem. Phys. **38**, 2572.
Huxley, L. G. H., and R. W. Crompton, 1962, in *Atomic and Molecular Processes*, edited by D. R. Bates (Academic, New York), Chap. 10.
Huxley, L. G. H., and R. W. Crompton, 1974, *The Diffusion and Drift of Electrons in Gases* (Wiley, New York).
Huzinaga, S., 1957, Prog. Theor. Phys. **17**, 62.
Huzinaga, S., 1965, J. Chem. Phys. **42**, 1293.
Itikawa, Y., 1969, J. Phys. Soc. Jpn. **27**, 444.
Itikawa, Y., 1970, J. Phys. Soc. Jpn. **28**, 1062.
Itikawa, Y., 1971a, J. Phys. Soc. Jpn. **30**, 835.
Itikawa, Y., 1971b, J. Phys. Soc. Jpn. **31**, 1532.
Itikawa, Y., 1971c, Phys. Rev. A **3**, 831.
Itikawa, Y., 1972, J. Phys. Soc. Jpn. **32**, 217.
Itikawa, Y., 1974a, J. Phys. Soc. Jpn. **36**, 1121.
Itikawa, Y., 1974b, J. Phys. Soc. Jpn. **36**, 1127.
Itikawa, Y., 1974c, At. Data Nucl. Data Tables **14**, 1.
Itikawa, Y., 1976, J. Phys. Soc. Jpn. **41**, 619.
Itikawa, Y., 1977, J. Phys. Soc. Jpn. **42**, 1334.
Itikawa, Y., 1978a, Phys. Rep. **46**, 117.
Itikawa, Y., 1978b, At. Data Nucl. Data Tables **21**, 69.
Itikawa, Y., and D. Ashihara, 1971, J. Phys. Soc. Jpn. **30**, 1461.
Itikawa, Y., and K. Takayanagi, 1969a, J. Phys. Soc. Jpn. **26**, 1254.
Itikawa, Y., and K. Takayanagi, 1969b, J. Phys. Soc. Jpn. **27**, 1293.
Itikawa, Y., and K. Takayanagi, 1969c, in *VI ICPEAC Abstracts* (MIT Press, Cambridge, Mass.) p. 144.
James, H. M., and A. S. Coolidge, 1933, J. Chem. Phys. **1**, 825.
Johnson, K. H., 1973, in *Advances in Quantitative Chemistry*, edited by P. O. Löwdin (Academic, New York), Vol. 7, p.

143.

Jordan, K. D., and W. Luken, 1976, J. Chem. Phys. **64**, 2760.

Joy, H. W., and R. G. Parr, 1958, J. Chem. Phys. **28**, 448.

Kaldor, U., 1978, Chem. Phys. Lett. **58**, 509.

Kaldor, U., 1979a, Phys. Rev. A **19**, 105.

Kaldor, U., 1979b, private communication.

Kaldor, U., and A. Klonover, 1977, in *X ICPEAC Abstracts* (Commissariat A L'Energie Atomique Paris) p. 488.

Kambara, H., and K. Kuchitsu, 1972, Jpn. J. Appl. Phys. **11**, 609.

Kleban, P., and H. T. Davis, 1977, Phys. Rev. Lett. **39**, 456.

Klonover, A., and U. Kaldor, 1978, J. Phys. B **11**, 1623.

Klonover, A., and U. Kaldor, 1979a, J. Phys. B **12**, L61.

Klonover, A., and U. Kaldor, 1979b, J. Phys. B **12**, 323.

Klonover, A., and U. Kaldor, 1979c, J. Phys. B (to be published).

Kohn, W., and L. J. Sham, 1965, Phys. Rev. **140**, A1133.

Koike, F., 1975, J. Phys. Soc. Jpn. **39**, 1590.

Kollath, R. K., 1932, Ann. Phys. (Leipzig) **15**, 485.

Kolos, W., and C. C. Roothaan, 1960, Rev. Mod. Phys. **32**, 205.

Kolos, W., and L. Wolniewicz, 1965, J. Chem. Phys. **41**, 3663.

Kolos, W., and L. Wolniewicz, 1967, J. Chem. Phys. **46**, 142.

Kouri, D. J., 1968a, Phys. Rev. **49**, 4481.

Kouri, D. J., 1968b, J. Chem. Phys. **49**, 5205.

Krauss, M., and F. H. Mies, 1970, Phys. Rev. A **1**, 1592.

Krauss, M., and D. Neumann, 1972, Chem. Phys. Lett. **14**, 26.

Lan, V. K., M. Le Dourneuf, and B. I. Schneider, 1979, edited by K. Takayanagi and N. Oda (Society for Atomic Collisions Research, Japan) *XI ICPEAC Abstracts*.

Land, J. E., 1978, J. Appl. Phys. **49**, 5716.

Lane, A. M., and R. G. Thomas, 1958, Rev. Mod. Phys. **30**, 257.

Lane, N. F., 1979, in *Electron-Molecule Scattering*, edited by Sanborn C. Brown, (Wiley, New York), in press.

Lane, N. F., and S. Geltman, 1967, Phys. Rev. **160**, 53.

Lane, N. F., and S. Geltman, 1969, Phys. Rev. **184**, 46.

Lane, N. F., and R. J. W. Henry, 1968, Phys. Rev. **173**, 183.

Latter, R., 1955, Phys. Rev. **99**, 510.

Lee, C. M., 1974, Phys. Rev. A **10**, 584.

Levin, D. A., A. W. Fliflet, and V. McKoy, 1979 (private communication).

Levin, D. A., T. N. Rescigno, and V. McKoy, 1977, Phys. Rev. A **16**, 157.

Levy-Leblond, J. M., 1967, Phys. Rev. **153**, 1.

Levy-Leblond, J. M., and J. R. Provost, 1967, Phys. Lett. B **26**, 104.

Lewis, B. R., J. B. Furness, and P. J. O. Tuebner, 1974, J. Phys. B **1**, 1083.

Light, J. C., and R. B. Walker, 1976, J. Chem. Phys. **65**, 4272.

Linder, F., 1969, *VI ICPEAC Abstracts* (MIT Press, Cambridge, Mass.) p. 141.

Linder, F., 1977, *X ICPEAC, Electronic and Atomic Collisions: Invited Papers and Progress Reports*, edited by G. Watel (North-Holland, Amsterdam), p. 51.

Linder, F., and H. Schmidt, 1971a, Z. Naturforsch. A **26a**, 1603.

Linder, F., and H. Schmidt, 1971b, Z. Naturforsch. A **26a**, 1617.

Lindgren, I., and A. Rosen, 1974, in *Case Studies in Atomic and Molecular Physics* (North-Holland, Amsterdam), Vol. 4, p. 93.

Lippmann, B. A., and H. M. Schey, 1961, Phys. Rev. **121**, 1112.

Lowke, J. J., A. V. Phelps, and B. W. Irwin, 1973, J. Appl. Phys. **44**, 4664.

Marriott, R., 1958, Proc. R. Soc. London **72**, 121.

Maru, M. P., and H. S. Desai, 1975, J. Phys. B **8**, 1959.

Maru, M. P., and H. S. Desai, 1976, Indian J. Theor. Phys. **24**, 49.

Massey, H. S. W., 1931, Proc. Cambridge Philos. Soc. **28**, 99.

Massey, H. S. W., 1935, Trans. Faraday Soc. **31**, 556.

Massey, H. S. W., 1969, *Electronic and Ionic Impact Phenomena, Vol. II: Electron Collisions with Molecules and Photoionization* (Oxford University, London).

Massey, H. S. W., and E. H. Burhop, 1969, *Electronic and Ionic Impact Phenomena, Vol. I: Collisions of Electrons with Atoms* (Oxford University, London).

Massey, H. S. W., and R. O. Ridley, 1956, Proc. Phys. Soc. London A **69**, 659.

Mathur, D., and J. B. Hasted, 1977, J. Phys. B **10**, L265.

Mathur, K. C., 1978, Phys. Rev. A **18**, 2493.

McCurdy, C. W. Jr., T. N. Rescigno, and V. McKoy, 1976, J. Phys. B **9**, 691.

McLean, A. D., and M. Yoshimine, 1967, IBM J. Res. Dev. Suppl. Nov. 1967.

McLean, A. D., and M. Yoshimine, 1968, IBM J. Res. Dev. **12**, 206.

Miller, W. H., and F. T. Smith, 1978, Phys. Rev. A **17**, 939.

Mittleman, M. H., and V. P. Myerscough, 1966, Phys. Lett. **23**, 545.

Mittleman, M. H., J. L. Peacher, and B. F. Rozsnyai, 1968, Phys. Rev. **176**, 180.

Mittleman, M. H., and R. E. von Holdt, 1965, Phys. Rev. **140**, A726.

Moiseiwitsch, B. L., 1966, *Variational Principles* (Interscience, New York).

Morrison, D. J. T. and M. R. H. Rudge, 1967, Proc. Phys. Soc. London **91**, 565.

Morrison, M. A., and L. A. Collins, 1977, J. Phys. B **10**, L119.

Morrison, M. A., and L. A. Collins, 1978, Phys. Rev. A **17**, 918.

Morrison, M. A., L. A. Collins, and N. F. Lane, 1976, Chem. Phys. Lett. **42**, 356.

Morrison, M. A., and P. J. Hay, 1977, J. Phys. B **10**, L647.

Morrison, M. A., and N. F. Lane, 1975, Phys. Rev. A **12**, 2361.

Morrison, M. A., and N. F. Lane, 1977, Phys. Rev. A **16**, 975.

Morrison, M. A., and N. F. Lane, 1978, Bull. Am. Phys. Soc. **23**, 1082.

Morrison, M. A., N. F. Lane, and L. A. Collins, 1977, Phys. Rev. A **15**, 2186.

Morrison, M. A., and B. I. Schneider, 1977, Phys. Rev. A **16**, 1003.

Morse, P. M., 1929, Phys. Rev. **34**, 57.

Morse, P. M., 1953, Phys. Rev. **90**, 51.

Mott, N. F., and H. S. W. Massey, 1965, *The Theory of Atomic Collisions*, 3rd edition (Clarendon, Oxford).

Mukherjee, D., and F. T. Smith, 1978, Phys. Rev. A **17**, 954.

Mullaney, N. A., and D. G. Truhlar, 1978, Chem. Phys. Lett. **58**, 512.

Murtaugh, T. S., and W. P. Reinhardt, 1972, J. Chem. Phys. **57**, 2129.

Murtaugh, T. S., and W. P. Reinhardt, 1973, J. Chem. Phys. **59**, 4900.

Nagahara, S., 1953, J. Phys. Soc. Jpn. **8**, 165.

Nagahara, S., 1954, J. Phys. Soc. Jpn. **9**, 52.

Nesbet, R. K., 1964, J. Chem. Phys. **40**, 3619.

Nesbet, R. K., 1977, J. Phys. B **10**, L739.

Nesbet, R. K., 1979, Phys. Rev. A **19**, 551.

Newton, R. G., 1977, J. Math. Phys. **18**, 1348.

Ochkur, V. I., 1964, Sov. Phys. JETP **18**, 508.

Oksyuk, Y. D., 1966, Sov. Phys. JETP **22**, 873.

O'Malley, T. F., 1971, Adv. Atom. Mol. Phys. **7**, 223.

O'Malley, T. F., and H. S. Taylor, 1968, Phys. Rev. **176**, 207.

Omidvar, K., 1961, New York University Research Dept. CS-37.

Omidvar, K., 1974, Phys. Rev. A **133**, 970.

Onda, K., 1974, J. Phys. Soc. Jpn. **36**, 826.

Onda, K., 1976, J. Phys. Soc. Jpn. **40**, 1437.

Onda, K., and D. G. Truhlar, 1978, J. Chem. Phys. **69**, 1361.

Onda, K., and D. G. Truhlar, 1979a, J. Chem. Phys. **70**, 1681.

Onda, K., and D. G. Truhlar, 1979b, J. Phys. B **12**, 283.

Osborn, T. A., and D. Bolle', 1977, J. Math. Phys. **18**, 432.

Pacansky, J., U. Wahlgren, and P. S. Bagus, 1975, J. Chem. Phys. **58**, 479.

Pande, A. K., and R. S. Singh, 1977, Indian J. Pure Appl. Phys. **15**, 493.

Pavlovic, Z., M. J. W. Boness, A. Herzenberg, and G. J. Schulz, 1972, Phys. Rev. A **6**, 676.

Penner, S. S., and D. B. Olfe, 1968, *Radiation and Reentry* (Academic, New York).

Phelps, A. V., 1968, Rev. Mod. Phys. **40**, 399.

Phillips, J. C., and L. Kleinman, 1959, Phys. Rev. **116**, 287.

Potter, J. E., N. C. Steph, P. H. Dwivedi, and D. E. Golden, 1977, J. Chem. Phys. **66**, 5557.

Rahman, N. K., F. A. Gianturco, and U. T. Lamanna, 1978, Phys. Rev. A **18**, 74.

Ramien, H., 1931, Z. Phys. **70**, 353.

Ramsauer, C., and R. K. Kollath, 1927, Ann. Phys. (Leipzig) **83**, 1129.

Ramsauer, C., and R. K. Kollath, 1930a, Ann. Phys. (Leipzig) **4**, 91.

Ramsauer, C., and R. K. Kollath, 1930b, Ann. Phys. (Leipzig) **7**, 176.

Ramsauer, C., and R. K. Kollath, 1931, Ann. Phys. (Leipzig) **9**, 756.

Ramsauer, C., and R. K. Kollath, 1932, Ann. Phys. (Leipzig) **12**, 529.

Ray, S., and A. K. Barua, 1974, J. Phys. B **7**, 973.

Read, F. H., 1968a, J. Phys. B **1**, 893.

Read, F. H., 1968b, J. Phys. B **1**, 1056.

Read, F. H., 1972, J. Phys. B **5**, 255.

Reinhardt, W. P., D. W. Oxtoby, and T. N. Rescigno, 1972, Phys. Rev. Lett. **28**, 401.

Rescigno, T. N., C. F. Bender, C. W. McCurdy, and V. McKoy, 1976, J. Phys. B **9**, 2141.

Rescigno, T. N., C. W. McCurdy, and V. McKoy, 1974a, Chem. Phys. Lett. **27**, 401.

Rescigno, T. N., C. W. McCurdy, and V. McKoy, 1974b, Phys. Rev. A **10**, 2240.

Rescigno, T. N., C. W. McCurdy, and V. McKoy, 1975a, Phys. Rev. A **11**, 825.

Rescigno, T. N., C. W. McCurdy, and V. McKoy, 1975b, J. Phys. B **8**, L433.

Rescigno, T. N., C. W. McCurdy, and V. McKoy, and C. F. Bender, 1976, Phys. Rev. A **13**, 216.

Rescigno, T., V. McKoy, and B. Schneider, 1979, editors, *Electron and Photon Molecule Collisions* (Plenum, New York).

Riley, M. E., and A. Kupperman, 1968, Chem. Phys. Lett. **1**, 537.

Riley, M. E., and D. G. Truhlar, 1975, J. Chem. Phys. **63**, 2182.

Riley, M. E., and D. G. Truhlar, 1976, J. Chem. Phys. **65**, 792.

Ritchie, B., 1972, Phys. Rev. A **6**, 1456.

Robb, W. D., 1977, in *X ICPEAC, Electronic and Atomic Collisions: Invited Papers and Progress Reports*, edited by G. Watel (North-Holland, Amsterdam), p. 231.

Rohr, K., 1977a, J. Phys. B **10**, L399.

Rohr, K., 1977b, J. Phys. B **10**, 1175.

Rohr, K., 1977c, J. Phys. B **10**, L735.

Rohr, K., 1977d, J. Phys. B **10**, 2215.

Rohr, K., 1978, J. Phys. B **11**, 1849.

Rohr, K., 1979, J. Phys. B **12**, L185.

Rohr, K., and F. Linder, 1975, J. Phys. B **8**, L200.

Rohr, K., and F. Linder, 1976, J. Phys. B **9**, 2521.

Rose, M. E., 1957, *Elementary Theory of Angular Momentum* (Wiley, New York).

Rudge, M. R. H., 1965a, Proc. Phys. Soc. London **85**, 607.

Rudge, M. R. H., 1965b, Proc. Phys. Soc. London **86**, 763.

Rudge, M. R. H., 1973, Adv. Atom. Mol. Phys. **9**, 48.

Rudge, M. R. H., 1974, J. Phys. B **7**, 1323.

Rudge, M. R. H., 1978a, J. Phys. B **11**, 1497.

Rudge, M. R. H., 1978b, J. Phys. B **11**, 1503.

Rudge, M. R. H., 1978c, J. Phys. B **11**, 2221.

Rudge, M. R. H., S. Trajmar, and W. Williams, 1976, Phys. Rev. A **13**, 2074.

Rumble, J. R., and D. G. Truhlar, 1979, J. Chem. Phys. **70**, 4101.

Sampson, D. H., and R. C. Mjolsness, 1965, Phys. Rev. **140**, 1466.

Sampson, D. H., and R. C. Mjolsness, 1966, Phys. Rev. **144**, 116.

Sams, W. N., L. Frommhold, and D. J. Kouri, 1972, Phys. Rev. A **6**, 1070.

Sams, W. N., and D. J. Kouri, 1969a, J. Chem. Phys. **51**, 4809.

Sams, W. N., and D. J. Kouri, 1969b, J. Chem. Phys. **51**, 4815.

Sanche, L., and G. J. Schulz, 1973, J. Chem. Phys. **58**, 479.

Sawada, T., P. S. Ganas, and A. E. S. Green, 1974, Phys. Rev. A **9**, 1130.

Schneider, B. I., 1974, Chem. Phys. Lett. **25**, 140.

Schneider, B. I., 1975a, Chem. Phys. Lett. **31**, 237.

Schneider, B. I., 1975b, Phys. Rev. **11**, 1957.

Schneider, B. I., 1976, Phys. Rev. A **14**, 1923.

Schneider, B. I., 1977a, *X ICPEAC, Electronic and Atomic Collisions: Invited Papers and Progress Reports*, edited by G. Watel (North-Holland, Amsterdam), p. 257.

Schneider, B. I., 1977b, Chem. Phys. Lett. **51**, 578.

Schneider, B. I., and R. S. Berry, 1969, Phys. Rev. **182**, 141.

Schneider, B. I., and P. J. Hay, 1976, Phys. Rev. A **13**, 2049.

Schneider, B. I., M. Le Dourneuf, and P. G. Burke, 1979, J. Phys. B **12** (to be published).

Schneider, B. I., M. Le Dourneuf, and V. K. Lan, 1979, private communication.

Schneider, B. I., M. Weinberg, J. C. Tully, and R. S. Berry, 1969, Phys. Rev. **182**, 133.

Schulz, G. J., 1959, Phys. Rev. **116**, 1141.

Schulz, G. J., 1962, Phys. Rev. **125**, 229.

Schulz, G. J., 1964, Phys. Rev. **135**, A988.

Schulz, G. J., 1973, Rev. Mod. Phys. **45**, 423.

Schulz, G. J., 1976, in *Principles of Laser Plasmas*, edited by B. Bekefi (Wiley, New York).

Schulz, G. J., and H. C. Koons, 1966, J. Chem. Phys. **44**, 1297.

Seaton, M. J., 1962, Proc. Phys. Soc. London **79**, 1105.

Seaton, M. J., 1974, J. Phys. B **7**, 1817.

Seng, G., and F. Linder, 1976, J. Phys. B **9**, 2539.

Seraph, H. E., 1964, Proc. Phys. Soc. London **83**, 763.

Shimamura, I., 1977a, J. Phys. B **10**, 2597.

Shimamura, I., 1977b, *X ICPEAC, Electronic and Atomic Collisions: Invited Papers and Progress Reports*, edited by G. Watel (North-Holland, Amsterdam), p. 213.

Shimamura, I., 1977c, unpublished (see Collins and Norcross, 1978).

Shimizu, M., 1963, J. Phys. Soc. Jpn. **18**, 811.

Shugard, M., and A. Hazi, 1975, Phys. Rev. A **12**, 1895.

Shyn, T. W., W. E. Sharp, and G. R. Carignan, 1978, Phys. Rev. A **17**, 1855.

Shyn, T. W., R. S. Stolarski, and G. R. Carignan, 1972, Phys. Rev. A **6**, 1002.

Siegel, J., and D. Dill, 1976, J. Chem. Phys. **64**, 3204.

Siegel, J., D. Dill, and J. L. Dehmer, 1978, Phys. Rev. A **17**, 2106.

Siegel, M. W., R. J. Celotta, J. L. Hall, J. Levine, and R. A. Bennett, 1972, Phys. Rev. A **6**, 607.

Sinfailam, A. L., 1970, Comput. Phys. Commun. **1**, 445.

Singh, Y., 1970, J. Phys. B **3**, 1222.

Slater, J. C., 1951, Phys. Rev. **81**, 385.

Slater, J. C., 1960a, *Quantum Theory of Atomic Structure*, Vol. 1 (McGraw-Hill, New York).

Slater, J. C., 1960b, *Quantum Theory of Atomic Structure*, Vol. 2 (McGraw-Hill, New York).

Slater, R. C., M. G. Fickes, W. G. Becker, and R. C. Stern, 1974a, J. Chem. Phys. **60**, 4697.

Slater, R. C., M. G. Fickes, W. G. Becker, and R. C. Stern, 1974b, J. Chem. Phys. **61**, 2290.

Slater, R. C., M. G. Fickes, and R. C. Stern, 1972, Phys. Rev. Lett. **29**, 333.

Sloan, I. H., 1968, J. Comput. Phys. **3**, 40.

Smith, K., R. J. W. Henry, and P. G. Burke, 1966, Phys. Rev. **147**, 21.

Spence, D., and G. J. Schulz, 1971, Phys. Rev. A **3**, 1968.

Spencer, F. E., and A. V. Phelps, 1976, in *Proceedings of the 15th Symposium on Engineering Aspects of MHD* (University of Pennsylvania, Philadephia).

Srivistava, S. K., A. Chutjian, and S. Trajmar, 1975, J. Chem. Phys. **63**, 2659.

Srivistava, S. K., A. Chutjian, and S. Trajmar, 1976, J. Chem. Phys. **64**, 1340.

Stamatovic, A., and G. J. Schulz, 1973, Phys. Rev. A **7**, 589.

Stauffer, A. D., and M. R. C. McDowell, 1966, Proc. Phys. Soc. London **89**, 289.

Stern, R. C., and W. G. Becker, 1975, *IX ICPEAC Abstracts*, edited by J. S. Risley and R. Geballe (Univ. of Wash., Seattle) p. 275.

Stevens, W. J., 1977, unpublished (see Collins and Norcross, 1978).

Stogryn, D. E., and A P. Stogryn, 1966, Mol. Phys. **11**, 371.

Subramanian, R., 1968, Zh. Eksp. Teor. Fiz. **55**, 363, [Sov. Phys. JETP **28**, 190 (1969)].

Swan, P., 1955, Proc. R. Soc. London A **228**, 10.

Szmytkowski, C., and M. Zubek, 1977, J. Phys. B **10**, L31.

Szmythowski, C., and M. Zubeck, 1978, Chem. Phys. Lett. **57**, 105.

Szmythowski, C., M. Zubeck, and J. Drewko, 1978, J. Phys. B **11**, L371.

Takayanagi, K., 1965a, J. Phys. Soc. Jpn. **20**, 562.

Takayanagi, K., 1965b, J. Phys. Soc. Jpn. **20**, 2297.

Takayanagi, K., 1966, J. Phys. Soc. Jpn. **21**, 507.

Takayanagi, K., 1967, Prog. Theor. Phys. Suppl. No. 40, 216.

Takayanagi, K., 1970, J. Phys. Soc. Jpn. **28**, 1527.

Takayanagi, K., 1972, Comments At. Mol. Phys. **3**, 95.

Takayanagi, K., 1973, Comments At. Mol. Phys. **4**, 59.

Takayanagi, K., 1974, Prog. Theor. Phys. **52**, 337.

Takayanagi, K., 1975a, in *Atomic Physics 4*, edited by G. Zu Putlitz, E. W. Weber, and A. Winnacker (Plenum, New York).

Takayanagi, K., 1975b, in *IX ICPEAC*, *The Physics of Electronic and Atomic Collisions: Invited Lectures, Review Papers, and Progress Reports*, edited by J. S. Risley and R. Geballe (University of Washington, Seattle), p. 219.

Takayanagi, K., and S. Geltman, 1964, Phys. Lett. **13**, 135.

Takayanagi, K., and S. Geltman, 1965, Phys. Rev. **138**, A1003.

Takayanagi, K., and Y. Itikawa, 1968, J. Phys. Soc. Jpn. **24**, 160.

Takayanagi, K., and Y. Itikawa, 1970a, Space Sci. Rev. **11**, 380.

Takayanagi, K., and Y. Itikawa, 1970b, Adv. At. Mol. Phys. **6**, 105.

Taylor, H. S., 1967, Proc. Phys. Soc. London **90**, 877.

Taylor, H. S., 1970, Adv. Chem. Phys. **17**, 91.

Taylor, H. S., E. Goldstein, and G. A. Segal, 1977, J. Phys. B **10**, 2253.

Taylor, H. S., and F. E. Harris, 1963a, Mol. Phys. **6**, 183.

Taylor, H. S., and F. E. Harris, 1963b, J. Chem. Phys. **38**, 2591.

Taylor, H. S., and F. E. Harris, 1963c, J. Chem. Phys. **39**, 1012.

Taylor, H. S., G. V. Nazaroff, and A. Golebiewski, 1966, J. Chem. Phys. **45**, 2872.

Taylor, H. S., and J. K. Williams, 1965, J. Chem. Phys. **42**, 4063.

Taylor, J. R., 1972, *Scattering Theory: The Quantum Theory of Non-Relativistic Collisions* (Wiley, New York).

Temkin, A., 1957, Phys. Rev. **107**, 1004.

Temkin, A., 1976, Comments At. Mol. Phys. **5**, 55.

Temkin, A., and F. H. M. Faisal, 1971, Phys. Rev. A **3**, 520.

Temkin, A., and J. C. Lamkin, 1961, Phys. Rev. **121**, 788.

Temkin, A., and E. C. Sullivan, 1974, Phys. Rev. Lett. **33**, 1057.

Temkin, A., and K. V. Vasavada, 1967, Phys. Rev. **160**, 109.

Temkin, A., K. V. Vasavada, E. S. Chang, and A. Silver, 1969, Phys. Rev. **186**, 57.

Thaddeus, P., 1972, Astrophys. J. **173**, 317.

Thomas, L. D., 1973, J. Comput. Phys. **13**, 348.

Tice, R. K., and D. Kivelson, 1967, J. Chem. Phys. **46**, 4748.

Trajmar, S., J. K. Rice, and A. Kuppermann, 1970, Adv. Chem. Phys. **17**, 15.

Trajmar, S., D. G. Truhlar, and J. K. Rice, 1970a, J. Chem. Phys. **52**, 4502.

Trajmar, S., D. G. Truhlar, J. K. Rice, and A. Kupperman, 1970b, J. Chem. Phys. **52**, 4516.

Tronc, M., A. Huertz, M. Landau, F. Pichon, and J. Reinhardt, 1975, J. Phys. B **8**, 1453.

Truhlar, D. G., 1972, J. Chem. Phys. **57**, 3260.

Truhlar, D. G., 1973, Phys. Rev. A **7**, 2217.

Truhlar, D. G., 1977, in *Semiempirical Methods of Electronic Structure Calculation, Part B: Applications*, edited by G. A. Segal (Plenum, New York).

Truhlar, D. G., and M. A. Brandt, 1976, J. Chem. Phys. **65**, 3092.

Truhlar, D. G., M. A. Brandt, A. Chutjian, S. K. Srivastava, and S. Trajmar, 1976, J. Chem. Phys. **65**, 2962.

Truhlar, D. G., M. A. Brandt, S. K. Srivastava, S. Trajmar, and A. Chutjian, 1977, J. Chem. Phys. **66**, 655.

Truhlar, D. G., D. A. Dixon, and R. A. Eades, 1979, J. Phys. B (in press).

Truhlar, D. G., and N. A. Mallaney, 1978, J. Chem. Phys. **68**, 1574.

Truhlar, D. G., K. Onda, R. A. Eades, and D. A. Dixon, 1979, Int. J. Quant. Chem. Symp. **13**, (in press).

Truhlar, D. G., and J. K. Rice, 1970, J. Chem. Phys. **52**, 4480.

Truhlar, D. G., S. Trajmar, and W. Williams, 1972, J. Chem. Phys. **57**, 3250.

Truhlar, D. G., and F. A. Van-Catledge, 1973, J. Chem. Phys. **59**, 3207.

Truhlar, D. G., and F. A. Van-Catledge, 1976, J. Chem. Phys. **65**, 5536.

Truhlar, D. G., and F. A. Van-Catledge, 1978, J. Chem. Phys. **69**, 3575.

Truhlar, D. G., F. A. Van-Catledge, and T. H. Dunning, 1972, J. Chem. Phys. **57**, 4788.

Truhlar, D. G., W. Williams, and S. Trajmar, 1972, J. Chem. Phys. **57**, 4307.

Tully, J. C., 1969, Phys. Rev. **181**, 7.

Tully, J. C., and R. S. Berry, 1969, J. Chem. Phys. **51**, 2056.

Turner, J. E., 1966, Phys. Rev. **141**, 21.

Turner, J. E., 1977, Am. J. Phys. **45**, 758.

Turner, J. E., and K. Fox, 1966, Phys. Lett. **23**, 547.

Varracchio, F., 1977, J. Phys. B **10**, 503.

Varracchio, F., 1979, private communication.

Vucelić, M., Y. Öhrn, and J. R. Sabin, 1973, J. Chem. Phys. **59**, 3003.

Vušković, L., S. K. Srivastava, and S. Trajmar, 1978, J. Phys. B **11**, 1643 .

Wadehra, J. M., and J. N. Bardsley, 1978, Phys. Rev. Lett. **41**, 1795.

Wang, S. C., 1928, Phys. Rev. **31**, 579.

Weatherford, C. A., and R. J. W. Henry, 1977, Can. J. Phys. **55**,**1**, 442.

Weatherford, C. A., and R. J. W. Henry, 1979 (private communication).

Weinbaum, S., 1933, J. Chem. Phys. **1**, 593.

White, R. A., and E. F. Hayes, 1972, J. Chem. Phys. **57**, 2985.

Wigner, E. P., 1946a, Phys. Rev. **70**, 15.

Wigner, E. P., 1946b, Phys. Rev. **70**, 606.

Wigner, E. P., and L. Eisenbud, 1947, Phys. Rev. **72**, 29.

Wilkins, K. L., and H. S. Taylor, 1967, J. Chem. Phys. **47**, 3532.

Winter, T. G., and N. F. Lane, 1975, Chem. Phys. Lett. **30**,

363.
Wolniewicz, L., 1966, J. Chem. Phys. **45**, 392.
Wong, S. 1978, private communication.
Wong, S., and L. Dubé, 1978, Phys. Rev. A **17**, 570.
Wong, S., and G. J. Schulz, 1974, Phys. Rev. Lett. **32**, 1089.
Wu, T. Y., 1947, Phys. Rev. **71**, 111.
Yoshimine, M., and A. D. McLean, 1967, Int. J. Quant. Chem. **1S**, 313.
Zarlingo, D. C., T. Ishihara, and R. T. Poe, 1972, Phys. Rev. Lett. **28**, 1093.
Ziesel, J. P., I. Nenner, and G. J. Schulz, 1975, J. Chem. Phys. **63**, 1943.
Zubek, M., and C. Szmytkowski, 1977, J. Phys. B **10**, L27.